Geoscience BC project – 2013-SK05
Geoscience BC Report 2017-09 (updated July 2017)

Hughes Range Paleomagnetic Study

Paleomagnetic evidence for extreme block faulting east of the Rocky Mountain Trench near Kimberley, BC

P.W. Ransom[1], T. Day[2] and R.J. Enkin[3]

1 Consultant, corresponding author: paul.ransom@corewhisperer.com

2 Department of Geography, Earth and Environmental Science, Okanagan College. Kelowna, BC

3 Geological Survey of Canada - Pacific, Sidney, BC

Geoscience BC is an independent, non-profit organization that generates earth science in collaboration with First Nations, local communities, government, academia and the resource sector. Our independent earth science enables informed resource management decisions and attracts investment and jobs. Geoscience BC gratefully acknowledges the financial support of the Province of British Columbia.

Abstract

The concept that steep west dipping normal faults were tilted into low angle normal faults (LANF) during block faulting of the Northern Hughes Range (NHR) east of the Rocky Mountain Trench (RMT) near Kimberley, British Columbia is supported by a reconnaissance paleomagnetic study of late Cretaceous stocks. The East Wild Horse and Nivlac stocks, 17 kilometres apart along the east side of the NHR, have down on east tilts of 42° and 56° respectively, the largest tilts of intrusions obtained to date in British Columbia. Contradictory results in the western part of the range from a small plug at Estella mine and from a 0.5 m wide dike at Saugum Canyon are probably intrusions that postdate the rotation. Two stocks and a small dike outside the NHR have magnetic remanances that overlap the mid Cretaceous value at the 95% confidence level.

Introduction

Regional Geology

Faults developed above deep crustal sutures influenced sedimentation patterns of the Belt-Purcell Supergroup and younger Proterozoic and Phanerozoic craton marginal sequences in southeastern British Columbia. Many of these same breaks were reactivated during late Jurassic to Early Cretaceous crustal shortening and subsequent Eocene block faulting. Some of these faults localized and became stitched by late Cretaceous igneous intrusions. East side down tilts of mid Cretaceous intrusions on the east side of the NHR, determined by this paleomagnetic study, provides the measure of tilting of the NHR block including once steep west dipping faults. Regional geology of the NHR of the Rocky and of adjacent Purcell Mountains near Kimberley, BC is shown in Figure 1.

The 10 to 30 kilometres wide valley between the Purcell and Rocky Mountains is part of the RMT, a physiographic feature that extends beyond the length of the province. Subdued topography of the eastern Purcell Mountains with strata that generally dip moderately into the trench contrast with the dramatic 2 kilometres high face on the east led earliest geologists to suggest a major fault on the east side; Daly (1912) described the RMT as a down flexure and Schofield (1915) called it an asymmetric graben that was initiated in the Eocene. A series of west dipping normal faults is inferred along the valley (Leech 1958). These ideas, including age of the faulting, still remain valid. The major right lateral reverse Moyie and St Mary faults of the Purcell Mountains continue directly across the Trench without lateral offset into the Rockies as the Dibble and Boulder Creek faults respectively (Rice, 1937; Leech, 1962). Known to have been growth faults during Proterozoic and, on the Moyie-Dibble fault at least during Paleozoic, episodes of extension these major structures became tear faults during compression (Leech, 1962; Lis et al, 1976). Subsequently, during Eocene extension, sections of the faults were likely block fault boundaries (Leech, 1962). Topography along parts of the RMT in this area has a block faulted appearance (Photos 1 and 2). A cross section from the eastern Purcells to the western Rockies at the latitude of Sullivan mine is an interpretation supported by this study that shows the Lakit LANF in the NHR block (Figure 2).

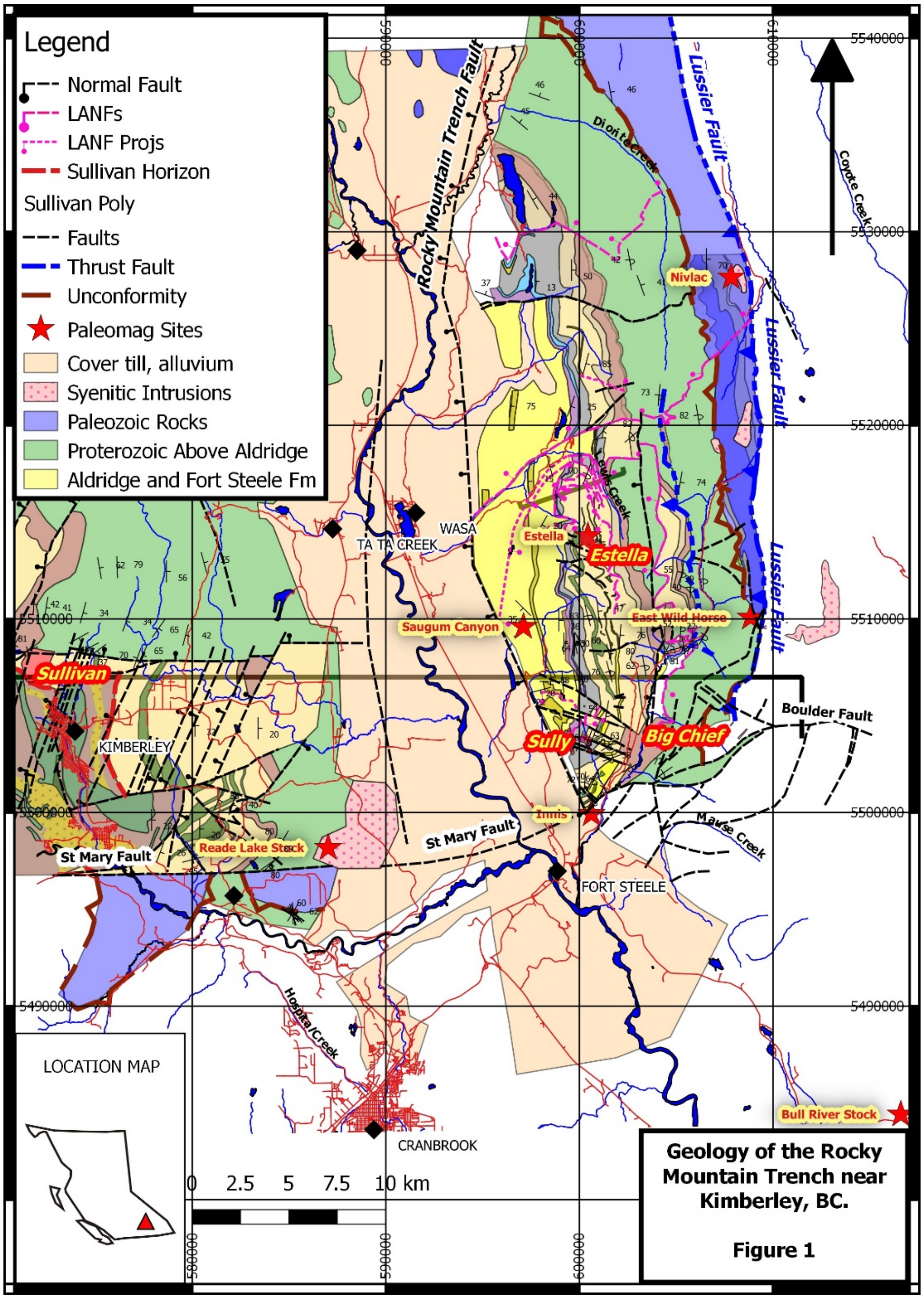

Figure 1. **I**n the Kimberley area the RMT valley is about 10 km wide between the Purcell and Rocky Mountains. On the east is the northern Hughes Range (NHR) of the Rockies. Rocks are predominantly Proterozoic, bounded above an unconformity on the east by Paleozoic strata. Major structures are the RMT and Kimberley normal faults, the Lussier Thrust and a major recumbent fold that extends along the entire NHR. Low angle normal faults (LANFs) have been mapped throughout the NHR. Near the south end of the NHR mapped litho-stratigraphic units in the lowest Proterozoic Aldridge Formation indicate a cumulative offset of 5 km in a 0.5 to 1 km zone of parallel LANFs. Stars indicate location of paleomagnetic sampling sites of post folding plutons and small dikes within and outside of the NHR.

Photo 1. View south along the RMT from about 1 km west of Cranbrook airport. Mt Baker on right is in the middle of the trench is a large block with significant east side down tilt, reminiscent of "sinking ships" in the Basin and Range. Steeples Range of southern Hughes Range on left.

Photo 2. View north along the RMT from about 1 km west of Cranbrook airport. Northern Hughes Range is on the right. Tilted blocks are apparent on both sides of trench. Mt Fairmont with slope down to west in the distance is 78 km north.

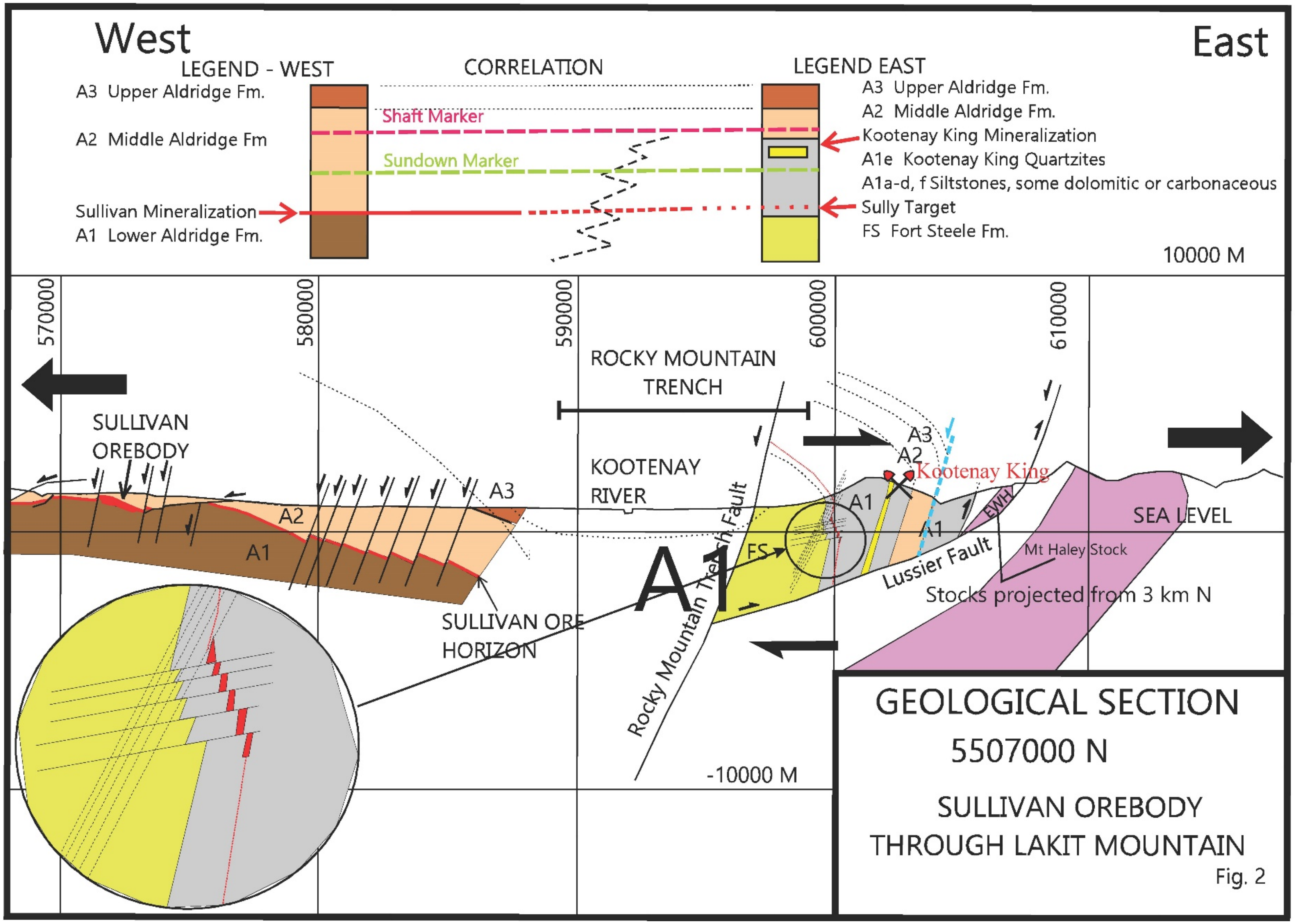

Figure 2. West to East cross section, Sullivan to Lussier Fault. In a rotated NHR any faults that had a steep west orientation would become LANFs.

Rocks are predominantly Mesoproterozoic strata of the Belt-Purcell Supergroup. In the easternmost part of the area shown in Figure 1 are two Neoproterozoic unconformities. The second cuts the first and has younger Neoproterozoic to Paleozoic strata above and it extends south to the east trending Boulder Creek Fault. An unconformity is also developed on sections immediately south of the St Mary Fault. An unconformity with Cambrian strata above is south of the St Mary Fault. For the purposes of this report the Mesoproterozoic successions are divided into Aldridge - Fort Steele Formations and above Aldridge.

The Aldridge Formation is present throughout the Purcell Mountains and comprises lower and middle and upper divisions. The several kilometres of lower and middle Aldridge is dominated by deep water turbidites. Within the 2.5 kilometres thick middle Aldridge Formation about a dozen laminite units 0.1 to 10 m thick contain sets of dark and light grey laminations in bar-code like patterns that provide absolute stratigraphic correlation (Hubschman, 1973) over distances up to 300 kilometres.

Unique to the NHR are the Fort Steele Formation at least 1 kilometres thick and above it the Hughes Range Facies of the Aldridge Formation (HRFA), that comprises units A1a through A1f, also about 1 kilometres thick (Höy, 1993). Mapping and drilling show that some of these strata thicken and contain evidence of having been deposited in progressively deeper water to the south up to where they are inferred to terminate against the Boulder Creek Fault. The HRFA passes up into the upper half of the barcode marker bearing interval of the middle Aldridge Formation indicating transgression and widening of the Belt-Purcell basin. The same bar code markers found in the NHR have been identified in the limited areas of Aldridge strata immediately south of the Boulder Fault. These sedimentological and stratigraphic trends indicate a growth fault existed roughly coincident with the Boulder Creek Fault. Similarly, transition of these strata to deep water turbidites to the west appears to be a facies change roughly coincident with the RMT.

Mesoproterozoic strata above the Aldridge Formation comprise the Creston (shallow water to subaerial) siliciclastic rocks), Kitchener (shallow water dolomitic siltstones), Van Creek (shallow water to subaerial) siliciclastic rocks), Nicol Creek (basaltic lava) formations and limited Upper Purcell Supergroup strata.

Early to mid-Cretaceous batholiths intrude many of the right hand reverse faults that cross from the Purcells into the Rockies and therefore provide an upper limit for the times of last displacement on them and linked thrust faults (Price, 1981). In the study area three stocks of similar age outcrop adjacent to the north trending Lussier Fault appear to have been intruded along it. One large mid-Cretaceous stock plugs the east trending St Mary Fault southeast of Kimberley. Several felsic to monzonitic porphyry dikes outcrop sparsely through the southern part of the NHR almost as far west as the RMT Fault including a swarm of dikes and small plugs near the Estella.

Structure

Facies changes are commonly an indication of growth faults and underlying structural breaks. The facies changes described mark growth faults along the traces of the RMT above a deep basement ramp (Varsek et al, 1994) and Boulder Creek faults that are probably related crustal breaks that have been active since the Proterozoic (Lis et al, 1976, Höy 1993).

A recumbent anticline with amplitude of several kilometres is mapped along the extent of the NHR (Leech, 1958). Strata on the upper limb dip gently, generally east but SW in the Saugum Canyon area. Strata on the steep limb dip steeply east to overturned west. Small scale folds have an east vergence and plunge gently north or south. In general cleavage throughout the range dips moderately to gently west. The only exception to the generality of these trends is close to the Boulder Creek Fault where structures appear to have been rotated and steepened in a sense indicating the north plate moved up and east against a lateral ramp during thrusting. (A similar pattern exists along the Kimberley Fault in the Purcells, Figure 1). Although this major fold is characteristic of structures formed during Jurassic-Early Cretaceous compression that formed the Purcell and western Rocky Mountains however the extent of the overturn and associated moderate west dip of cleavage is anomalous.

Höy first mapped LANFs in the NHR (1973). Based on subsequent mapping, diamond drilling and reinterpretation, known LANFs in the NHR are as shown in Figure 1. South of Lewis Creek a number of these localities consist of several parallel faults spaced over at least 500 metres with a net cumulative offset of 3 to 6 kilometres. These LANF localities south of Lewis Creek appear to be aligned and project into one another, and together they comprise the Lakit Fault. Key localities are:

1. On Estella Ridge are several parallel LANFs spaced over 500 metres interpreted from mapping and a 700 metre deep diamond drill hole that have a cumulative offset of at least 2 kilometres (Figure 3, Photo 3) (Ransom (1991).
2. Eight kilometres southeast of Estella Ridge, a LANF with an estimated offset of 3 kilometres was mapped (Thompson, 2010).
3. Along the road on the northwest side of Wild Horse Creek, two kilometres south of, and 400 m in elevation below location 2 is a fenster of NHRA strata below Upper Aldridge and younger rocks that indicate a lower LANF with substantial offset (Figures 1 and 2).
4. Drilling on the Sully property five kilometres southwest of the fenster and 14 kilometres south of Estella Ridge intersected six LANFs that repeat an overturned unique 20 metre thick lithostratigraphic sub-unit within HRFA unit A1a. The faults were intersected below 700 metres in the 1250 deep diamond drill hole SU14-07 (dip -70°E that flattened to -56°E). Cumulative offset on these 6 faults is about 400 metres. It is suspected the sole fault of the Lakit Fault set is below the drill hole and that these NHRA strata on the west side of the NHR are displaced from a location in the fenster 3 kilometres to the east.

The Lakit Fault system must have a total cumulative offset of at least 6 kilometres as indicated by the combined offsets of the fenster and mapped fault above and 2 km north. These widespread localities of the Lakit LANF define a plane that dips about 13°-252° (Dip-Dip Direction is the convention for planar geometry used in this report, unless otherwise stated).

Lakit Fault as interpreted here must project across Lewis Creek valley. A fault in that position but with a 25°NW dip runs from the RMT along Lewis Creek and over the range into structures mapped as the Nicol Creek Fault that is here reinterpreted as a LANF. That Lewis Creek forms the deepest valley across the NHR is an indication that a structure hidden in the valley may explain the differences in orientation of the Lakit and Lewis - Nicol Creek LANFs.

Photo 3. LANF on Estella Ridge. UTM 11 600554 5517580, elevation 1575. Three metre portion of LANF exposed in road cut. Fault material is incohesive gouge of rock flour and chips with about 10% rock fragments to 5 cm. Planar alignment of the gouge is 20°-258°.

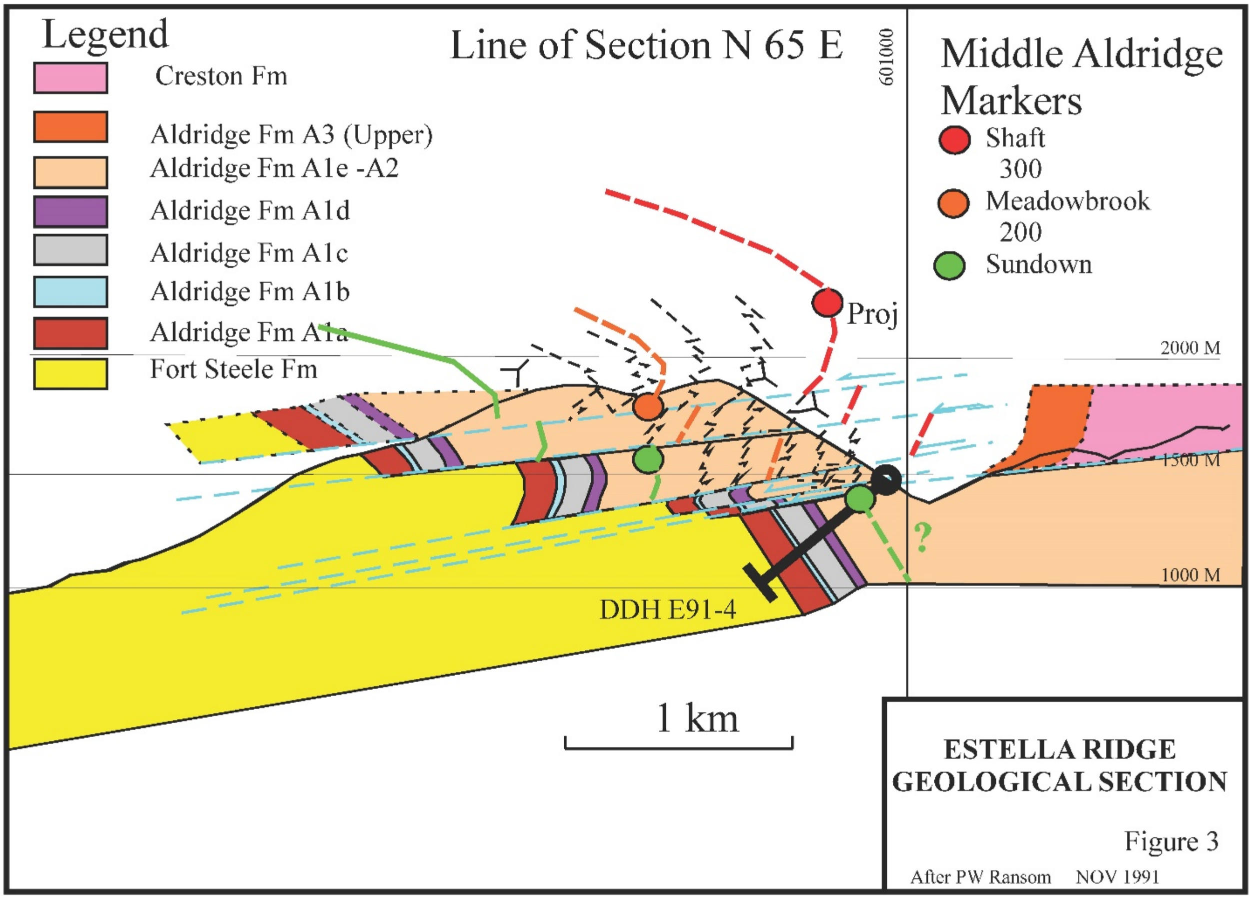

Figure 3. Low angle normal faults (Lakit Fault set) indicated by mapping and drilling at the north end of Estella ridge indicate a cumulative offset of at least 2 km.

Basic mechanical concepts imply the force of friction on planes less than 45° exceeds material strength (Coulomb , 1776). Movement on shallow dip normal faults is possible if friction is reduced by the presence of fluids and if sufficient force, such as an extreme topographic differential, acts on the hanging wall. Tectonic considerations suggest neither of these conditions existed and another mechanism is required to explain the origin of these major structures.

A cross section from Sullivan Mine in the Purcell Mountains to the NHR shows steep west dipping "Sullivan type faults" west of the RMT, the Trench and RMT Fault, Lakit LANF, and the East Wild Horse and Mt Haley stocks straddling the Lussier Fault (Figure 2). It is apparent from this drawing that the LANF may have originally been a steep structure, probably a precedent of the RMT Fault that after translation several kilometres to the east during thrusting was tilted down on the east above a listric normal fault during Eocene extension. Listric normal faulting along the RMT km (Bally et al., 1966) is shown to have taken place in the study area (Cook et al, 1995; van der Velden et al., 1996). Subsequent adjustments during block faulting could explain differences in trends of LANFs north and south of Lewis Creek valley.

The up to 3 kilometres of alluvium in the present RMT is a first order estimate of the amount of recent displacement on the RMT Fault. The minimum 6 kilometres of cumulative offset on the LANFs at the fenster and above, is an estimate of pre-thrust and pre-tilt offset above the same crustal break (that even earlier had influenced sediment deposition between the Purcells and Rockies). The 9 kilometres combined total of these estimates is in keeping with offset on the RMT Fault shown in sections of deep seismic interpretations (Cook et al, 1995) and as interpreted at the latitude near the study area by van der Velden (1996).

Aeromagnetic Contours

Aeromagnetic contours from GSC surveys carried out in the 1960s and 1970s (Figure 4) outline the larger plutons in the study area. Contours associated with plutons spaced along the Lussier Fault suggest there is a single source north-trending dike-like feature at depth that is about 20 kilometres long. These contours have an asymmetry that indicates the source has a westerly inclination (Larson et al., 2006). It is suggested that this asymmetry is extreme and that the body has a gentle west dip. Contours associated with the large Reade Lake pluton west of the RMT are only slightly asymmetric suggesting it has only a slight down on the east tilt. The studied dikes and small plugs at Estella are not reflected in these surveys however they show up in lower altitude helicopter surveys.

Geochronology

Significant ages pertinent to this paleomagnetic study are summarized in Table 1. See sources for details. Note that the U/Pb age of the Reade Lake stock is 28 Ma younger than that based on the K/Ar maximum discussed in Höy (1993). K/Ar dating is affected by Ar contamination that can result in an interpreted age significantly older than more robust dating techniques. In his discussion of the Estella stock, Höy states that the 115 Ma age is considered to be a maximum. Höy also suggests the Estella stock is epizonal indicating that it may be a later stage of an intrusive system. Höy examined felsic dikes in the Saugum Canyon area and stated their age was probably Cretaceous(?) or Tertiary (Höy, 2010).

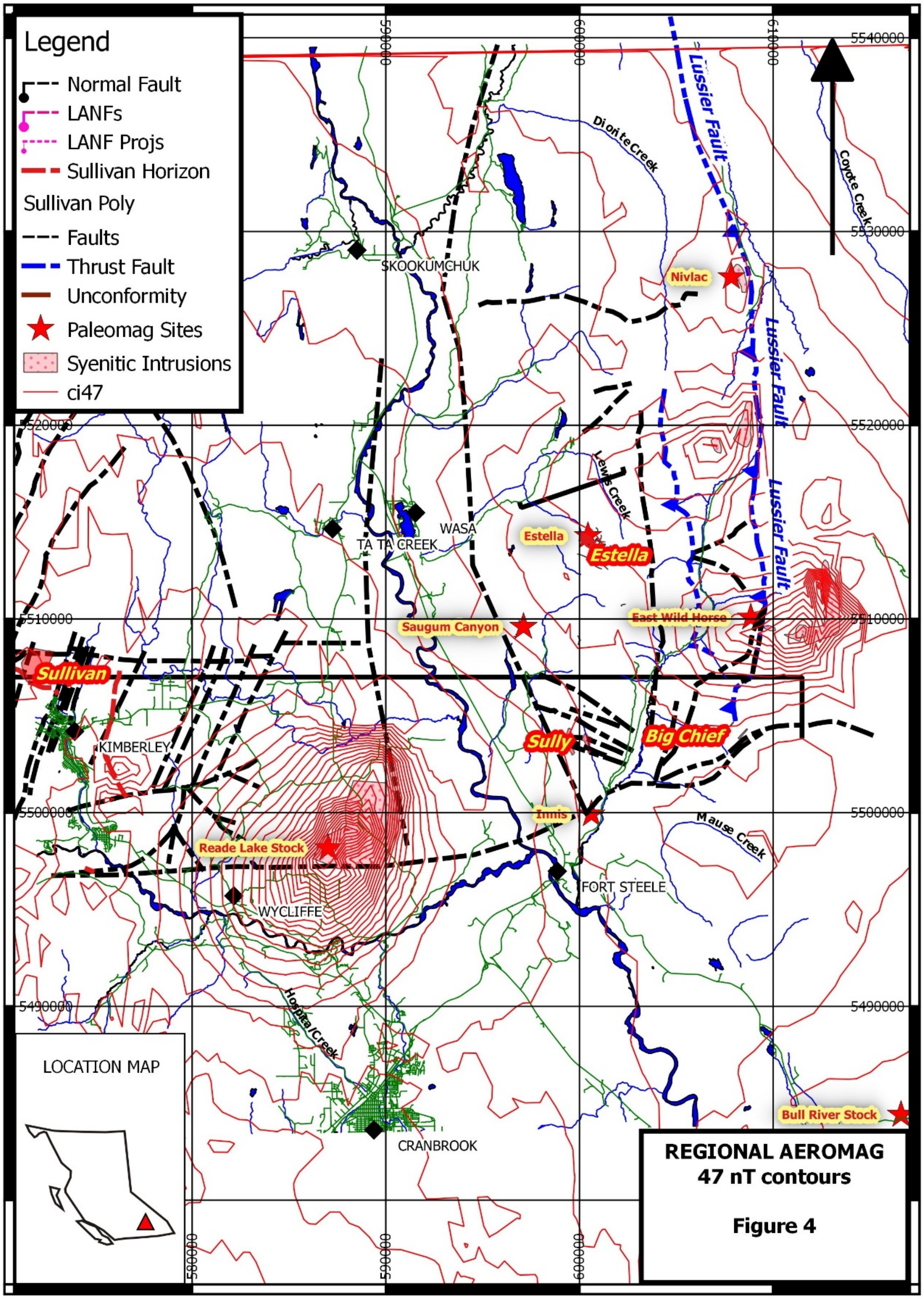

Figure 4. Aeromagnetic contours reveal extreme asymmetry over plutons in the NHR compared to that over the adjacent Reade Lake stock and supports the interpretation of paleomagnetic measurements (Figures 5a and 5b) suggest that an initially vertical north trending pluton in the NHR now dips about 40 degrees west.

Table 1. Summary of geochronology of sampled post-Laramide intrusions in and adjacent to the Hughes Range.

Intrusion	Date	Method	Comment	Source
Reade Lake stock	94 Ma	U/Pb	Mesozonal, lower intercept considered a minimum age	Höy et al (1988)
Reade Lake stock	103-146 Ma 122 Ma maximum	K/Ar	Excess Ar	Höy (1993)
Estella stock	115±4 Ma	K/Ar	Epizonal, biotite, maximum age because of possible excess Ar	Höy (1993)
Mt Haley	108.2±0.7 Ma	Ar/Ar	Muscovite plateau age, muscovite from within intrusion	Larson et al (2006)
Lussier	107.7±0.6 Ma	Ar/Ar	Muscovite, single crystal in skarn of intrusion aureole	Larson et al (2006)

Paleomagnetic Background

Age dates of plutons sampled for this study are all within the extended period of mid Cretaceous stability (126 to 84 Ma) when the North American craton moved little with respect to Earth's axis. Between 124 and 84 Ma the currently accepted values of the paleomagnetic pole for cratonic North America range from 73.1-76.6°N; 193.9-207.4°E (Besse and Courtillot, 2002). The 90±10 Ma pole for North America from Besse and Courtillot is 75.5°N; 207.4°E has α_{95}=5.1°. If the study area (49.7°N; 115.6°W) were attached to the North American craton, the resulting paleomagnetic declination would be 342° and inclination would be 74° (Butler, 1992). The sampling area is part of a wedge that was accreted to the North American plate that rotated 30° clockwise about an Euler pole located near Helena Montana (Price et al. 2000). A substantial amount of that rotation took place subsequent to emplacement of some of the intrusions that are the focus of this study. Irving and Archibald (1990) studied the 94-99 Ma Skelly Creek batholith (49.4°N, 116.6°W) 90 kilometres southwest of the project area and observed a mean direction of D=349°, I=74° (13 sites, k=290, α_{95}=6°). The paleomagnetic pole determined from Skelly is indistinguishable from that based on determinations from the North American craton. The paleomagnetic direction of the Skelly intrusion is the reference direction used for this report with the following limitations: its tilt is constrained to be <5° and vertical axis rotations are unknown.

Paleomagnetic studies of Eocene and mid Cretaceous intrusions in southern British Columbia have shown that some of the intrusions have rotated as much as 39° around a horizontal axis above extensional faults (Marquis et al., 1990, Irving et al., 1990, Wingate et al., 1994). The largest mid Cretaceous intrusions in the vicinity of the northern Hughes Range are located on and stitch the major St Mary-Boulder Creek right lateral reverse fault and Lussier thrust fault. Scattered within and adjacent to the range are a few dikes up to 15 metres wide and one area about 500 m across (Estella) with several plugs and dikes that were initially believed to be time equivalent to the larger intrusions. Paleomagnetic orientations of samples from seven intrusion localities, four within and three outside the NHR block, were measured to compare with assumed orientations the bodies acquired when they solidified.

Sampling Program

Sites were selected a short distance from vehicle access. Core samples were obtained using a gasoline powered chainsaw motor equipped with a water-cooled diamond coring bit designed for paleomagnetic work. Eight to twelve 25 mm diameter cores up to about 10 cm long were drilled at each locality investigated. Initially a circle mark was made with the drill then the hole proper started offset from this circle by a fraction of the diameter. The circle mark provides a reference on top of the core so it could later be accurately repositioned in its original orientation for mark up. Orientation parameters of the hole were measured using a device with an adjustable plate hinged to the top of a tube that fits snugly in the completed hole. Hole trend (180 degrees from the plunge direction) was obtained using a Brunton compass on the levelled plate; the co-plunge (hade) was measured from a scale on the side of the device. From a groove on the tube top a mark was made at the top of the hole. With the orienting device removed and the core oriented back in the hole, a mark corresponding to the mark previously made of the top of the hole was made on the top of the core. An aluminum angle bar was used to draw a line extending this mark along the top of the core with markings indicating direction toward the start of the hole. The sample was marked with a hole name, the trend and co-plunge. When conditions allowed the sun shadow azimuth was measured and compared with solar azimuth provided by the Mr. Sun app. (Solar azimuth was generally within 2 degrees of the value provided by Mr. Sun indicating there were no significant local deviations.) Sample site UTM locations, hole names, orientations and solar direction measurements are in Appendix 1.

Measurements and Plotting

Sample cores were cut into 2.2 cm long specimens and measured on an Agico JR5A spinner magnetometer, and/or Molspin fluxgate spinner magnetometer at Okanagan College in Kelowna. Results from the two instruments were comparable to the low 10-2 A/m range. At lower intensities the Molspin gave unreliable results and only the JR5A results are included. Specimens were progressively demagnetized in three orientations in a Sapphire Instruments SI-4 static alternating field demagnetizer. The order of the specimen orientations was systematically changed during progressive demagnetization in order to detect spurious anhysteretic remanent magnetism (ARM). No ARM was detected. Results were plotted and statistical analysis performed with PuffinPlot (Lurcock and Wilson, 2012). The Characteristic Remanent Magnetism was identified by Principal Components Analysis (PCA) on selected demagnetization stages (Kirschvink, 1980). The selection procedure described by Kirvschvink finds the most points within the demagnetization steps of a specimen that fall closest a straight line anchored to the origin.

All final measurements are in Appendix 2 and representative results are shown on standard summary paleomagnetic graphs produced using Puffin Plot in Appendix 3.

Each of the diagrams in Appendix 3 includes information on the declination and inclination of the Principal Components Analysis (PCA) derived Characteristic Remanent Magnetism of the specimen. The Fisher statistics (Fisher, 1953) refer to the mean declination and inclination for the entire suite of specimens from a locality based on the individually determined PCAs. "α95" is the radius of the cone of

95% confidence around the mean (smaller is better), and κ is the Fisher precision parameter (larger is better). Although not utilized for this study, the diagrams also show values for (Maximum Angular Deviation (MAD) a measure of angular uncertainty (smaller is better), MAD1 and MAD3 indicate how nearly the points lie within a plane or along a single line respectively.

Sampling sites - Geological descriptions

The East Wild Horse stock, exposed in an area about 300 by 700 m, is believed to be a segment of the extreme west and narrow end of the Mt Haley stock less than 1 kilometres west of the Lussier Fault; the bulk of Mt Haley stock extends as much as 4.5 kilometres east of the Lussier Fault. It intrudes either or both Kitchener and Jubilee carbonates, now tremolitic dolomite, along strike of overturned west strata and the nearby Neoproterozoic unconformity. The samples were collected from an outcrop area about 30m across that consists of medium grained quartz monzonite porphyry that contains 5 to 10% unrecognizable mafic grains. Fine fractures are indicative of some post solidification deformation.

The Nivlac stock is about 1 by 2 kilometres across and is entirely west of the Lussier Fault. It intrudes Paleozoic strata and therefore is east of the Neoproterozoic unconformity. Adjacent strata dip steeply east to, adjacent to the Lussier Fault, overturned. The locality sampled is the highest exposure at the north end of the stock. The samples are from a syenite porphyry containing 30% aligned coarse plagioclase laths to 40 mm long surrounded by intergrown coarse grains of potassic feldspar and about 10% unidentified fine, uniformly distributed, dull black, mostly equant grains.

Reade Lake stock is outside the northern Hughes Range and is immediately west of the RMT. This intrusion was collected for comparison, reference and background purposes. The stock has a prominent and extensive, slightly asymmetric aeromagnetic signature. Outcrops are scattered about an area 3 kilometres across. The samples for paleomagnetic study were obtained from a 100x30 m outcrop at the north end of a 400 m diameter area of abundant outcrop of the west part of the stock. Reade Lake stock is typically mega crystic quartz monzonite porphyry. One kilometre south and SW are outcrops of folded Cambrian strata situated above an erosional unconformity on the south side of the St Mary Fault. Nearest outcrops north of the fault are sparse outcrops of Creston strata in an arc 2 kilometres to the west, north and northeast.

Bull River stock is 25 kilometres south of the NHR and was collected for comparison, reference and background purposes. It is near the base of the south end of Steeples Range. It probably intrudes middle Aldridge Fm strata between the top of the bar code marker interval and upper Aldridge that outcrop about 1 kilometres east. Bull River stock has a narrow weak east trending aeromagnetic signature. The sampling locality consists of several outcrops in an area 50 metres across. In contrast to the other sites investigated, this one has a 20 to 40 mm weathered rind that made drilling extremely difficult. The rock is a porphyry consisting of 60% coarse phenocrysts, rarely exceeding 1 cm of zoned and saussuritizsed plagioclase and much lesser featureless pink orthoclase. The remaining 40% is a very fine grained biotitic felsic matrix. Fine fractures are common; however it is uncertain if the fractures are related to weathering or deformation.

The Innis Springs sample is from a 5 m wide near-vertical dike that strikes approximately 080° that intrudes folded Kitchener Fm strata. Bedding dip is moderate to steep north adjacent to the dike. This location is 200 m south of a northeast striking segment of the near vertical, right lateral, reverse Boulder Creek Fault. The dike consists of 10-20% relicts of saussuritized plagioclase that merge into a greenish, fine grained felsic siliceous matrix, 10% orthoclase to 20 mm across, 20% hornblende to 10 mm long (1 to rarely 2 mm wide), rare dark patches appear to be partially assimilated xenoliths.

The Saugum Canyon sample site is 1 kilometre west of the base of the NHR in the RMT, 10 kilometres north of the Boulder Creek Fault. Samples were obtained from a near-vertical dike 0.5 m wide that strikes 068° in a large area of moderately SW dipping Fort Steele Fm. The dike is a felsic rock with faint granular texture suggesting that it might be a well silicified, coarse or medium grained slightly porphyritic monzonite.

The Estella stock is actually a 500 metre diameter cluster of small plugs and dikes that outcrop near the Estella mine. Strata nearby are upper NHRA and upper bar-code marker portion of the middle Aldridge above. This area is on the lower limb of the regional recumbent anticline. The samples were collected from a plug that is about 150 by 75 metres across. The sampling site is on the west side of a creek close to the mine portal. It appears to be quartz monzonite porphyry consisting of 30% plagioclase to 30 mm long and 10% orthoclase to 10 mm across, 20% patchy quartz and a fine grained biotitic siliceous matrix.

Results

Magnetic remanances of Intrusions in the Northern Hughes Range are summarized in Table 2. These results are shown graphically on a stereo net (Figure 5a and 5e). All raw data are presented in Appendix 2, Hughes Range Reconnaissance Paleomagnetic Data. Standard paleomagnetic plots of all the data prepared using Puffin Plot software are presented in Appendix 3, Hughes Range Reconnaissance Paleomagnetic Data Plots. Fisher Statistics of all samples analyzed at a site are shown on each Puffin Plot from that site.

Table 2. Magnetic remanances of Intrusions in the Northern Hughes Range.

SUITE (number of samples measured)	Declination [°]	Inclination [°]	α_{95} [°]	k
Reade Lake Stock (9)	343.8	71.5	9.1	33.1
Bull River (8)	10.2	66.9	6.2	81.2
Nivlac (10)	251.6	39.5	8.7	31.5
East Wild Horse (6)	289.8	43.8	8.7	60.7
Estella (9)	335.6	72.7	10.7	24.3
Saugum Canyon (6)	334.9	83.4	23.8	8.9
Innis Springs (6)	337.0	66.6	15.3	20.0

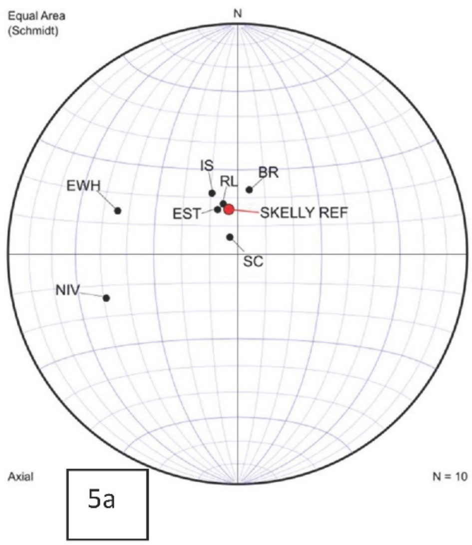

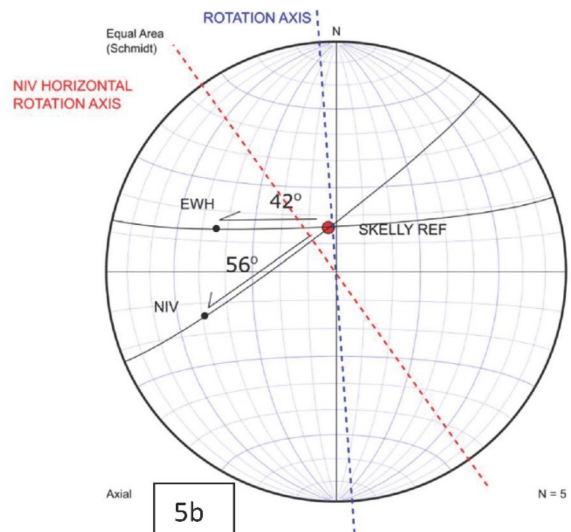

Figure 5. Stereo net plots of paleomagnetic inclinations obtained in this study. (NHR – Northern Hughes Range. Sampled intrusions: EWH – East Wild Horse, NIV – Nivlac, EST – Estella, SC – Saugum Canyon, IS – Innis Springs, BR – Bull River, RL – Reade Lake).

(a) EWH, NIV, EST, SC are within the NHR, IS is in the NHR but south of the Boulder Fault, BR and RL are outside of the NHR. Red is the Cretaceous reference Skelley intrusion located 100 km west of the study area. The Skelly reference is indistinguishable from the North American mid Cretaceous average. Inclinations of the two large plutons within the NHR diverge substantially from the reference, a small dike and plug do not.

(b) Stereo net plot of angular divergence of the East Wild Horse and Nivlac sites that assumes block rotation around a horizontal axis is obtained by measuring the arc of a small circle through the poles for the site and reference.

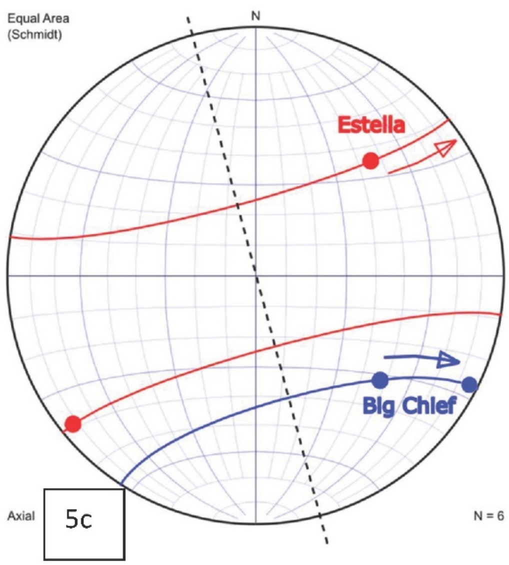

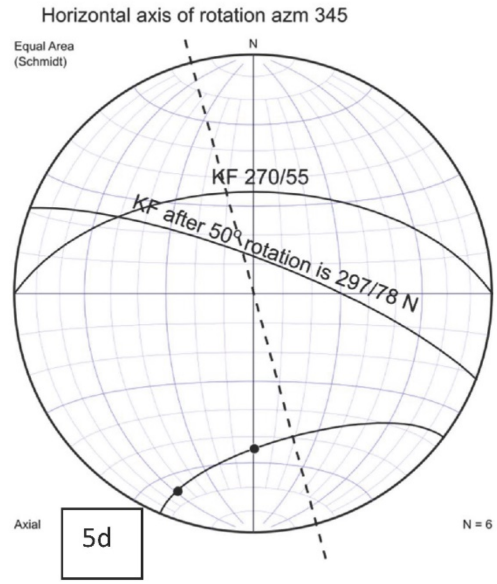

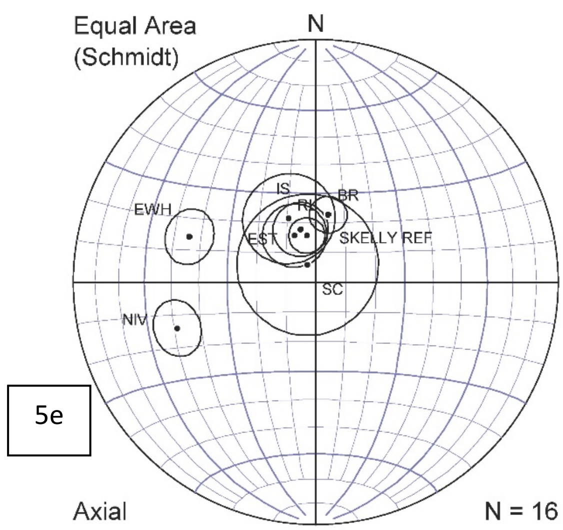

Figure 5. Stereo net plots of paleomagnetic inclinations obtained in this study. (NHR – Northern Hughes Range. Sampled intrusions: EWH – East Wild Horse, NIV – Nivlac, EST – Estella, SC – Saugum Canyon, IS – Innis Springs, BR – Bull River, RL – Reade Lake). **(c)** Stereo net plot that shows the calculation of rotating the 55 SW dipping Estella sulphide vein and the 55 NW dipping Big Chief (gold prospect) dikes by 50 degrees around a horizontal axis trending 345 to restore them to the pre-tilt orientation they would have had. Both features restore to near the perimeter of the net indicating they would have been near vertical.

(d) The Kimberley Fault (KF) dips N 55 degrees off-setting one of the world's largest lead, zinc, iron sulphide deposits down 2.5 km and about 3 km NW. At the eastern limit of the fault, apparent stratigraphic separation is about 6 km. In contrast to the left lateral offset, strain indicated by folding in the hanging wall is dextral. Unlike other major faults such as the Moyie and St Mary, the KF does not appear to have a counterpart in the Rockies. If the conclusions of this study are correct the KF would have been included in the rotated block. The net shows that rotation of the KF by the amount indicated by this study it would dip 78 and strike 291. With this rotation continuation of the KF can be assumed to be entirely within the RMT.

(e) Stereo net plots of paleomagnetic inclinations obtained in this study (as in 5a) with α95 small circles representing cones of 95% confidence.

Interpretation

The most interesting results are from the East Wild Horse and Nivlac stocks. They are the most easterly sites studied and are the only large intrusions sampled within the NHR. These stocks are 17.5 kilometres apart and they are immediately west of the Lussier Fault. Stereo net small circles with horizontal axes through the remanence direction pole of each intrusion and the Skelly reference provide a first order estimate of tilts (Figure 5b). For East Wild Horse the amount of tilt is 42° down on the east around a horizontal axis that trends 357°; for Nivlac it is 56° down on the northeast around a horizontal axis that trends 323°. At the 10 to 15 degree 95% confidence level these remanences appear to be robust. The amounts of rotation are similar. The trends of the axes of rotation are aligned with the local tectono-stratigraphic trend. These are the largest horizontal axis rotations of intrusions determined by paleomagnetic measurement in British Columbia to date. These results support the hypothesis this project was designed to test.

The Reade Lake and Bull River intrusions were sampled for comparison, background and reference purposes and have remanances that overlap the mid Cretaceous value at the 95% confidence level. At Reade Lake the tilt sense and amount is about 6° down on the east, consistent with slight asymmetry of the associated aeromagnetic signature. Remanance of the Bull River intrusion indicates it has a west side down tilt of 6° that suggests the block containing may have tilted slightly above a fault antithetic to the RMT Fault. This observation may be important because it supports other evidence of little or no tilt south of the St Mary-Boulder Creek Fault such as presence of numerous steep normal faults (McMechan, 1979) and an absence of LANFs.

Remanence direction at the Innis Springs site overlaps the mid Cretaceous value at the 95% confidence level, suggesting little or no tilt took place since intrusion. The Innis Springs site was selected because it is south of the east trending St. Mary-Boulder Creek right lateral reverse fault and therefore south of the inferred rotated block. Some of the Innis Springs samples have a reversed magnetic overprint (possibly a lightning induced IRM) otherwise the Fisher statistics show no significant departure from the mid Cretaceous geomagnetic field direction. The results support this inference, but not totally because age of the dike is unknown.

Remanence direction obtained at the Saugum Canyon site overlaps the mid Cretaceous value at the 95% confidence level, suggesting little or no post-intrusion tilt took place. Saugum Canyon samples 1 and 3 are erratic, however other samples closer to the road where sampling was done are not erratic suggesting that road building equipment or heavy vehicles are unlikely to be responsible.

Remanance direction at the Estella site overlaps the mid Cretaceous value at the 95% confidence level and indicates that the small intrusion sampled did not rotate significantly.

Discussion

Figure 6 shows the minimum and maximum west limits of the rotated Hughes Range block indicated by this study. The tilted block probably continues north to a splay of the Hall Lake right lateral reverse fault east of the RMT, a few kilometres north of the map, or it may continue 20 kilometres to structures that follow Kootenay River.

The two localities on the western side of the NHR with remanances that that do not support the tilting may actually postdate it. As mentioned in the section on geochronology, the U/Pb age of the Reade Lake stock is 28 Ma less than that determined by K/Ar. It can be argued that Estella stock may be as much as 28 Ma younger than its K/Ar 115 Ma maximum age and if so it could postdate tilting. Remanence direction of the vertical Saugum Canyon dike indicates it has not been rotated. Similar dikes nearby with different strikes are also vertical, another indication that the Saugum dikes have not been tilted. The assumption that the dike has the same age as the large intrusions to the east may be incorrect. Therefore the Saugum dike either postdates tilting, or if older it provides the minimum west limit to the rotated block shown in Figure 6.

Unlike the near vertical Moyie and St Mary faults, the 55°N dipping Kimberley Fault does not have a counterpart in the Rockies. The possibility that it continues east of the Trench in faults along Lewis Creek has been considered however once faults shown to be LANFs are excluded, only a small fault remains that lacks expected trend, magnitude and strain characteristics. The missing segment of the Kimberley Fault should be within the tilted NHR block. Figure 5d is a stereonet example of a calculation that shows the approximate expected orientation of the KF plane within the rotated block becomes 78°-021° (strike 291°). Also, the axis of rotation of the NHR block is probably closer to the Lussier Fault than to the RMT. Continuation of the Kimberley Fault in the rotated block must be a substantial distance to the north and because there is no corresponding structure with the appropriate orientation in the NHR, the most likely outcome is that the Kimberley Fault continues from some unknown distance to the north from the west side of the RMT into the trench and that it is segmented and down dropped by younger normal faulting within the confines of the RMT. This supports the maximum west extent of the rotated block as shown in Figure 6.

Implications of Block Faulting for Nearby Mineral Occurrences

Big Chief and Estella

The Big Chief is a 200 m wide swarm of ten parallel syenite dikes on Boulder Creek that flows northwest into Wild Horse River. Dikes are 3 to 10 m thick and dip about 55° toward 310° (MacDougall, 1968; probably based on CM&S plane table mapping, McEachern (1945)). Small amounts of gold have been found along the hanging wall of one of the dikes and this locality is one possible source of gold in the Wild Horse placers. This location is at the southeast corner of the tilted Hughes Range block, close to both bounding Lussier and Boulder Creek faults.

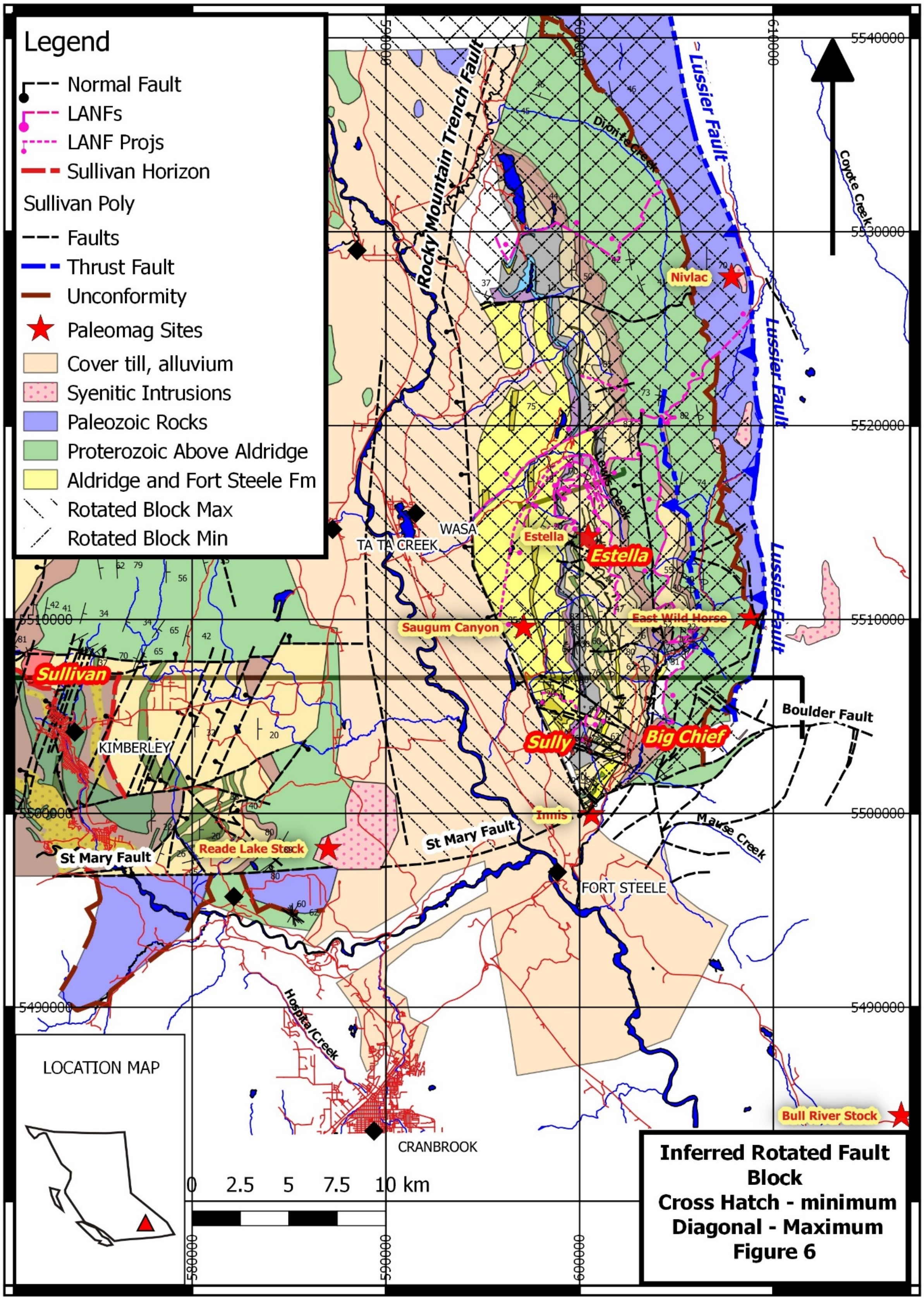

Figure 6. Minimum and maximum possible extents of rotated block indicated by this study.

The Estella is a lead-zinc-iron massive sulphide vein on Estella Ridge that dips between 40° and 70° toward 225. This location is central and toward the west side of the rotated block. Lead isotope age of Estella is comparable to that of Sullivan; therefore it is possible the vein was formed by remobilization from a Proterozoic deposit.

Figure 5 c is a stereo net showing small circles drawn with a horizontal axis of 345° (an average of the Lussier and Nivlac rotation axes) through poles to the Big Chief dike swarm trend and Estella vein. Arrows indicate 45°rotations toward pre tilt orientations near the perimeter of the net, indicating they were near vertical before tilting.

Sullivan and the Kimberley Fault

The giant Sullivan SEDEX Ag-Pb-Zn deposit is offset by the Kimberley Fault that dips 55°N (Figure 1). The Kimberley Fault is a shear zone with right-lateral, reverse strain hanging wall deformation zone 1-2 kilometres wide comparable to that associated with other major faults in the region. Net offset on the Kimberley Fault is, however, left lateral. By 1998 Cominco had identified the Sullivan sub-basin (Ransom, 2000) and general location of the faulted segment of the ore body. In 2004 Stikine Gold Corporation discovered the unique microstratigraphic sequence of massive sulphide and waste beds that comprises the Sullivan deposit in a 2900 m deep hole (Ransom 2004). Subsequently two more massive sulphide intersections were obtained at similar depths spaced over several kilometres (Ransom 2004-2007). The massive sulphide intersections are barren and are too thin to ever be mined. The discovery established net offset on the Kimberley fault to be about 3 kilometres northwest and down 2.5 kilometres. The suggestion that the Kimberley Fault was a penecontemporaneous structure crucial to formation of Sullivan (Turner et al., 2000) can almost be ruled out by the continuity across it of the unique microstratigraphic sub-basin assemblage of massive sulphide and waste beds, mud volcano deposits, reflected beds and slurry accumulations and laminites. This study indicates that the Kimberley Fault was probably a bounding structure during Eocene extension and block faulting and that is when Sullivan was offset from its post-thrusting position.

Bul River Mine

Remanance of the Bull River intrusion indicates a west side down tilt, antithetic to the RMT Fault. This intrusion postdates folding and, like other monzonitic bodies in the region, is likely mid-Cretaceous. The intrusion and Bul (as spelled by the company with the mine) River Mine 3 kilometres east have separate highs within the same narrow east-west aeromagnetic trend. The mine is a narrow stockwork of near-vertical east-west quartz-siderite veins containing pyrite, pyrrhotite and chalcopyrite. The 350° C emplacement temperature of the veins (Morton, 1999) suggests an epizonal setting and possible relationship to the granitic intrusion. Age dating of the vein has not yielded a robust date; K/Ar ages from muscovite-rich selvedges are Cambrian to latest Proterozoic (Morton, 1999). A shallow east dipping thrust in the west part of the mine, and a steep west dipping to near-vertical reverse fault in the east part, appear to define a pop-up, now with a west side down tilt. This pop-up structure, near an apparent offset of the RMT Fault is indicative of formation in a transpressional strike-slip setting (McClay et al, 2001; Langhi et al, 2008).

Sully

Diamond drilling on the Sully prospect in the southwest part of the NHR totaling 7 kilometres in 9 holes 350 to 1550 metres long has detailed the structure of Fort Steele Formation and NHRA strata on the steep and overturned limb of the NHR fold. Of particular interest to this study, as previously mentioned, is intersection between 700 m and the1289 m end of DDH SU14-07 of several repeats of a 20 metre thick lithostratigraphic marker on a series of 5 LANFs (the Lakit Fault set). True dips of strata provided by oriented core assisted with this interpretation. These LANFs are on trend with those on Estella Ridge and in Tackle Creek that together make up the Lakit Fault system. Lack of one for one correspondence of the LANFs in deep drilling to the west is explained by intervening steep west dipping faults that cut off the LANFs. These steep faults likely developed as the block rotated in a manner similar to that documented at Yerrington, Nevada (Proffitt, 1974).

At Sully, parallel coincident gravity and aeromagnetic anomalies believed to be coincident with Sullivan time equivalent unit HRFA unit A1c are under investigation. Unit A1c is substantially thicker than near Estella 10 kilometres to the north and it contains numerous iron sulphide laminations, abundant 1-20 mm thick quartz-dolomite-iron sulphide beds and intervals containing elevated lead-zinc, and in one hole it contains several pebble fragmentals, all indicators of a sub basin with a massive sulphide deposit. Steep dip of strata and of an assumed stratabound massive sulphide body is at odds with the interpreted modest east dip of the cause of the gravity anomaly. LANFs offsetting a steep dipping stratabound massive sulphide body in the manner described for the Lakit Fault set provides the perfect explanation why a gravity potential field that indicates a target with a modest east dip.

Conclusions

1) Paleomagnetic data support the hypothesis of significant east side down tilt of the northern Hughes Range west of the Lussier Fault.
2) LANFs are a major tectonic component of the northern Hughes Range.
3) Steep faults that formed above the same basement structure as the modern RMT faults were carried east above the Lussier Thrust were subsequently tilted during block faulting are now the Lakit LANF set and the, possibly equivalent, Nicol Creek Fault.
4) The Lakit Fault set projects north across Lewis Creek toward the Nicol Creek Fault however because the latter dips northwest, like at least one other LANF further north, the structural history to the north is unresolved.
5) The major recumbent fold of the Hughes Range probably formed as a ramp anticline above the Lussier Thrust.
6) Corrections for tilting indicate the Estella sulphide vein and Big Chief syenitic dikes may have initially been emplaced as vertical features normal to the least principal stress axis.
7) The Kimberley Fault initially a right-lateral, reverse high strain zone with unknown displacement formed during regional compressional mountain building and it was reactivated during block faulting. Net displacement of Sullivan about 3 kilometres northwest and down 2.5 kilometres.

8) The Kimberley Fault disappears east into the RMT and as part NHR block was rotated into a steep north easterly dipping orientation, segmented and down dropped within the trench. No counterpart to the KF has been identified east of the RMT.
9) Effects and extent of Basin and Range tectonics at shallow crustal levels extend substantial distances further east and west of the RMT than previously thought.
10) The Lakit LANFs are a major structural feature at depth in the Sully area and explain apparent east dip of the east Sully geophysical anomaly and why the anomaly cause has not been intersected.

A new interpretation of block faulting with major tilting of the Northern Hughes Range is supported by this paleomagnetic study. Non-conforming data of two small features sampled is rationalized by assuming a younger age of intrusion. This new interpretation indicates the 55° SW dipping Estella massive sulphide vein and the 55 NW dipping Big Chief syenite dike set were near-vertical features before block faulting, in keeping with intrusion into extension joints normal to the local horizontal least principal stress direction. The results of this study provide new insight into most recent movement on Kimberley Fault, important because it offsets one of Earth's largest lead zinc deposits; the study explains why the fault does not have a counterpart east of the RMT. It is apparent from this study that the effects of Eocene relaxation extend well beyond the confines of the Trench. The work of many geologists in this area has created a rich knowledge base and an evolving improved interpretation. Further studies can only refine the fascinating and complex geological puzzle in the Kimberley area.

Recommendations

1) Continue paleomagnetic investigations in the Hughes Range, in particular:
   a) Sample Mt Haley stock east of Lussier Fault to establish that the Lussier Fault is the east limit of tilting.
   b) Sample the Lussier Stock (mapped entirely west Lussier Fault) located midway between Nivlac and Mt Haley.
   c) Sample the Big Chief dike swarm on Boulder Creek to test the inference that the dikes were vertical when intruded
   d) Sample additional sites from Nivlac stock,
   e) Sample other dikes to obtain a broader coverage within the northern Hughes Range.
   f) Expand sampling of plugs and dikes in the Estella Stock area.
2) Obtain age dates on dikes sampled and use improved techniques of radiometric dating on intrusions that this study indicates may post-date block faulting.
3) Conduct geological mapping to constrain fault traces, especially north of Lewis Creek where only one middle Aldridge bar-code type marker has been identified in outcrop.

Acknowledgements

Trygve Höy support the idea for this project and for a field trip to the Saugum Canyon site. Russell Hartlaub recognized the potential of this project and allocated Geoscience BC SEEK Project funding for it. The efforts of Andrea Clifford, Christa Pellet and Janice Fingler of Geoscience BC for their roles in setting up and reviewing the project are most appreciated. Margot McMechan provided valuable comments on an early draft of this report. Margot McMechan is thanked as an invited peer reviewer. Encouragement of Scott Broughton of Santa Fe Metals is greatly appreciated. Many discussions with Brian Jones on magnetic and gravity interpretation were especially helpful. Some unreferenced individuals who provided assistance, shared information or who did field work for private companies in the northern Hughes Range include: G. Delaney, A.S. Hagen, C. Kennedy, M. Kennedy, S. Kennedy, P. Klewchuk, B. Kostiuk, I.D. McCartney, K.R. McClay, D.L. Pighin, C.S. Schultze, M. Seabrook.

References

NOTE AR refers to Assessment Report, British Columbia Ministry of Mines.

Anderson, D.A. (2012). Diamond Drilling Report for the Dewdney Trail Property. (AR 32758).

Anderson, M.H. (1951). The Dynamics of Faulting, Edinburgh, Oliver and Boyd, 206 p.

Besse, J. and Courtillot, V. (2002). Apparent and true polar wander and the geometry of the geomagnetic field over the last 200 Myr, Journal of Geophysical Research, V107, No. B11, 2300.

Butler, R.F. (1992). Paleomagnetic Poles; in *Paleomagnetism*: Magnetic Domains to Geologic Terranes, Blackwell Scientific Publications, Chapter 7, p. 121-136.

Clague, J.J. (1973). Late Cenezoic Geology of the southern Rocky Mountain Trench, British Columbia. PhD Thesis, UBC.

Cook, F.A. and van der Velden, A.J. (1995). Three-dimensional crustal structure of the Purcell Anticlinorium in the Cordillera of southwestern Canada, Geological Society of America Bulletin, v. 107, p. 642-664.

Coulomb, C. A. (1776). *Essai sur une application des regles des maximis et minimis a quelquels problemesde statique relatifs, a la architecture.* Mem. Acad. Roy. Div. Sav., vol. 7, pp. 343–387.

Doughty, P.T. and Price, R.A. (2000). Geology of the Purcell Trench rift valley and Sandpoint Conglomerate: Eocene en echelon faulting and synrift sedimentation along the eastern flank of the Priest River metamorphic complex, northern Idaho, Geological Society of America Bulletin 2000; 112, no. 9; 1356-1374.

Dvorak, Z. and Klein, J. (1990). Geophysical Report on an Airborne EM, Magnetic and VLF –EM Survey on the Estella/Kootenay King Property, Fort Steele M.D., B.C. (AR 20175).

Eardley, A.J. (1951). Structural Geology of North America, New York, Harper and Brothers, 624 p.

Fisher, R.A., 1953. Dispersion on a sphere. Proceedings of the Royal Society of London, Series A, 217: 295 –305

Garland, G.D. and Tanner, J.G. (1957). Investigations of Gravity and Isostasy in the Southern Canadian Cordillera, Publications of the Dominion Observatory, Ottawa, Vol. 19, No. 5, pp 169-222.

Geological Survey of Canada (1988). Map 19522G, Geophysical Series (Aeromagnetic), Fernie Alberta-British Columbia, 1:250,000.

Hagen, A.S. and Ransom, P.W. (1985). The Kimberley Fault – 1985, internal company report, Cominco Ltd.

Höy, T. (1979). Geology of the Estella – Kootenay King area, Hughes Range, Southeastern British Columbia, Preliminary Map 36, Province of British Columbia, Ministry of Energy, Mines and Petroleum Resources.

Höy, T. (1993). Geology of the Purcell Supergroup in the Fernie west-half map area, southeastern British Columbia, Province of British Columbia Geological Survey Branch, Bulletin 84.

Höy, T. (2010). Geology of the Saugum Gold Property, Southern Hughes Range, southeastern British Columbia, (AR 31711).

Höy, T. and van der Heyden, P. (1988). Geochemistry, Geochronology and Tectonic Implications of Two Quartz Monzonite Intrusions, Purcell Mountains, Southeastern Brtitish Columbia, Canadian Journal of Earth Sciences, Volume 25, p 106-115.

Höy, T., Anderson, D., Turner, R.J.W., and Leitch, C.H.B. (2000): Tectonic, magmatic and metallogenic history of the early synrift phase of the Purcell Basin, southeastern British Columbia; Chapter 4 in The Geological Environment of the Sullivan Deposit, British Columbia, (ed.) J.W. Lydon, T. Höy, J.F. Slack and M. Knapp; Geological Association of Canada, Mineral Deposits Division, MDD Special Volume No. 1.

Huebschman, R.P. (1973). Correlation of Fine Carbonaceous Bands across a Precambrian Stagnant Basin. Journal of Sedimentary Petrology, v 43, p 688-699.

Irving, E. and Archibald, D.A. (1990). Bathozonal Tilt Corrections to Paleomagnetic Data from Mid-Cretaceous Plutonic Rocks: Examples from the Omineca Belt, British Columbia. Journal of Geophysical Research, V95, No B4, p. 4579-4585.

Kirschvink, J. L. (1980). The least-squares line and plane and the analysis of palaeomagnetic data. *Geophysical Journal of the Royal Astronomical Society*, 62(3), 699-718.

Larson, K. P., Price, R. A., and Archibald, D. A. (2006). Tectonic Implications of 40Ar/39Ar muscovite dates from Mt. Haley stock and Lussier River stock near Fort Steele, British Columbia. Canadian Journal of Earth Sciences, V43, p.1673-1684.

Leech, G.B. (1958). Fernie Map-Area, West Half, British Columbia. Geological Survey of Canada, Paper 58-10.

Lis, M.G. and Price, R.A. (1976). Large-scale block faulting during deposition of the Windermere Supergroup (Hadrynian) in southeastern British Columbia, Geological Survey of Canada Paper 76-1A. p. 241-279.

Lurcock, P. C. and Wilson, G. S. (2012). PuffinPlot: A versatile, user-friendly program for paleomagnetic analysis. *Geochemistry, Geophysics, Geosystems,* 13, Q06Z45, doi:10.1029/2012GC004098.

McDougall, R.J. (1968). Report of Progress on the Boulder Creek Mineral Claim in Second Prospectus for Boulder Creek Mines Ltd.

McEachern, R.G. (1945). Report on Examination of Free Trader Group, Boulder Creek, private report for Consolidated Mining and Smelting Company Ltd.

Marquis, G. and Irving, E. (1990). Observing Tilts in Midcrustal Rocks by Paleomagnetism: Examples from Southeast British Columbia. Tectonics, V 9, No 5, p. 925-934.

McClay, K.R. and Bonora, M. (2001). Analog models of restraining stepovers in strike-slip fault systems, AAPG Bulletin, v. 85, no. 2 (February 2001), pp. 233–260.

McMechan, M.E. (1979). Geology of the Mount Fisher – Sand Creek area. British Columbia Ministry of Energy, Mines and Petroleum Resources, Preliminary Map 34.

Price, R.A. 1965. Flathead Map-Area, British Columbia and Alberta, Geological Survey of Canada, Memoir 336.

Price, R. A. 1981. The Cordilleran foreland thrust and fold belt of the southern Canadian Rocky Mountains, Thrust and Nappe Tectonics, The Geological Society of London, 427-448.

Price, R.A. and Sears, J.W. (2000). A preliminary palinspastic map of the Mesoproterozoic Belt-Purcell Supergroup, Canada and USA: Implications for the tectonic setting and structural evolution of the Purcell anticlinorium and the Sullivan deposit; Chapter 5 in The Geological Environment the Sullivan Deposit, British Columbia, (ed) J.W. Lydon, T. Höy, J.F. Slacl and M.E. Knapp; Geological Association of Canada, Mineral Deposits Division, Special Publication No. 1, p. 61-81.

Price, R.A. (2013). Geology, Fernie British Columbia-Alberta; Geological Survey of Canada, Map 2200A, scale 1:125 000, doi:10.4095/292659

Proffitt, J.M. 1977. Cenozoic geology of the Yerington district, Nevada, and implications for the nature and origin of Basin and Range faulting, Geological Society of America Bulletin, v.88, p.247-266.

Ransom, P.W. (1991). 1991 Exploration Report, Estella Property, Fort Steele Mining Division, B.C. (AR 21935).

Ransom, P.W. (1992). 1991 Estella Year End Report, Cominco Ltd.

Ransom, P.W. and Lydon, J.W. (2000). Geology, Sedimentology, and Evolution of the Sullivan Sub-Basin; Chapter 23 in The Geological Environment of the Sullivan Deposit, British Columbia, (ed.) J.W. Lydon, T. Höy, J.F. Slack and M. Knapp; Geological Association of Canada, Mineral Deposits Division, MDD Special Volume No. 1.

Ransom, P.W. (2004-2007). Drill logs and interpretation drawings of the Sullivan Deeps project prepared for Stikine Gold Corporation, private records.

Thompson, R.I. (2010). Geology of the Rocky Mountains Claim Block with Recommendations for Further Exploration, Fort Steele Mining Division British Columbia. (AR 31437).

Thompson, T.L. (1962). Origin of the Rocky Mountain Trench in Southeastern British Columbia by Cenozoic Block Faulting, Journal of the Alberta Society of Petromeum Geologists, v.10-7, p 408-427.

Turner, R.J.W, Leitch, C.H.B., Höy, T., Ransom, P.W., Hagen, A.S., and Delaney, G.D. (2000). Sullivan Graben System: District-scale setting of the Sullivan Deposit. Chapter 21 in The Geological Environment of the Sullivan Deposit, British Columbia, (ed.) J.W. Lydon, T. Höy, J.F. Slack and M. Knapp; Geological Association of Canada, Mineral Deposits Division, MDD Special Volume No. 1.

van der Velden, A.j., and Cook, F.A. (1996). Structure and tectonic development of the southern Rocky Mountain Trench, Tectonics, V . 15, No. 3, p. 517-544.

Wernicke, B. (1981). Low-angle normal faults in the Basin and Range Province: nappe tectonics in an extending orogeny, Nature, Lond. 291, 645-648.

Wingate, M.T.D., and Irving, E. (1994). Extension in high-grade terranes of the southern Omineca Belt, British Columbia: Evidence from paleomagnetism. Tectonics, V. 13, No. 2, p. 686-711.

Appendices

Appendix 1

Location information

Notes on magnetic directions and corresponding solar azimuth readings

Magnetic susceptibility observations

Miscellaneous notes

Appendix 1

PWR Sampling for Paleomag Log

Year 2013

GPS locations are in UTM Zone 11

Sample orientations are out of hole standard, in other words the orientation recorded is the dip and dip-direction of the plane normal to the hole.

When possible, on sunny days, azimuth to the sun was recorded, time of recording noted and the result was compared to azimuth from the Mr Sun iPhone app, either at the same time if the app was "live" (the app was able to detect location) or later calculated for the time and location in which case the sites first Mr Sun value is preceded with letter P. The only location where no sun readings were taken at all was East Wild Horse.

Samples were located where magnetic susceptibility readings were elevated compared to the immediately surrounding area. In most situations it was necessary to be quite selective in doing this as most readings were less than 1 e-3. The desirable level of around 10 e-3 and higher was not commonly obtained. In many situations a high value could not be repeated and such spots were generally avoided. After drilling some sites ms was taken again. Results are in the ms column, additional readings or ranges of values appear in the comments.

Reade Lake Stock

The area sampled is at the north end of a series of outcrops over an area 300 by 500 m.

Sample	Date	Mag Sus	Orientation	Sun Az	time(MDT)	Mr Sun	Comments
RL 1	Jun-29	7.5	32-275	261	5:45	261	WPT190 Set declination with this reading, 15 degrees, same as declination app for same time.
RL 2	Jul-11	7	30-275				ms of core 5. 20m south of RL1.
RL 3	Jul-11	10	53-277				ms of core 5.6.
RL 4	Jul-11	16	33-132.5				ms of core 5.3
RL 5	Jul-11	7	63-110				ms of core 5.5. Five m south of RL3 and RL4.
RL 6	Jul-11	13	62-224				ms of core 7
RL 7	Jul-11	9	57-264				ms of spec 7
RL 8	Jul-11	10	67.5-266	125	11.04	127.1	8,7 around hole. Ms of spec is 4.35. WPT 243 for holes 5-8.
RL 9	Aug-31	2	29.5-353	146	12.11	146.7	WPT 244 for holes 9-11, about 15m south of WPT 243.
RL 10	Aug-31	7	35-286	155	12.36	155.2	
RL 11	Aug-31	11	41.5-139	166	1.01	164.2	

Innis Springs Dike

Porphyritic syenite dike

Sample	Date	Mag Sus	Orientation	Sun Az	time(MDT)	Mr Sun	Comments
IS 1	Jul-18	21	57-254	123	?	125.6	
IS 2	Jul-18	25	32-137	121	11:24	122	
IS 3	Jul-18	22	87.5-251	126	?	128.6	
IS 4	Jul-18	24	40-203	129.5	?	131.5	
IS 5	Jul-18	19	45-227	136	12:05	135.1	WPT225 this wpt for IS1-5.

IS 6 Jul-18 20 36-198 174.5 1:36 174 WPT226 ~ 25m East, for IS 6-8
IS 7 Jul-18 24 67-255 179.5 1:46 178.9
IS 8 Jul-18 18 66-248 184 2:00 185.7

Saugum Canyon
Felsic dike crosses road
Strike 068, vertical. Swarm of sub-parallel felsic filled fractures on west side of road dip 81 toward 340.
Cross fractures with felsic fill dip 48 toward 048.
Cross bedded quartzites of Fort Steele Fm.
WPT 227 is point on east side of road on line with dike.
Rock hard to drill, even new bit polished fairly rapidly.

Sample Date Mag Sus Orientation Sun Az time(MDT) Mr Sun Comments
SC 1 Jul-22 2 64-336 204.5 2:44 205.6 3 m east of road. Broke core while drilling, connected back for orientation just fine.
SC 2 Jul-22 5 65-352 211 3:00 212.3 Piece stayed attached.
SC 3 Jul-22 2 to 5 21-140.5 214 3:11 216.4 top 3 cm broke off, fits fine.
SC 4 Jul-22 3 to 37 51.5-335 core stayed attached.
SC 5 Jul-22 0.2 to 5 12-258 226 3:46 228 core broke off bottom, fit back fine.
SC 6 Jul-22 3 to 14 39-327 232 3:59 233.1 2 cm piece broke off top, fit on stub fine.
SC 7 Jul-22 0.5 to 2.5 12-244 236 4:10 236.4 0.5 by 1.5 m patch on west side of road on line assume outcrop. More weathered than 1 to 6, Two 5 and 3 cm pieces.
SC 8 Jul-22 1.5 to 3 20-203.5 241.5 4:33 242.9 OC 2.5 x 3 m on line with dike. (This is an area with 10 metre blocks strewn about by glaciation!) Two pieces 2 and 5 cm of core. Poor fit back in hole, registration circles used to orient.

Nivlac
(Note, samples marked as LN (Lussier North). It is the northernmost intrusion sampled, however this is at the south end of Lussier River, this northern intrusion area was named Nivlac to differentiate it from the Lussier intrusion 5-10 km to the south. Mr Sun app not functioning live.

Sample Date Mag Sus Orientation Sun Az time(MDT) Mr Sun Comments
L 1 Aug-20 11 15.5-189 WPT 240 obvious outcrop in floor of log landing.
L 2 Aug-20 6 25-066.5 225 3:52 P 225
L 3 Aug-20 5 17-223.5 226 3:58 227 Top mark mostly broken off, but fit seems reasonable, possible source of error.
L 4 Aug-20 NR 66-225 230 4:10 231 hole all by itself
L 5 Aug-20 4 45-326 233 4:22 234 Cluster (of samples?) on road at upper exit from landing near contact with marble. (This is close to WPT 241.)
L 6 Aug-20 5 48-316 236.5 4:30 236
L 7 Aug-20 3 28.5-310.5 238 4:39 239
L 8 Aug-20 5 56-298 241 4:51 242 3 pieces
L 9 Aug-20 8 60-265.5 244.5 5:06 245
L 10 Aug-20 4 52-303 246 5:17 248 WPT 241 westernmost holes, 2 m above contact with marble. 2.5 m above level of road.
L 11 Aug-20 4 52-303.5 248 5:26 250 same level, 3 m east of L10

Estella

Sample	Date	Mag Sus	Orientation	Sun Az	time(MDT)	Mr Sun	Comments
Est 1	Aug-27	5	62-038	197	2:41	P 201	WPT 242 Sun info obtained

across creek, about 5 m northeast of 1-3.

Sample	Date	Mag Sus	Orientation	Sun Az	time(MDT)	Mr Sun	Comments
Est 2	Aug-27	6	61-015	218	3:30	218	
Est 3	Aug-27	2.5	50-110	224.5	3:54	226	
Est 4	Aug-27	6	48-034	238	4:35	237	
Est 5	Aug-27	2	91-210				
Est 6	Aug-27	3	35-359	256	6:07	257	
Est 7	Aug-27	4	48-336.5				
Est 8	Aug-27	4	58-343.5				
Est 9	Aug-27	4	60-335				

E9 15 cm from E8, mostly below. E6-E9 in 1 m area about 15 m upstream and 5 m elev above E1-E5.
Brass water fitting broke at drill. Considerable corrosion of the aluminium of the drill housing.

Bull River

Occurrence north of gravel road about 1 km east of junction from Fort Steele - Wardner paved highway.
WPT 250 on SE corner of outcrop area nearest road. Samples from here to 20 m W and NW.
Site was difficult to drill. Crumbling (weathered) collars and abrasive rock, slow drilling, repeated sharpening of bits required. Finished all 3 bits the kit came with. Ordered 3 more.

Sample	Date	Mag Sus	Orientation	Sun Az	time(MDT)	Mr Sun	Comments
BR 1	Sep-05	4	35-141	221	3:44	221.8	Mag sus near 0.6, 0.2, 0.3, 0.6.
BR 2	Sep-05	4	48-202.5	225.5	4:01	226.6	mag sus around 1, 7, 0.4, 2.
BR 3	Sep-09	3.4	46-284	137	11:19	134.9	Mag sus 0.9 to 2 around hole.

Core jammed in bit, had to extrac t at home Sept 5, surveyed BR 3 Sept 9.

Sample	Date	Mag Sus	Orientation	Sun Az	time(MDT)	Mr Sun	Comments
BR 4	Sep-09	4.6	37.5-188	178	1:39	180.3	Mag Sus around about 1.

BR 4 sample not ideal, hovever the Bull River sampling has finished off two bits already. Having to drill 2 to 4 holes before an acceptable sample is obtained.

Sample	Date	Mag Sus	Orientation	Sun Az	time(MDT)	Mr Sun	Comments
BR 5	Sep-09	5	67.5-222	191	2:14	192.4	Mag sus likely low, not rec.
BR 6	Sep-09	10	48-268	199	2:38	200.6	mag sus ± 0.5.
BR 7	Sep-09	11	65-209	209	3:08	210.4	Mag sus likely low, not rec.
BR 8	Sep-09	8	65-231	224.5	4:01	226.1	Mag sus 0.5 all around.
BR 9	Sep-09	6, 3	72-174	228	4:12	229	Mag sus <0.5 all around.
BR 10	Sep-09	5	50-213.5	240	5:03	241.6	Mag sus around 1.5, 0.5, 0.5, 1.

BR 10 - Burned last bit here after two failed starts.

East Wild Horse

Outlier to Mt Haley stock. It is the furthest west part of Mt Haley sampled. It is north of the Boulder (St Mary Fault extension) Fault. (The Big Chief on Boulder Creek, 10 km further west was visited. The main body had very low mag sys and would have been diffiult to get equipment to. Some rubble near by had very high mag sus but it is not known if outcrops; and access is difficult.)

Howie Mason provided guiding, Rino transport to this locality and assistance, 5 km from truck access on Wild Horse Creek.

Cool and raining. No Sun readings.

WPT 280

Sample	Date	Mag Sus	Orientation	Sun Az	time(MDT)	Mr Sun	Comments
EWH 1	Sep-22	10	50-105				
EWH 2	Sep-22	8	50-101				
EWH 3	Sep-22	12	47-113				
EWH 4	Sep-22	3	57-98.5				Mag sus of 7 once!
EWH 5	Sep-22	5	31-103				
EWH 6	Sep-22		68-095				
EWH 7	Sep-22	7	54-099				
EWH 8	Sep-22	7	56-089				Mag sus 0.1-1.4 around.

Sully

215 m west of DDH SU13-06 currently being drilled by Santa Fe Metals.

Dike about 1 to 2 m wide, steep, intrudes along cleavage.

Although appears to be porphyritic, the phenocrysts are corroded or resorbed and not as distinct as in many of the other sites sampled.

This dike was sampled to see if paleo mag measurements were discernable. Samples were not useable.

WPT 276 Overcast and in trees, no sun.

Sample	Date	Mag Sus	Orientation	Sun Az	time(MDT)	Mr Sun	Comments
SU 1	Sep-27	0.12	69.5-180				Main line along core is more accurate than the start tick which was off a line width.
SU 2	Sep-27	0.21	18-196				
SU 3	Sep-27	0.19	30-173				
SU 4	Sep-27	0.11	27-245.5				This is 5 m south of SU1-SU3.

Waypoint information:

190	11 U 586991 5498195	Reade Lake Stock	
243	11 U 587010 5498172	Reade Lake Stock	
244	11 U 587008 5498162	Reade Lake Stock	
225	11 U 600567 5499930	Innis Springs Dike	
226	11 U 600591 5499933	Innis Springs Dike	
227	11 U 600591 5499933	Saugum Canyon	
240	11 U 607975 5527563	Nivlac	
241	11 U 607941 5527501	Nivlac	
242	11 U 600437 5514278	Estella	
250	11 U 613863 5483220	Bull River	
280	11 U 608792 5510214	East Wild Horse	
276	11 U 599620 5503519	Sully	(Waypoint recorded on reconaissance day).

Appendix 2

Raw Data

Appendix 2 Hughes Range Paleomagnetic Study Raw Data

Abbreviations:

SC	Saugum Canyon
RL	Reade Lake
EWH	East Wild Horse
IS	Innis Springs
L	Nivlac
E	Estella
BR	Bull River

Sample	Demag	Dec	Inc	Int
SC1-1	0	49.6	68.8	51.54
SC1-1	5	28.6	68.3	33.36
SC1-1	10	44.7	59.1	20.63
SC1-1	15	42	59.1	13.71
SC1-1	20	30.3	69.3	11.72
SC1-1	30	54.8	60.6	6.33
SC1-1	40	57.5	58.5	6.33
SC1-1	50	60	61.2	6.23
SC1-1	60	72.5	67.7	6.11
SC1-1	70	72.9	51.5	5.4
SC2-3	0	313.9	82.5	105.04
SC2-3	5	3.2	76.8	55.41
SC2-3	10	343.1	70.4	30.26
SC2-3	15	289.2	70.2	17.85
SC2-3	20	326.4	67.1	13.46
SC3-2	0	187.7	41	1391.18
SC3-2	5	181.2	44.9	396.2
SC3-2	10	183	54.4	79.64
SC3-2	20	225	57.3	19.85
SC4-1	0	243.9	74.2	84.79
SC4-1	5	303.4	72.2	57.88
SC4-1	10	325.6	71.9	33.9
SC4-1	15	338.2	69.1	23.72
SC4-1	20	327.9	58.8	20.84
SC4-1	25	336.5	53.3	16.48
SC6-1	0	324.5	78.1	20.09
SC6-1	5	326.4	83.1	15.35
SC6-1	10	316.7	85.5	12.66
SC6-1	15	237	85	11.34
SC6-1	20	245.5	86.8	10.62
SC6-1	25	258.4	75.2	10.93
SC6-1	30	212.8	74.9	10
SC8-1	0	51.7	86.3	76.57
SC8-1	5	337.4	79.4	41.36
SC8-1	10	318.9	70.3	22.9
SC8-1	15	337.3	74.1	16.58

SC8-1	20	344.6	70.3	10.88
RL1-3	0	194.7	86.8	219.22
RL1-3	5	357	83	121.11
RL1-3	10	355.5	75.5	71.41
RL1-3	20	336.5	76.5	38.01
RL1-3	40	356.7	76.3	17.87
RL1-3	80	340.7	77.7	14.72
RL1-3	160	4.6	40.4	13.24
RL2-1	0	342.2	74	283.6
RL2-1	5	326.2	76.8	179.6
RL2-1	10	333.6	71.8	113.46
RL2-1	20	351.8	69.8	60.9
RL2-1	40	327.4	68.2	29.08
RL2-1	80	307.7	56.4	22.26
RL2-1	160	322.7	53.3	13
RL3-3	0	35.7	72.7	359.37
RL3-3	5	31.4	68.8	230.71
RL3-3	10	32.7	54.9	141.18
RL3-3	20	47.7	69.6	65.94
RL3-3	40	58.8	62.4	30.07
RL3-3	80	10.8	63.5	17.83
RL3-3	160	358.4	63.6	11.4
RL4-1	0	355.9	69.3	397.19
RL4-1	5	350.3	65.5	256.42
RL4-1	10	343	65.5	165.1
RL4-1	20	330.9	67	96.4
RL4-1	40	331.6	57.8	48.48
RL4-1	80	329.2	53	28.44
RL4-1	160	338.4	59	20.8
RL5-1	0	0.4	59.3	164.94
RL5-1	5	350.9	64	123.06
RL5-1	10	335.6	67.1	85.74
RL5-1	20	318.7	67.7	53.02
RL5-1	40	295.7	62.7	30.76
RL5-1	80	318.3	74.3	16.01
RL5-1	160	286.1	52.6	7.7
RL6-1	0	357.6	54.2	293.67
RL6-1	5	352.5	52.3	185.91
RL6-1	10	346.6	51.9	119.46
RL6-1	20	345.7	52.4	73.33
RL6-1	40	338.6	50.9	37.68
RL6-1	80	328.2	50.8	30.44
RL6-1	160	332.1	42.6	17.36
RL7-1	0	282.1	79.1	279.95
RL7-1	5	299.9	76.1	185.3
RL7-1	10	304.4	74.6	121.15
RL7-1	20	316.5	67.5	81.62

RL7-1	40	325.2	68.2	42.74
RL7-1	80	318.5	55.2	28.14
RL7-1	160	340.6	78.4	10.46
RL8-1	0	13.6	76.2	276.57
RL8-1	5	4.8	74.1	184.3
RL8-1	10	354.6	70.7	107.56
RL8-1	20	345.9	64.9	52.17
RL8-1	40	352.1	65.6	24.66
RL8-1	80	7.9	54.9	16.51
RL8-1	160	325.7	35	14.15
RL9-1	0	145.8	82.8	2188.48
RL9-1	5	119.4	82.7	926.81
RL9-1	10	99.1	84.6	372.41
RL9-1	20	42.5	86.5	146.67
RL9-1	40	46.2	83.6	57.95
RL9-1	80	0.5	77.1	22.79
RL9-1	160	302.1	81.4	16.9
EWH1-1	0	304.8	56.1	224.91
EWH1-1	5	296.2	48.7	189.99
EWH1-1	10	293	45.4	163.48
EWH1-1	20	287.6	43.9	125.2
EWH1-1	40	284.5	42.9	97.48
EWH1-1	80	284.3	42.3	73.08
EWH1-1	160	273	49.7	42.62
EWH3-3	0	278.1	56.7	191.44
EWH3-3	5	286.5	48	162.87
EWH3-3	10	286.1	44.9	141.64
EWH3-3	20	286.3	42.6	111.67
EWH3-3	40	285.3	36.5	88.52
EWH3-3	80	284.8	36.2	74.14
EWH3-3	160	291.8	35.6	49.81
EWH5-1	0	305.5	62	259.8
EWH5-1	5	297.8	53.3	188.31
EWH5-1	10	293.8	49.2	149.33
EWH5-1	20	292.6	47.7	112.39
EWH5-1	40	290.1	44.9	79.54
EWH5-1	80	292.6	46	51.92
EWH5-1	160	298.8	44.7	35.46
EWH6-1	0	279.7	60.9	219.96
EWH6-1	5	291.1	53.9	175.57
EWH6-1	10	291.2	52.7	141.86
EWH6-1	20	290.3	49.5	97.76
EWH6-1	40	291.7	49.7	58.38
EWH6-1	80	283.1	54	40.75
EWH6-1	160	276.1	28.1	18.18
EWH6-2	0	294.2	54.2	255.46
EWH6-2	5	295.5	51.3	238.76

EWH6-2	10	293.5	49.8	201.71
EWH6-2	20	290.9	48.6	138.54
EWH6-2	40	291.7	48	78.6
EWH6-2	80	294.2	46.6	42.45
EWH6-2	160	275.8	37.4	24.75
EWH7-1	0	301.8	10.8	177.65
EWH7-1	5	295.4	18.7	137.93
EWH7-1	10	292.1	23.7	108.14
EWH7-1	20	289.5	25.8	80.18
EWH7-1	40	285.4	22	56.36
EWH7-1	80	288.2	25.7	41.62
EWH7-1	160	283.3	25.2	35.19
IS2-1	0	310.4	-13.1	630.89
IS2-1	5	323.3	41.3	135.48
IS2-1	10	327.2	61	70.19
IS2-1	15	322.2	65.6	46.75
IS2-1	20	314.8	67	34.08
IS2-1	25	304.1	67.5	27.92
IS2-1	30	298.8	63.8	21.31
IS2-1	40	289	55	15.73
IS2-1	50	296.8	57.7	15.52
IS2-1	60	287.9	63.2	8.91
IS2-2	0	11.7	57.5	292.05
IS2-2	10	356.7	71.6	80.13
IS2-2	20	355.8	77.6	35.11
IS2-2	30	311.1	84.2	22.24
IS2-2	40	267.3	82.9	16.91
IS2-2	60	297.7	82.6	13.44
IS2-2	80	230.3	76.1	10.59
IS2-2	100	252.6	57.65	6.52
IS3-1	0	334.5	-44.5	1789.07
IS3-1	5	347	-27.8	335.57
IS3-1	10	353.2	12.8	62.83
IS3-1	20	0.3	56.7	26.28
IS3-1	40	353	43.8	15.69
IS3-1	80	29.8	44.5	13.14
IS3-1	160	24.6	19.9	8.28
IS4-1	0	50.3	-25.6	947.2
IS4-1	5	59.8	-27.9	510.83
IS4-1	10	68.3	-25.3	196.94
IS4-1	20	67.3	0.1	35.48
IS4-1	40	7.7	56.2	14.21
IS4-1	80	317	70.7	8.11
IS4-1	160	285.9	47.7	7.02
IS5-1	0	10	68.3	275.96
IS5-1	5	354.3	66.3	136
IS5-1	10	345.2	66.5	67.35

IS5-1	20	339	67.6	35.11
IS5-1	40	325	63.8	25.29
IS5-1	80	325.6	55.4	7.43
IS5-1	160	317.1	40	6.11
IS6-1	0	346.2	58.7	190.9
IS6-1	5	348.5	66.9	100.24
IS6-1	10	347.5	67.2	52.54
IS6-1	20	336.4	65.6	25.48
IS6-1	40	326.9	63.5	14.91
IS6-1	80	322.9	44.7	8.43
IS6-1	160	326.3	59.7	5.34
IS6-2	0	35.9	71.8	155.35
IS6-2	5	18.2	73.1	82.41
IS6-2	10	9.7	75.5	41.17
IS6-2	15	352.9	76.2	26.29
IS6-2	20	325.5	73.8	17.74
IS6-2	25	312.1	69.1	13.43
IS6-2	30	316.8	70.7	12.49
IS6-2	35	330.5	62.4	7.61
IS6-2	40	281.1	73.5	9.91
IS7-3	0	60	78.9	134.21
IS7-3	5	285.1	64.2	85.36
IS7-3	10	270.5	57.4	47.79
IS7-3	20	270.3	47.9	29.23
IS7-3	40	271	40	20.8
IS7-3	80	304.4	41.9	12.15
L1-3	0	190.5	67.4	209.76
L1-3	5	218.8	46.9	111.24
L1-3	10	224.5	43.8	94.6
L1-3	20	224.8	43.9	68.98
L1-3	40	220.8	40	32.54
L1-3	80	224.3	23.3	16.76
L1-3	160	300.2	74.3	6.63
L2-1	0	282.8	77.3	143.4
L2-1	5	260.6	68.5	74.34
L2-1	10	260.6	59	57.69
L2-1	20	254.3	53.7	45.44
L2-1	40	256.6	52.8	22.76
L2-1	80	243.7	52.2	15.59
L2-1	160	242.7	49.1	7.46
L4-2	0	286	57.9	255.54
L4-2	5	279.4	42.2	226.97
L4-2	10	275.9	40	191.43
L4-2	20	277	39	144.34
L4-2	40	281	30.1	98
L4-2	80	281.7	25	69.29
L4-2	160	283.6	22.6	16.5

L5-1	0	253.6	46.8	535.56
L5-1	5	253.7	41.8	500.06
L5-1	10	255.2	40.5	449.05
L5-1	20	252.4	38.3	371.03
L5-1	40	247.1	31.5	291.19
L5-1	80	247.8	34.1	190.1
L5-1	160	242.5	33.2	53.32
L6-1	0	253.5	43.5	263.16
L6-1	5	260.4	44.7	241.99
L6-1	10	261.4	45.7	219.34
L6-1	20	261.7	43	166.93
L6-1	40	257.1	40.3	113.71
L6-1	80	258.2	40.8	59.99
L6-1	160	258.7	41.7	28.19
L7-1	0	261	43	461.18
L7-1	5	265.4	42.7	441.53
L7-1	10	257.4	39.2	400.64
L7-1	20	266.1	40.8	299.62
L7-1	40	263.2	39.8	206.88
L7-1	80	263.3	40.4	112.81
L7-1	160	264.4	37	54.87
L8-2	0	243.1	41.9	454.41
L8-2	5	252.6	39.7	423.33
L8-2	10	250.7	37.8	369.08
L8-2	20	249.3	36.4	272.32
L8-2	40	243.7	32	189.5
L8-2	80	243.2	30.1	116.15
L8-2	160	250.4	38.6	50.93
L9-1	0	255.1	35.1	374.45
L9-1	5	254.1	35.4	361.31
L9-1	10	257.1	34.3	321.3
L9-1	15	255.3	34.3	277.74
L9-1	20	247.9	32.7	239.37
L9-1	30	256.5	34.5	182.23
L9-1	40	255.2	34.7	144.73
L9-1	50	255.6	32.4	118.36
L9-1	60	252	32.5	96.1
L9-1	70	251.8	35.1	79.07
L9-1	80	256.4	34.5	65.69
L9-1	90	250.8	33.8	53.67
L9-1	100	251.2	34.8	46.03
L9-1	120	252.4	36.1	34.86
L9-1	140	250.1	38.6	28.63
L10-3	0	218.4	51.5	82.49
L10-3	5	231.4	46.9	52.3
L10-3	10	232.1	40.5	38.66
L10-3	20	233.5	44.1	25.37

L10-3	40	230	37.6	13.5
L10-3	80	250	31.2	6.06
L10-3	160	191	27	4.01
L11-2	0	253.9	41.1	500.15
L11-2	5	252.1	36.8	472.11
L11-2	10	254	37.5	387.09
L11-2	20	254.3	36.3	263.07
L11-2	40	253	33.8	185.89
L11-2	80	251	33.7	117.71
L11-2	160	246.7	34.5	52.2
E1-1	0	346.15	85.7	82.8
E1-1	5	339.3	77.3	45.41
E1-1	10	347.2	78.5	30.13
E1-1	15	320.6	74.4	22.61
E1-1	20	29.5	80.4	17.9
E1-1	30	61.4	82.3	12.78
E1-1	40	10.9	82.3	7.47
E2-2	0	296.7	70.9	29.12
E2-2	5	344.7	61.3	19.37
E2-2	10	358.7	65.9	14.47
E2-2	20	327.1	65.3	10.23
E2-2	40	200.6	81.2	6.42
E3-2	0	324.5	47.2	44.41
E3-2	5	320.4	48.8	24.98
E3-2	10	314	55.3	16.77
E3-2	20	319.4	62.6	11.48
E3-2	40	302.5	59.3	7.57
E3-2	50	308.9	62.8	5.21
E4-2	0	321.8	68	58.43
E4-2	5	326.6	65.9	31.4
E4-2	10	313.8	62.2	23.16
E4-2	15	315.4	64.9	19.55
E4-2	20	312.6	60.2	15.23
E4-2	30	293.8	53.7	11.57
E4-2	40	288.6	51.2	9.88
E4-2	50	279.7	53.2	7.23
E5-2	0	78.5	66.7	53.98
E5-2	5	106.5	71.8	33.11
E5-2	10	111.6	70	22.5
E5-2	15	102.1	66.7	18.62
E5-2	20	108.9	53.9	17.3
E5-2	30	102.1	60.7	12.02
E5-2	40	86	54	10. 59
E5-2	50	89.1	60.1	7.97
E6-3	0	12	81.4	63.59
E6-3	5	27.8	73.9	34.87
E6-3	10	350.7	75.2	18.91

E6-3	15	311	72.4	14.38
E6-3	20	333	73.1	11.37
E6-3	30	357.7	75.9	7.89
E6-3	40	352.8	70.1	8.3
E7-2	0	355.4	66.3	50.81
E7-2	5	356.2	65.2	32.01
E7-2	10	352.1	63.1	19.14
E7-2	15	334.5	67.5	13.26
E7-2	20	331.3	69.7	9.9
E7-2	25	315.8	60.5	10.19
E7-2	30	326.3	65.1	8.08
E7-2	35	314.7	57.6	7.65
E7-2	40	301.2	52.9	7.98
E8-3	0	256.3	66.4	62.91
E8-3	5	292.9	75	31.34
E8-3	10	275.5	72.7	18.25
E8-3	15	280.7	71	11.34
E8-3	20	288.6	73.1	7.74
E8-3	30	265.4	84.9	6.87
E8-3	40	269	65.5	5.12
E9-1	0	340.9	78.3	64.34
E9-1	5	343.5	68	36.58
E9-1	10	337.7	65.6	20.75
E9-1	15	354.4	57	13.99
E9-1	20	344.4	55.4	12.04
E9-1	30	352.7	51.2	10.97
E9-1	40	334.5	59.1	8.54
BR1-1	0	5	78.2	130.165
BR1-1	5	1.7	79.3	100.28
BR1-1	10	353.9	75	69.87
BR1-1	20	353	75.7	43.17
BR1-1	40	341.6	74.5	21.7
BR1-1	80	319.2	68.3	13.69
BR1-1	160	262.5	54.6	4.54
BR2-2	0	8.9	70.2	118.46
BR2-2	5	11.2	68.1	98.29
BR2-2	10	12.7	67.7	79.125
BR2-2	20	5.2	65.7	49.32
BR2-2	40	7.9	67	26.34
BR2-2	80	358.3	51.2	7.68
BR2-2	160	10.1	36.2	5.02
BR3-1	0	33.8	86.1	92.59
BR3-1	5	339.5	79.9	79.33
BR3-1	10	339	75.8	64.02
BR3-1	20	336.4	73.5	45.73
BR3-1	40	321.7	74.3	28.03
BR3-1	80	319.6	57.7	15.63

BR3-1	160	298.4	55.7	6.84
BR5-2	0	43.4	68	184.98
BR5-2	5	35.1	68.5	138.67
BR5-2	10	30.6	68.6	96.22
BR5-2	20	23.5	65.2	56.12
BR5-2	40	25.5	65.2	23.15
BR5-2	80	338.2	49.8	8.67
BR5-2	160	29.3	26.5	3.39
BR7-1	0	69.85	53.7	82.02
BR7-1	5	51.6	64.1	63.03
BR7-1	10	44.3	65.3	50.4
BR7-1	20	26	60.9	33.68
BR7-1	40	27.8	54.8	17.45
BR7-1	80	18.6	54.4	7.38
BR7-1	160	353.2	-1	2.81
BR8-1	0	33.1	51	174.81
BR8-1	5	14.9	59.3	123.33
BR8-1	10	8.4	58.8	82.16
BR8-1	20	4.8	60.7	48.69
BR8-1	40	355.4	53.9	25.38
BR8-1	80	351.2	45.3	12.13
BR8-1	160	353.3	41.95	8.15
BR9-1	0	9.1	58.9	213.61
BR9-1	5	6.8	62	171.67
BR9-1	10	359.2	63.7	120.02
BR9-1	20	7.9	63.2	63.23
BR9-1	40	12.9	63.6	22.17
BR9-1	80	343.5	61.4	8.51
BR9-1	160	39.2	44	2.93
BR10-1	0	11.9	61	114.53
BR10-1	5	7.5	63.1	84.77
BR10-1	10	6.2	63.1	66.23
BR10-1	20	8.4	59.6	42.26
BR10-1	40	11	55.3	20.57
BR10-1	80	357.6	47	9.6
BR10-1	160	340.8	9.2	4.34

Appendix 3

Paleomagnetic Plots

Standard presentations of representative paleomagnetic data from selected samples from every site prepared with Puffin Plot software.

Sample: SC1-1

Site: Saugum Canyon

PCA dec 45.09 / inc 61.36 Fisher dec 334.9 / inc 83.4 / a95 23.8 / k 8.9

PCA MAD1 38.87 / MAD3 5.60

(0.34 0.34 0.88)t

□ vertical

■ horizontal

Units: A/m ×102

Updated July 2017

	demag.	dec.	inc.	int.	m.s.
	0	49.6	68.8	5.15e-02	NaN
	5	28.6	68.3	3.34e-02	NaN
*	10	44.7	59.1	2.06e-02	NaN
*	15	42.0	59.1	1.37e-02	NaN
*	20	30.3	69.3	1.17e-02	NaN
*	30	54.8	60.6	6.33e-03	NaN
*	40	57.5	58.5	6.33e-03	NaN
*	50	60.0	61.2	6.23e-03	NaN
*	60	72.5	67.7	6.11e-03	NaN
	70	72.9	51.5	5.40e-03	NaN

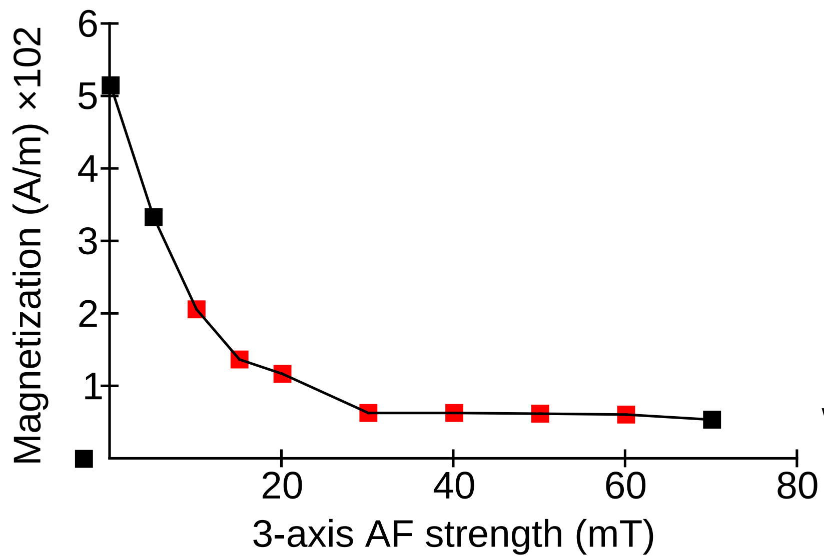

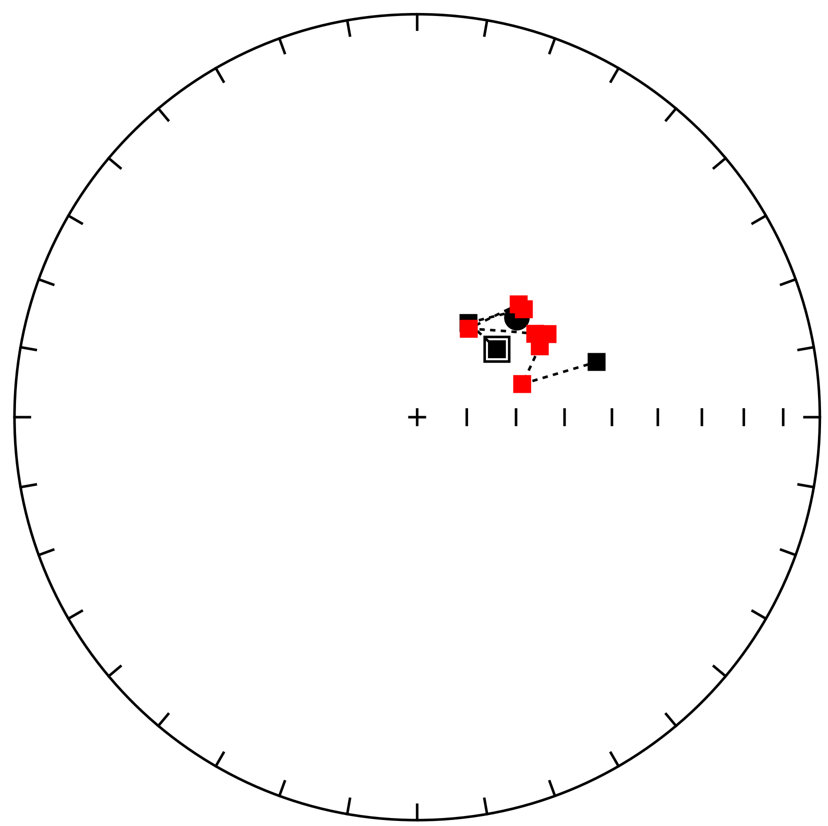

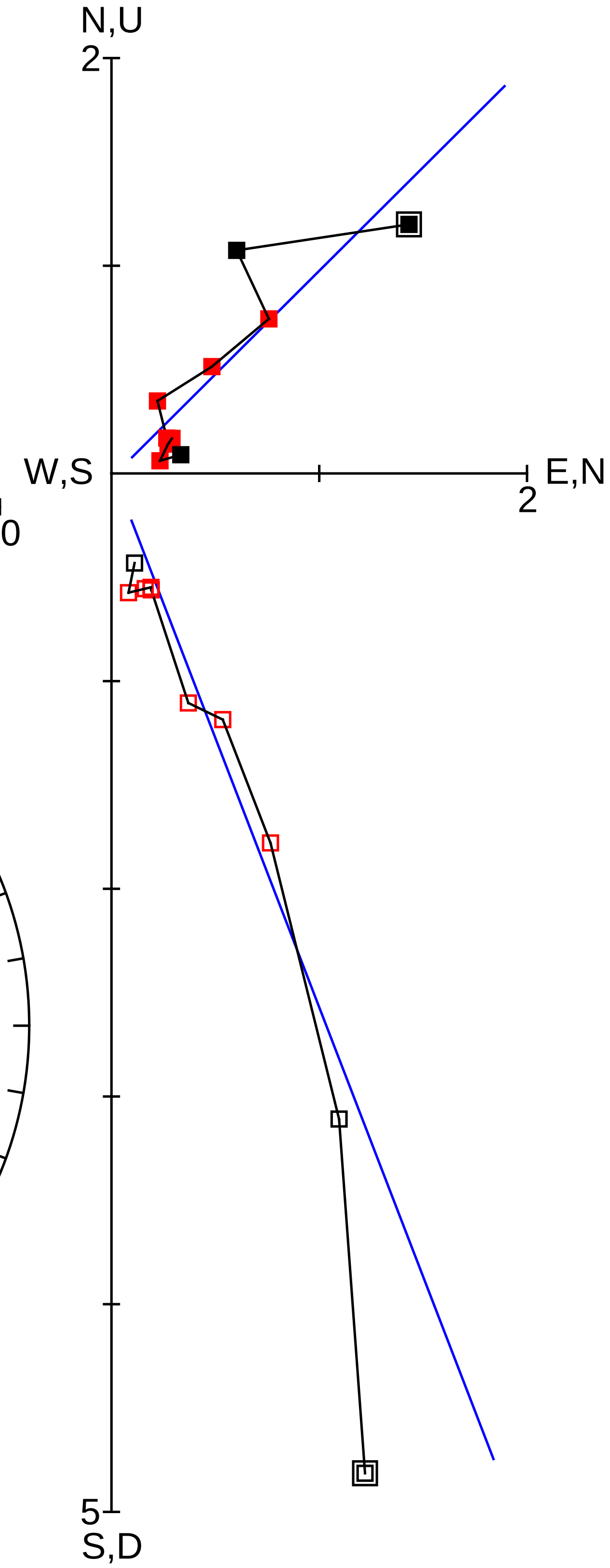

Sample: SC2-3

Site: Saugum Canyon

PCA dec 329.53 / inc 71.23 Fisher dec 334.9 / inc 83.4 / a95 23.8 / k 8.9
PCA MAD1 12.99 / MAD3 7.34
(0.28 -0.16 0.95)t

vertical
horizontal
Units: A/m ×102

Updated July 2017

	demag.	dec.	inc.	int.	m.s.
	0	313.9	82.5	1.05e-01	NaN
	5	3.2	76.8	5.54e-02	NaN
*	10	343.1	70.4	3.03e-02	NaN
*	15	289.2	70.2	1.79e-02	NaN
*	20	326.4	67.1	1.35e-02	NaN

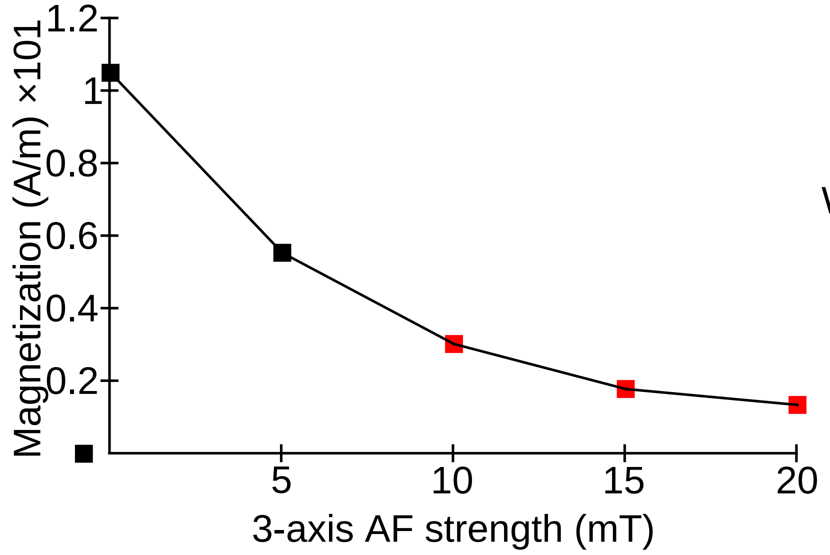

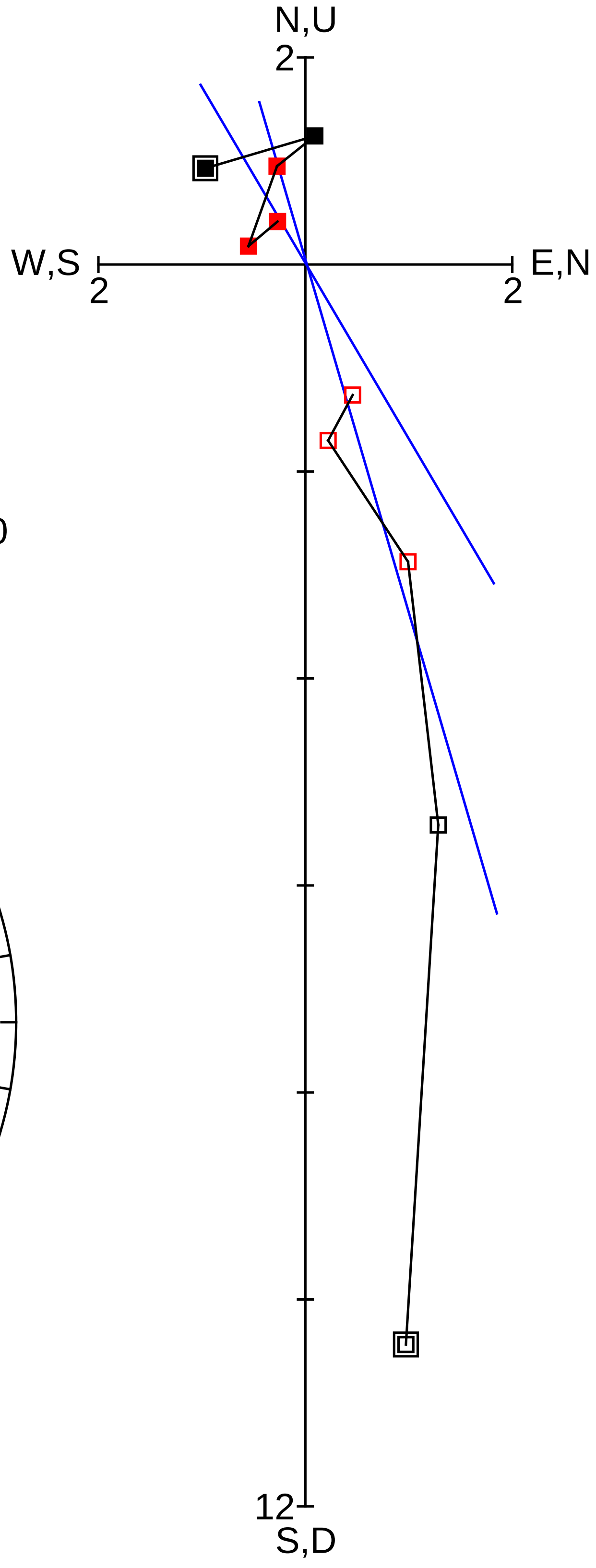

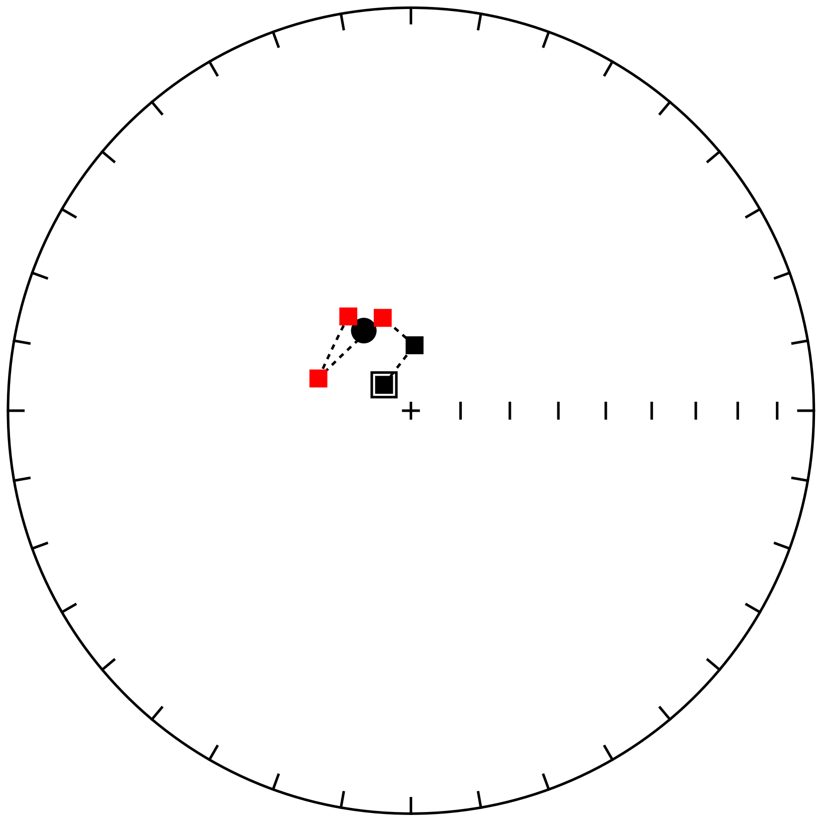

Sample: SC3-2

Site: Saugum Canyon

PCA dec 181.26 / inc 45.26 Fisher dec 334.9 / inc 83.4 / a95 23.8 / k 8.9
PCA MAD1 0.00 / MAD3 1.84
(-0.70 -0.02 0.71)t

vertical
horizontal
Units: A/m ×101

Updated July 2017

	demag.	dec.	inc.	int.	m.s.
	0	187.7	41.0	1.39e+00	NaN
*	5	181.2	44.9	3.96e-01	NaN
*	10	183.0	54.4	7.96e-02	NaN
	20	225.0	57.3	1.99e-02	NaN

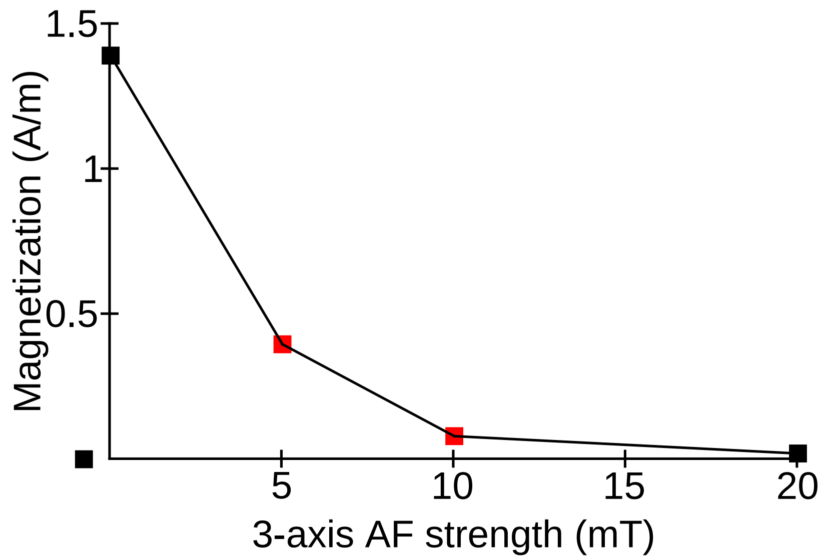

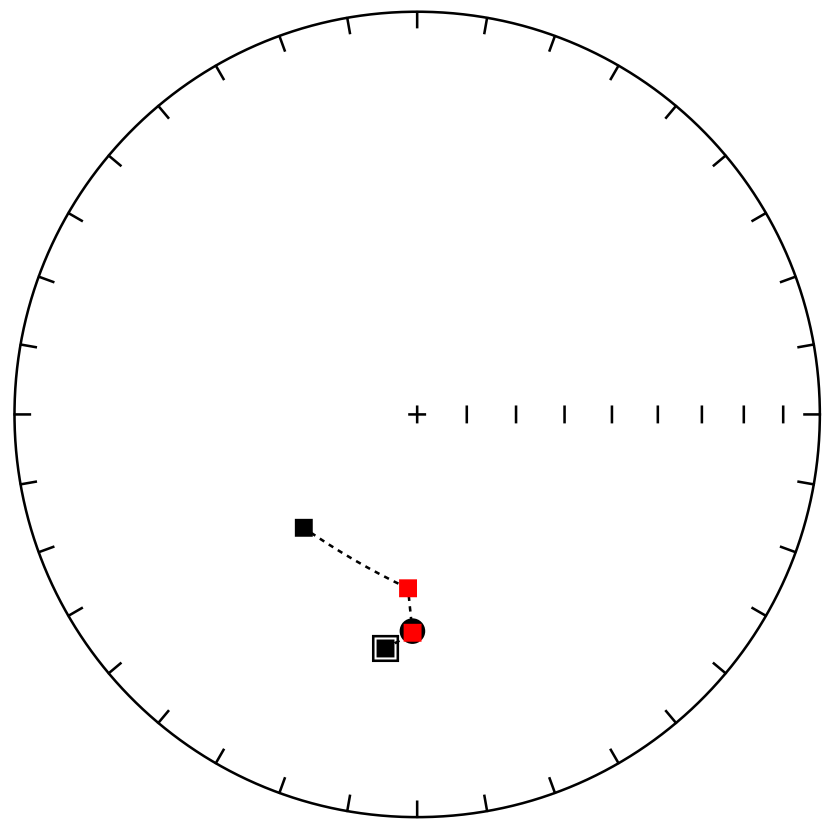

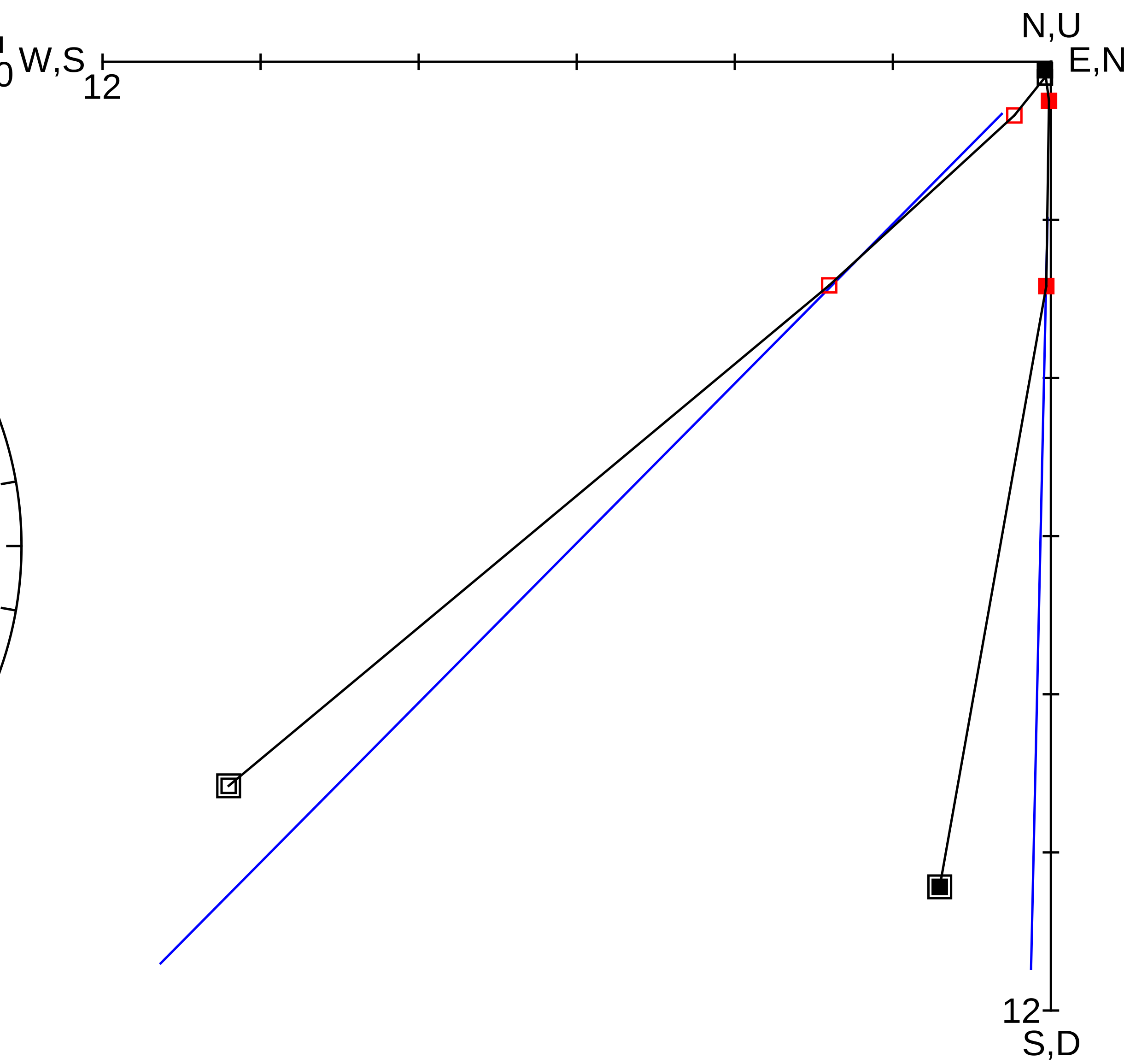

Sample: SC4-1
Site: Saugum Canyon

PCA dec 330.67 / inc 66.96 Fisher dec 334.9 / inc 83.4 / a95 23.8 / k 8.9
PCA MAD1 16.31 / MAD3 7.06
(0.34 -0.19 0.92)t

vertical
horizontal
Units: A/m ×102

Updated July 2017

	demag.	dec.	inc.	int.	m.s.
	0	243.9	74.2	8.48e-02	NaN
	5	303.4	72.2	5.79e-02	NaN
*	10	325.6	71.9	3.39e-02	NaN
*	15	338.2	69.1	2.37e-02	NaN
*	20	327.9	58.8	2.08e-02	NaN
*	25	336.5	53.3	1.65e-02	NaN

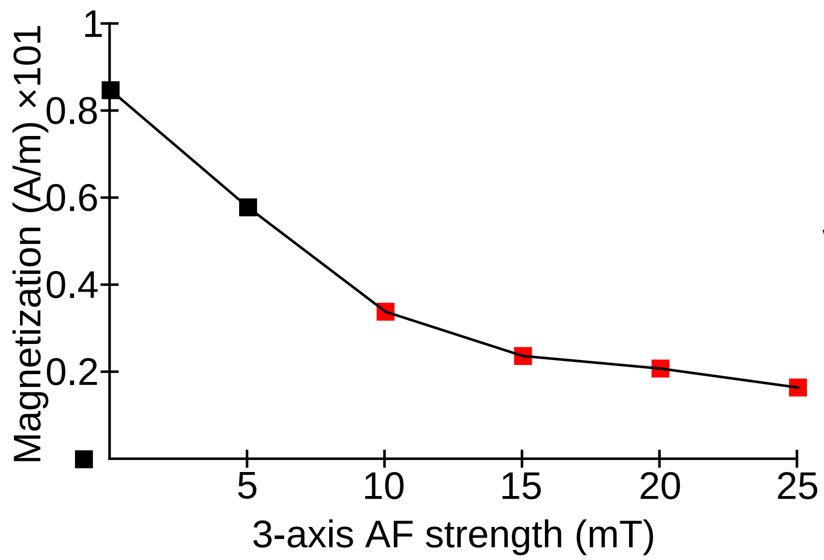

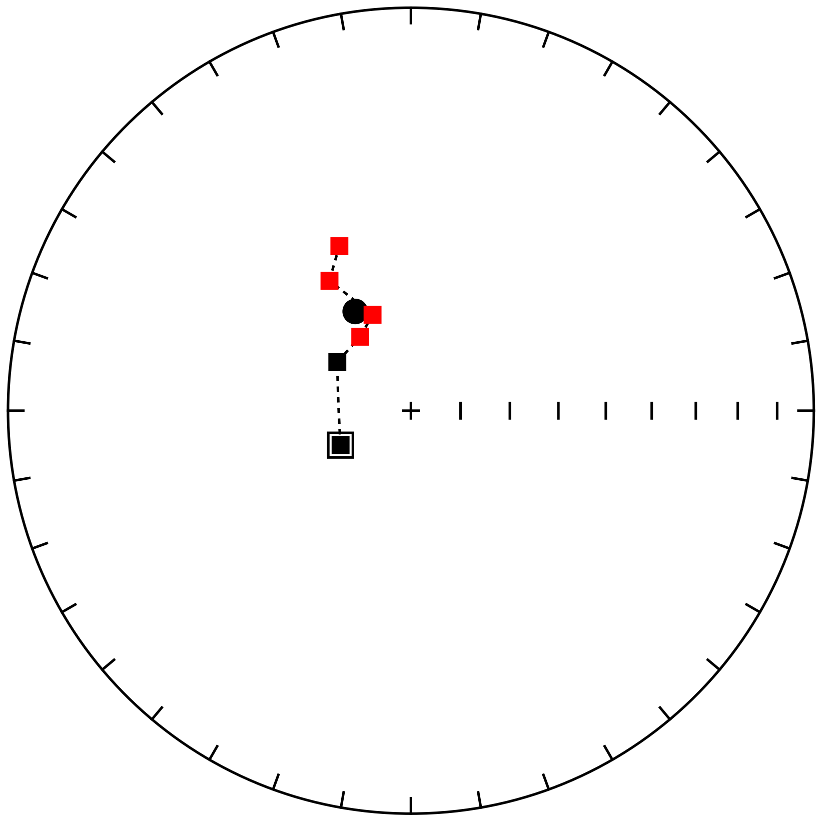

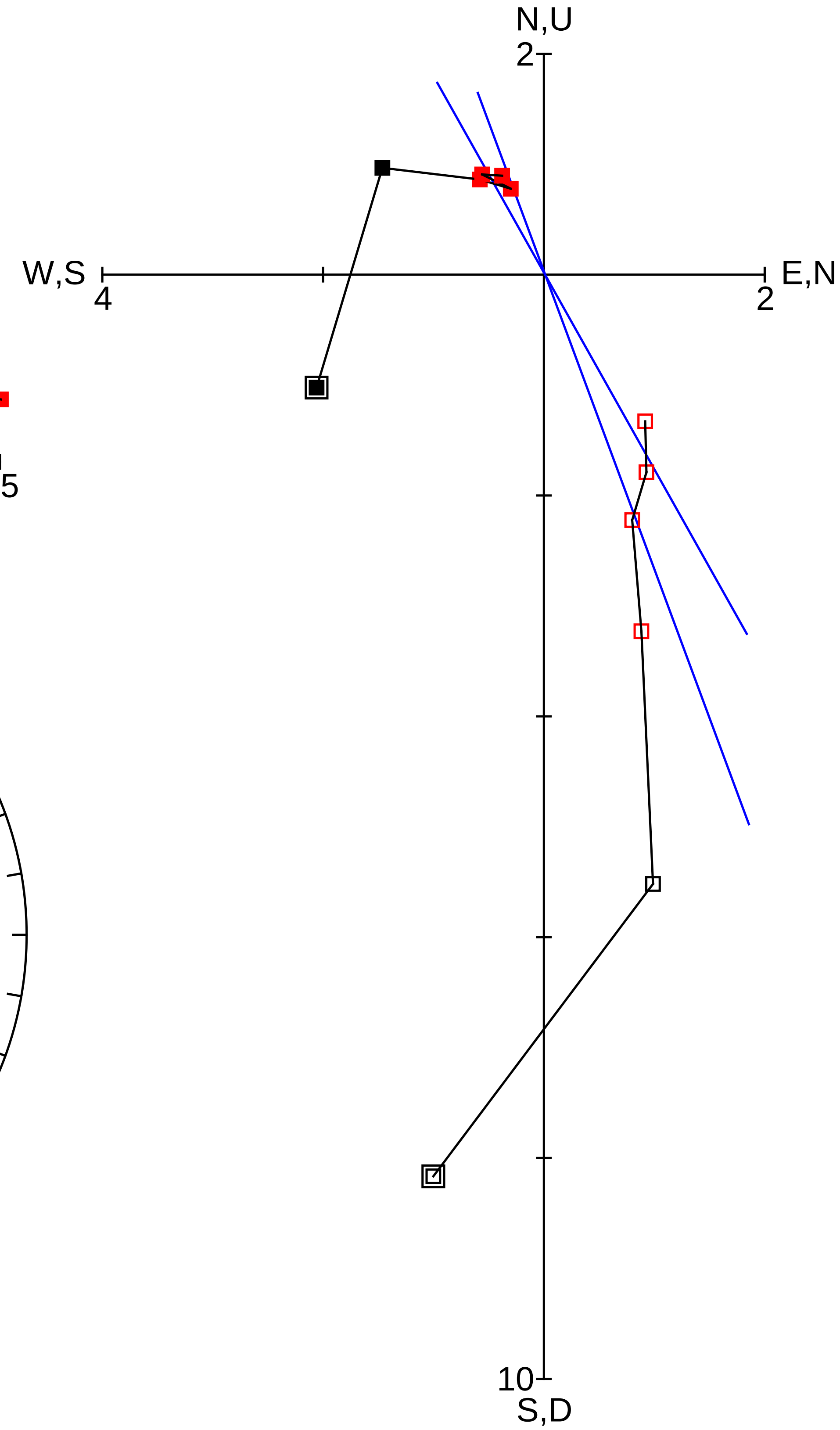

Sample: SC6-1
Site: Saugum Canyon

PCA dec 308.37 / inc 85.29 Fisher dec 334.9 / inc 83.4 / a95 23.8 / k 8.9
PCA MAD1 6.57 / MAD3 3.40
(0.05 -0.06 1.00)t

□ vertical
■ horizontal
Units: A/m ×103

Updated July 2017

	demag.	dec.	inc.	int.	m.s.
	0	324.5	78.1	2.01e-02	NaN
*	5	326.4	83.1	1.54e-02	NaN
*	10	316.7	85.5	1.27e-02	NaN
*	15	237.0	85.0	1.13e-02	NaN
	20	245.5	86.8	1.06e-02	NaN
	25	258.4	75.2	1.09e-02	NaN
	30	212.8	74.9	1.00e-02	NaN

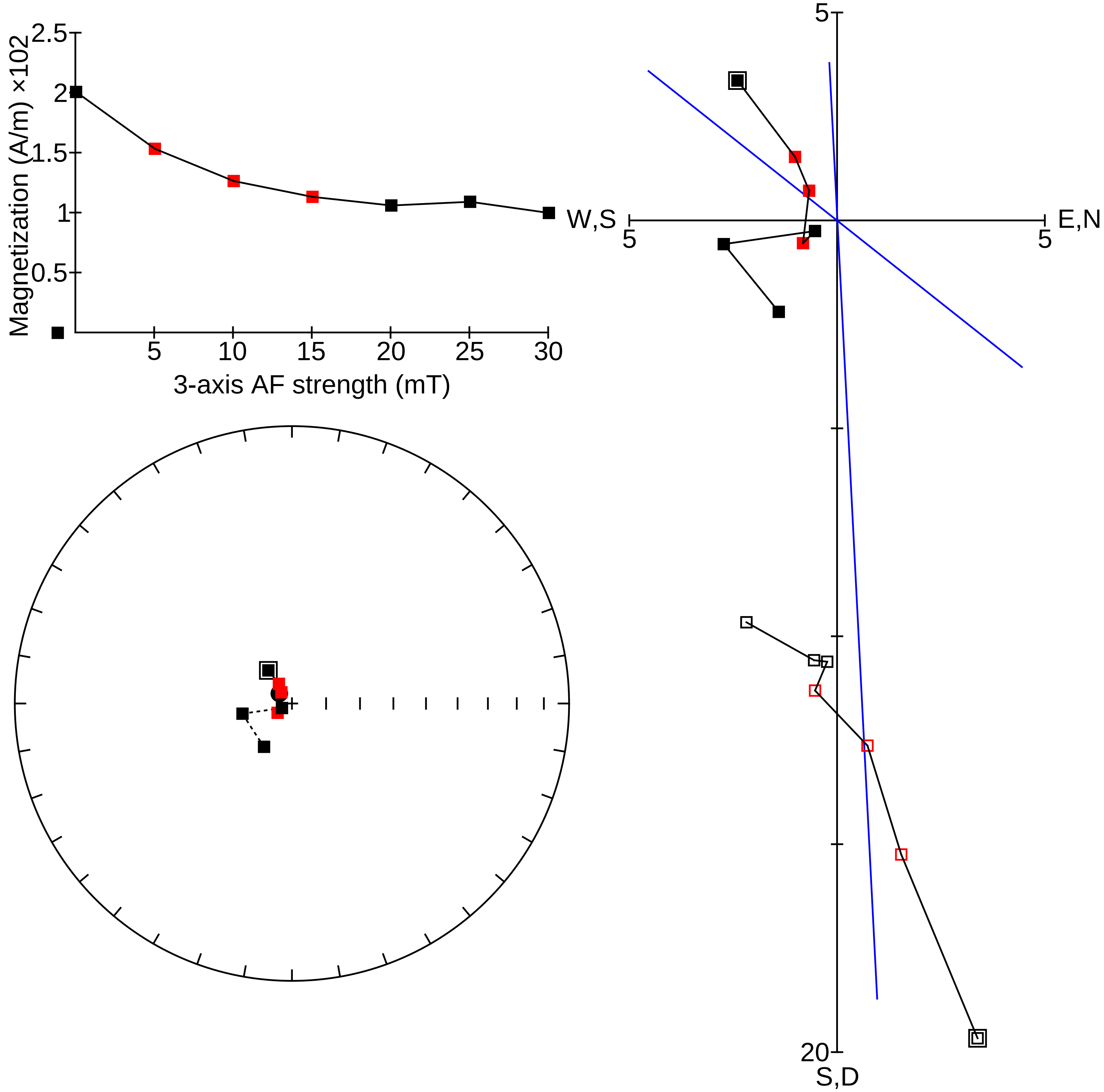

Sample: SC8-1

Site: Saugum Canyon

PCA dec 327.11 / inc 71.73 Fisher dec 334.9 / inc 83.4 / a95 23.8 / k 8.9
PCA MAD1 19.32 / MAD3 3.74
(0.26 -0.17 0.95)t

vertical
horizontal
Units: A/m ×102

Updated July 2017

	demag.	dec.	inc.	int.	m.s.
	0	51.7	86.3	7.66e-02	NaN
	5	337.4	79.4	4.14e-02	NaN
*	10	318.9	70.3	2.29e-02	NaN
*	15	337.3	74.1	1.66e-02	NaN
*	20	344.6	70.3	1.09e-02	NaN

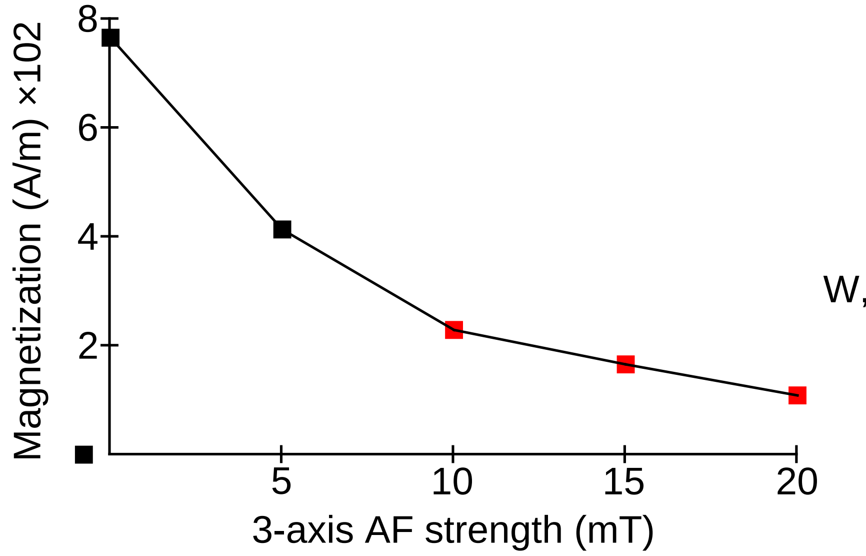

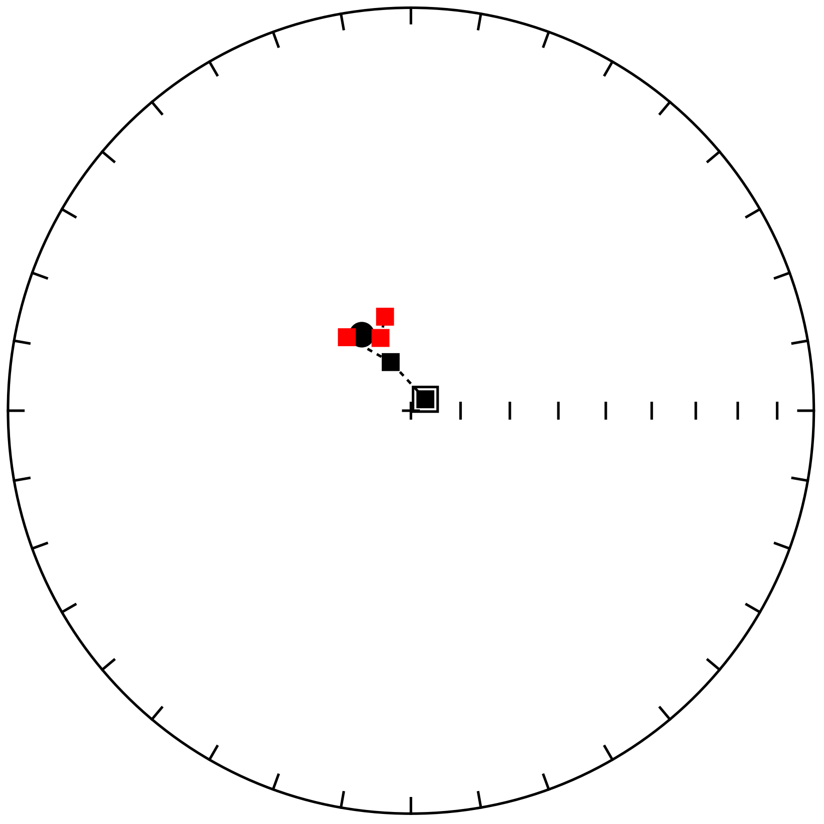

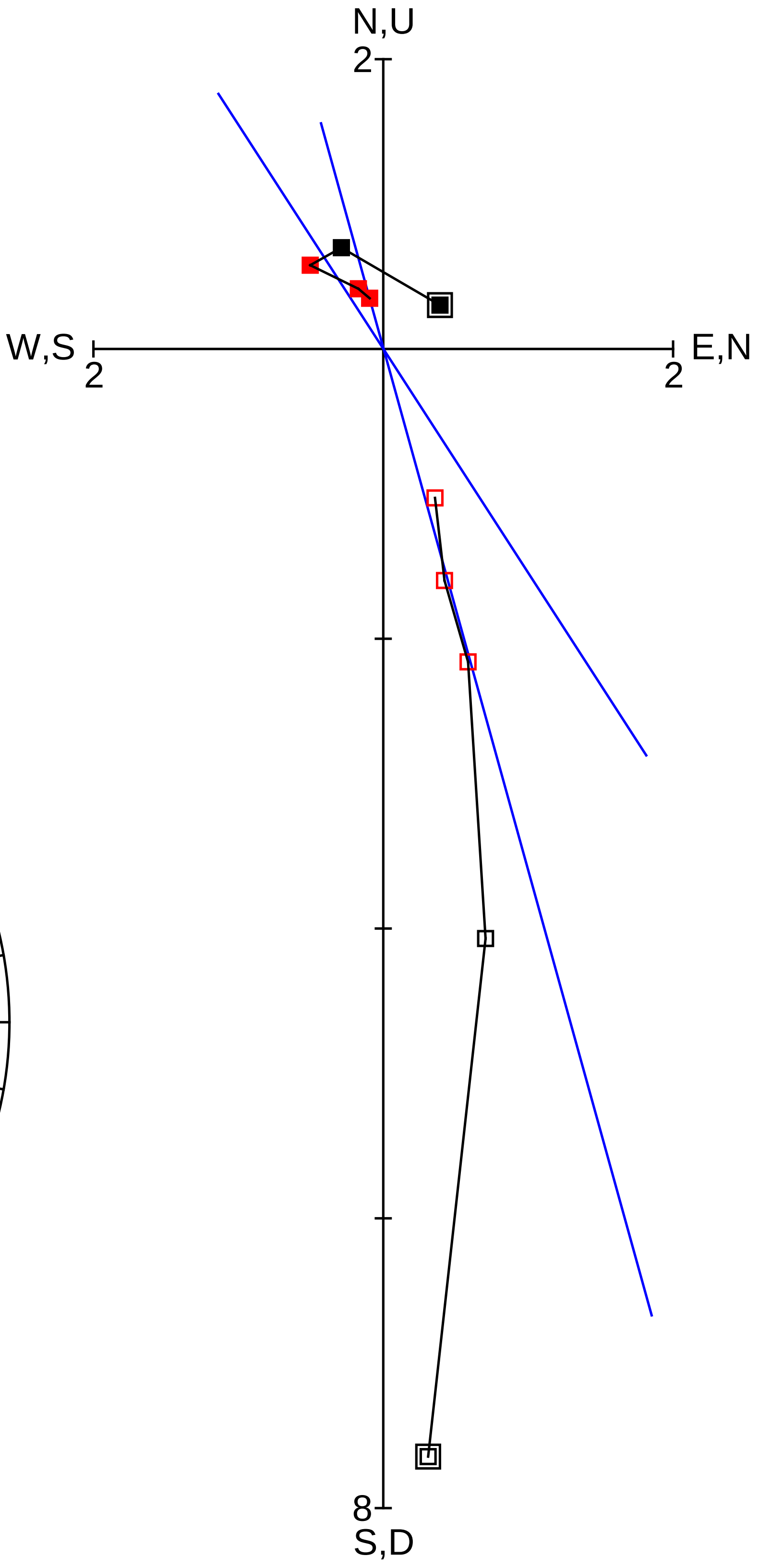

Sample: RL1-3

Site: Reade Lake Stock

PCA dec 351.50 / inc 75.93 Fisher dec 343.8 / inc 71.5 / a95 9.1 / k 33.1

PCA MAD1 8.05 / MAD3 1.96

(0.24 -0.04 0.97)t

Updated July 2017

	demag.	dec.	inc.	int.	m.s.
	0	194.7	86.8	2.19e-01	NaN
	5	357.0	83.0	1.21e-01	NaN
*	10	355.5	75.5	7.14e-02	NaN
*	20	336.5	76.5	3.80e-02	NaN
*	40	356.7	76.3	1.79e-02	NaN
*	80	340.7	77.7	1.47e-02	NaN
	160	4.6	40.4	1.32e-02	NaN

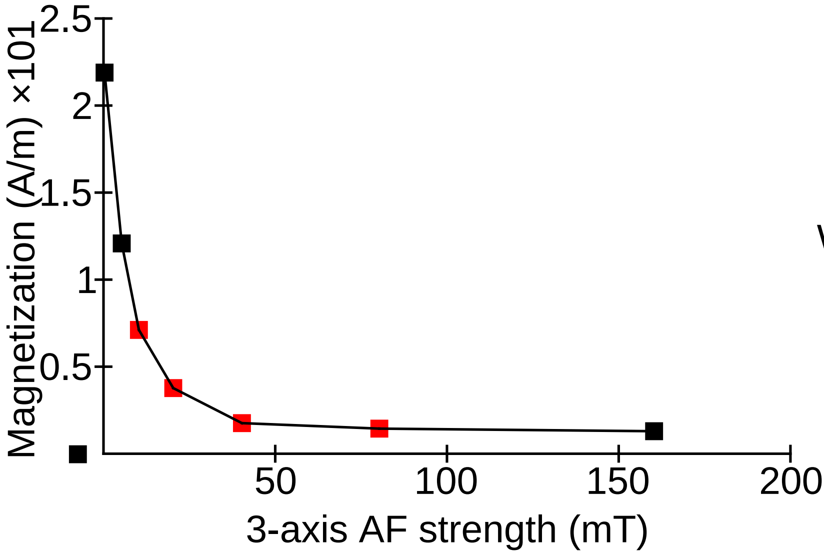

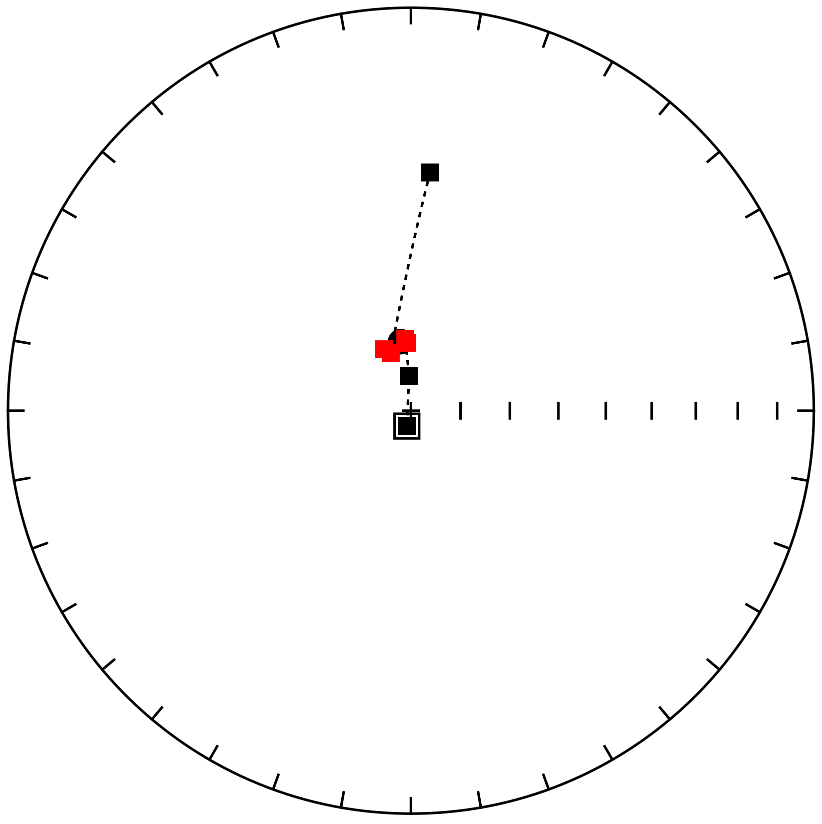

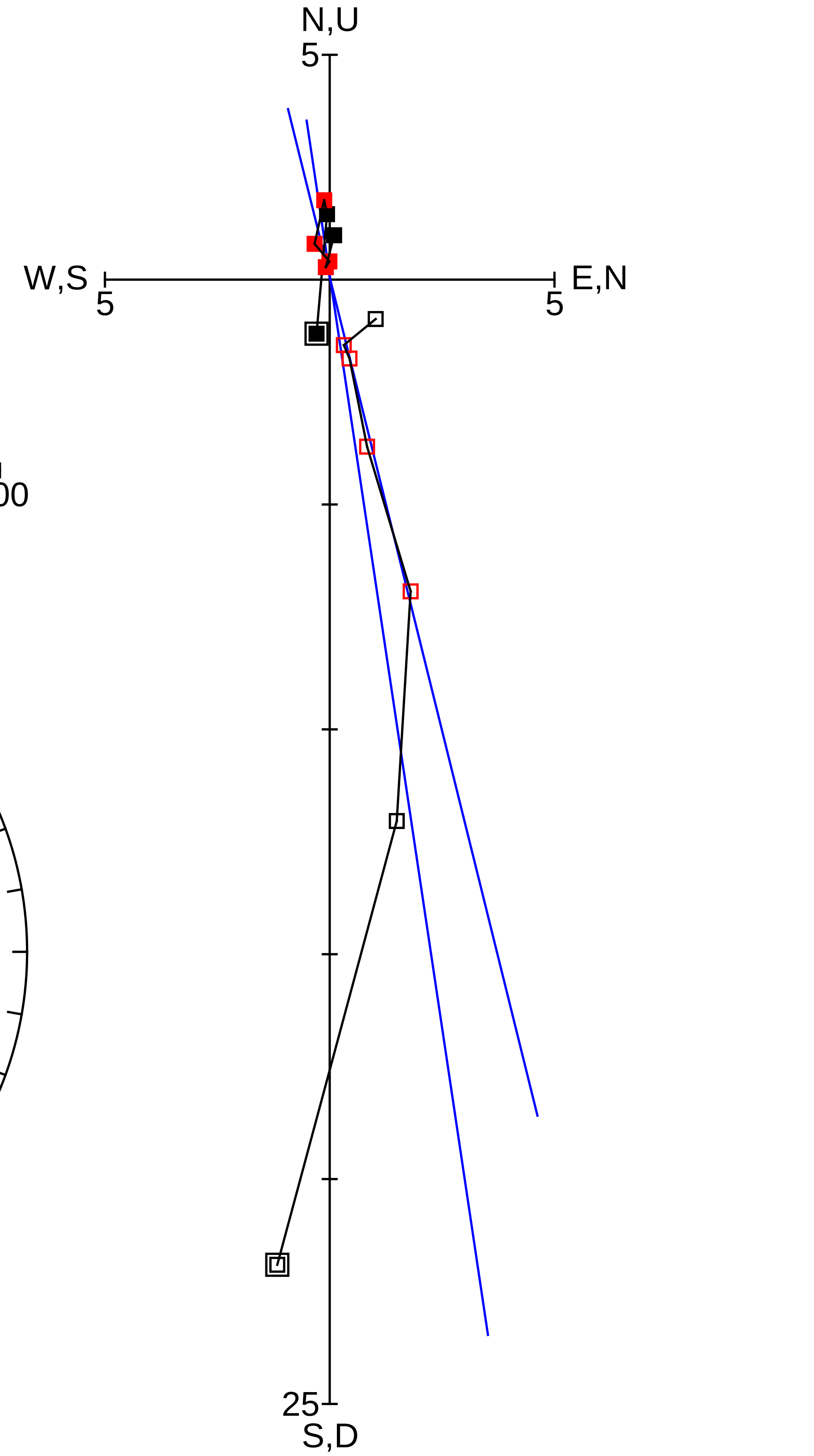

Sample: RL2-1

Site: Reade Lake Stock

PCA dec 337.36 / inc 71.37 Fisher dec 343.8 / inc 71.5 / a95 9.1 / k 33.1

PCA MAD1 16.68 / MAD3 2.76

(0.29 -0.12 0.95)t

□ vertical

■ horizontal

Units: A/m ×102

Updated July 2017

	demag.	dec.	inc.	int.	m.s.
	0	342.2	74.0	2.84e-01	NaN
	5	326.2	76.8	1.80e-01	NaN
*	10	333.6	71.8	1.13e-01	NaN
*	20	351.8	69.8	6.09e-02	NaN
*	40	327.4	68.2	2.91e-02	NaN
	80	307.7	56.4	2.23e-02	NaN
	160	322.7	53.3	1.30e-02	NaN

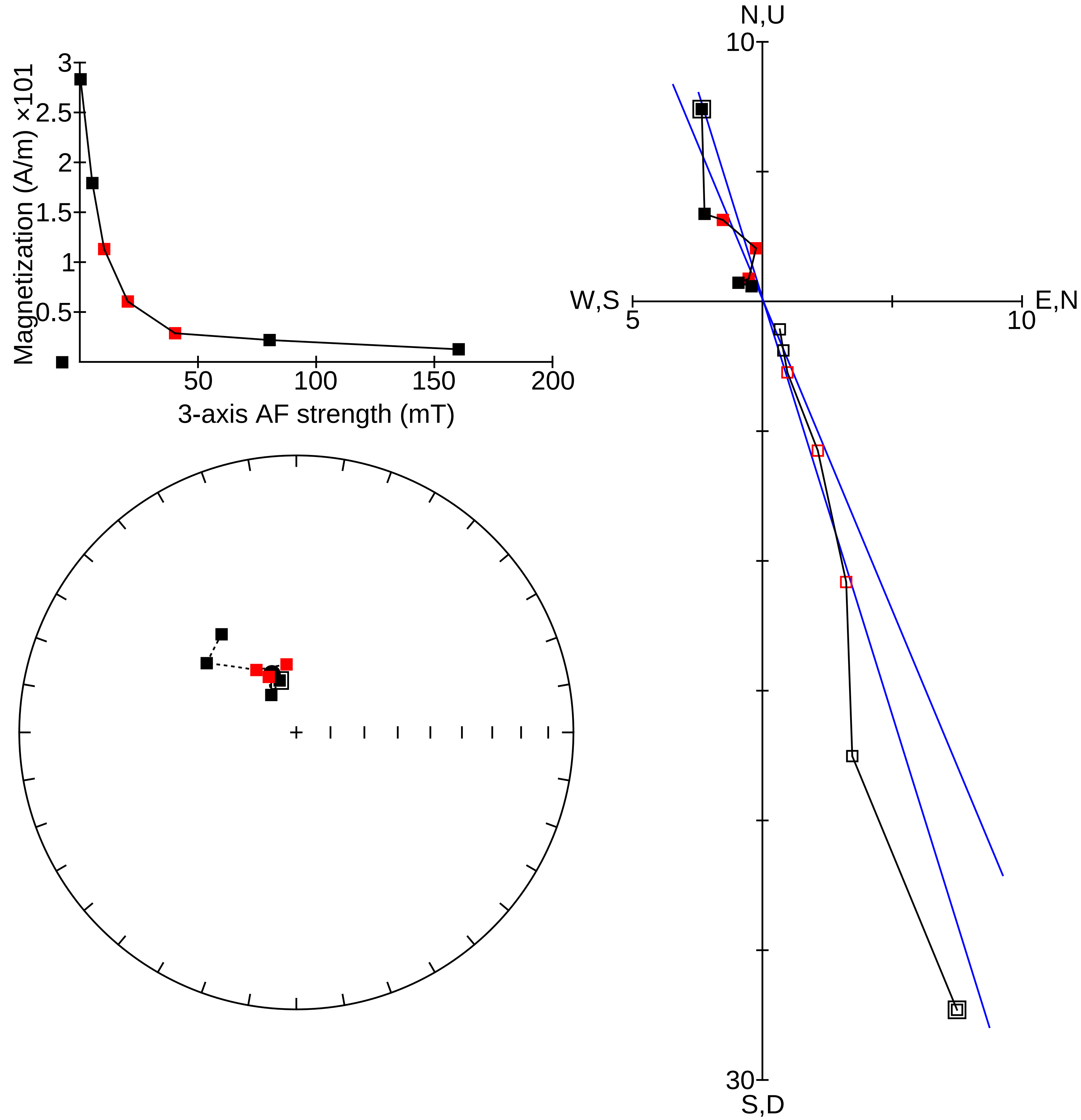

Sample: RL3-3

Site: Reade Lake Stock

PCA dec 46.49 / inc 68.51 Fisher dec 343.8 / inc 71.5 / a95 9.1 / k 33.1

PCA MAD1 22.40 / MAD3 5.65

(0.25 0.27 0.93)t

□ vertical

■ horizontal

Units: A/m ×102

Updated July 2017

	demag.	dec.	inc.	int.	m.s.
	0	35.7	72.7	3.59e-01	NaN
	5	31.4	68.8	2.31e-01	NaN
	10	32.7	54.9	1.41e-01	NaN
*	20	47.7	69.6	6.59e-02	NaN
*	40	58.8	62.4	3.01e-02	NaN
*	80	10.8	63.5	1.78e-02	NaN
*	160	358.4	63.6	1.14e-02	NaN

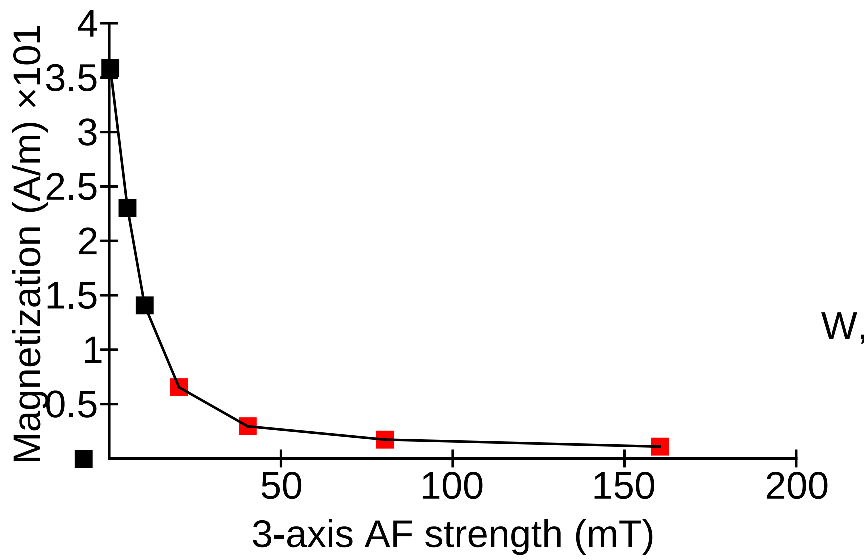

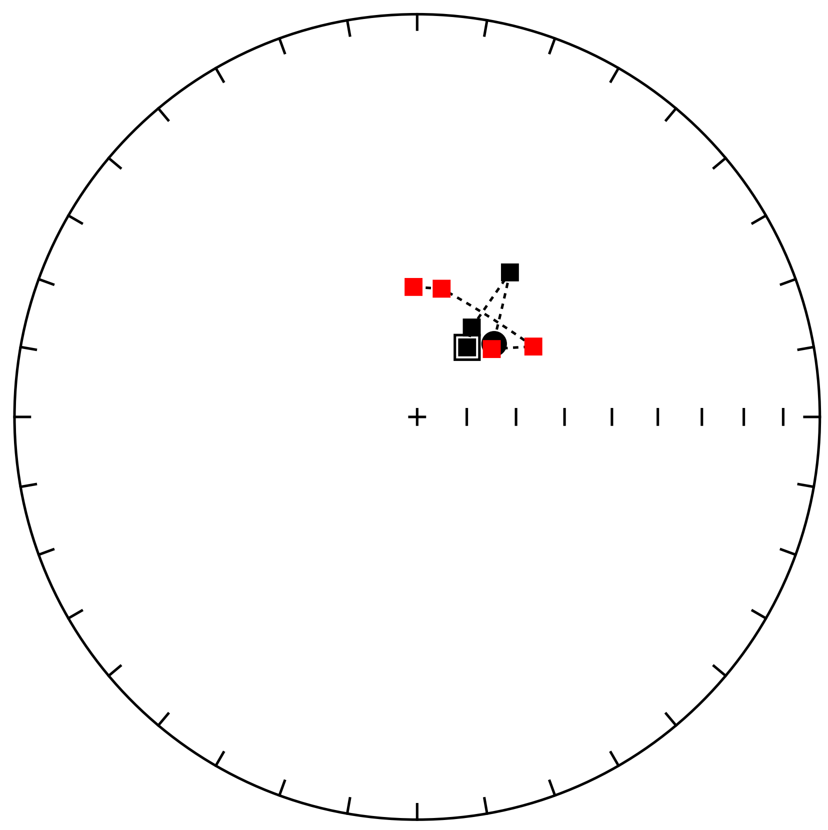

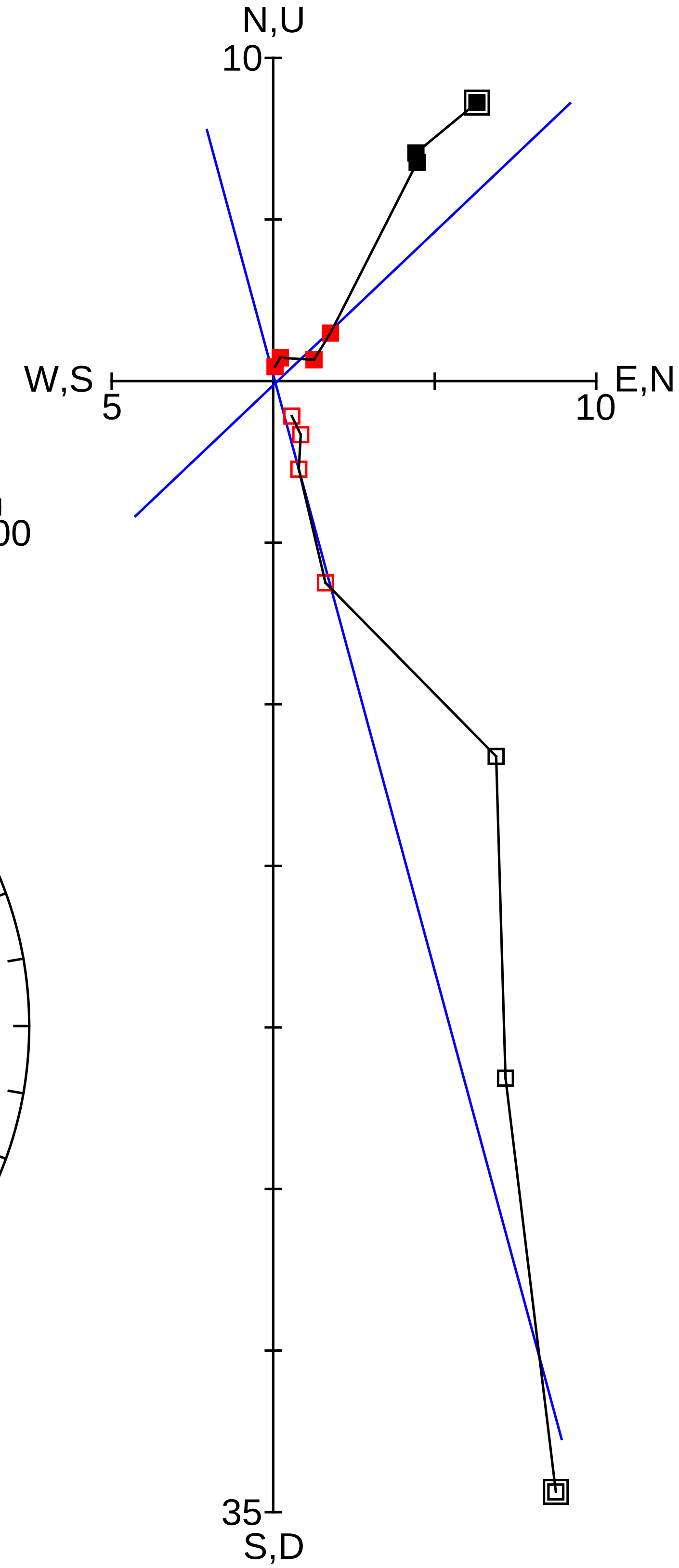

Sample: RL4-1

Site: Reade Lake Stock

PCA dec 331.21 / inc 64.21 Fisher dec 343.8 / inc 71.5 / a95 9.1 / k 33.1

PCA MAD1 9.20 / MAD3 4.72

(0.38 -0.21 0.90)t

□ vertical

■ horizontal

Units: A/m ×102

Updated July 2017

	demag.	dec.	inc.	int.	m.s.
	0	355.9	69.3	3.97e-01	NaN
	5	350.3	65.5	2.56e-01	NaN
	10	343.0	65.5	1.65e-01	NaN
*	20	330.9	67.0	9.64e-02	NaN
*	40	331.6	57.8	4.85e-02	NaN
*	80	329.2	53.0	2.84e-02	NaN
*	160	338.4	59.0	2.08e-02	NaN

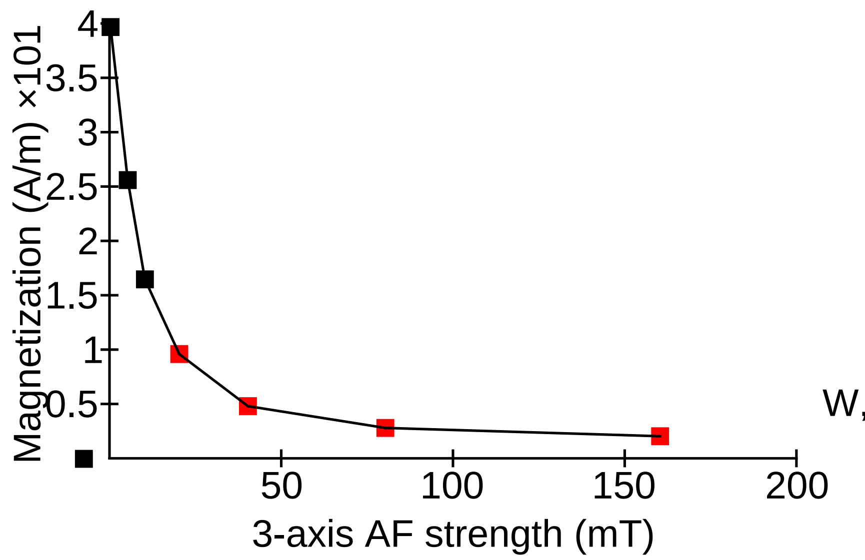

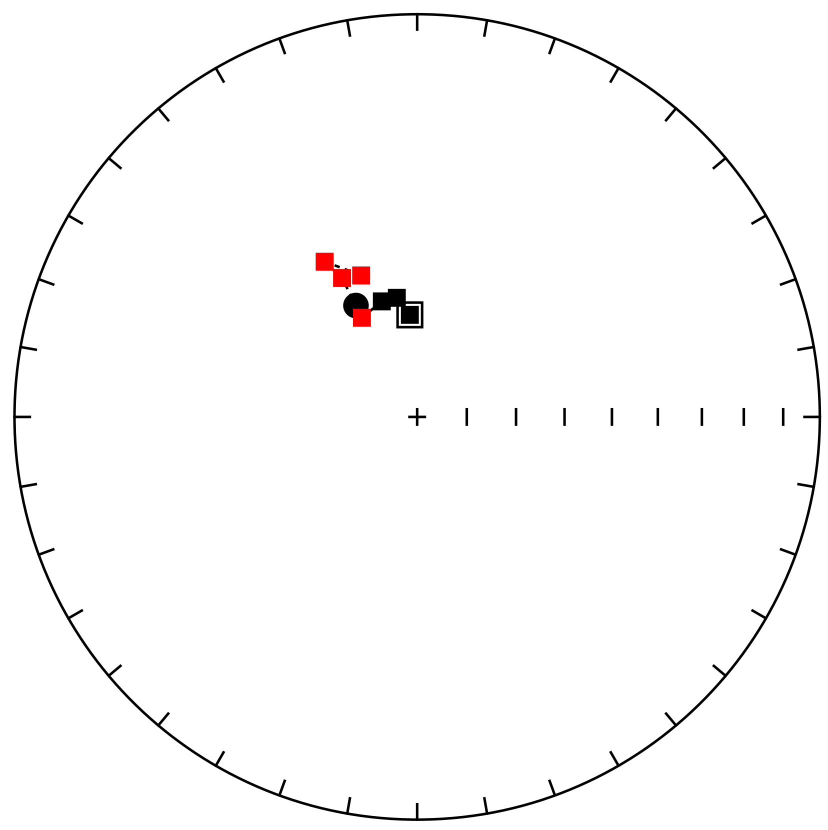

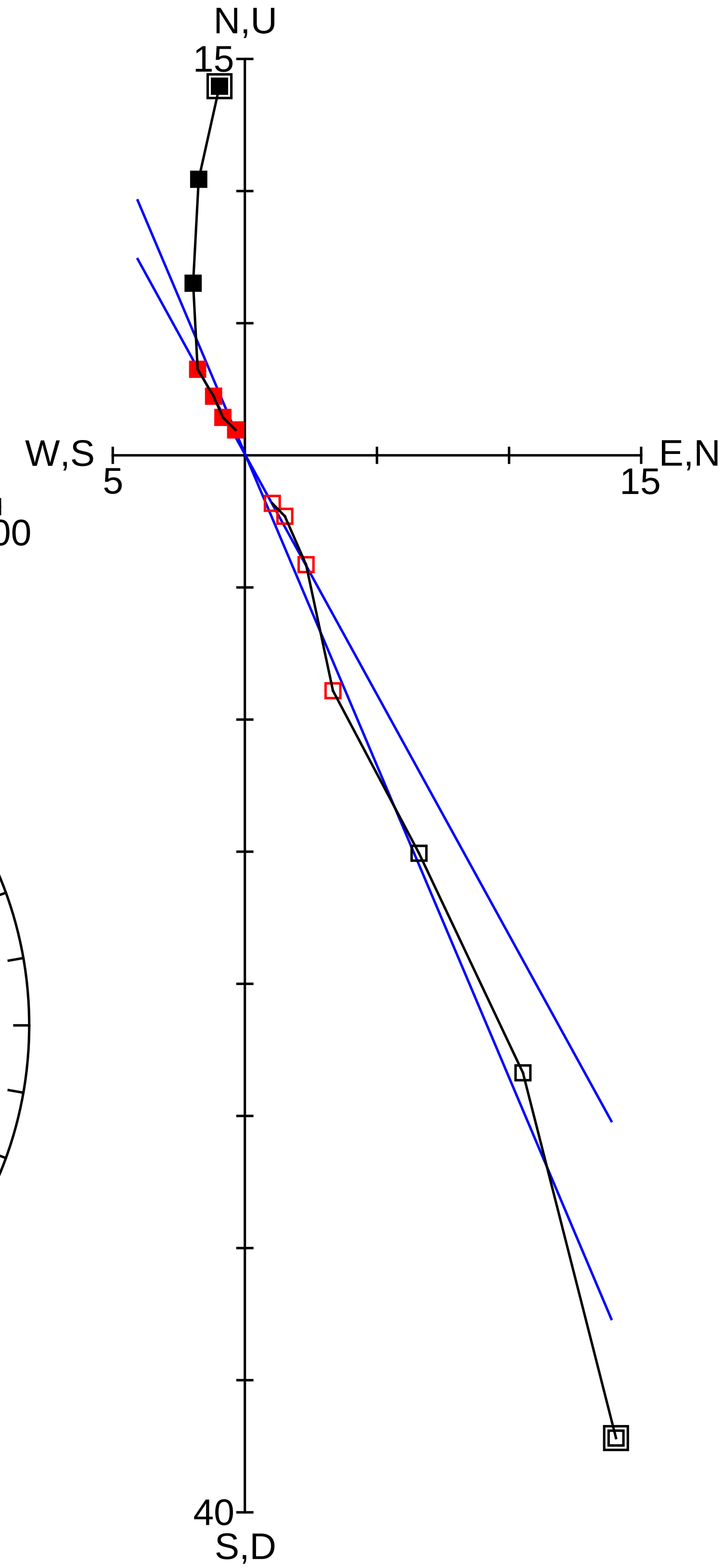

Sample: RL5-1
Site: Reade Lake Stock

PCA dec 311.87 / inc 67.12 Fisher dec 343.8 / inc 71.5 / a95 9.1 / k 33.1
PCA MAD1 16.53 / MAD3 5.38
(0.26 -0.29 0.92)t

vertical
horizontal
Units: A/m ×102

Updated July 2017

	demag.	dec.	inc.	int.	m.s.
	0	0.4	59.3	1.65e-01	NaN
	5	350.9	64.0	1.23e-01	NaN
	10	335.6	67.1	8.57e-02	NaN
*	20	318.7	67.7	5.30e-02	NaN
*	40	295.7	62.7	3.08e-02	NaN
*	80	318.3	74.3	1.60e-02	NaN
*	160	286.1	52.6	7.70e-03	NaN

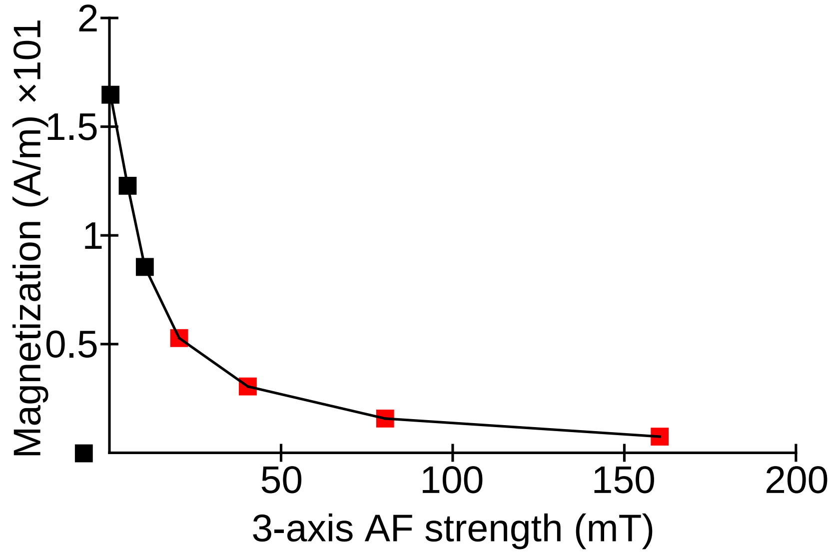

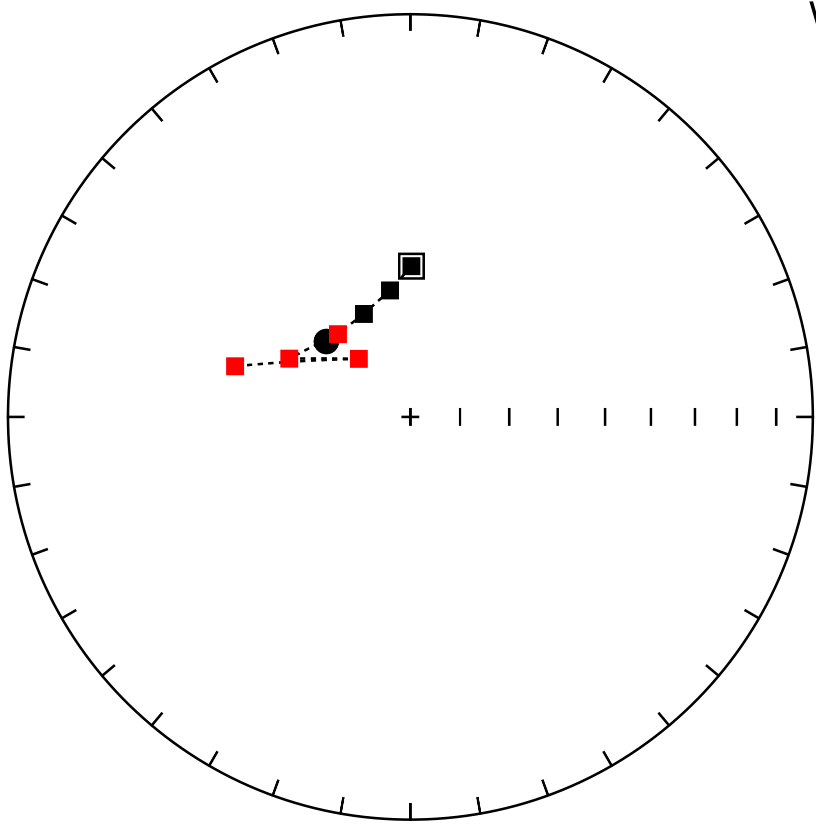

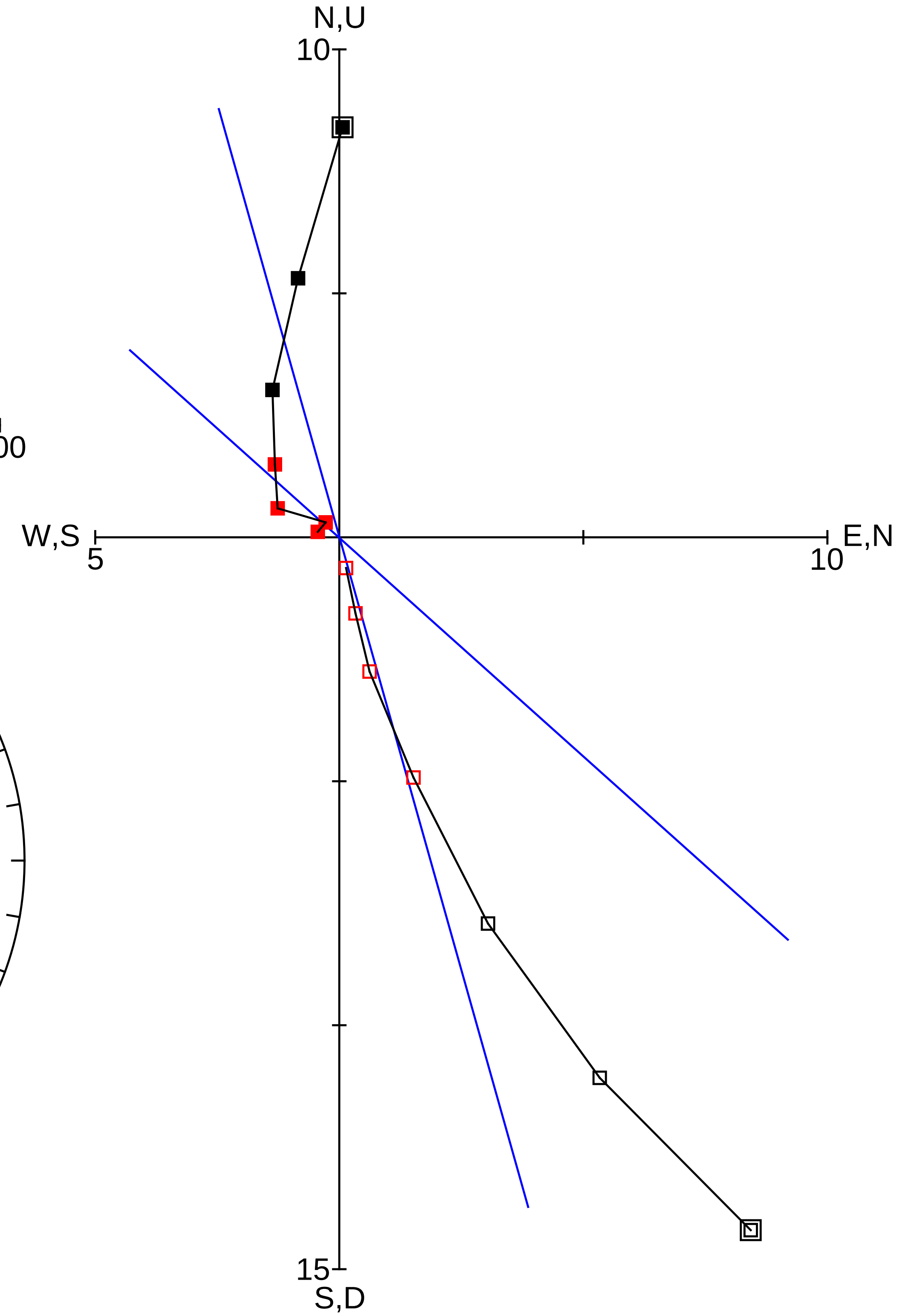

Sample: RL6-1
Site: Reade Lake Stock

PCA dec 344.88 / inc 51.87 Fisher dec 343.8 / inc 71.5 / a95 9.1 / k 33.1
PCA MAD1 18.01 / MAD3 2.92
(0.60 -0.16 0.79)t

□ vertical
■ horizontal
Units: A/m ×102

Updated July 2017

	demag.	dec.	inc.	int.	m.s.
	0	357.6	54.2	2.94e-01	NaN
	5	352.5	52.3	1.86e-01	NaN
*	10	346.6	51.9	1.19e-01	NaN
*	20	345.7	52.4	7.33e-02	NaN
*	40	338.6	50.9	3.77e-02	NaN
*	80	328.2	50.8	3.04e-02	NaN
*	160	332.1	42.6	1.74e-02	NaN

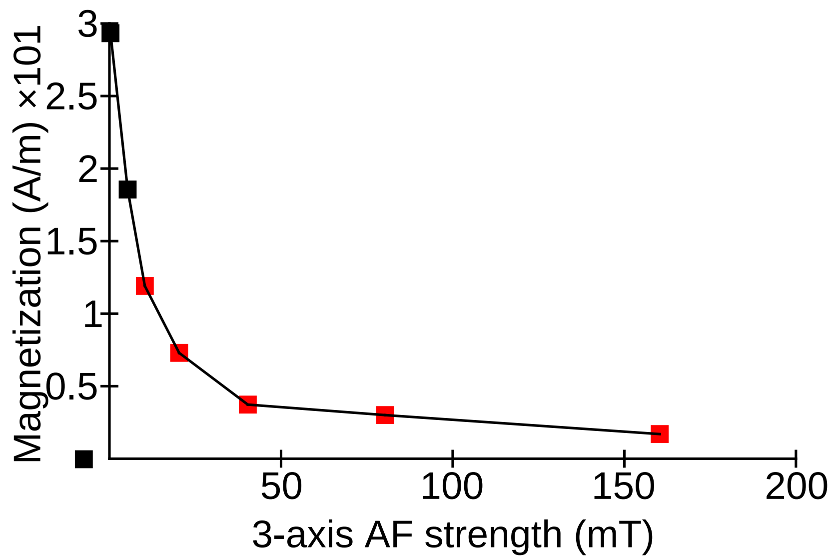

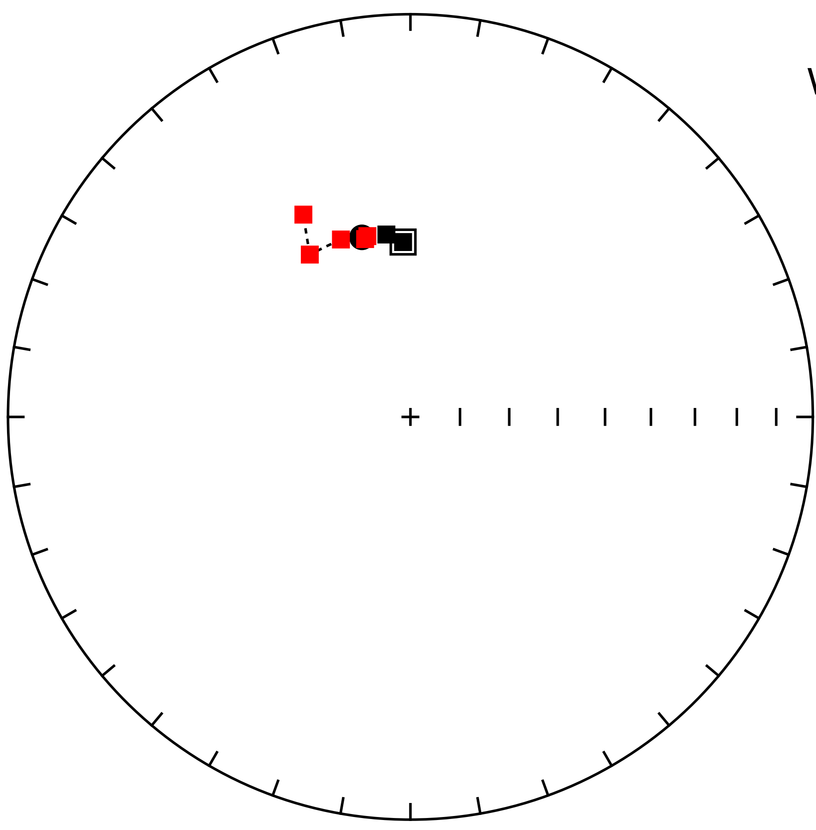

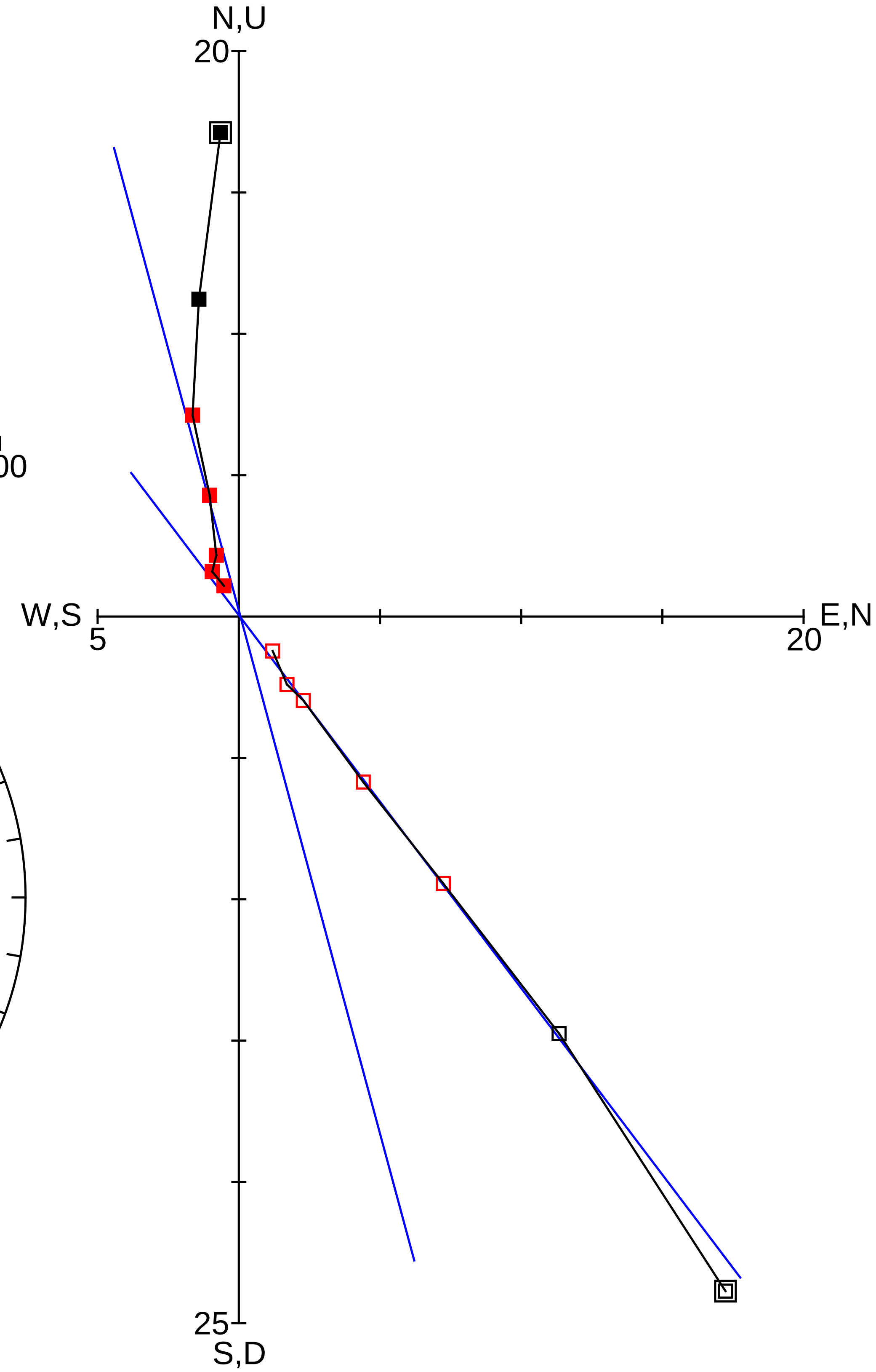

Sample: RL7-1

Site: Reade Lake Stock

PCA dec 318.34 / inc 66.65 Fisher dec 343.8 / inc 71.5 / a95 9.1 / k 33.1
PCA MAD1 20.09 / MAD3 3.71
(0.30 -0.26 0.92)t

□ vertical
■ horizontal
Units: A/m ×102

Updated July 2017

	demag.	dec.	inc.	int.	m.s.
	0	282.1	79.1	2.80e-01	NaN
	5	299.9	76.1	1.85e-01	NaN
	10	304.4	74.6	1.21e-01	NaN
*	20	316.5	67.5	8.16e-02	NaN
*	40	325.2	68.2	4.27e-02	NaN
*	80	318.5	55.2	2.81e-02	NaN
	160	340.6	78.4	1.05e-02	NaN

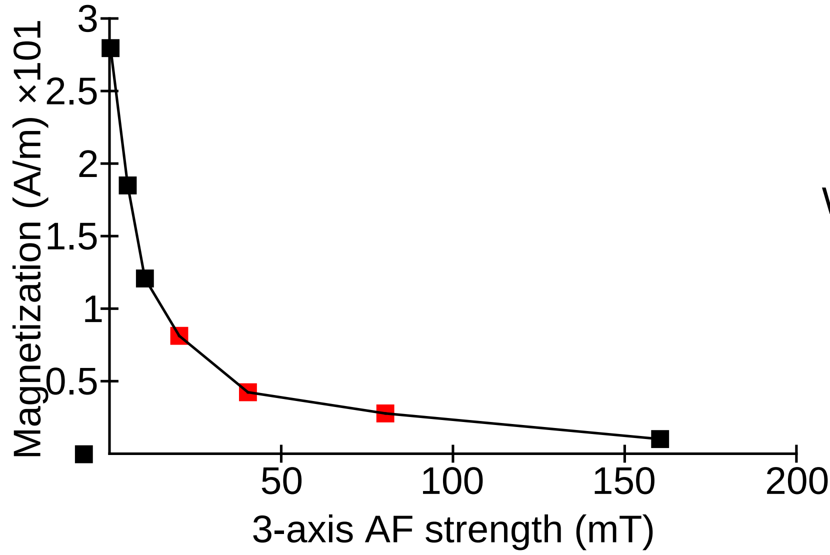

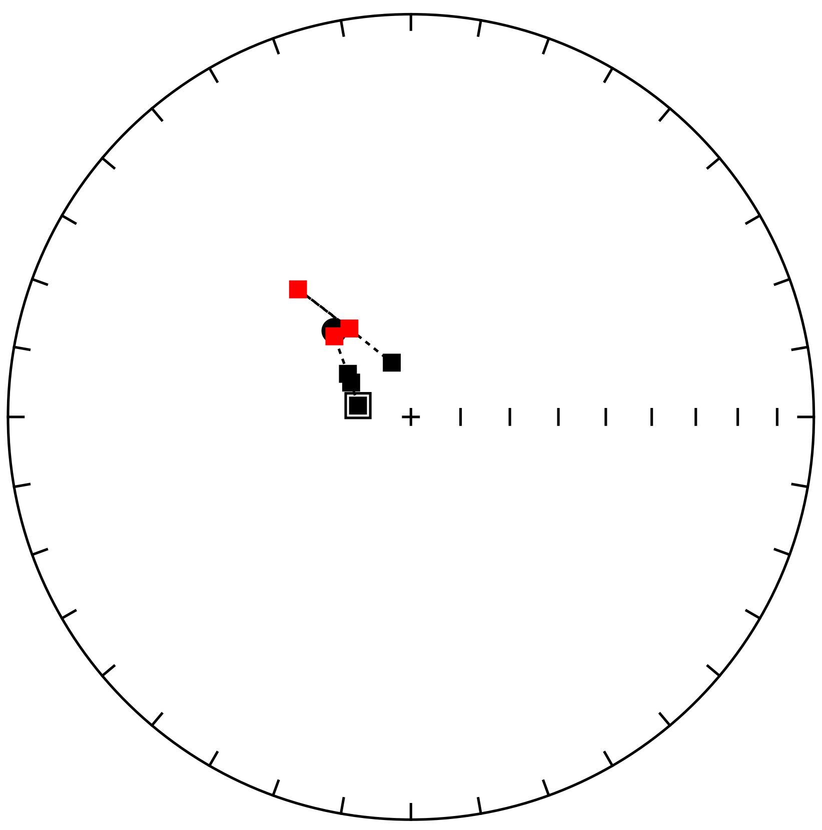

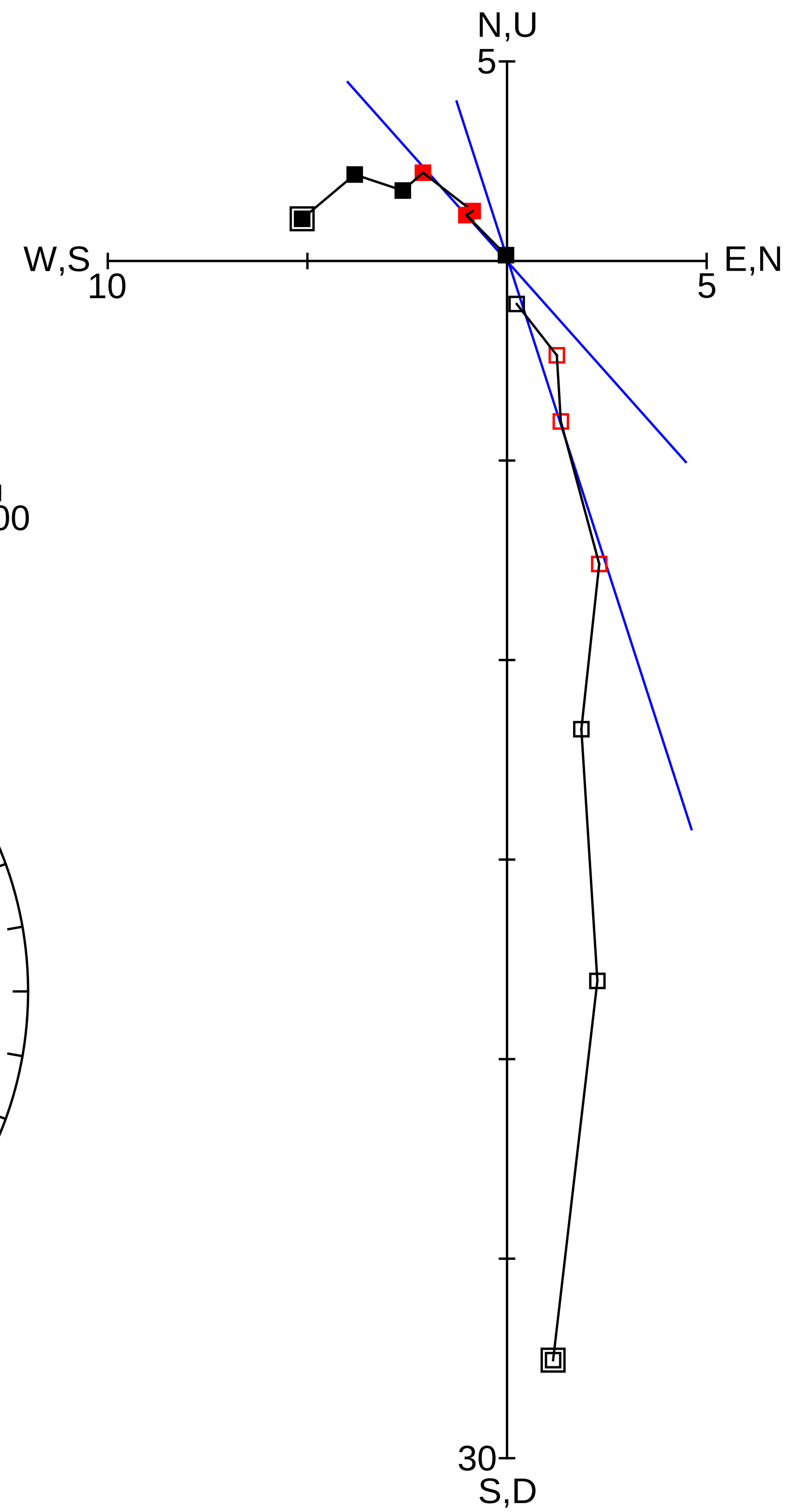

Sample: RL8-1

Site: Reade Lake Stock

PCA dec 352.57 / inc 69.47 Fisher dec 343.8 / inc 71.5 / a95 9.1 / k 33.1

PCA MAD1 7.99 / MAD3 2.68

(0.35 -0.05 0.94)t

□ vertical

■ horizontal

Units: A/m ×102

Updated July 2017

	demag.	dec.	inc.	int.	m.s.
	0	13.6	76.2	2.77e-01	NaN
	5	4.8	74.1	1.84e-01	NaN
*	10	354.6	70.7	1.08e-01	NaN
*	20	345.9	64.9	5.22e-02	NaN
*	40	352.1	65.6	2.47e-02	NaN
	80	7.9	54.9	1.65e-02	NaN
	160	325.7	35.0	1.42e-02	NaN

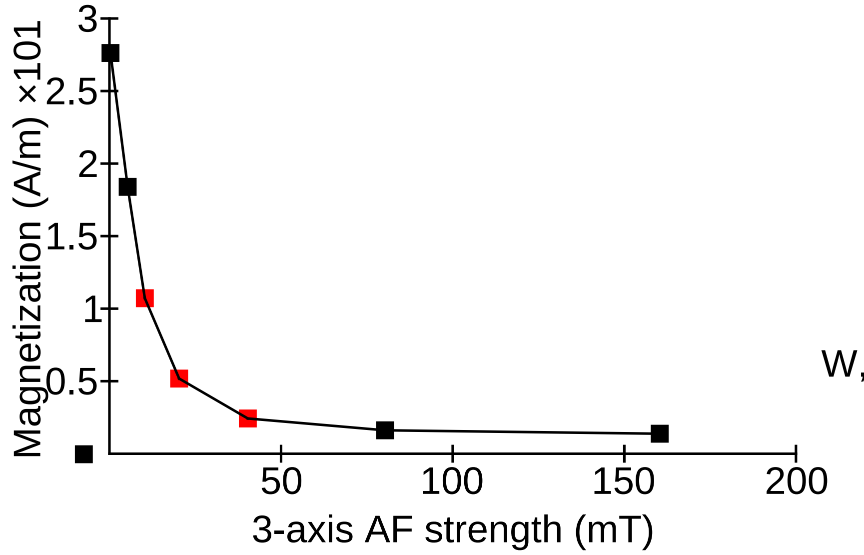

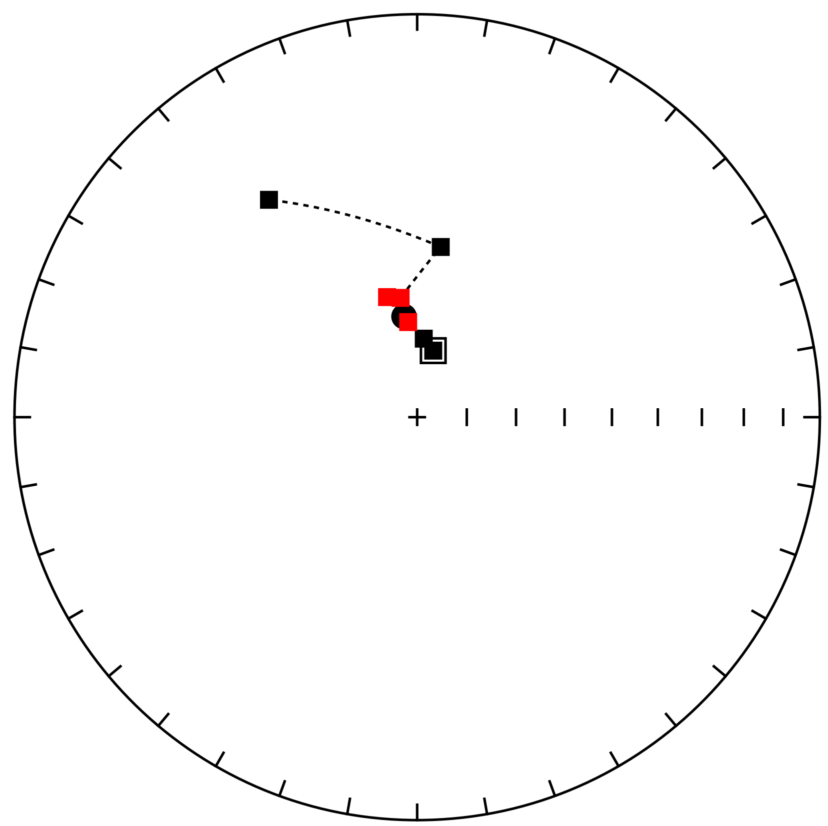

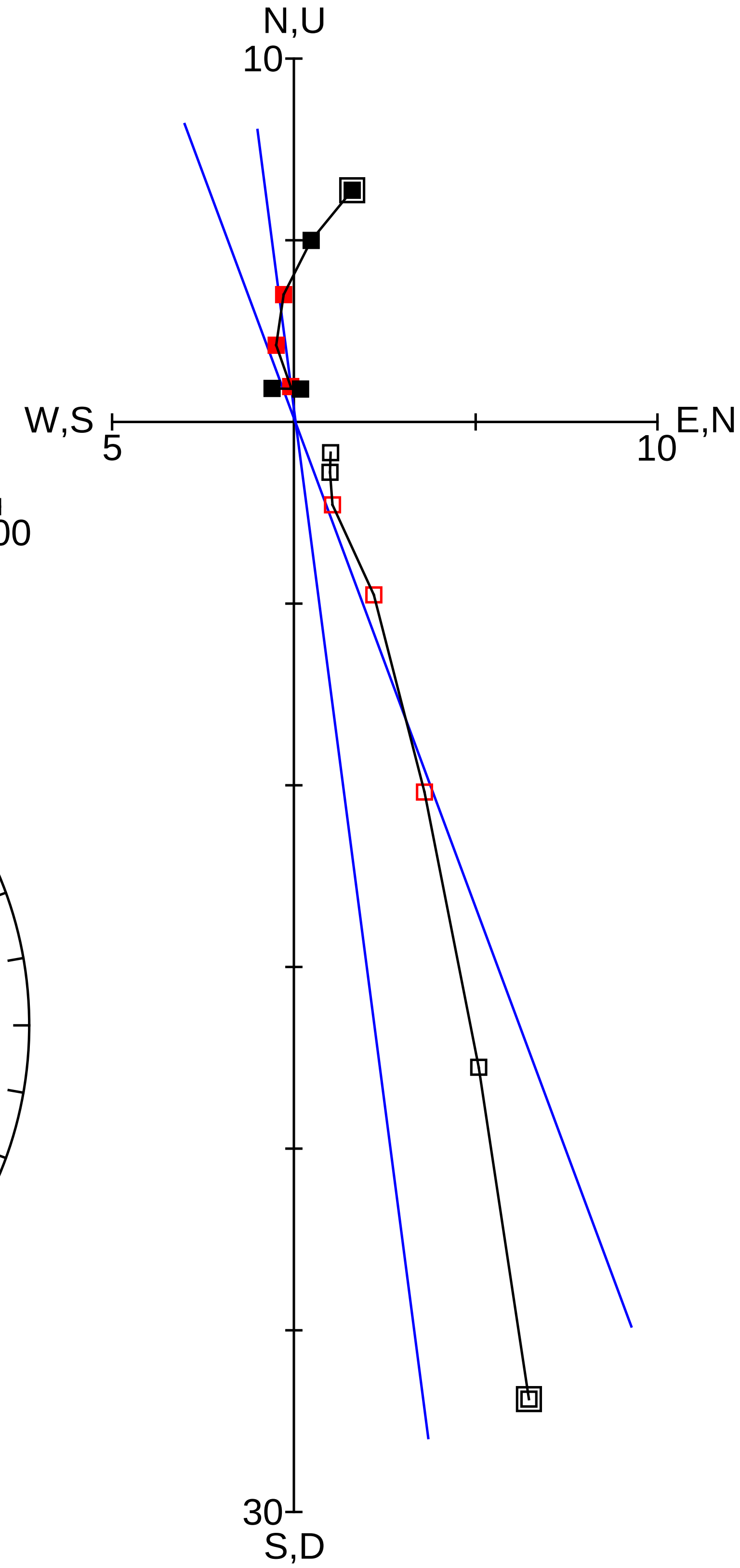

Sample: RL9-1

Site: Reade Lake Stock

PCA dec 92.96 / inc 85.08 Fisher dec 343.8 / inc 71.5 / a95 9.1 / k 33.1

PCA MAD1 13.56 / MAD3 1.85

(-0.00 0.09 1.00)t

□ vertical

■ horizontal

Units: A/m ×101

Updated July 2017

	demag.	dec.	inc.	int.	m.s.
	0	145.8	82.8	2.19e+00	NaN
	5	119.4	82.7	9.27e-01	NaN
*	10	99.1	84.6	3.72e-01	NaN
*	20	42.5	86.5	1.47e-01	NaN
*	40	46.2	83.6	5.80e-02	NaN
*	80	0.5	77.1	2.28e-02	NaN
	160	302.1	81.4	1.69e-02	NaN

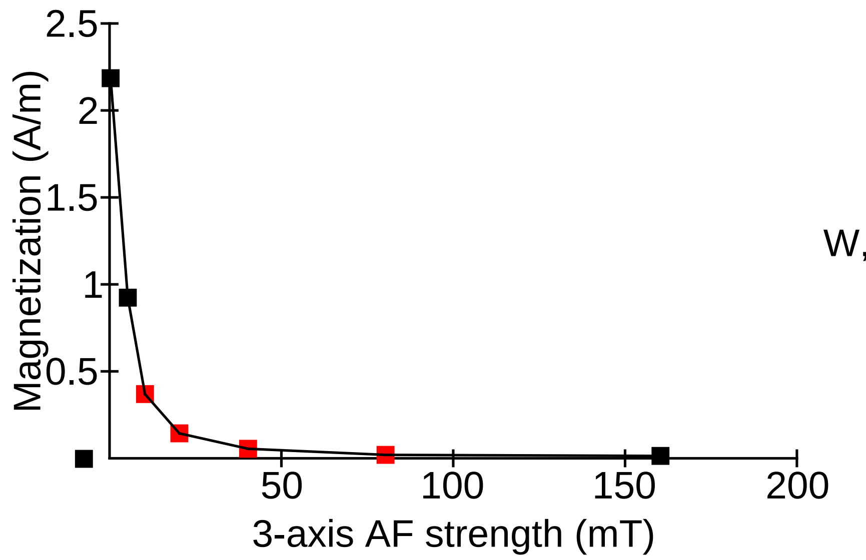

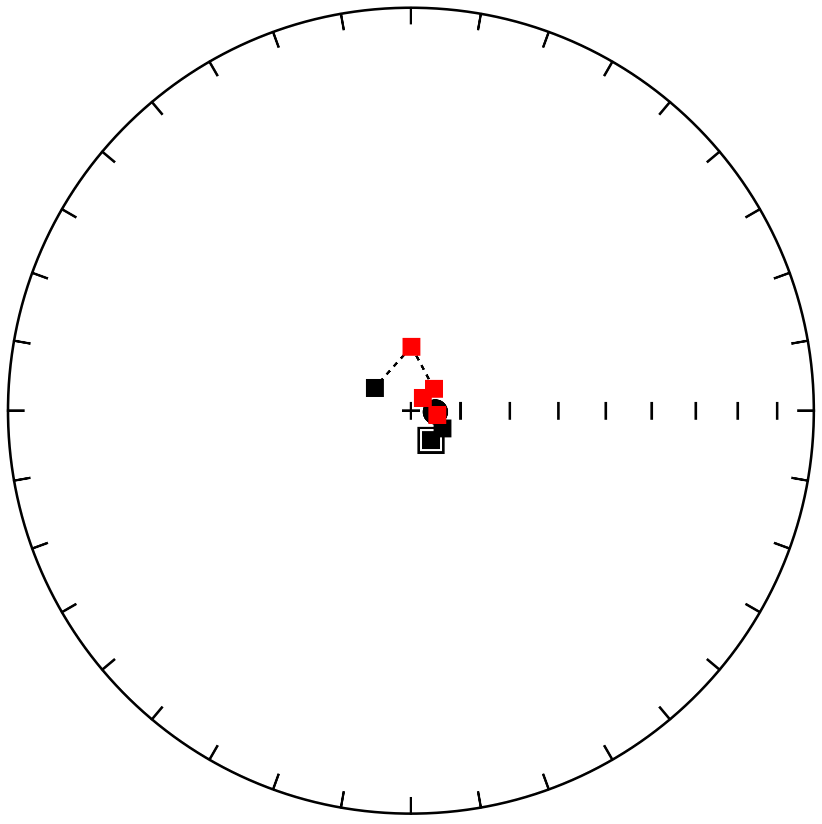

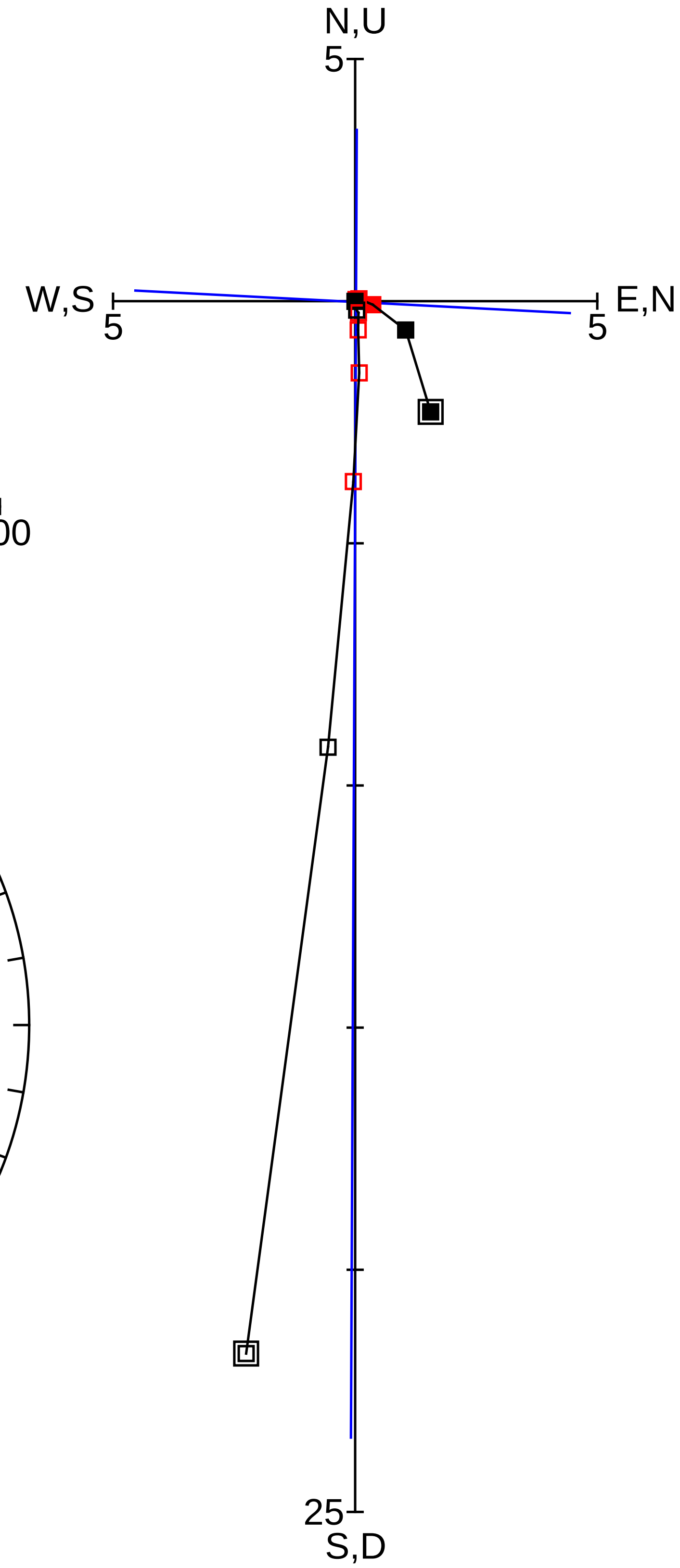

Sample: EWH1-1

Site: East Wild Horse

PCA dec 286.04 / inc 43.32 Fisher dec 289.8 / inc 43.8 / a95 8.7 / k 60.7

PCA MAD1 6.58 / MAD3 1.32

(0.20 -0.70 0.69)t

□ vertical

■ horizontal

Units: A/m ×102

Updated July 2017

	demag.	dec.	inc.	int.	m.s.
	0	304.8	56.1	2.25e-01	NaN
	5	296.2	48.7	1.90e-01	NaN
	10	293.0	45.4	1.63e-01	NaN
*	20	287.6	43.9	1.25e-01	NaN
*	40	284.5	42.9	9.75e-02	NaN
*	80	284.3	42.3	7.31e-02	NaN
	160	273.0	49.7	4.26e-02	NaN

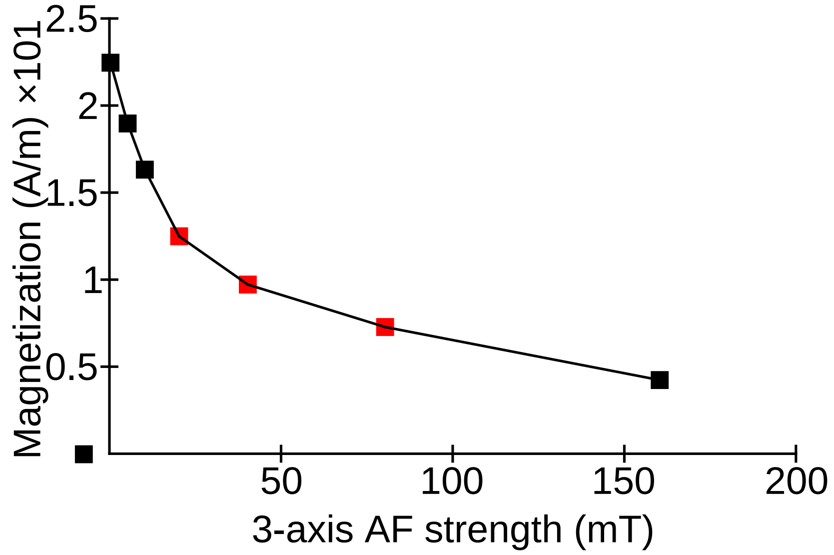

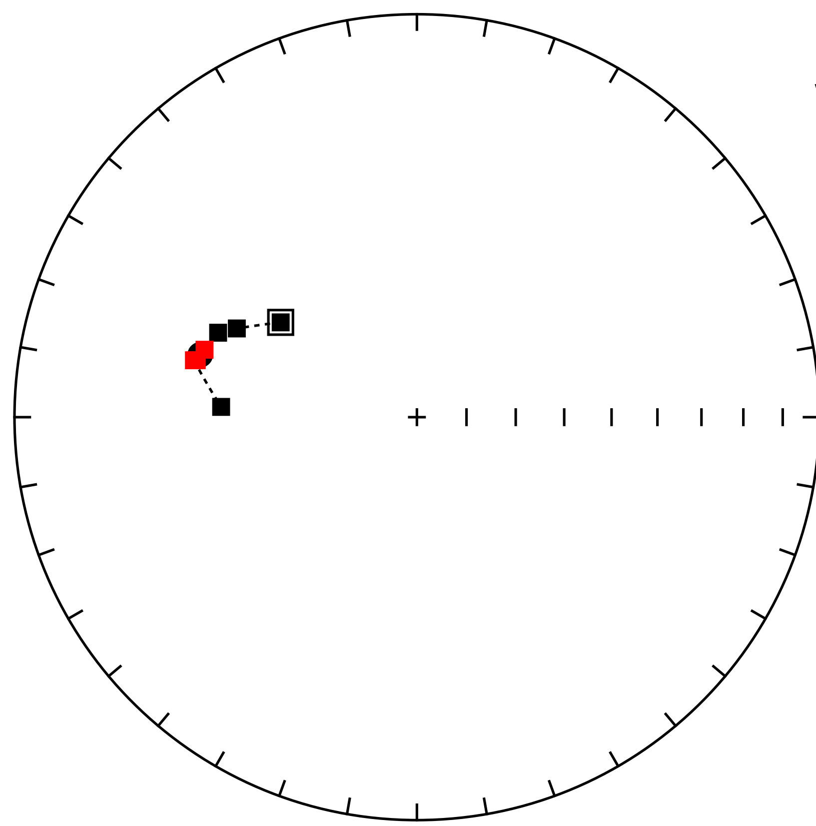

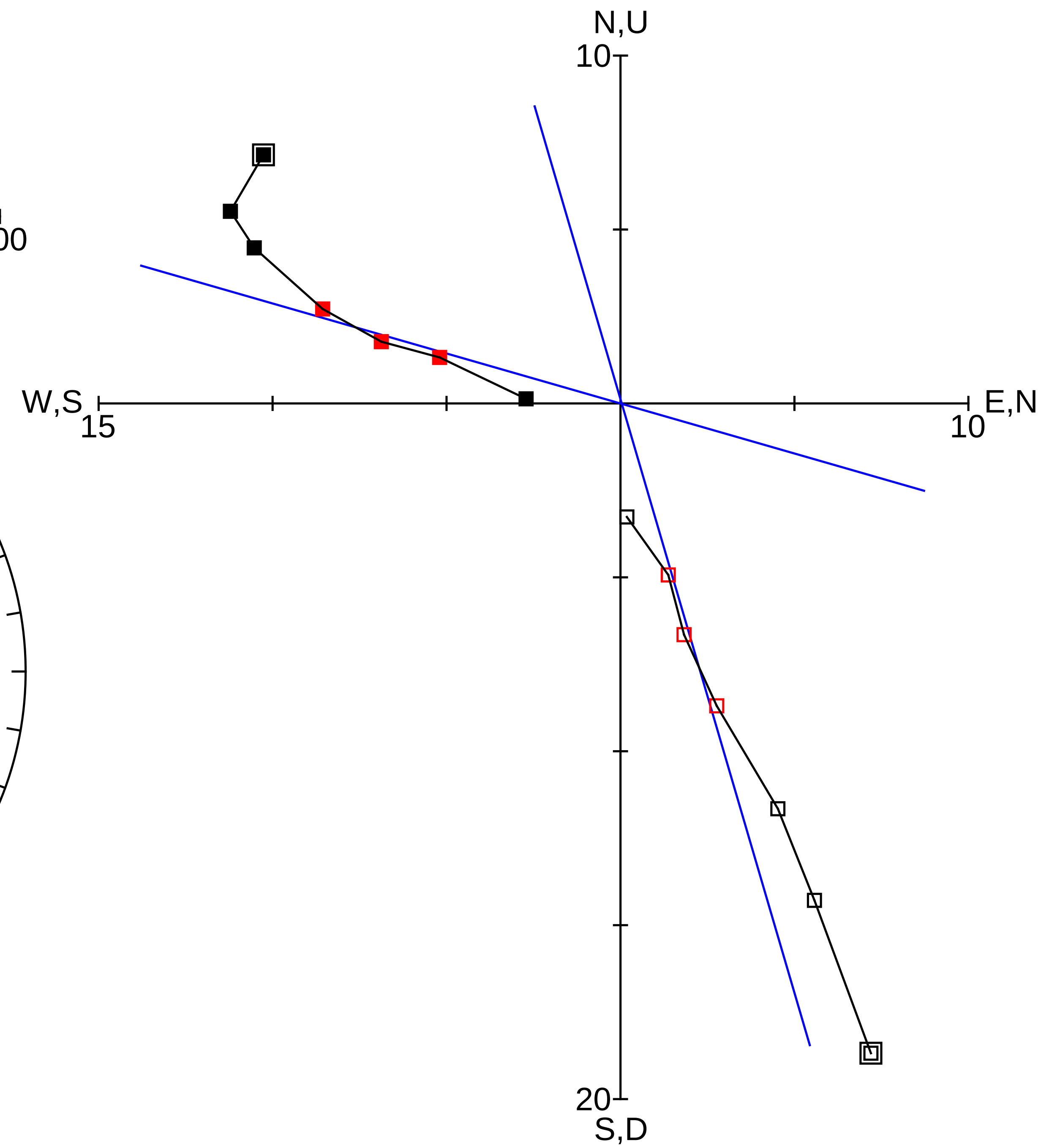

Sample: EWH3-3
Site: East Wild Horse

PCA dec 286.28 / inc 43.81 Fisher dec 289.8 / inc 43.8 / a95 8.7 / k 60.7
PCA MAD1 12.03 / MAD3 4.42
(0.20 -0.69 0.69)t

Updated July 2017

	demag.	dec.	inc.	int.	m.s.
	0	278.1	56.7	1.91e-01	NaN
*	5	286.5	48.0	1.63e-01	NaN
*	10	286.1	44.9	1.42e-01	NaN
*	20	286.3	42.6	1.12e-01	NaN
*	40	285.3	36.5	8.85e-02	NaN
*	80	284.8	36.2	7.41e-02	NaN
*	160	291.8	35.6	4.98e-02	NaN

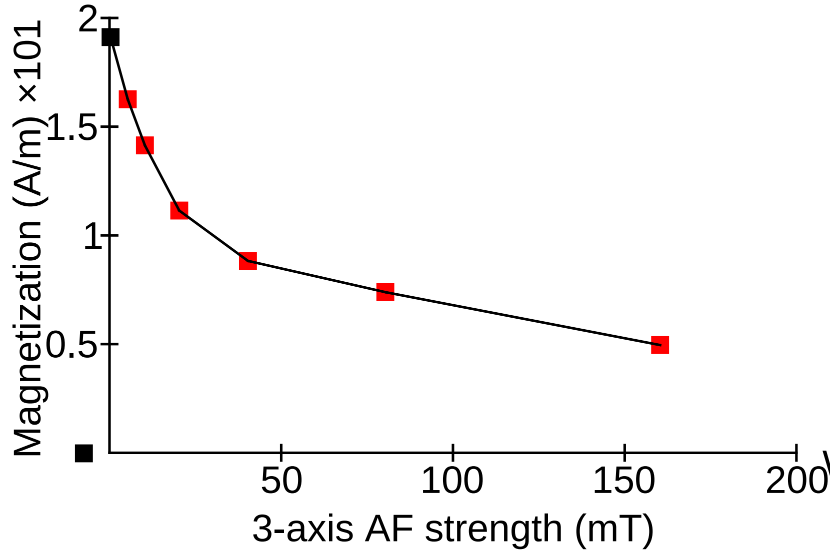

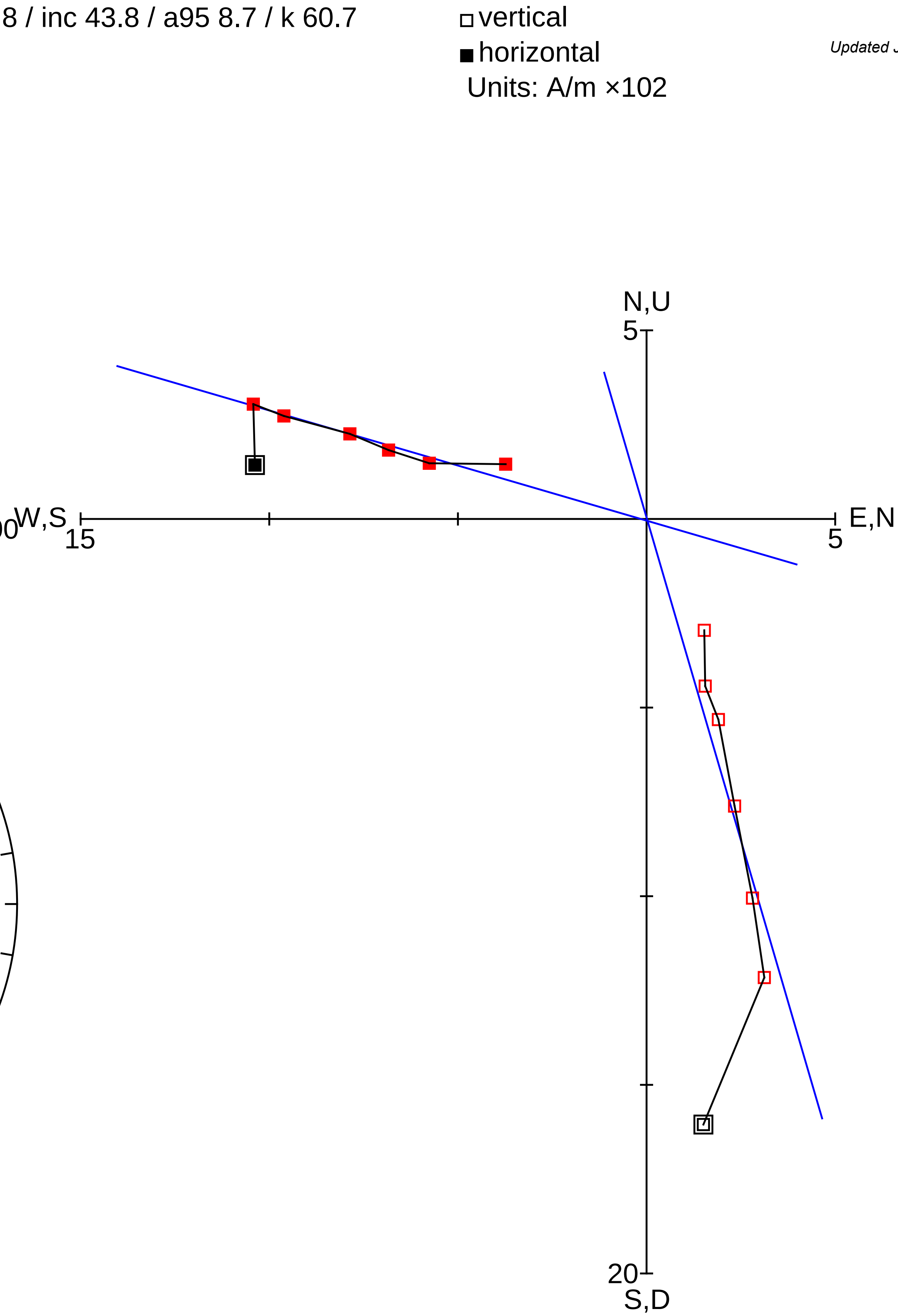

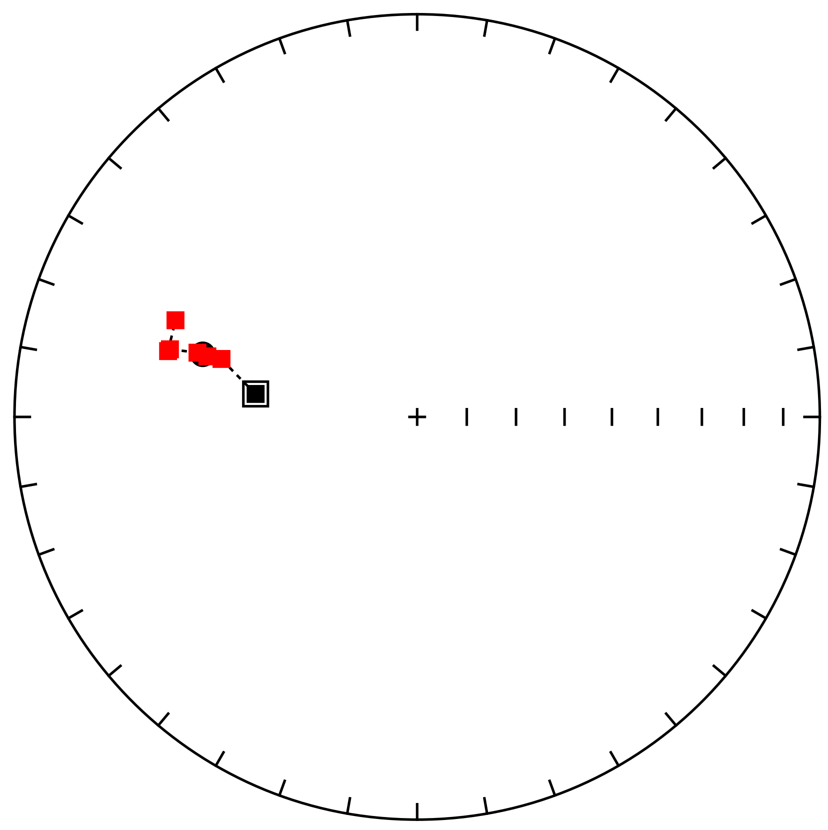

Sample: EWH5-1

Site: East Wild Horse

PCA dec 292.99 / inc 47.88 Fisher dec 289.8 / inc 43.8 / a95 8.7 / k 60.7

PCA MAD1 27.05 / MAD3 1.94

(0.26 -0.62 0.74)t

□ vertical

■ horizontal

Units: A/m ×102

Updated July 2017

	demag.	dec.	inc.	int.	m.s.
	0	305.5	62.0	2.60e-01	NaN
	5	297.8	53.3	1.88e-01	NaN
*	10	293.8	49.2	1.49e-01	NaN
*	20	292.6	47.7	1.12e-01	NaN
*	40	290.1	44.9	7.95e-02	NaN
*	80	292.6	46.0	5.19e-02	NaN
*	160	298.8	44.7	3.55e-02	NaN

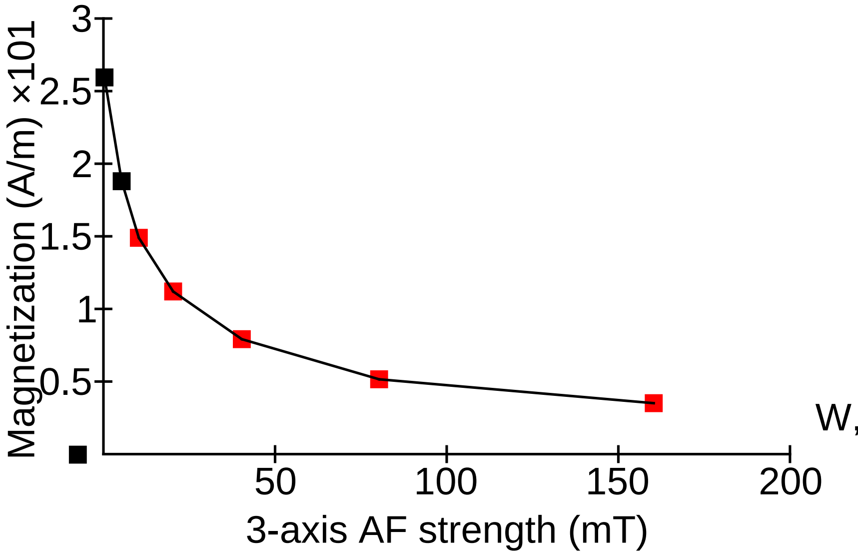

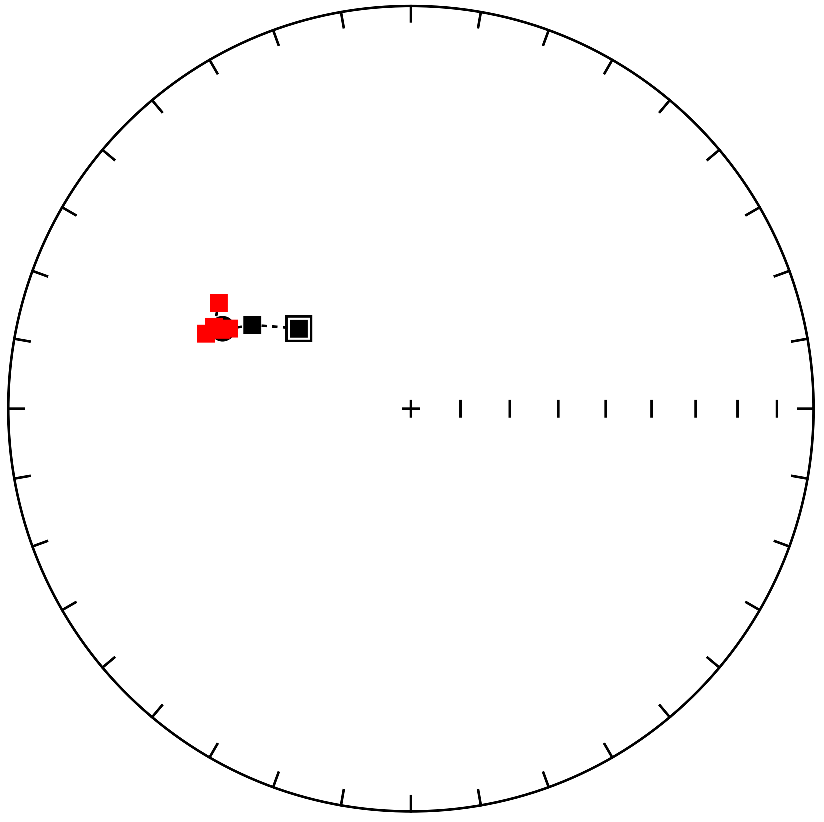

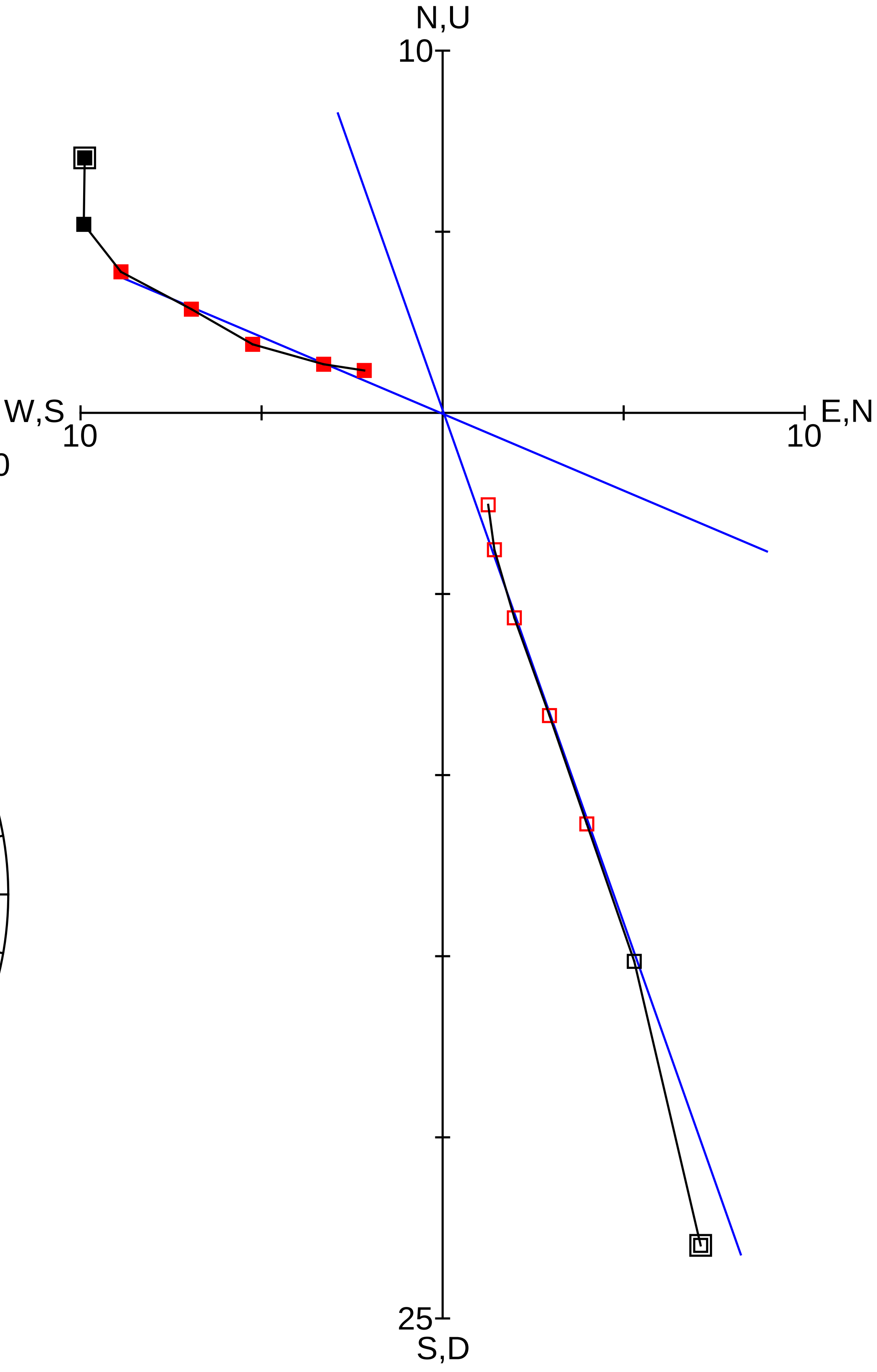

Sample: EWH6-1
Site: East Wild Horse

PCA dec 290.84 / inc 52.68 Fisher dec 289.8 / inc 43.8 / a95 8.7 / k 60.7
PCA MAD1 24.91 / MAD3 1.81
(0.22 -0.57 0.80)t

Updated July 2017

	demag.	dec.	inc.	int.	m.s.
	0	279.7	60.9	2.20e-01	NaN
*	5	291.1	53.9	1.76e-01	NaN
*	10	291.2	52.7	1.42e-01	NaN
*	20	290.3	49.5	9.78e-02	NaN
*	40	291.7	49.7	5.84e-02	NaN
*	80	283.1	54.0	4.08e-02	NaN
	160	276.1	28.1	1.82e-02	NaN

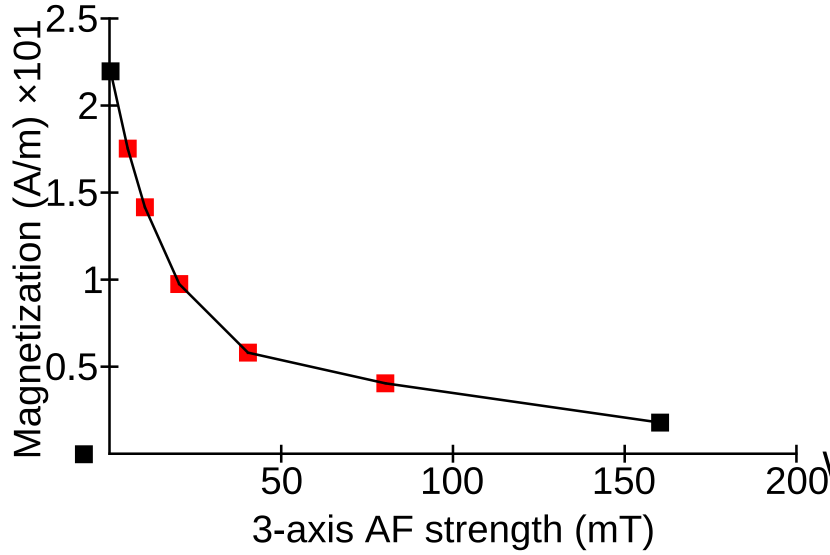

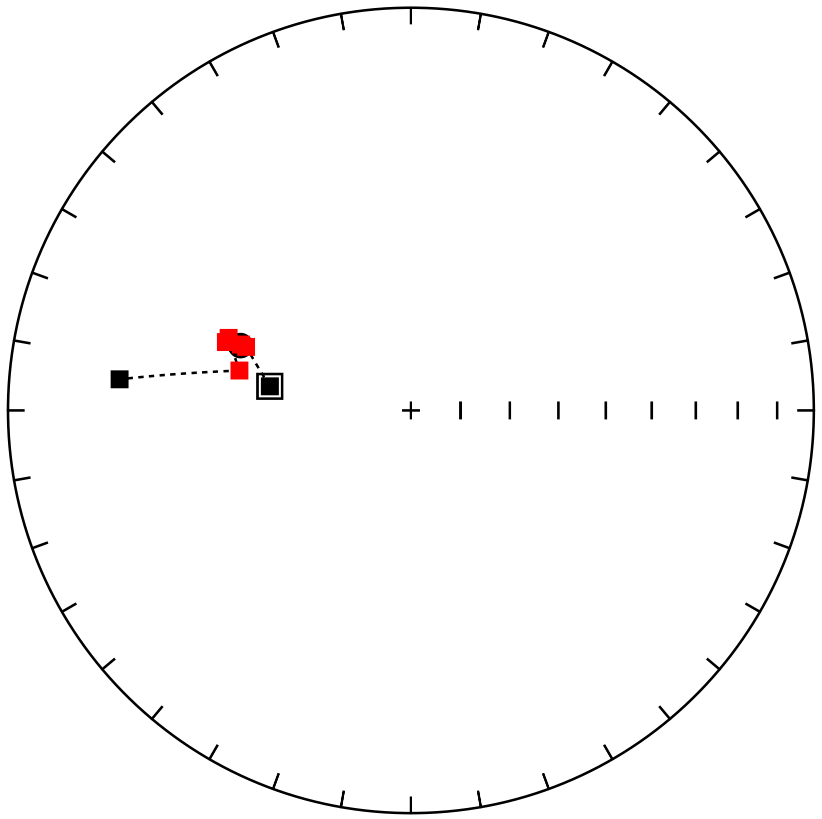

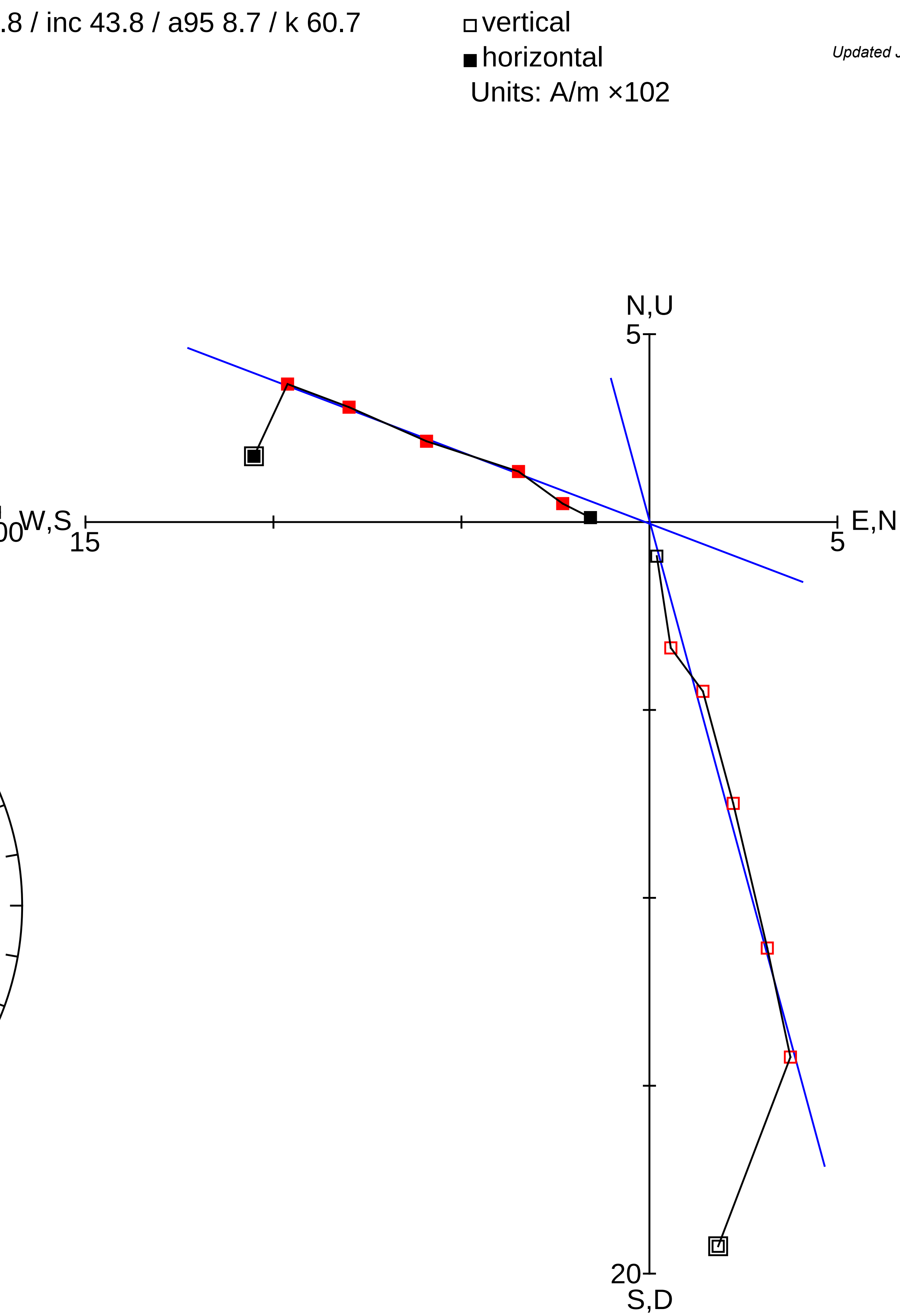

Sample: EWH6-2

Site: East Wild Horse

PCA dec 293.90 / inc 50.18 Fisher dec 289.8 / inc 43.8 / a95 8.7 / k 60.7
PCA MAD1 12.98 / MAD3 1.61
(0.26 -0.59 0.77)t

□ vertical
■ horizontal
Units: A/m ×102

Updated July 2017

	demag.	dec.	inc.	int.	m.s.
	0	294.2	54.2	2.55e-01	NaN
*	5	295.5	51.3	2.39e-01	NaN
*	10	293.5	49.8	2.02e-01	NaN
*	20	290.9	48.6	1.39e-01	NaN
*	40	291.7	48.0	7.86e-02	NaN
*	80	294.2	46.6	4.25e-02	NaN
	160	275.8	37.4	2.47e-02	NaN

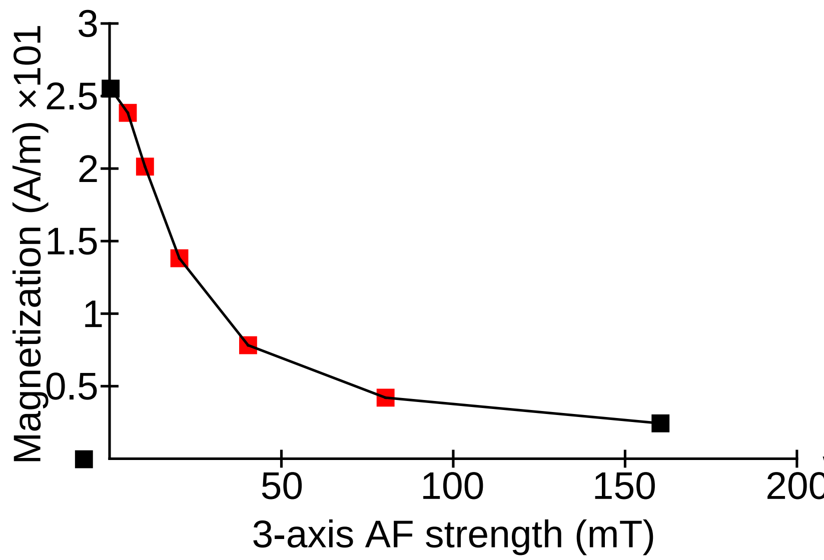

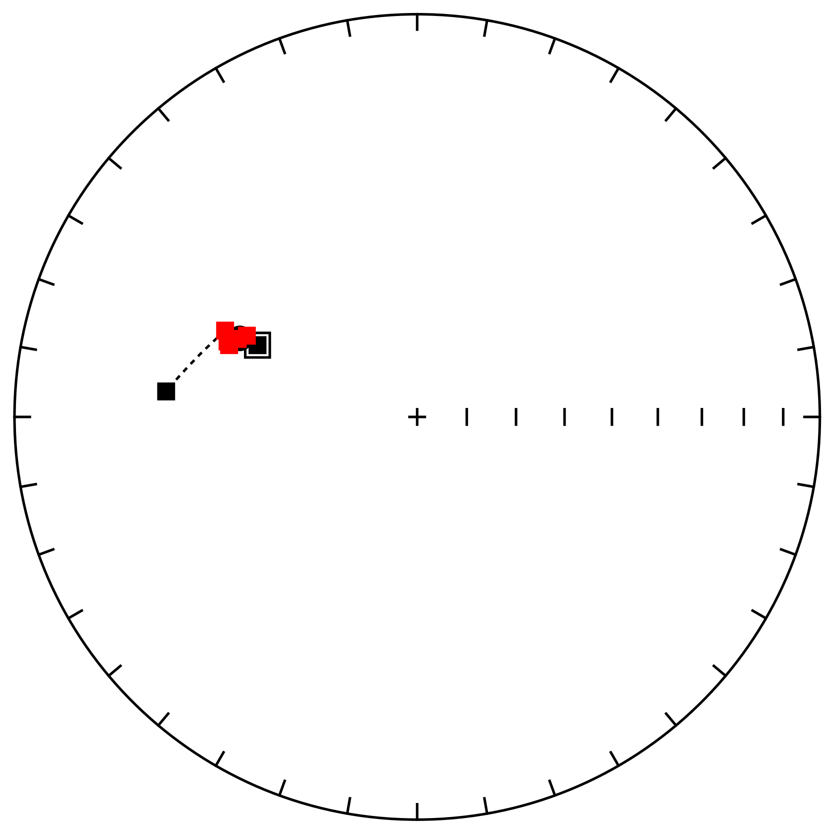

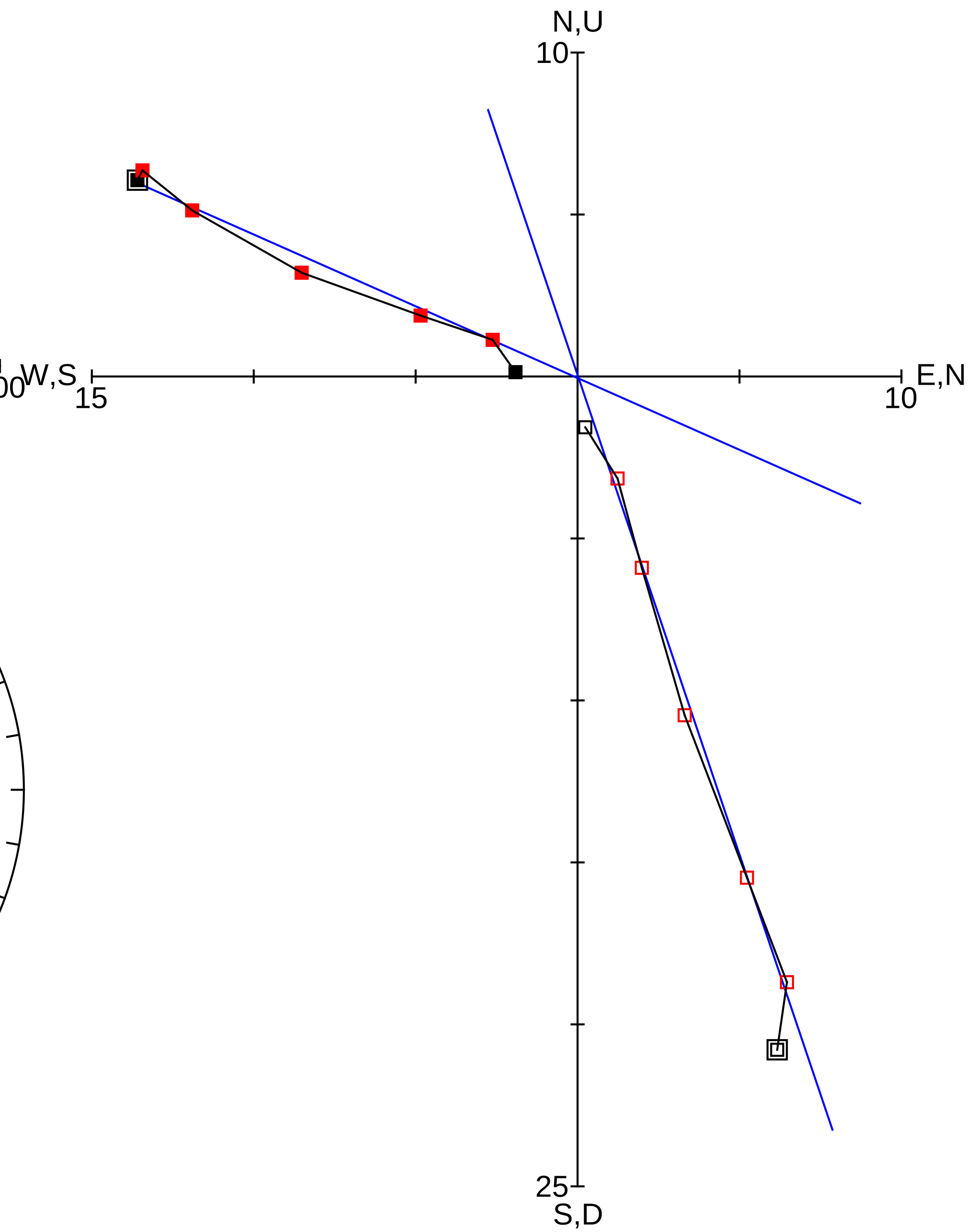

Sample: EWH7-1

Site: East Wild Horse

PCA dec 289.81 / inc 24.28 Fisher dec 289.8 / inc 43.8 / a95 8.7 / k 60.7
PCA MAD1 26.95 / MAD3 2.80
(0.31 -0.86 0.41)t

□ vertical
■ horizontal
Units: A/m ×102

Updated July 2017

	demag.	dec.	inc.	int.	m.s.
	0	301.8	10.8	1.78e-01	NaN
	5	295.4	18.7	1.38e-01	NaN
*	10	292.1	23.7	1.08e-01	NaN
*	20	289.5	25.8	8.02e-02	NaN
*	40	285.4	22.0	5.64e-02	NaN
*	80	288.2	25.7	4.16e-02	NaN
*	160	283.3	25.2	3.52e-02	NaN

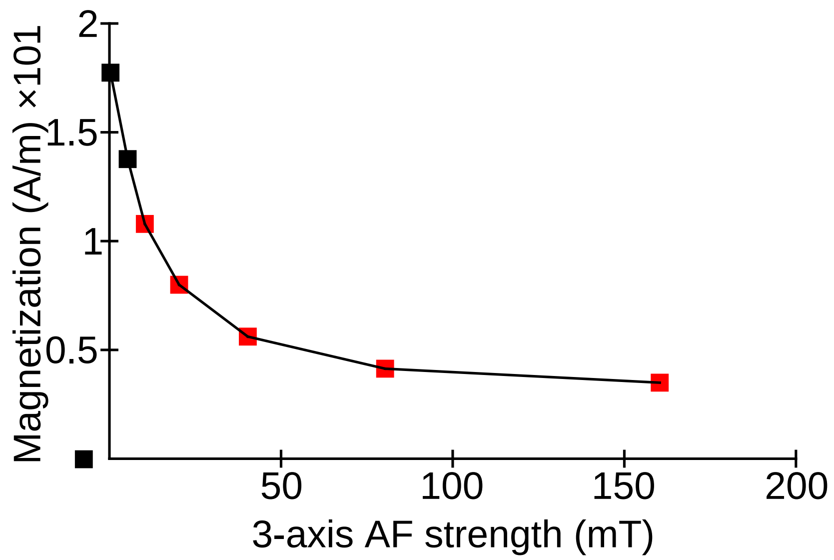

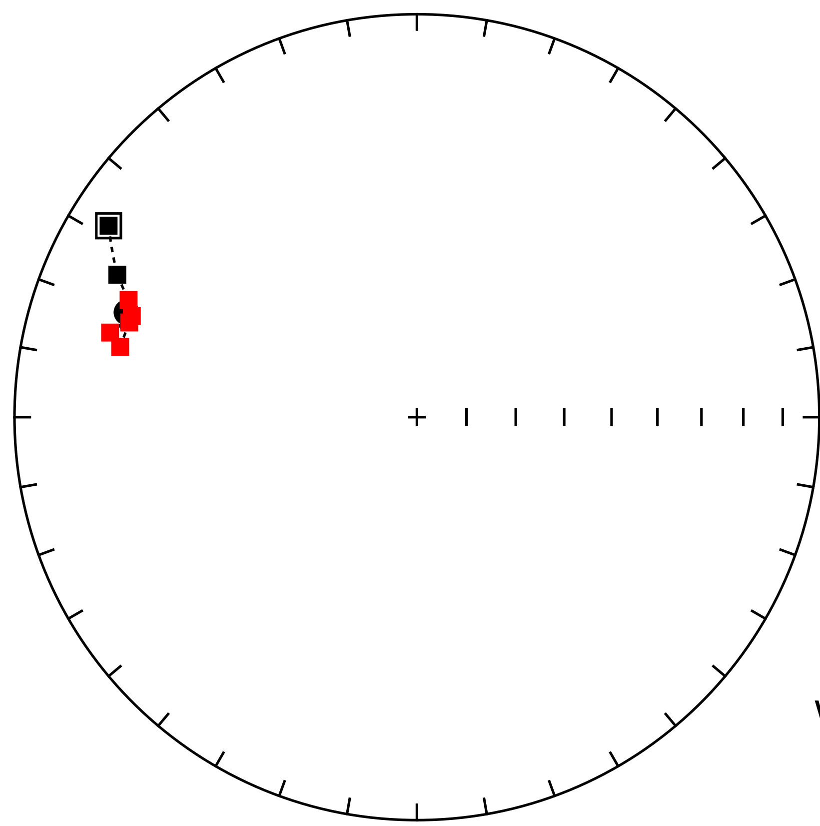

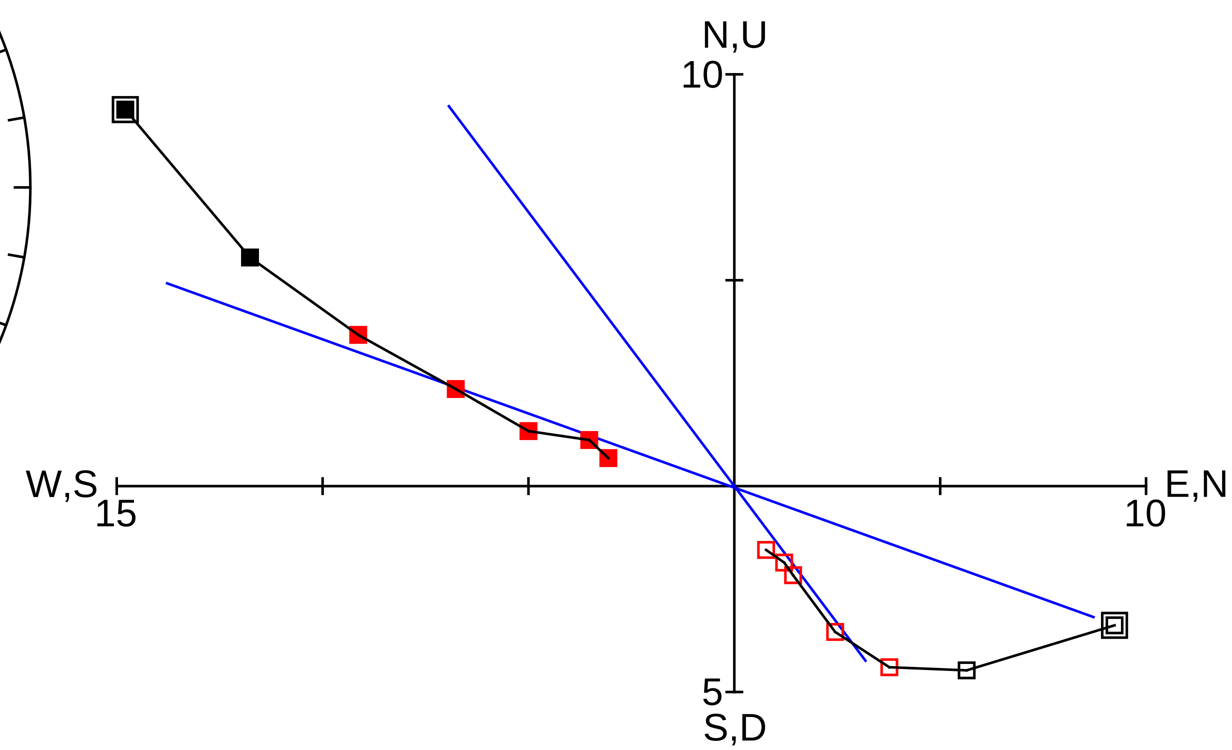

Sample: IS2-2

Site: Innis Springs

PCA dec 354.44 / inc 74.12 Fisher dec 337.0 / inc 66.6 / a95 15.3 / k 20.0

PCA MAD1 7.45 / MAD3 5.33

(0.27 -0.03 0.96)t

□ vertical

■ horizontal

Units: A/m ×102

Updated July 2017

	demag.	dec.	inc.	int.	m.s.
	0	11.7	57.5	2.92e-01	NaN
*	10	356.7	71.6	8.01e-02	NaN
*	20	355.8	77.6	3.51e-02	NaN
*	30	311.1	84.2	2.22e-02	NaN
*	40	267.3	82.9	1.69e-02	NaN
*	60	297.7	82.6	1.34e-02	NaN
	80	230.3	76.1	1.06e-02	NaN
	100	252.6	57.7	6.52e-03	NaN

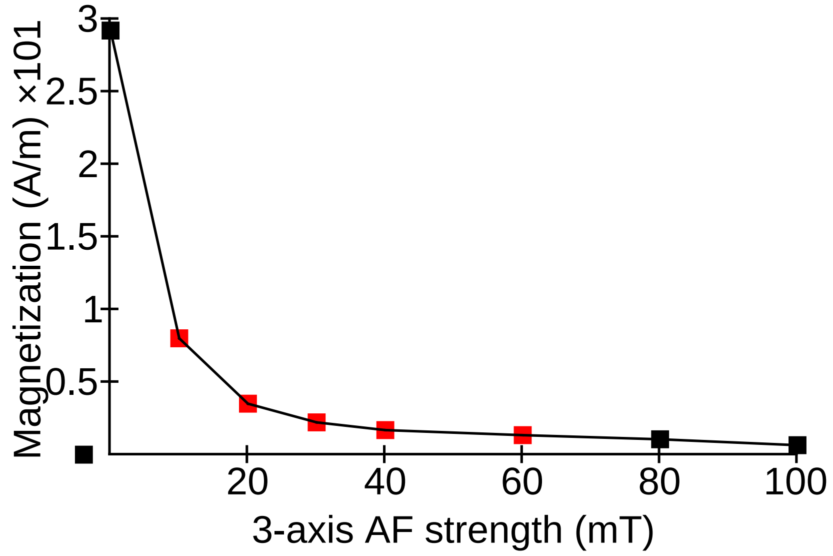

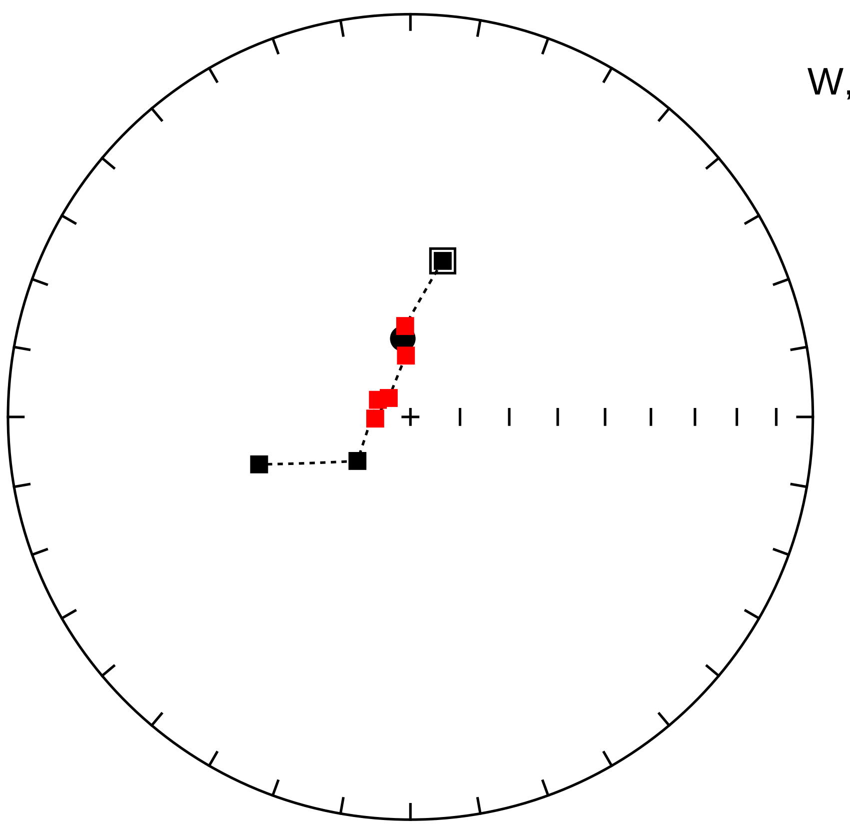

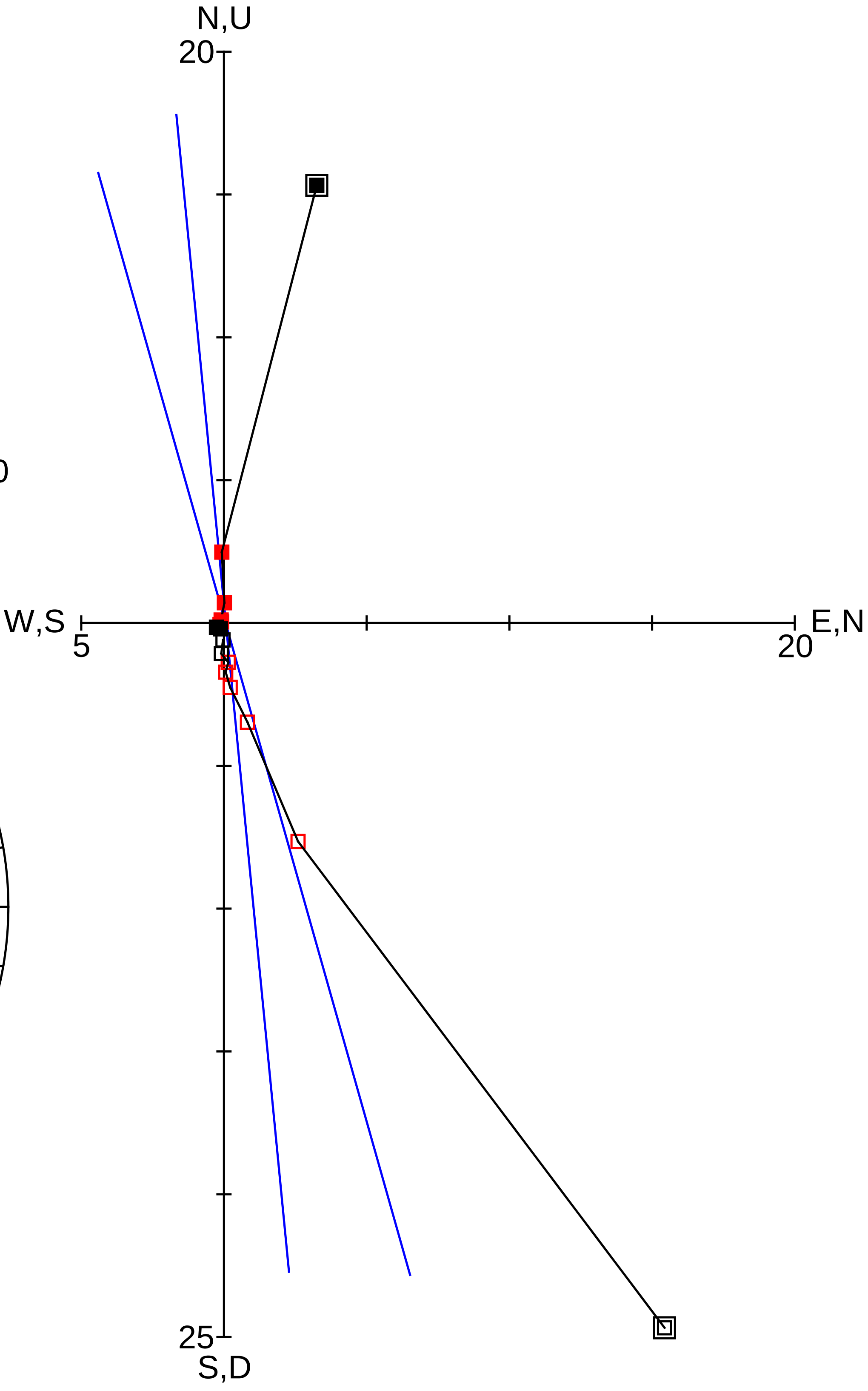

Sample: IS3-1
Site: Innis Springs

PCA dec 3.38 / inc 52.69 Fisher dec 337.0 / inc 66.6 / a95 15.3 / k 20.0
PCA MAD1 33.64 / MAD3 9.77
(0.61 0.04 0.80)t

□ vertical
■ horizontal
Units: A/m ×101

Updated July 2017

	demag.	dec.	inc.	int.	m.s.
	0	334.5	-44.5	1.79e+00	NaN
	5	347.0	-27.8	3.36e-01	NaN
	10	353.2	12.8	6.28e-02	NaN
*	20	0.3	56.7	2.63e-02	NaN
*	40	353.0	43.8	1.57e-02	NaN
*	80	29.8	44.5	1.31e-02	NaN
	160	24.6	19.9	8.28e-03	NaN

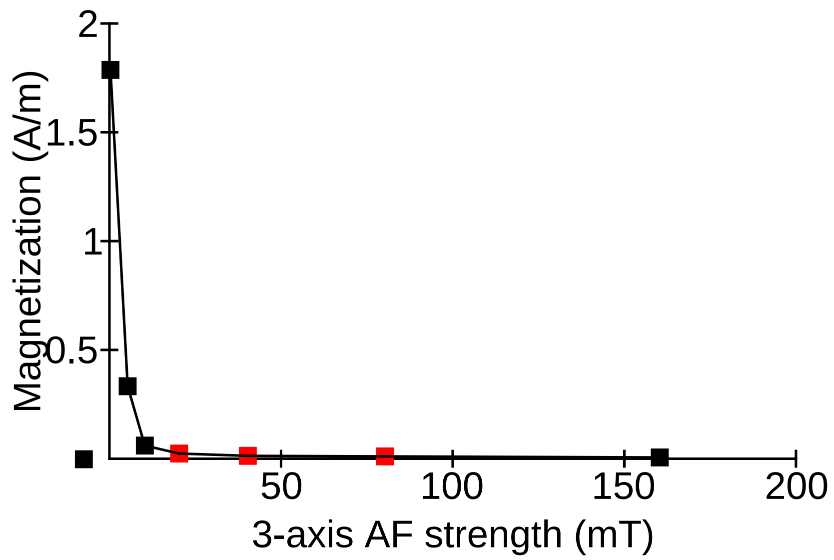

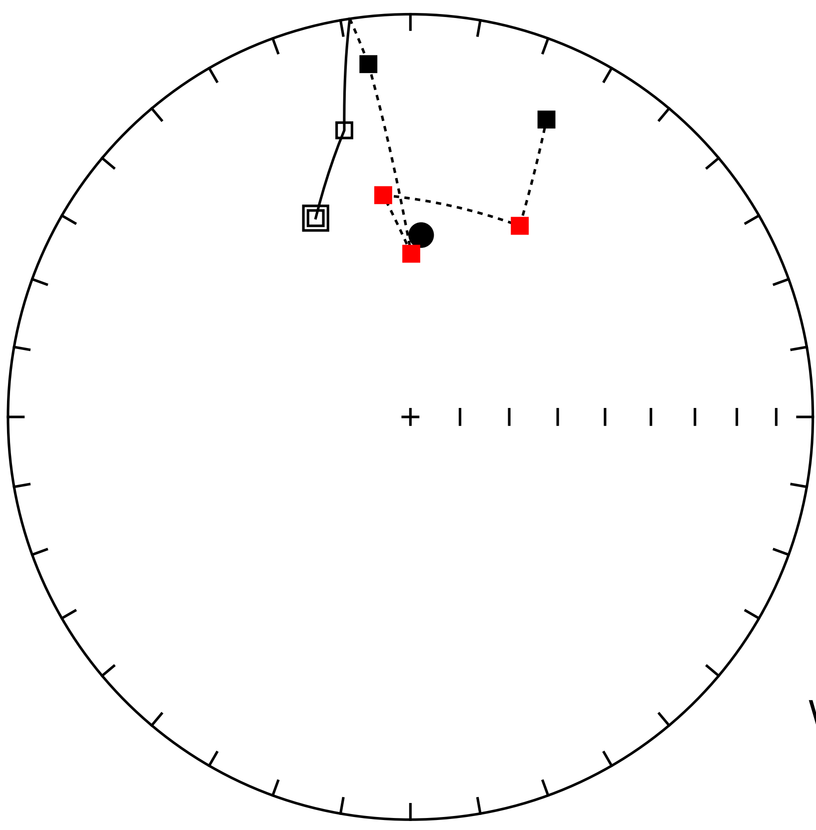

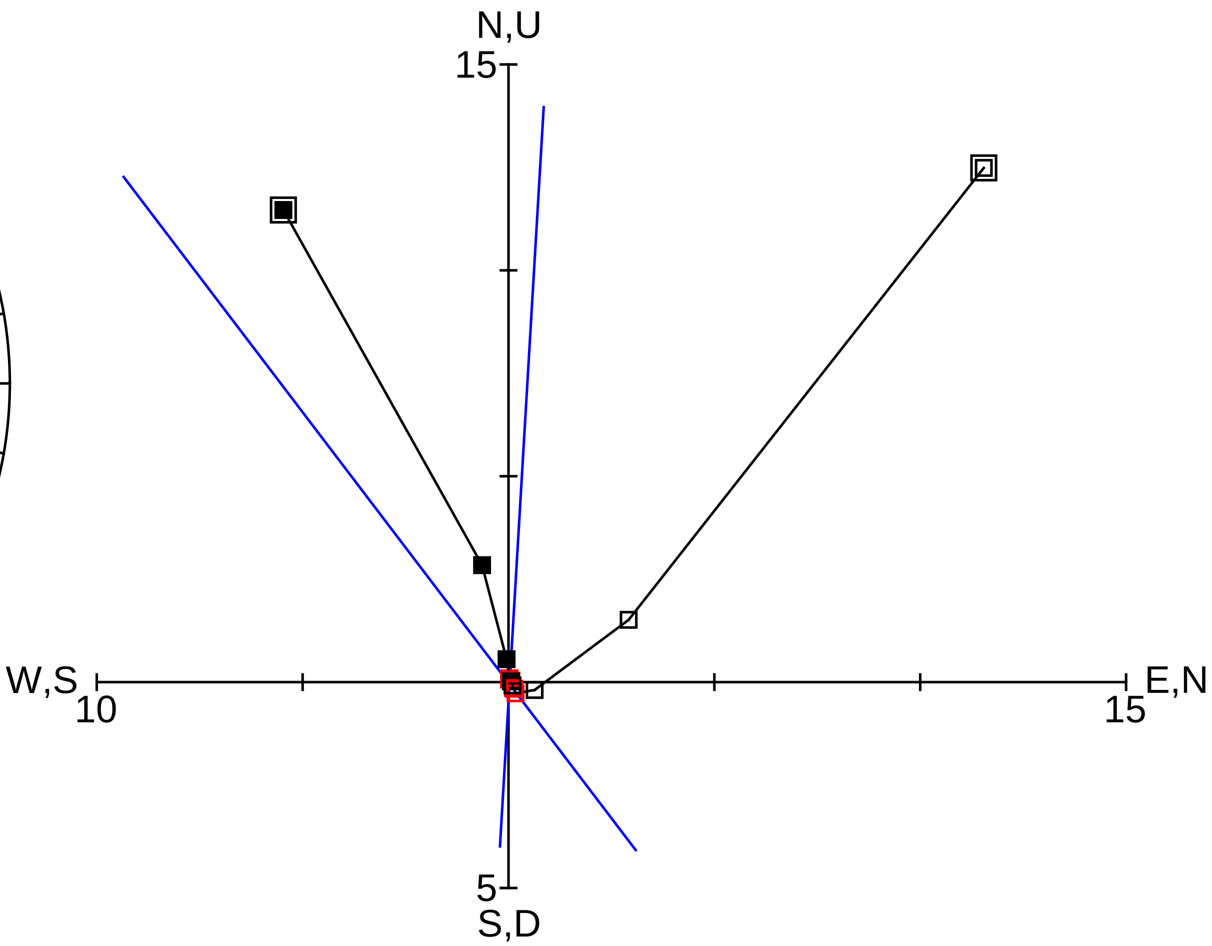

Sample: IS4-1
Site: Innis Springs

PCA dec 349.31 / inc 62.12 Fisher dec 337.0 / inc 66.6 / a95 15.3 / k 20.0
PCA MAD1 14.74 / MAD3 17.96
(0.46 -0.09 0.88)t

vertical
horizontal
Units: A/m ×101

Updated July 2017

	demag.	dec.	inc.	int.	m.s.
	0	50.3	-25.6	9.47e-01	NaN
	5	59.8	-27.9	5.11e-01	NaN
	10	68.3	-25.3	1.97e-01	NaN
	20	67.3	0.1	3.55e-02	NaN
*	40	7.7	56.2	1.42e-02	NaN
*	80	317.0	70.7	8.11e-03	NaN
*	160	285.9	47.7	7.02e-03	NaN

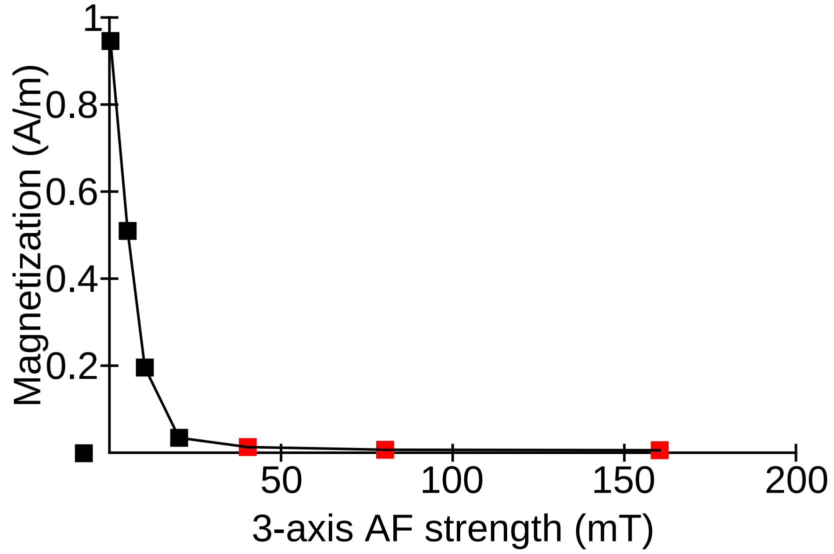

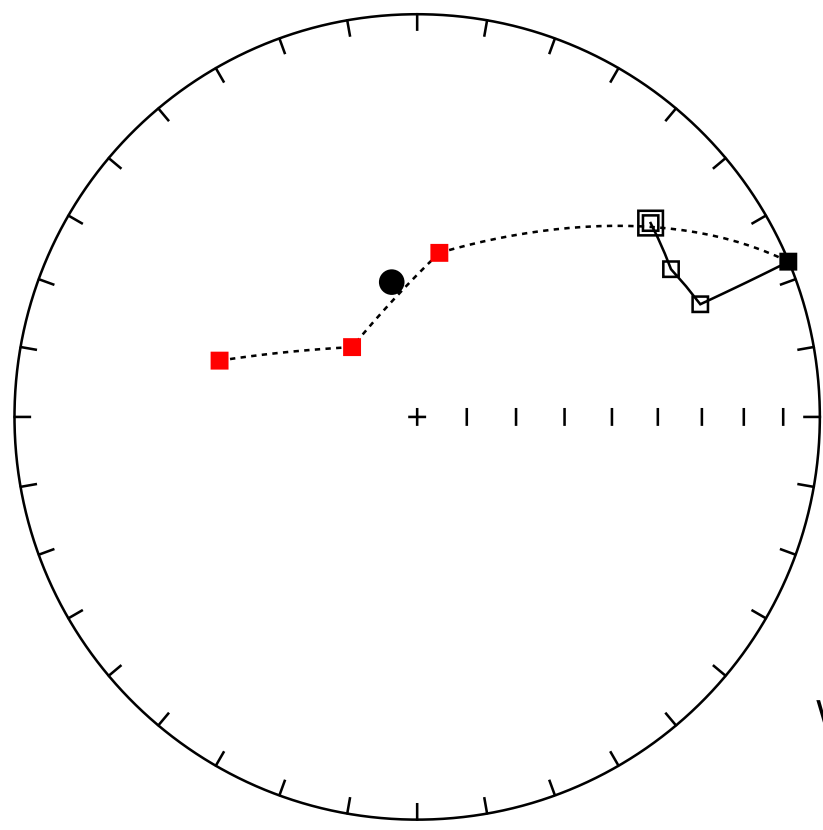

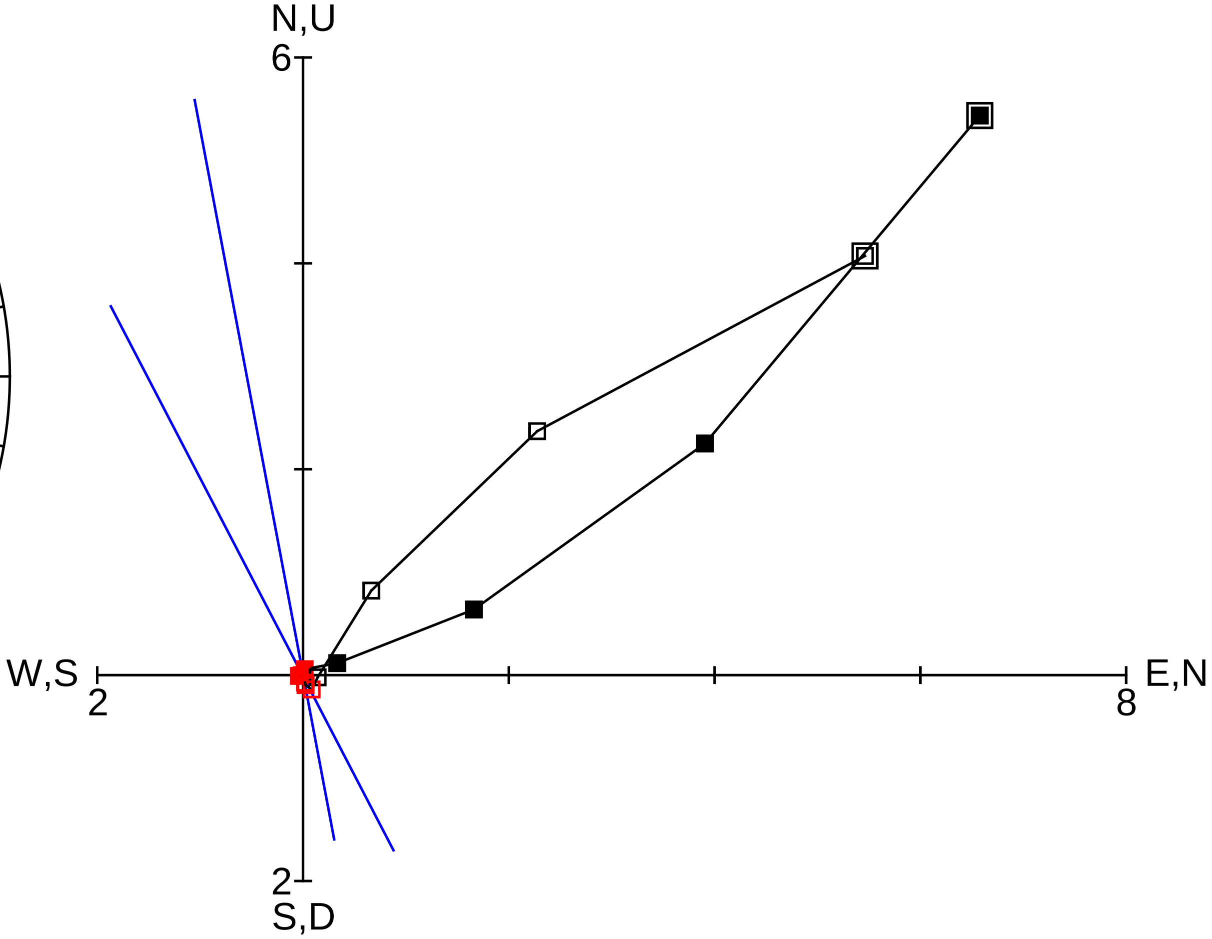

Sample: IS5-1

Site: Innis Springs

PCA dec 341.69 / inc 66.49 Fisher dec 337.0 / inc 66.6 / a95 15.3 / k 20.0

PCA MAD1 18.25 / MAD3 2.98

(0.38 -0.13 0.92)t

□ vertical

■ horizontal

Units: A/m ×102

Updated July 2017

	demag.	dec.	inc.	int.	m.s.
	0	10.0	68.3	2.76e-01	NaN
	5	354.3	66.3	1.36e-01	NaN
*	10	345.2	66.5	6.74e-02	NaN
*	20	339.0	67.6	3.51e-02	NaN
*	40	325.0	63.8	2.53e-02	NaN
*	80	325.6	55.4	7.43e-03	NaN
	160	317.1	40.0	6.11e-03	NaN

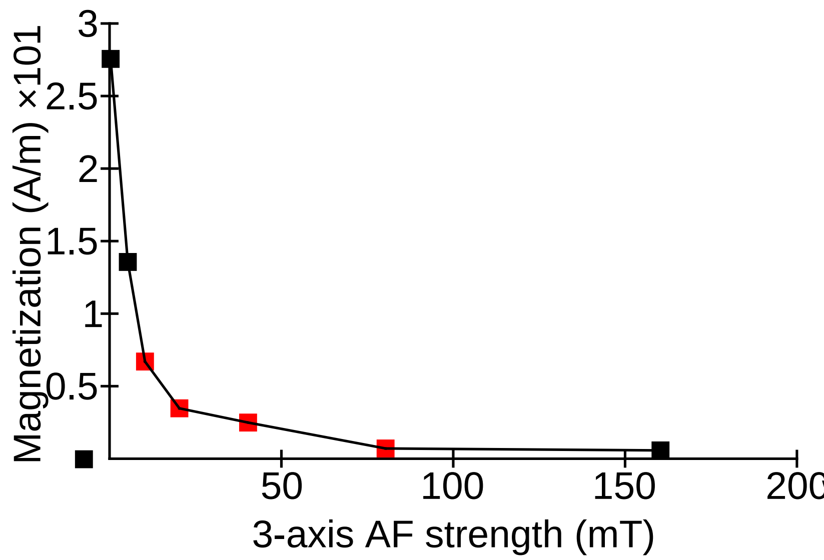

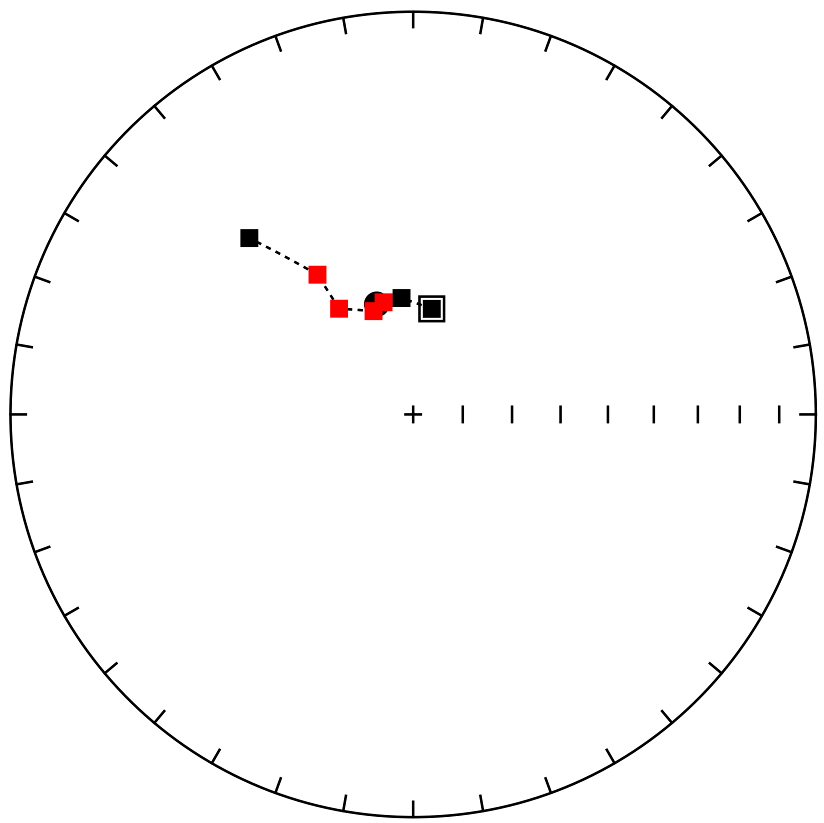

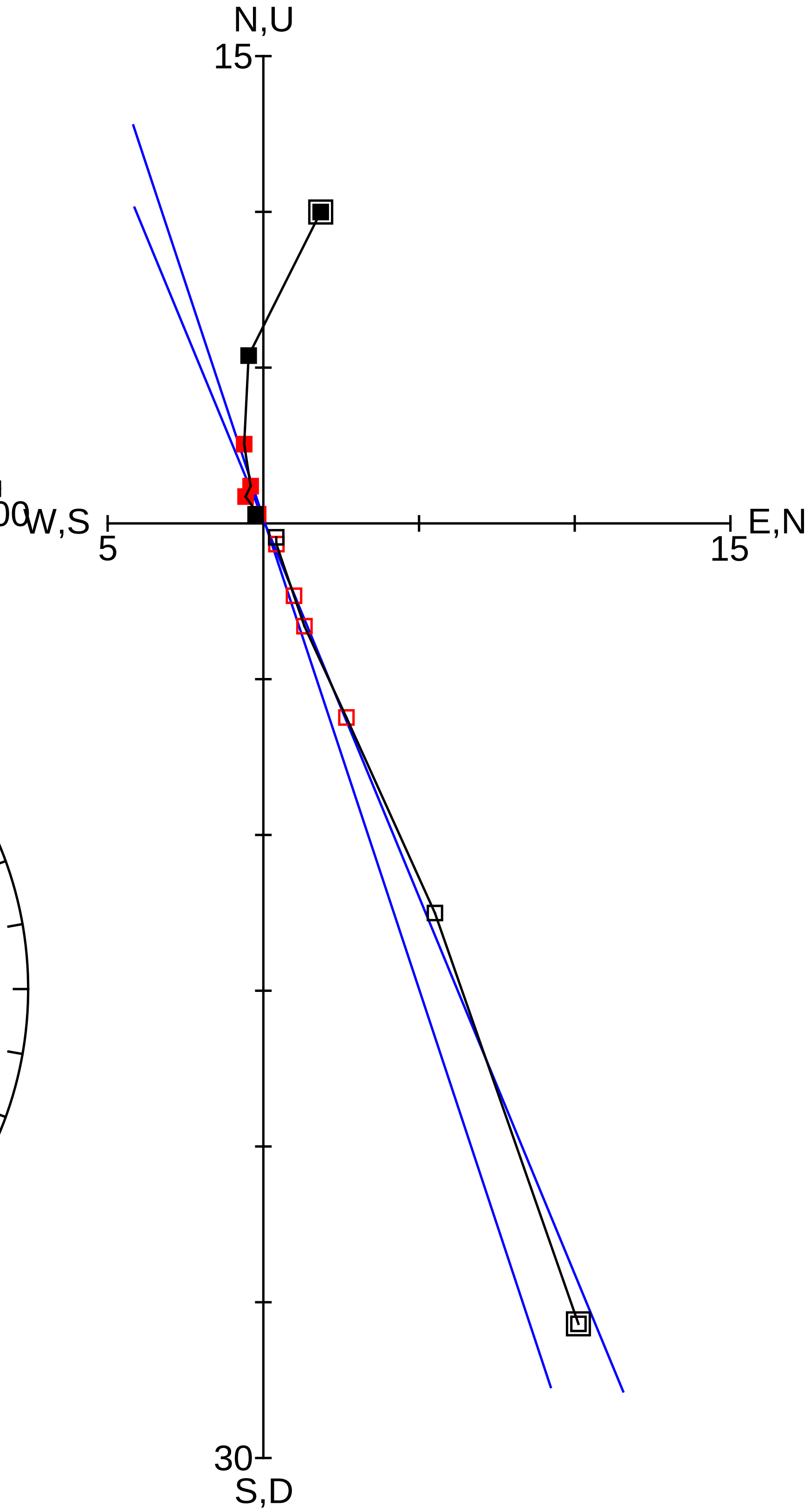

Sample: IS6-1

Site: Innis Springs

PCA dec 347.06 / inc 66.79 Fisher dec 337.0 / inc 66.6 / a95 15.3 / k 20.0

PCA MAD1 17.76 / MAD3 2.44

(0.38 -0.09 0.92)t

□ vertical

■ horizontal

Units: A/m ×102

Updated July 2017

	demag.	dec.	inc.	int.	m.s.
	0	346.2	58.7	1.91e-01	NaN
*	5	348.5	66.9	1.00e-01	NaN
*	10	347.5	67.2	5.25e-02	NaN
*	20	336.4	65.6	2.55e-02	NaN
*	40	326.9	63.5	1.49e-02	NaN
*	80	322.9	44.7	8.43e-03	NaN
*	160	326.3	59.7	5.34e-03	NaN

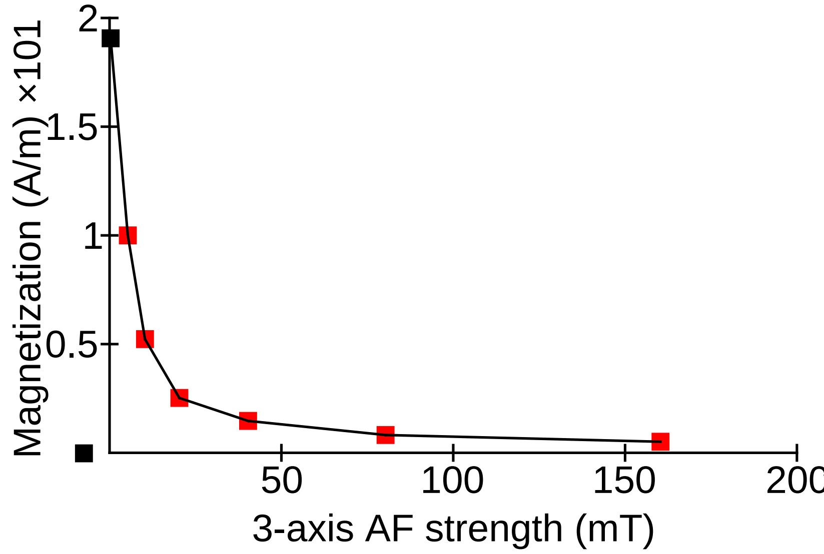

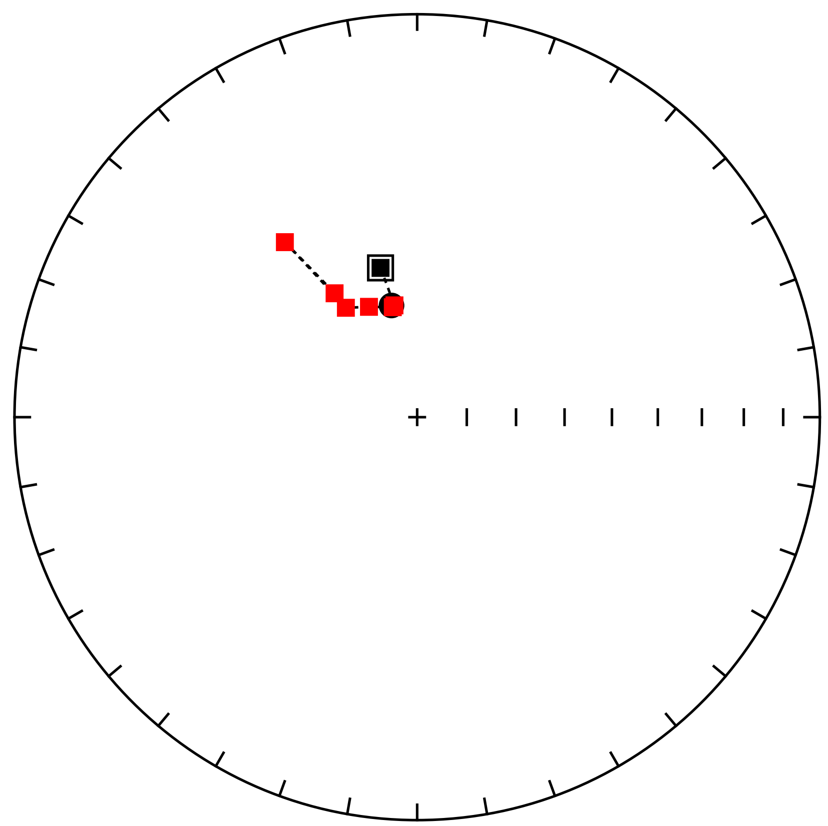

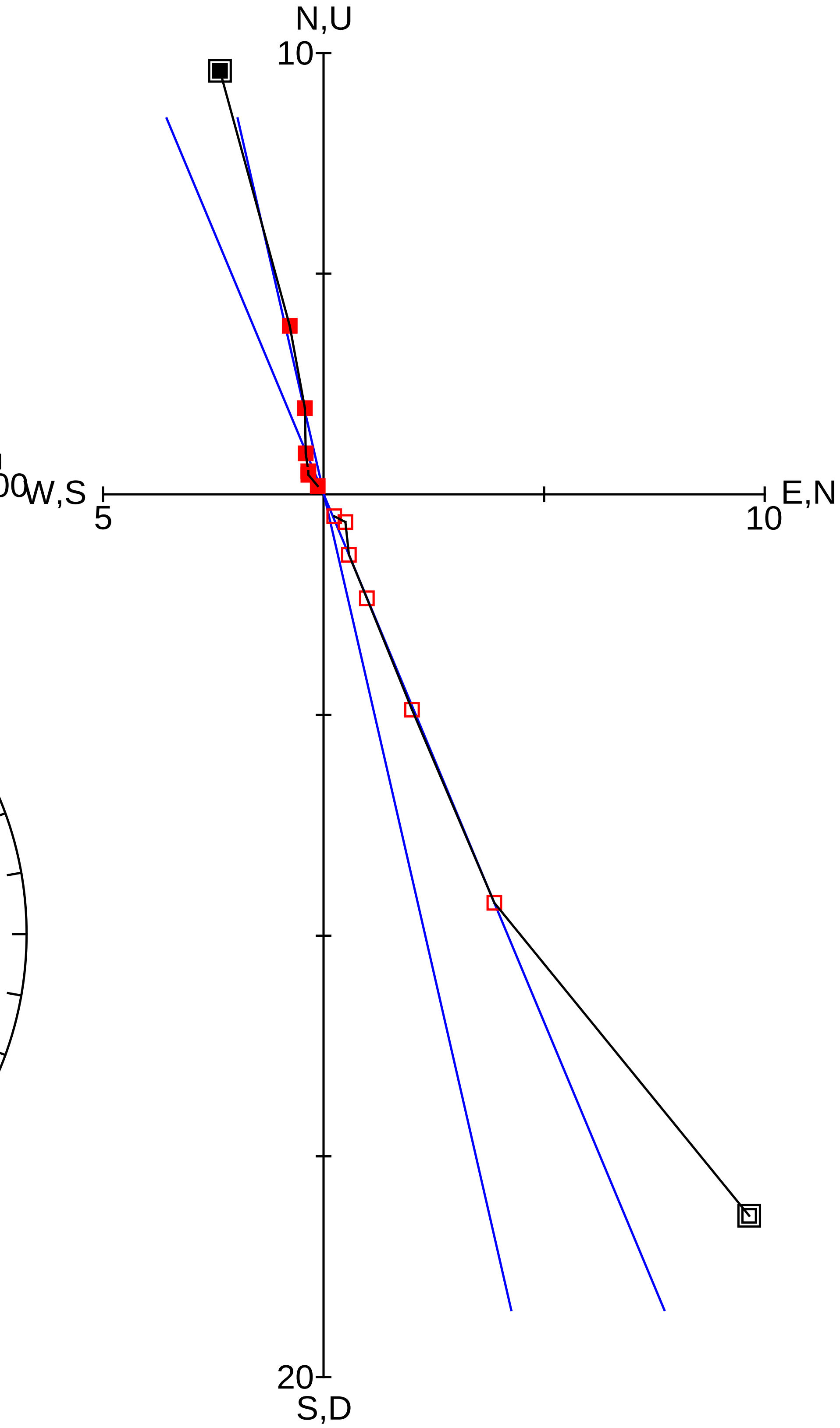

Sample: IS7-3

Site: Innis Springs

PCA dec 270.52 / inc 53.07 Fisher dec 337.0 / inc 66.6 / a95 15.3 / k 20.0
PCA MAD1 1.21 / MAD3 6.23
(0.01 -0.60 0.80)t

□ vertical
■ horizontal
Units: A/m ×102

Updated July 2017

	demag.	dec.	inc.	int.	m.s.
	0	60.0	78.9	1.34e-01	NaN
	5	285.1	64.2	8.54e-02	NaN
*	10	270.5	57.4	4.78e-02	NaN
*	20	270.3	47.9	2.92e-02	NaN
*	40	271.0	40.0	2.08e-02	NaN
	80	304.4	41.9	1.22e-02	NaN

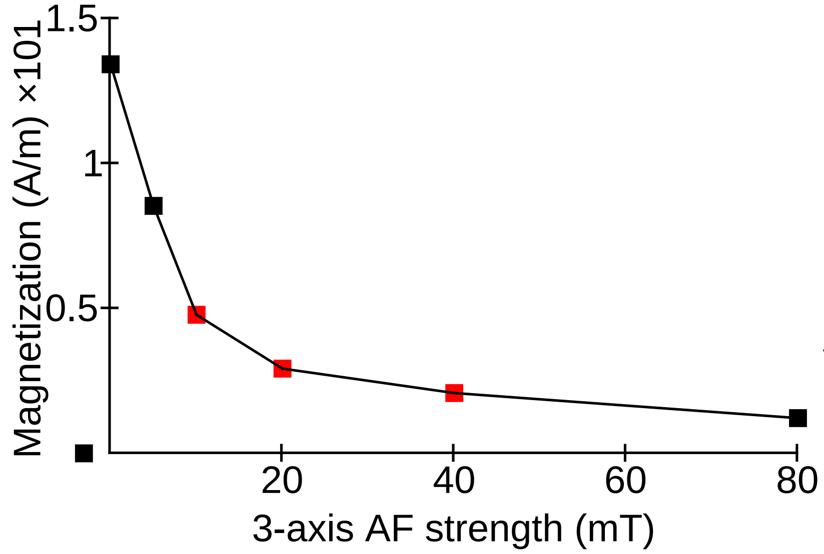

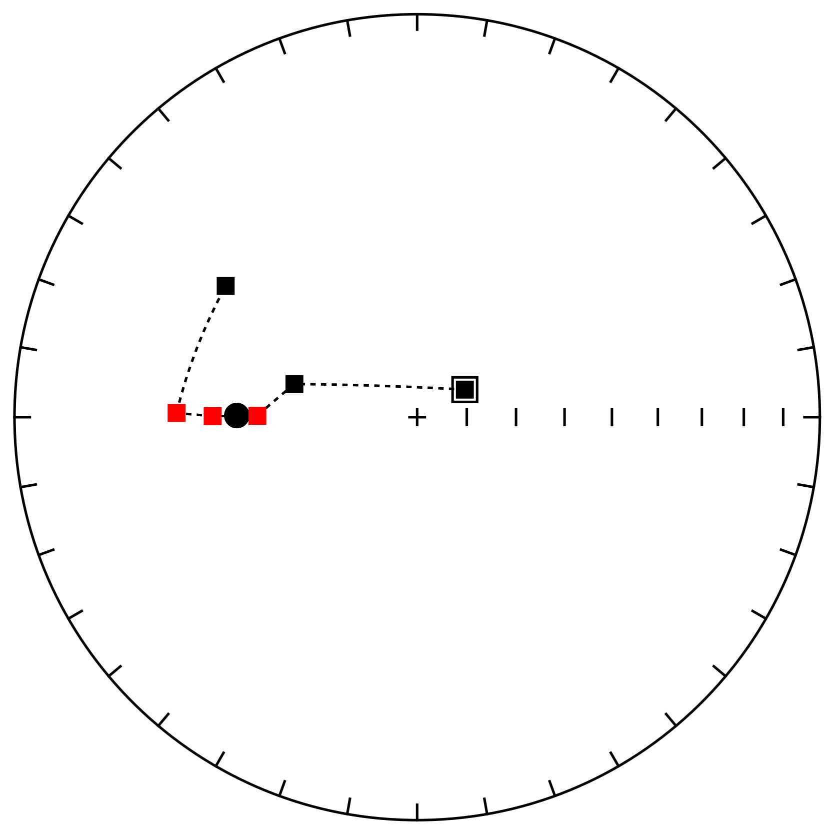

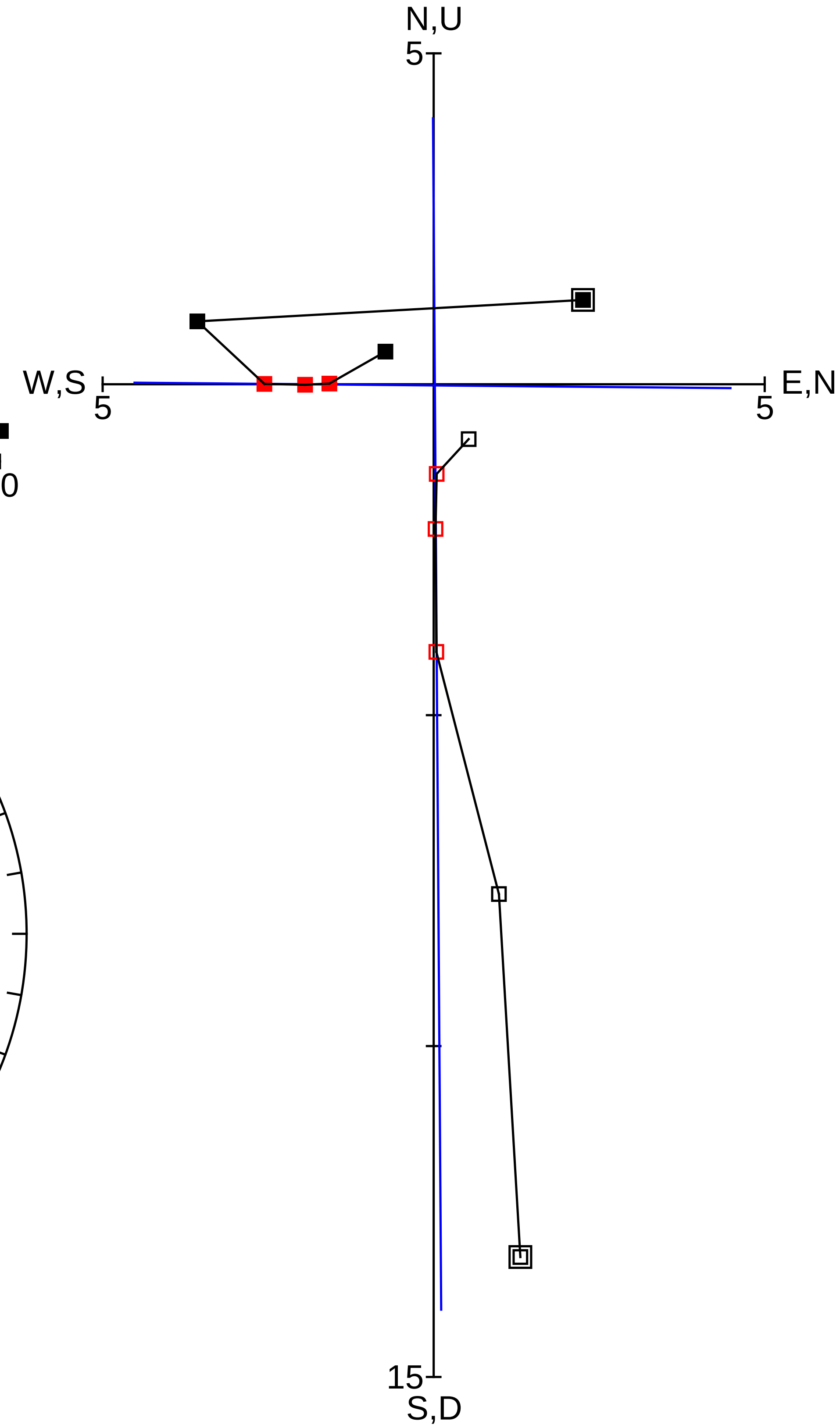

Sample: NV1-3

Site: Nivlac

PCA dec 224.32 / inc 43.57 Fisher dec 251.6 / inc 39.5 / a95 8.7 / k 31.5

PCA MAD1 2.33 / MAD3 1.23

(-0.52 -0.51 0.69)t

□ vertical

■ horizontal

Units: A/m ×102

Updated July 2017

	demag.	dec.	inc.	int.	m.s.
	0	190.5	67.4	2.10e-01	NaN
	5	218.8	46.9	1.11e-01	NaN
*	10	224.5	43.8	9.46e-02	NaN
*	20	224.8	43.9	6.90e-02	NaN
*	40	220.8	40.0	3.25e-02	NaN
	80	224.3	23.3	1.68e-02	NaN
	160	300.2	74.3	6.63e-03	NaN

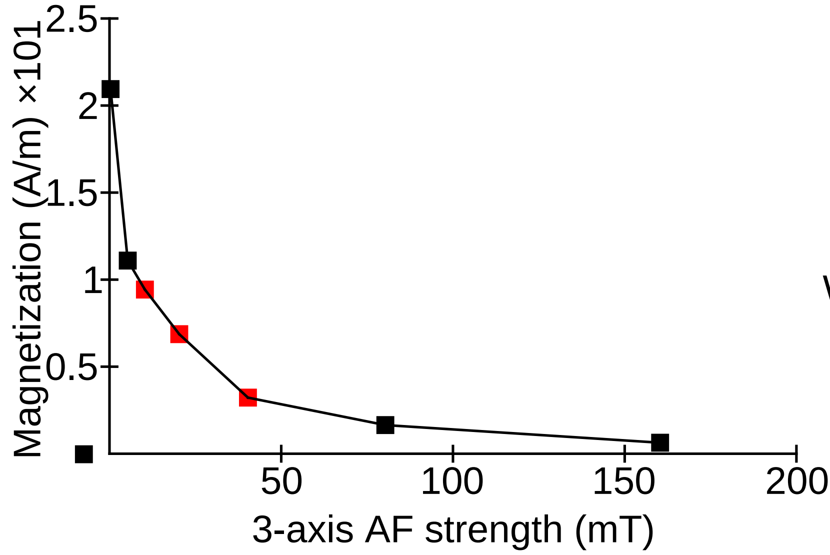

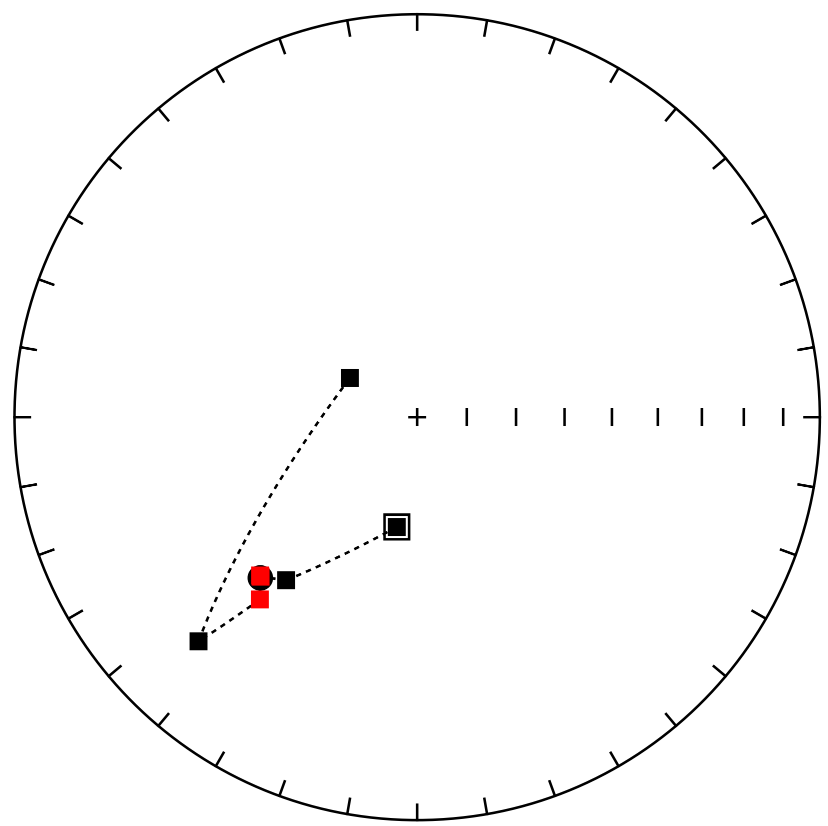

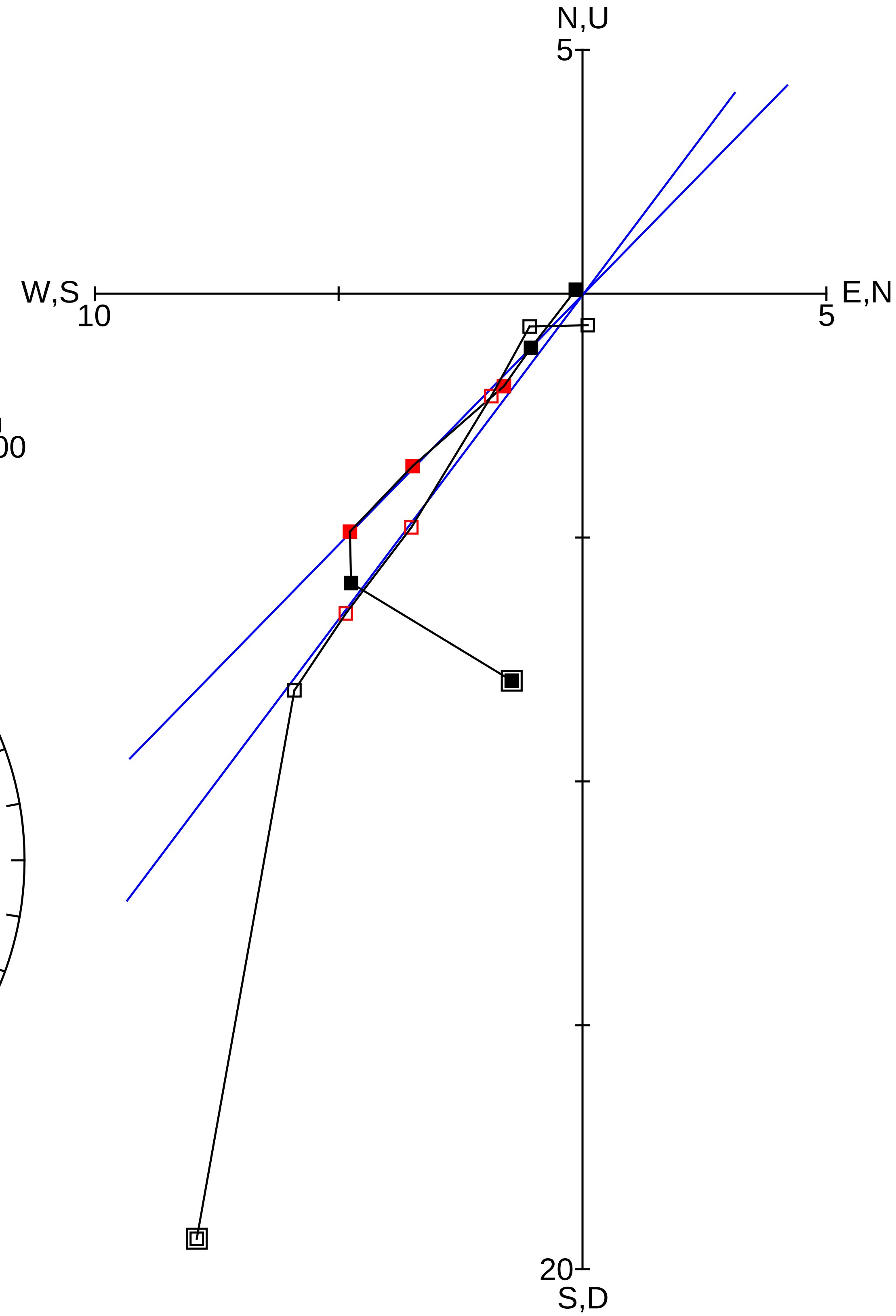

Sample: NV2-1
Site: Nivlac

PCA dec 253.57 / inc 53.38 Fisher dec 251.6 / inc 39.5 / a95 8.7 / k 31.5
PCA MAD1 13.79 / MAD3 2.28
(-0.17 -0.57 0.80)t

vertical
horizontal
Units: A/m ×102

Updated July 2017

	demag.	dec.	inc.	int.	m.s.
	0	282.8	77.3	1.43e-01	NaN
	5	260.6	68.5	7.43e-02	NaN
	10	260.6	59.0	5.77e-02	NaN
*	20	254.3	53.7	4.54e-02	NaN
*	40	256.6	52.8	2.28e-02	NaN
*	80	243.7	52.2	1.56e-02	NaN
*	160	242.7	49.1	7.46e-03	NaN

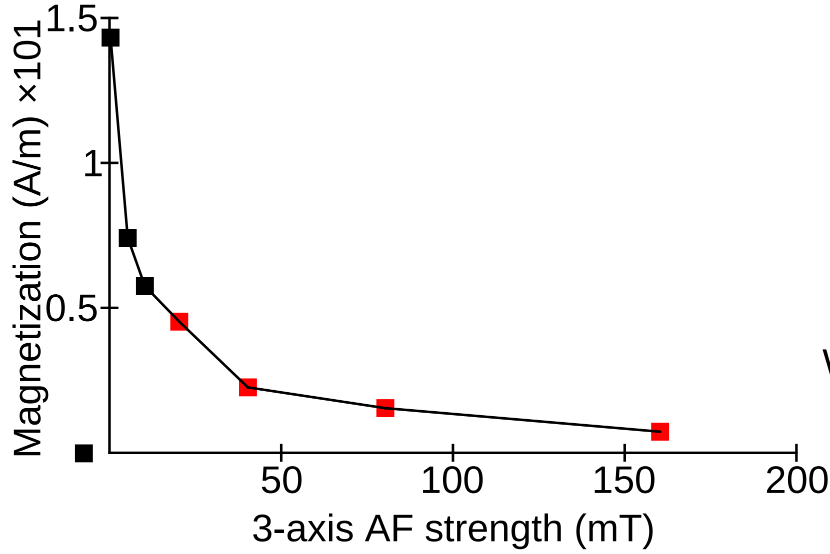

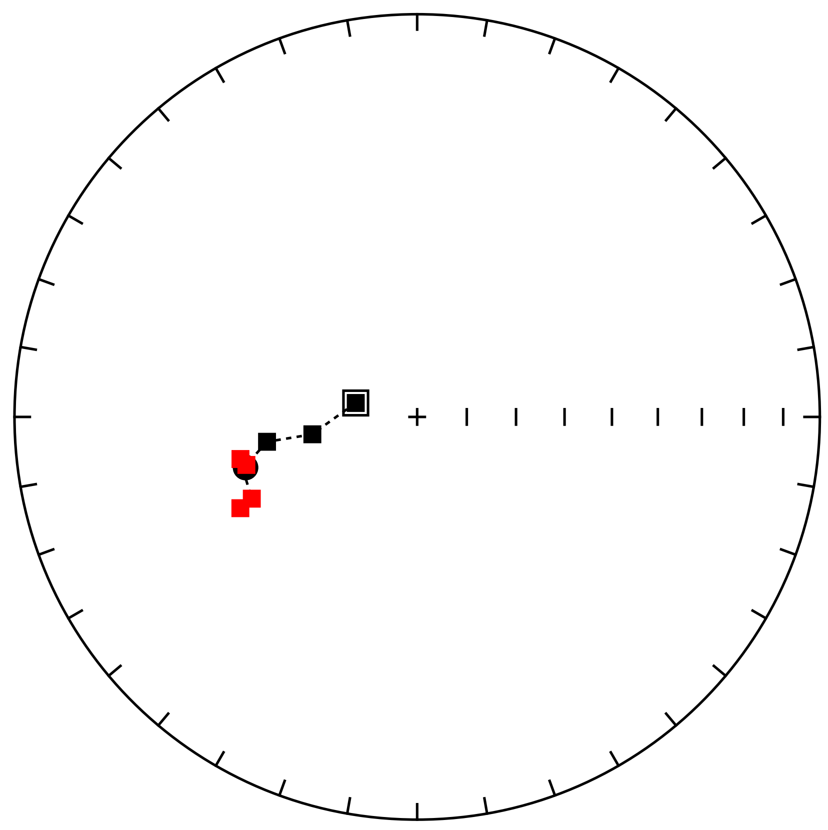

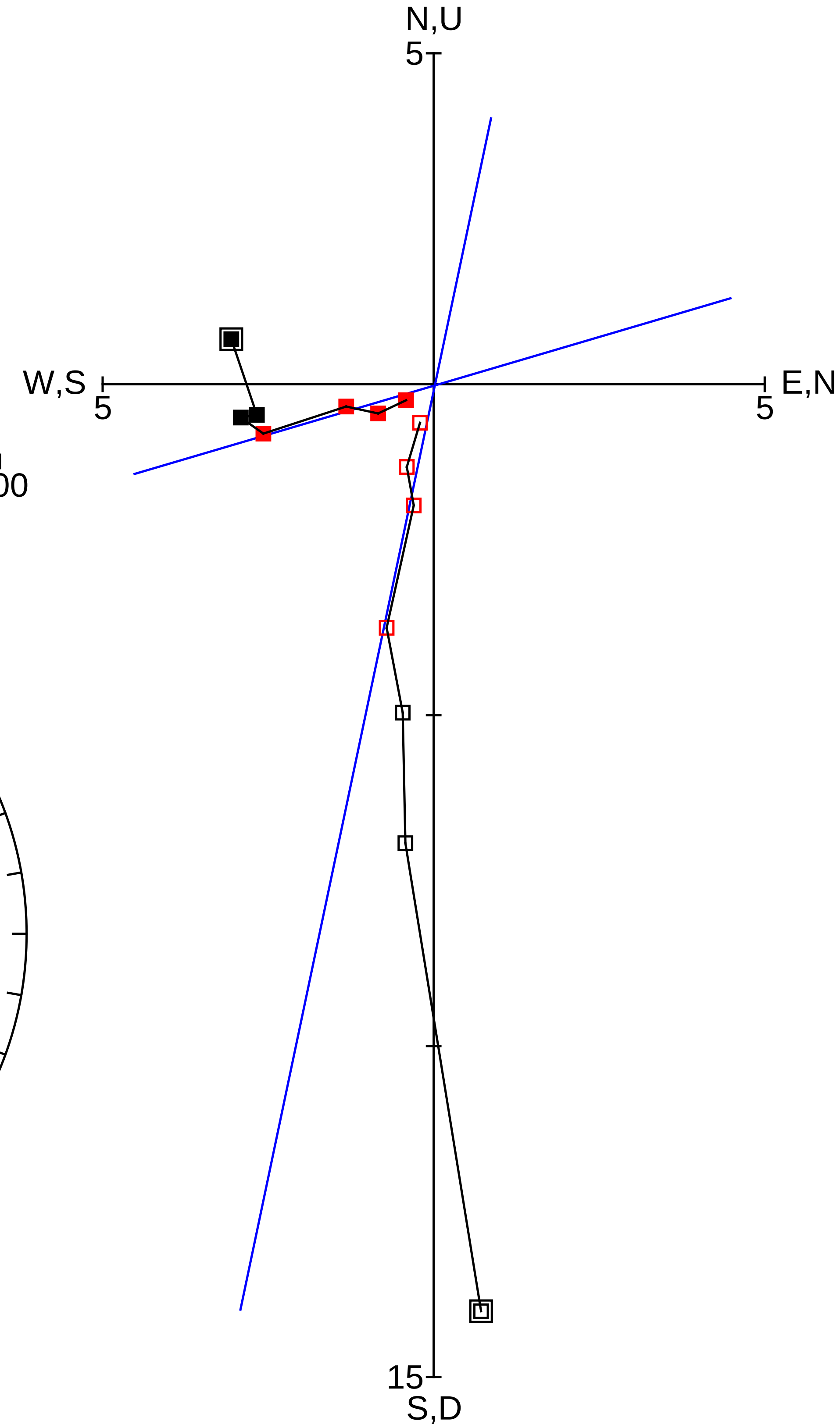

Sample: NV4-2

Site: Nivlac

PCA dec 281.29 / inc 28.30 Fisher dec 251.6 / inc 39.5 / a95 8.7 / k 31.5

PCA MAD1 4.22 / MAD3 2.54

(0.17 -0.86 0.47)t

□ vertical

■ horizontal

Units: A/m ×102

Updated July 2017

	demag.	dec.	inc.	int.	m.s.
	0	286.0	57.9	2.56e-01	NaN
	5	279.4	42.2	2.27e-01	NaN
	10	275.9	40.0	1.91e-01	NaN
	20	277.0	39.0	1.44e-01	NaN
*	40	281.0	30.1	9.80e-02	NaN
*	80	281.7	25.0	6.93e-02	NaN
*	160	283.6	22.6	1.65e-02	NaN

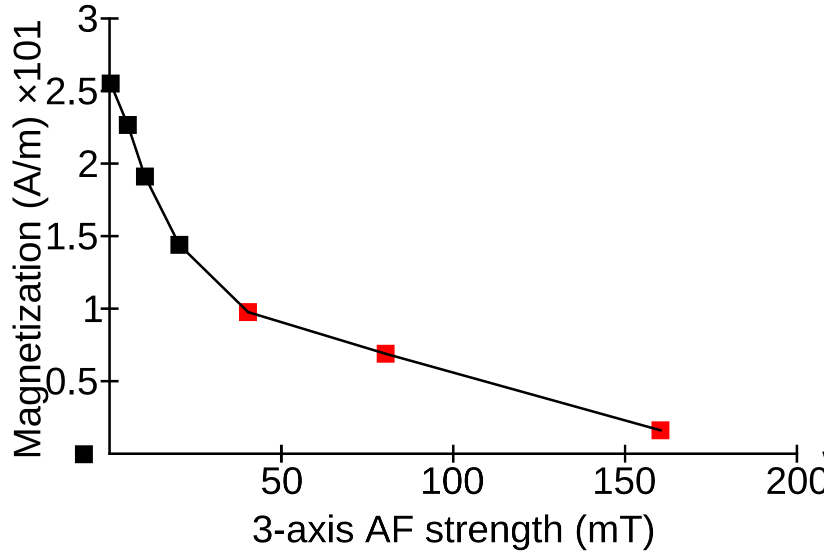

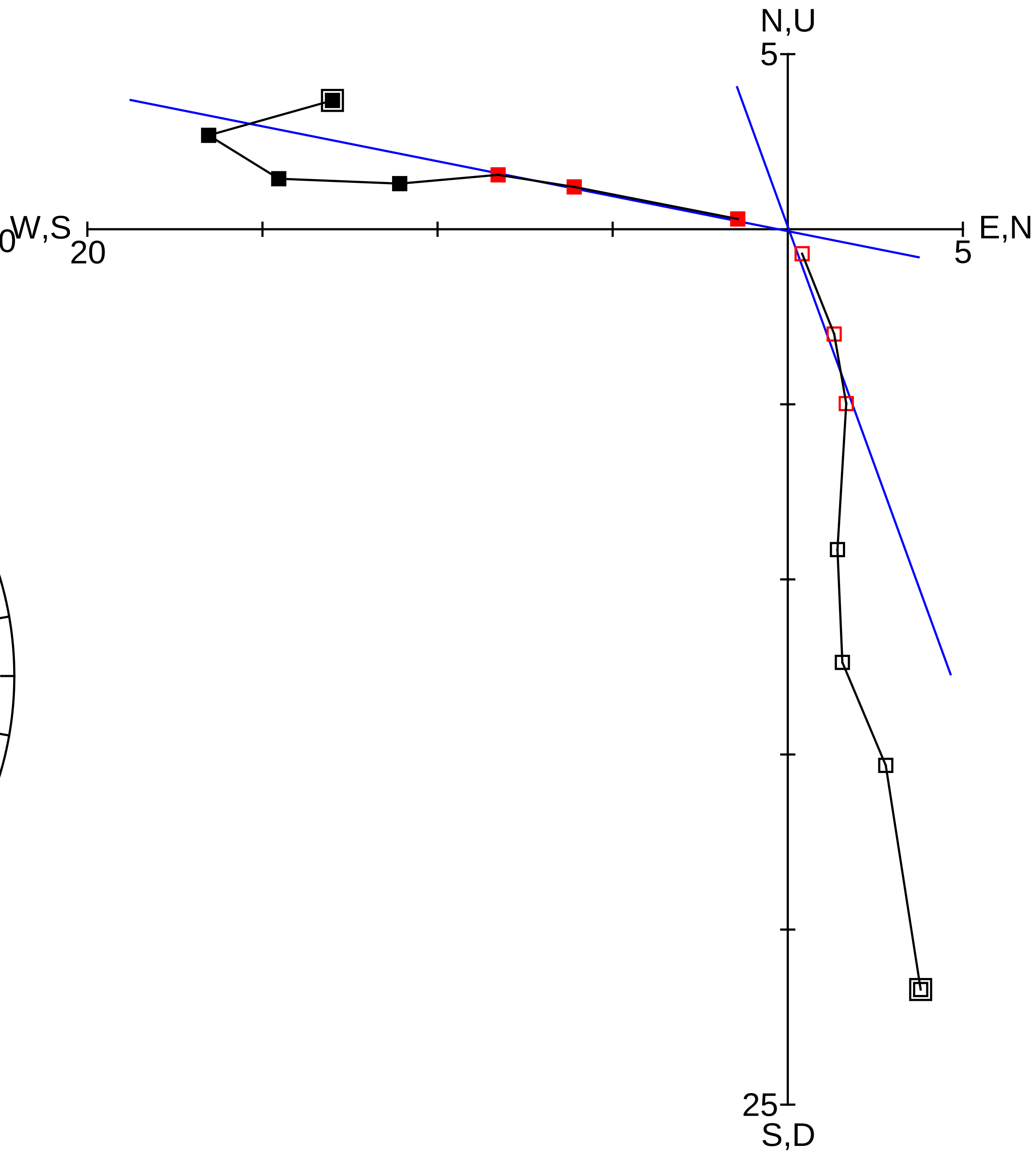

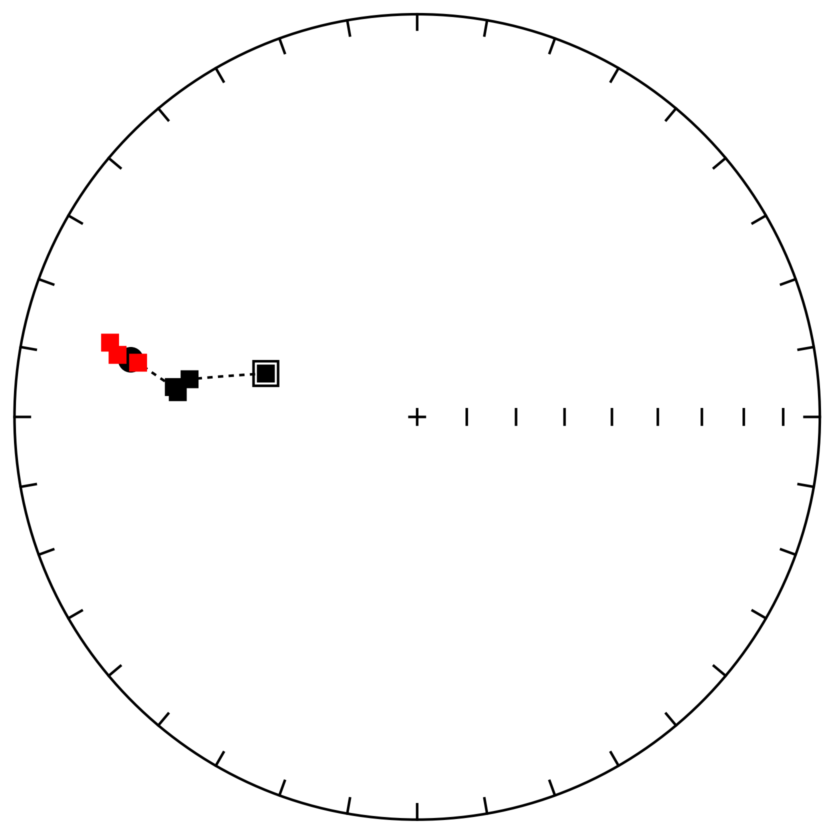

Sample: NV5-1
Site: Nivlac

PCA dec 247.20 / inc 32.30 Fisher dec 251.6 / inc 39.5 / a95 8.7 / k 31.5
PCA MAD1 27.22 / MAD3 1.36
(-0.33 -0.78 0.53)t

□ vertical
■ horizontal
Units: A/m ×102

Updated July 2017

	demag.	dec.	inc.	int.	m.s.
	0	253.6	46.8	5.36e-01	NaN
	5	253.7	41.8	5.00e-01	NaN
	10	255.2	40.5	4.49e-01	NaN
	20	252.4	38.3	3.71e-01	NaN
*	40	247.1	31.5	2.91e-01	NaN
*	80	247.8	34.1	1.90e-01	NaN
*	160	242.5	33.2	5.33e-02	NaN

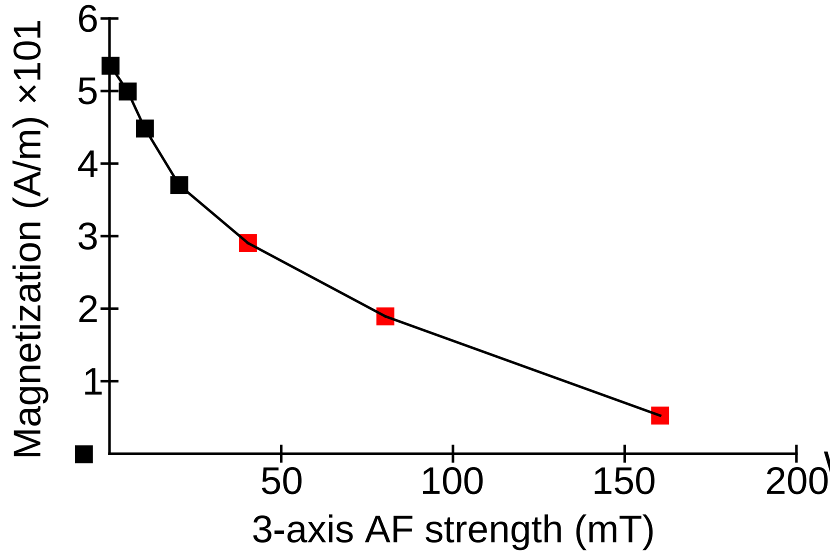

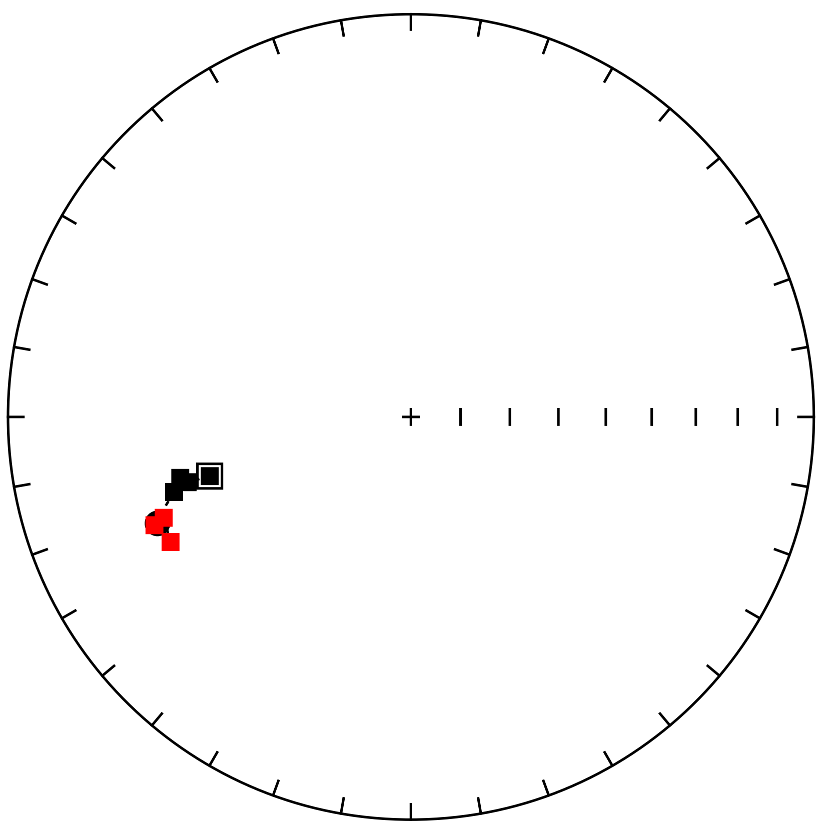

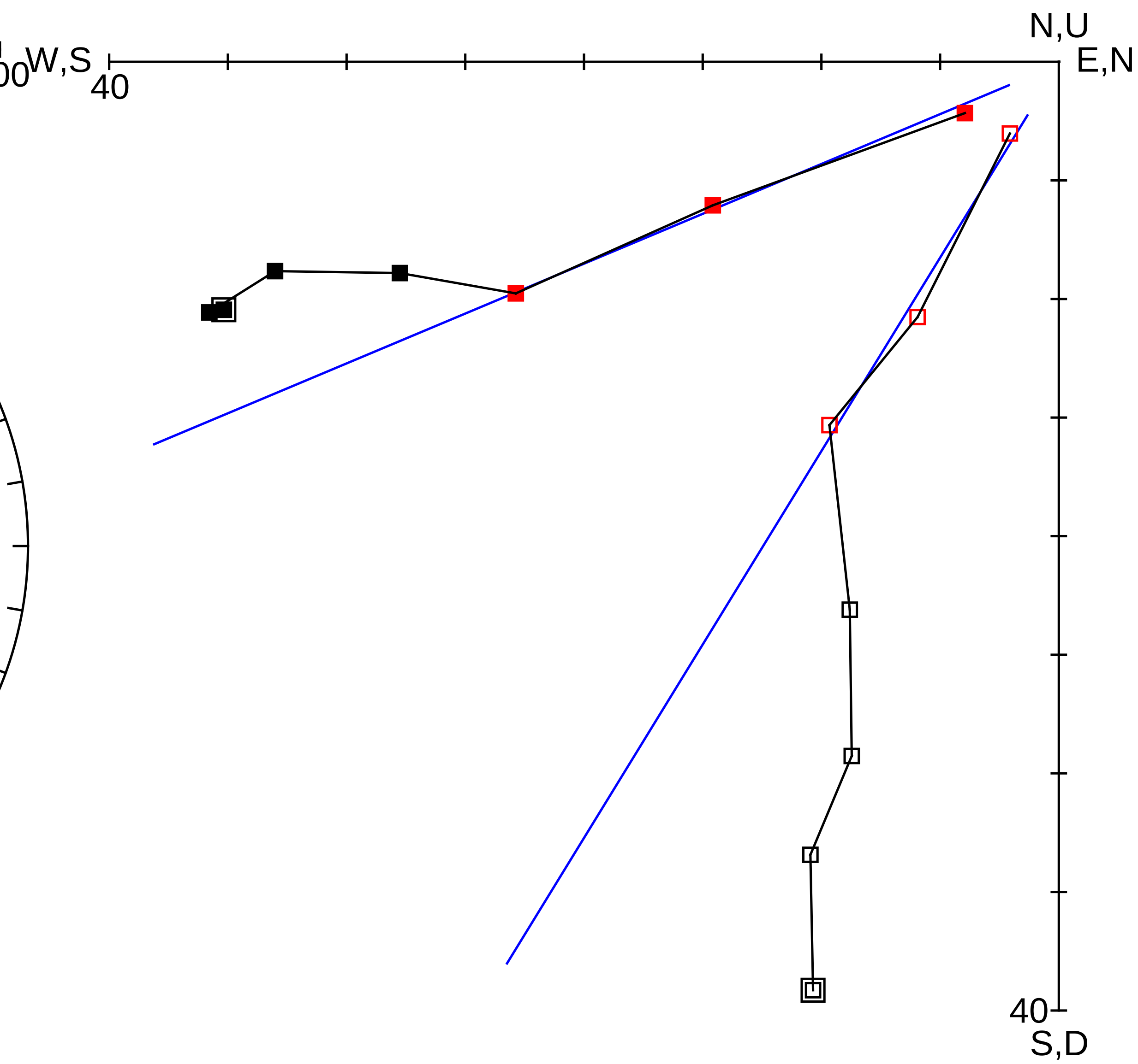

Sample: NV6-1
Site: Nivlac

PCA dec 257.40 / inc 40.47 Fisher dec 251.6 / inc 39.5 / a95 8.7 / k 31.5
PCA MAD1 10.33 / MAD3 0.52
(-0.17 -0.74 0.65)t

□ vertical
■ horizontal
Units: A/m ×102

Updated July 2017

	demag.	dec.	inc.	int.	m.s.
	0	253.5	43.5	2.63e-01	NaN
	5	260.4	44.7	2.42e-01	NaN
	10	261.4	45.7	2.19e-01	NaN
	20	261.7	43.0	1.67e-01	NaN
*	40	257.1	40.3	1.14e-01	NaN
*	80	258.2	40.8	6.00e-02	NaN
*	160	258.7	41.7	2.82e-02	NaN

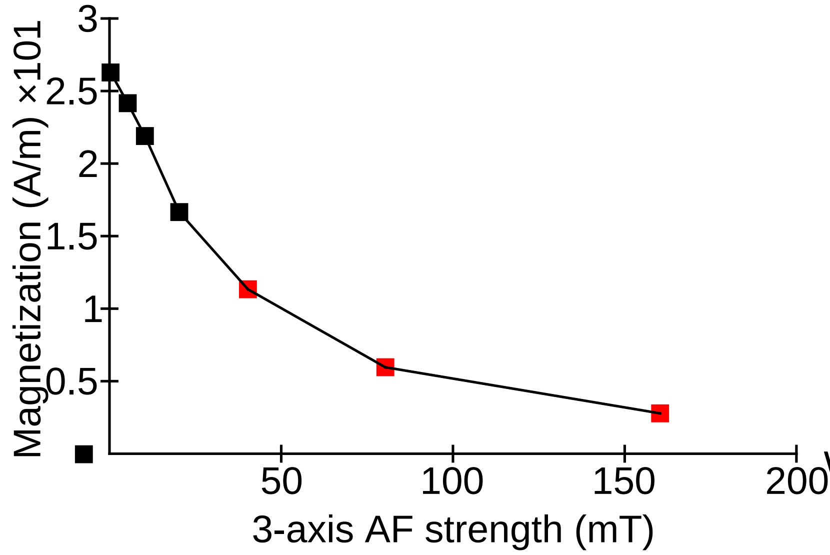

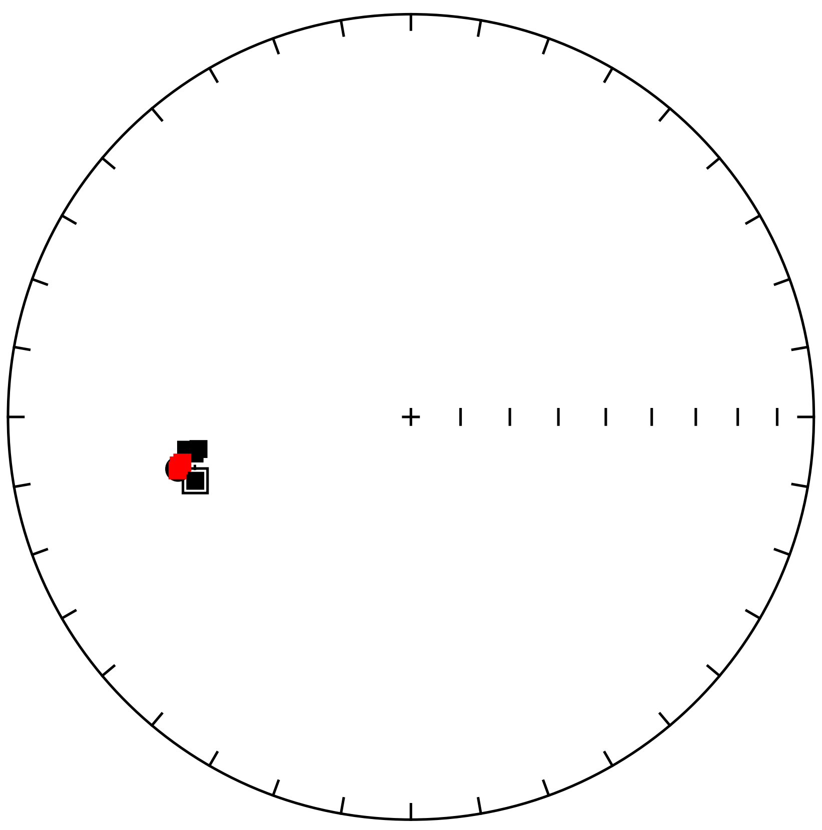

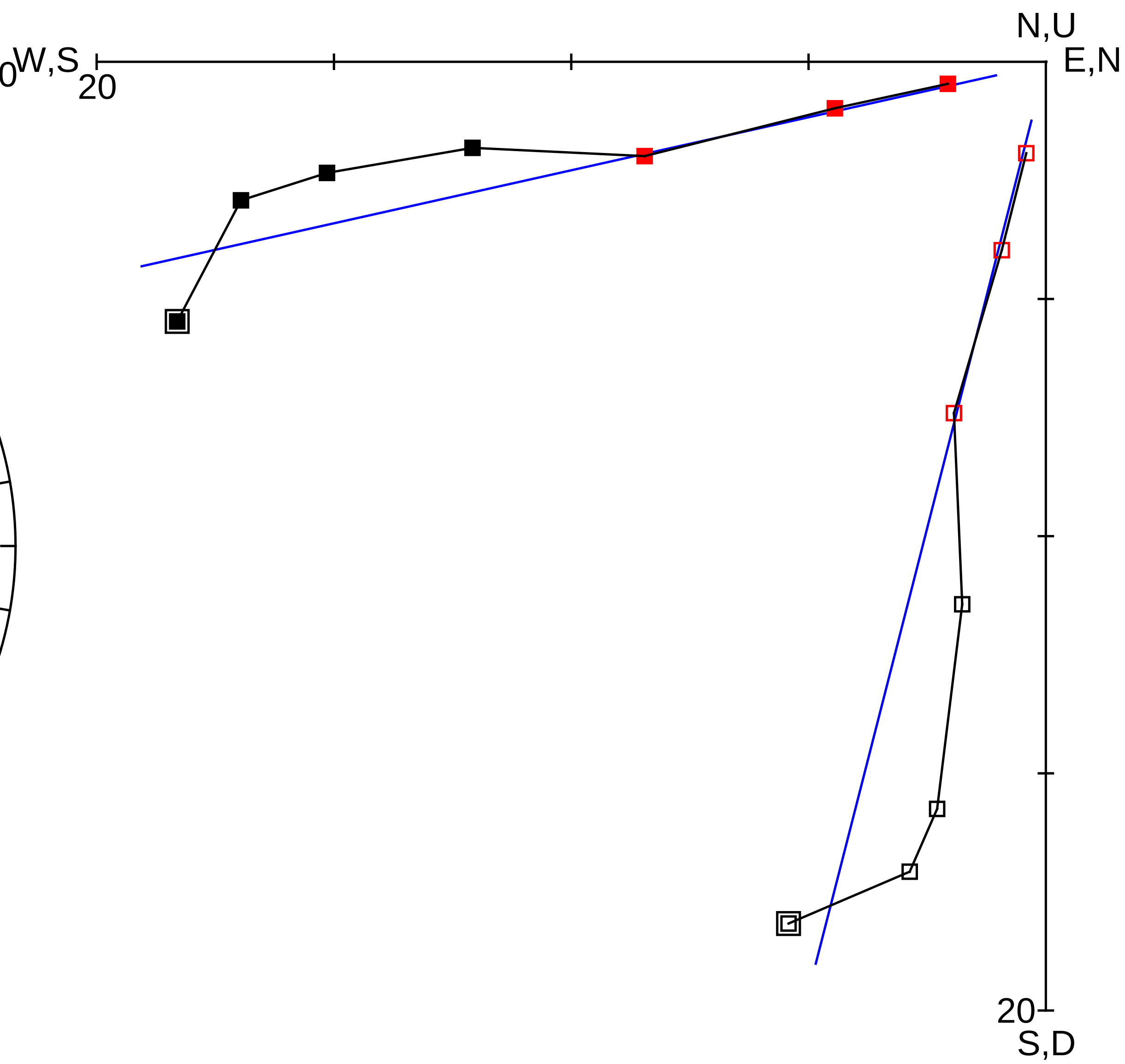

Sample: NV7-1
Site: Nivlac

PCA dec 263.29 / inc 39.79 Fisher dec 251.6 / inc 39.5 / a95 8.7 / k 31.5
PCA MAD1 7.90 / MAD3 0.72
(-0.09 -0.76 0.64)t

□ vertical
■ horizontal
Units: A/m ×102

Updated July 2017

	demag.	dec.	inc.	int.	m.s.
	0	261.0	43.0	4.61e-01	NaN
	5	265.4	42.7	4.42e-01	NaN
	10	257.4	39.2	4.01e-01	NaN
	20	266.1	40.8	3.00e-01	NaN
*	40	263.2	39.8	2.07e-01	NaN
*	80	263.3	40.4	1.13e-01	NaN
*	160	264.4	37.0	5.49e-02	NaN

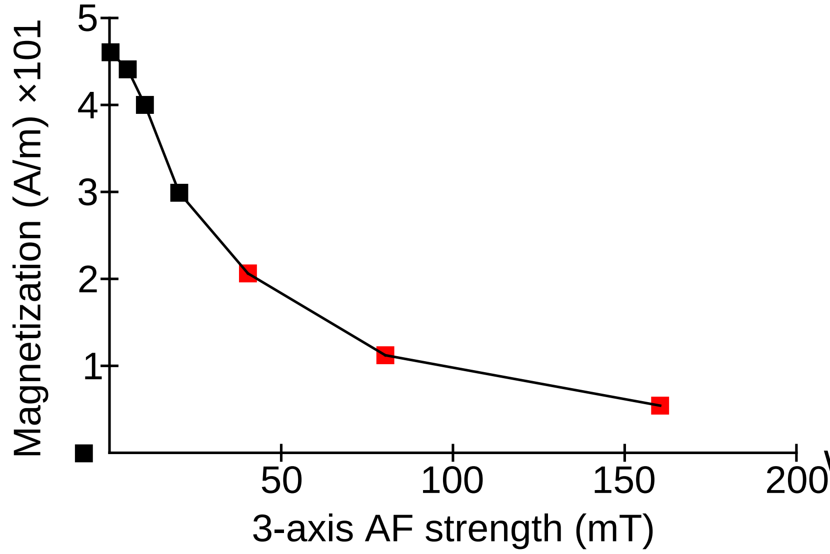

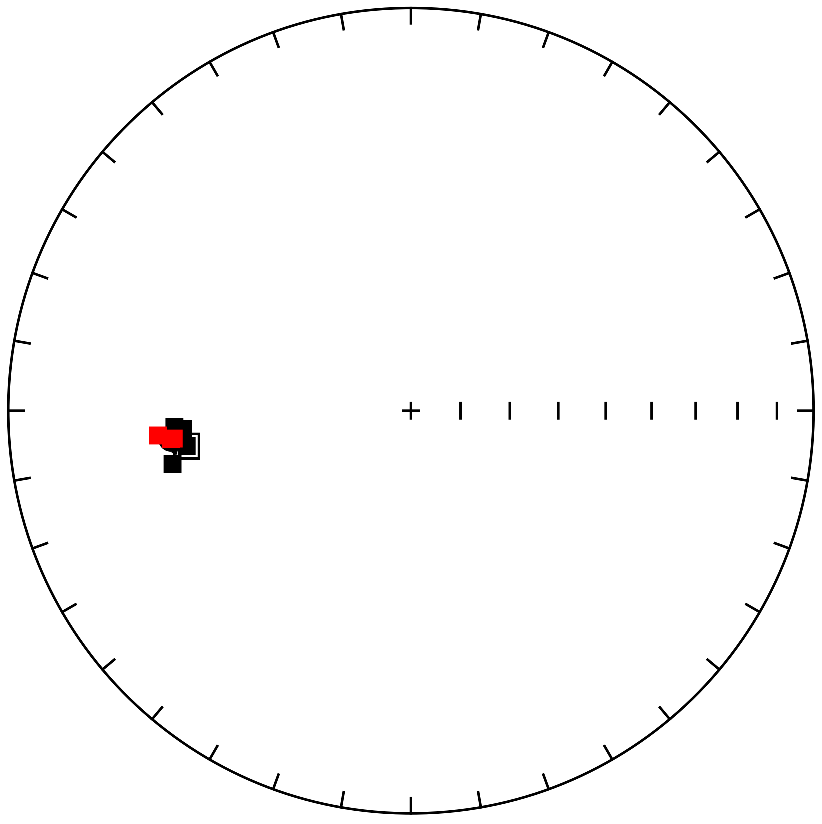

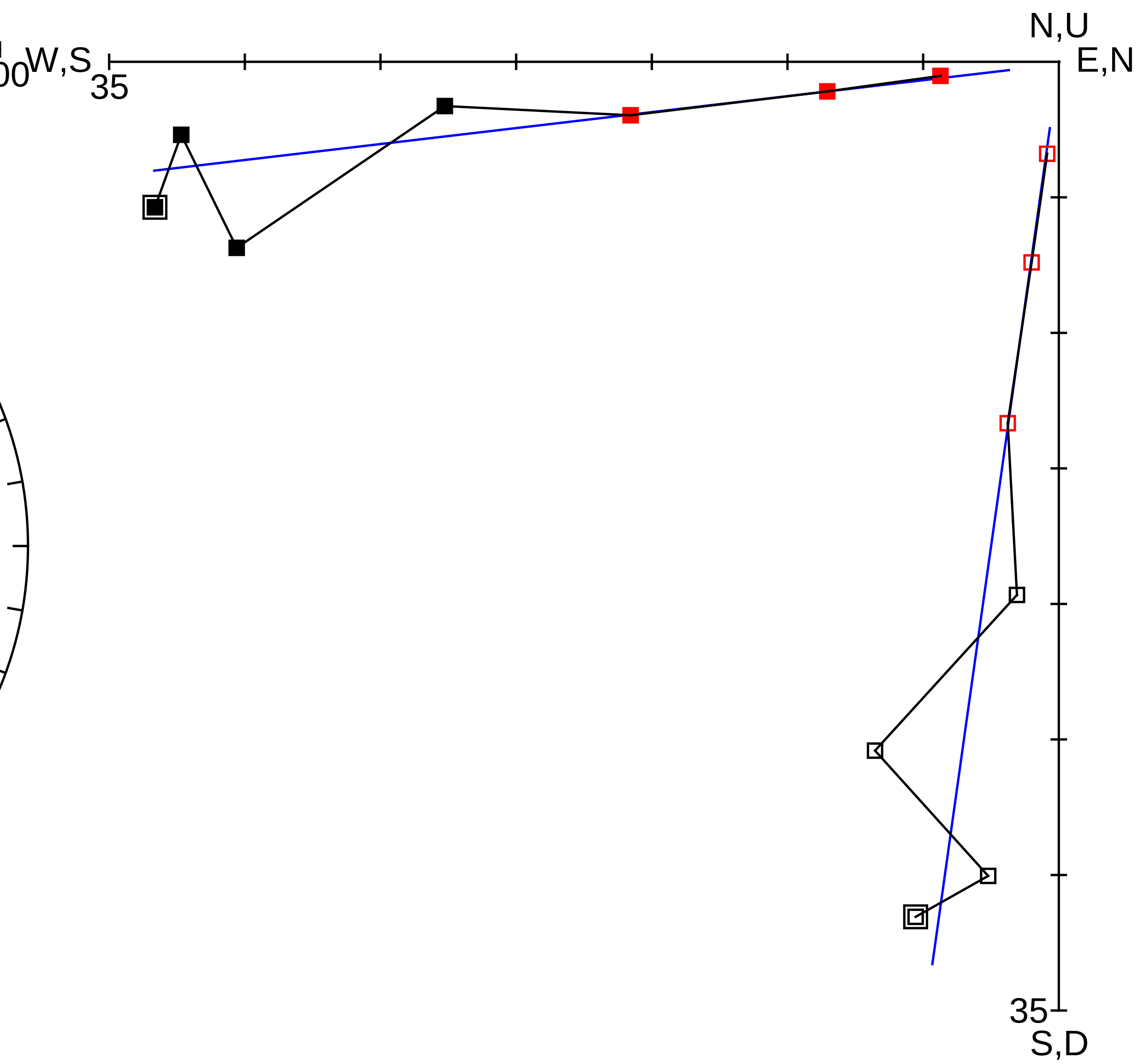

Sample: NV8-2

Site: Nivlac

PCA dec 243.87 / inc 31.84 Fisher dec 251.6 / inc 39.5 / a95 8.7 / k 31.5
PCA MAD1 8.43 / MAD3 2.14
(-0.37 -0.76 0.53)t

vertical
horizontal
Units: A/m ×102

Updated July 2017

	demag.	dec.	inc.	int.	m.s.
	0	243.1	41.9	4.54e-01	NaN
	5	252.6	39.7	4.23e-01	NaN
	10	250.7	37.8	3.69e-01	NaN
	20	249.3	36.4	2.72e-01	NaN
*	40	243.7	32.0	1.90e-01	NaN
*	80	243.2	30.1	1.16e-01	NaN
*	160	250.4	38.6	5.09e-02	NaN

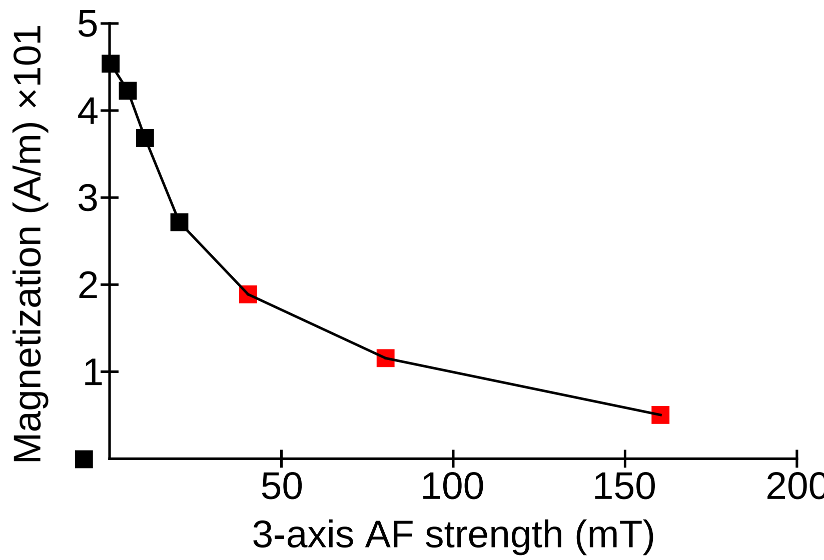

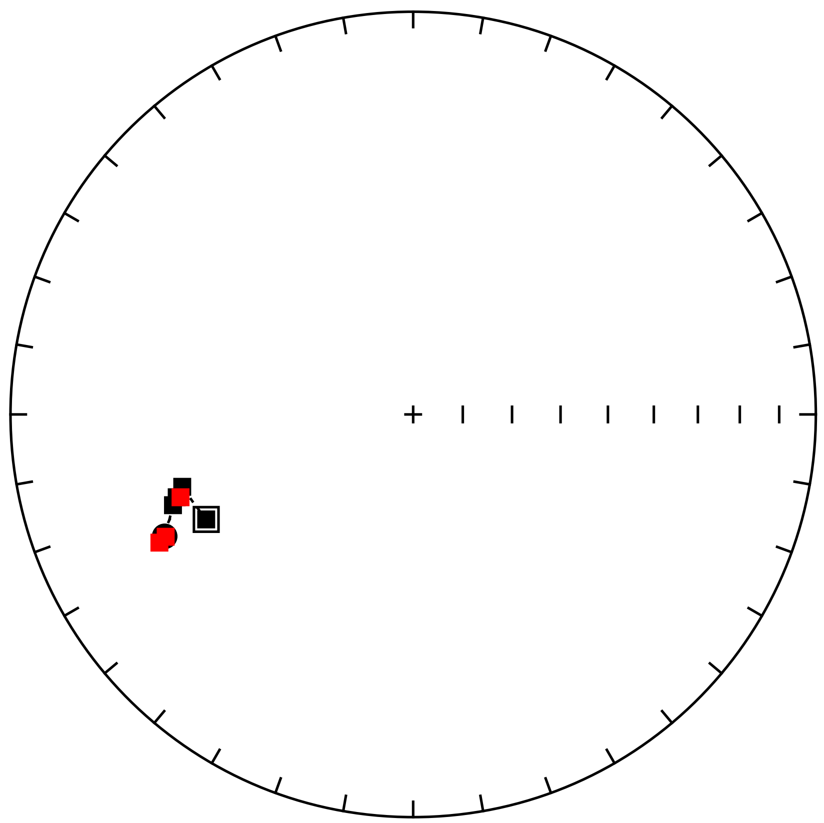

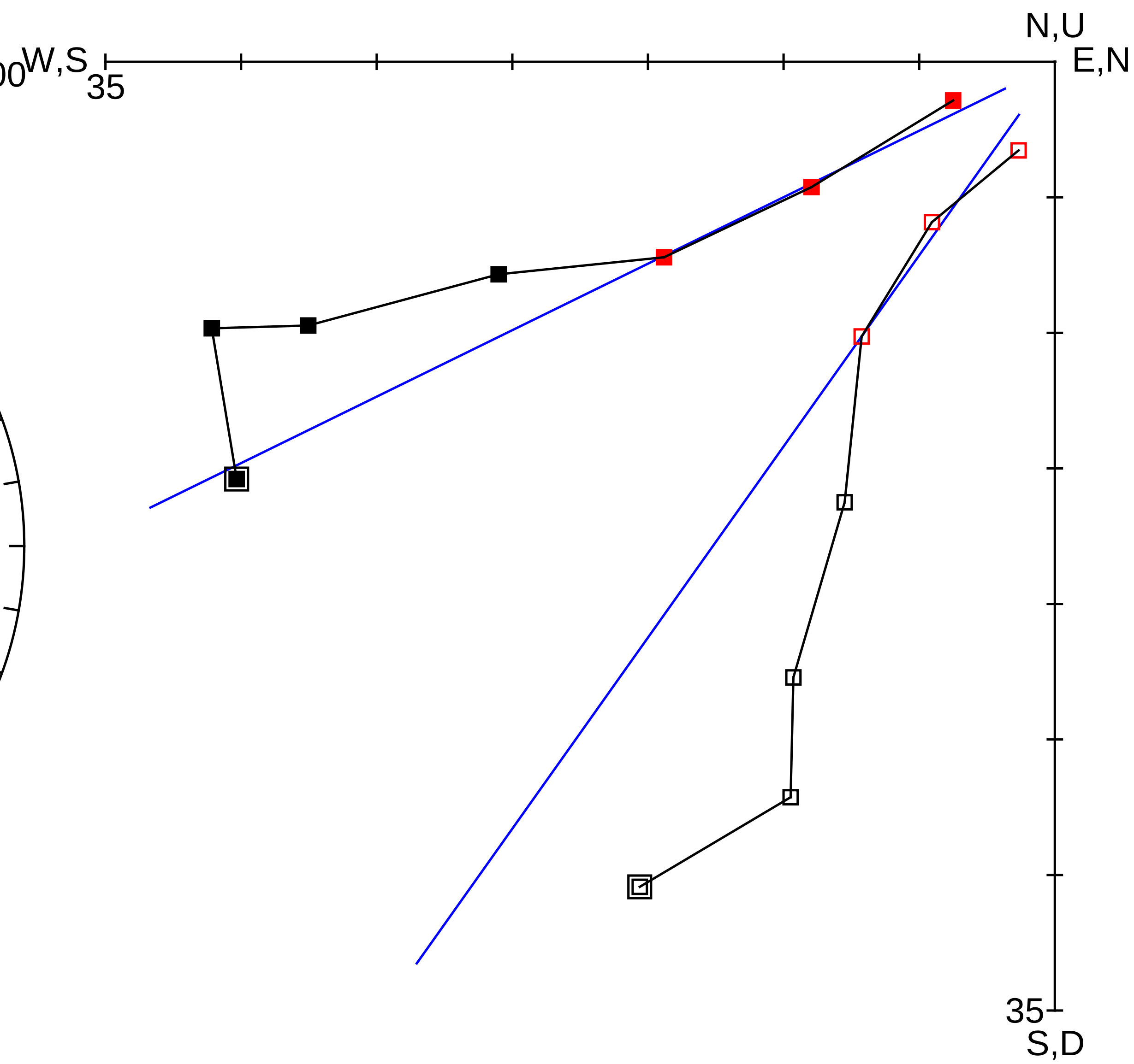

Sample: NV9-1
Site:Nivlac

PCA dec 254.93 / inc 34.14 Fisher dec 251.6 / inc 39.5 / a95 8.7 / k 31.5
PCA MAD1 33.96 / MAD3 1.90
(-0.22 -0.80 0.56)t

vertical
horizontal
Units: A/m ×102

Updated July 2017

	demag.	dec.	inc.	int.	m.s.
	0	255.1	35.1	3.74e-01	NaN
	5	254.1	35.4	3.61e-01	NaN
	10	257.1	34.3	3.21e-01	NaN
	15	255.3	34.3	2.78e-01	NaN
	20	247.9	32.7	2.39e-01	NaN
*	30	256.5	34.5	1.82e-01	NaN
*	40	255.2	34.7	1.45e-01	NaN
*	50	255.6	32.4	1.18e-01	NaN
*	60	252.0	32.5	9.61e-02	NaN
*	70	251.8	35.1	7.91e-02	NaN
*	80	256.4	34.5	6.57e-02	NaN
*	90	250.8	33.8	5.37e-02	NaN
*	100	251.2	34.8	4.60e-02	NaN
*	120	252.4	36.1	3.49e-02	NaN
*	140	250.1	38.6	2.86e-02	NaN

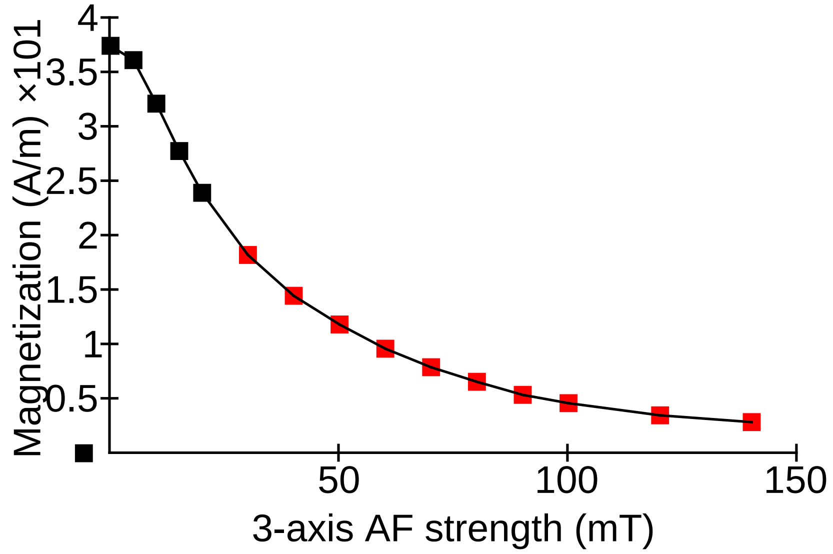

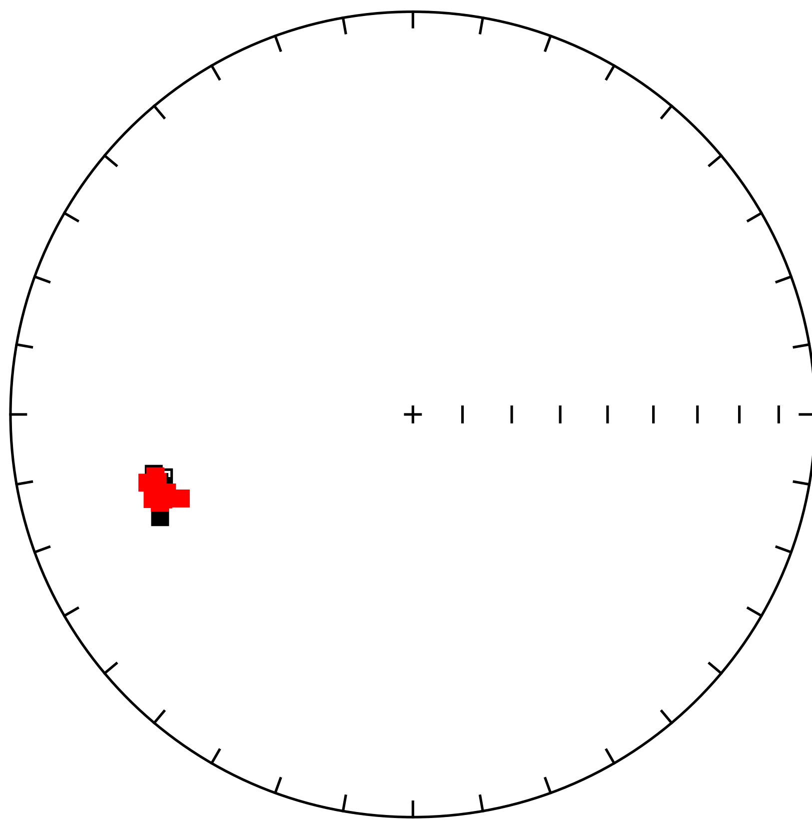

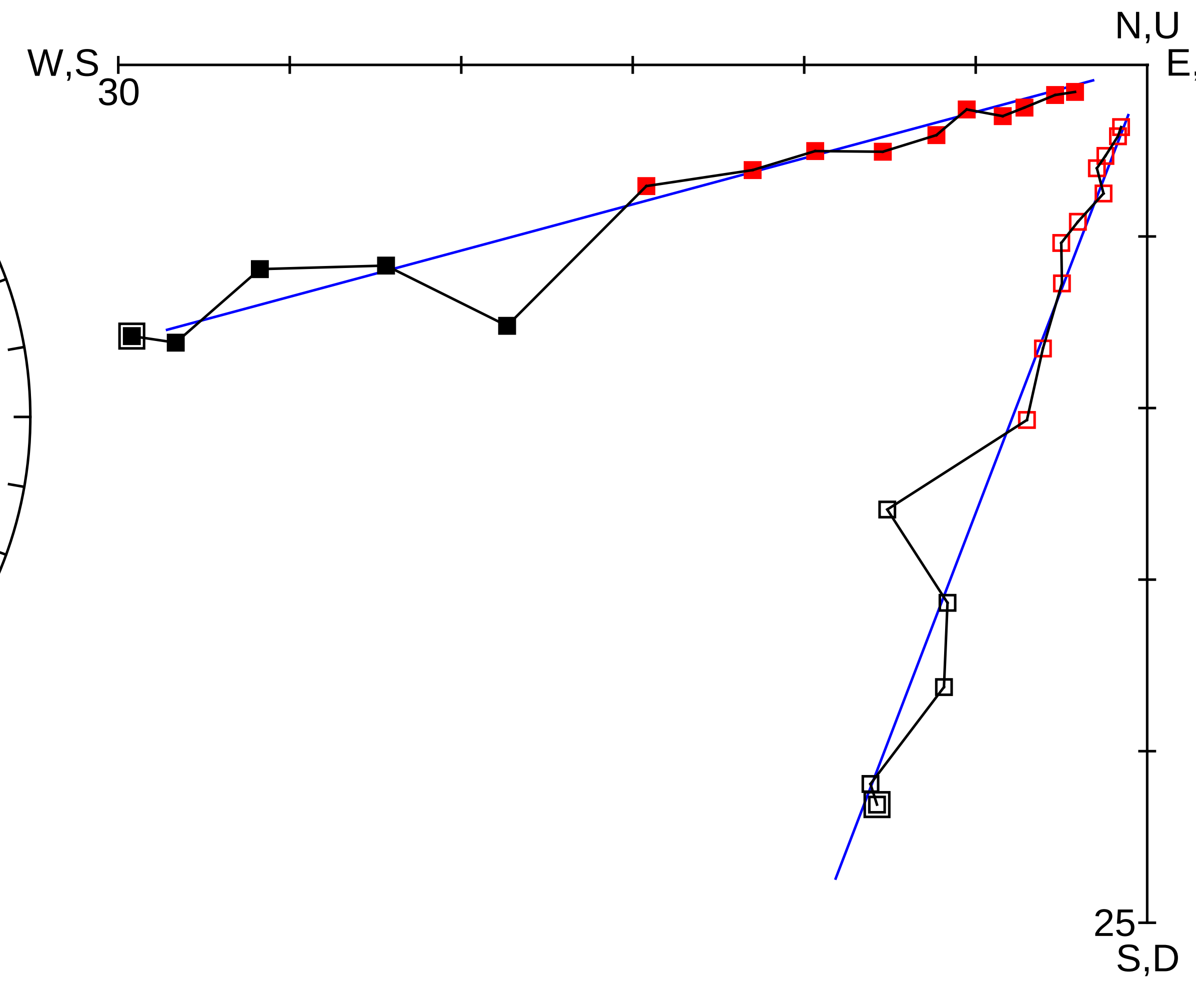

Sample: NV10-3

Site: Nivlac

PCA dec 231.83 / inc 44.32 Fisher dec 251.6 / inc 39.5 / a95 8.7 / k 31.5
PCA MAD1 10.18 / MAD3 3.14
(-0.44 -0.56 0.70)t

□ vertical
■ horizontal
Units: A/m ×102

Updated July 2017

	demag.	dec.	inc.	int.	m.s.
	0	218.4	51.5	8.25e-02	NaN
*	5	231.4	46.9	5.23e-02	NaN
*	10	232.1	40.5	3.87e-02	NaN
*	20	233.5	44.1	2.54e-02	NaN
*	40	230.0	37.6	1.35e-02	NaN
	80	250.0	31.2	6.06e-03	NaN
	160	191.0	27.0	4.01e-03	NaN

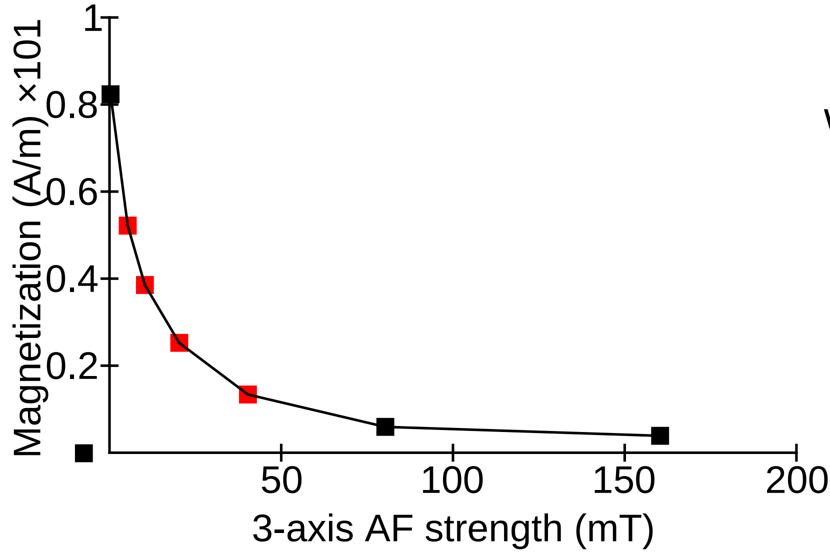

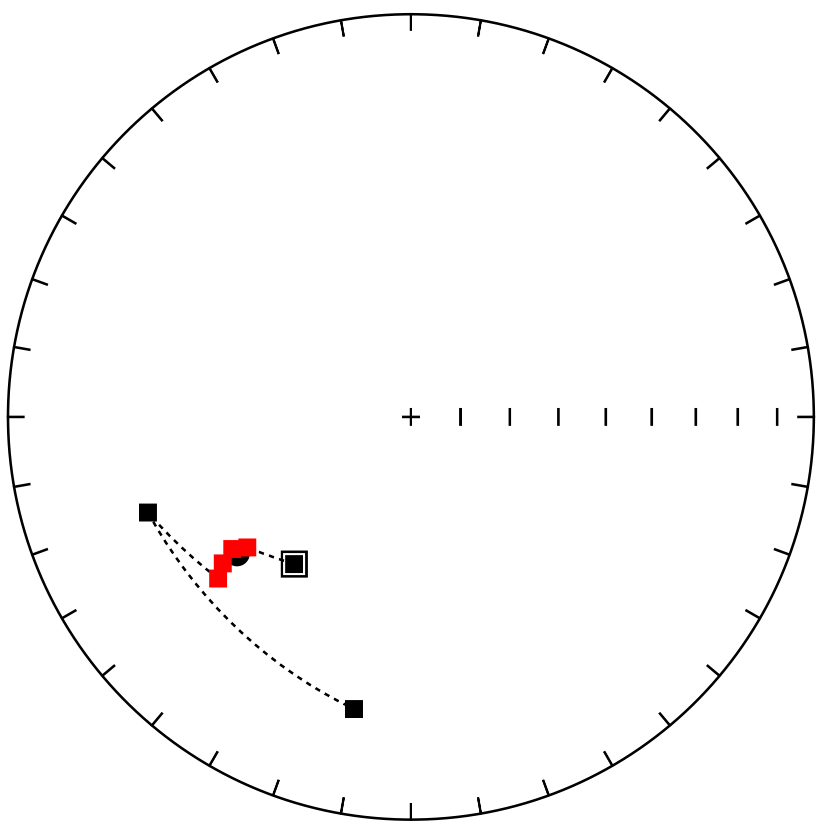

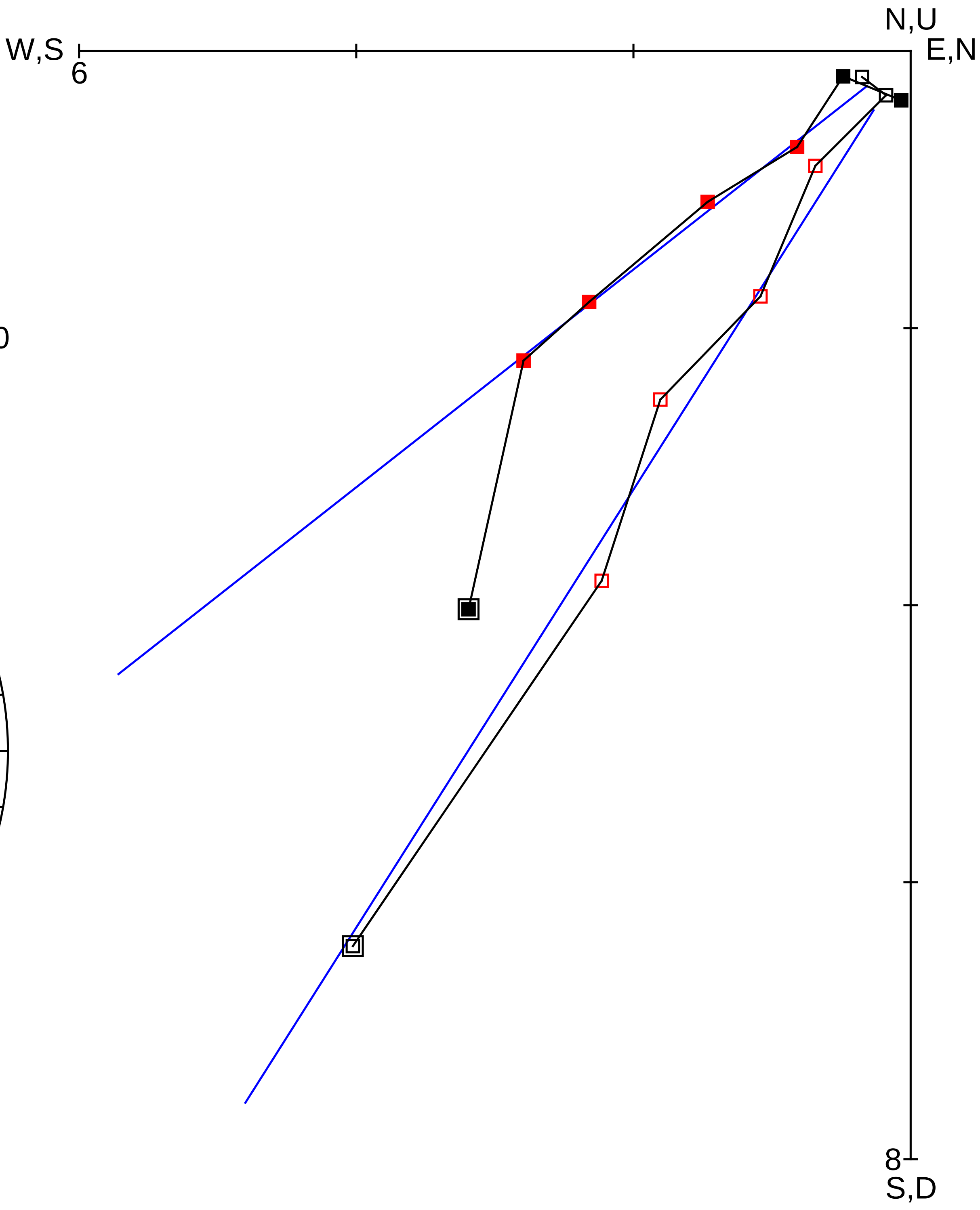

Sample: NV11-2
Site: Nivlac

PCA dec 252.98 / inc 36.64 Fisher dec 251.6 / inc 39.5 / a95 8.7 / k 31.5
PCA MAD1 34.80 / MAD3 1.37
(-0.23 -0.77 0.60)t

□ vertical
■ horizontal
Units: A/m ×102

Updated July 2017

	demag.	dec.	inc.	int.	m.s.
	0	253.9	41.1	5.00e-01	NaN
*	5	252.1	36.8	4.72e-01	NaN
*	10	254.0	37.5	3.87e-01	NaN
*	20	254.3	36.3	2.63e-01	NaN
*	40	253.0	33.8	1.86e-01	NaN
*	80	251.0	33.7	1.18e-01	NaN
*	160	246.7	34.5	5.22e-02	NaN

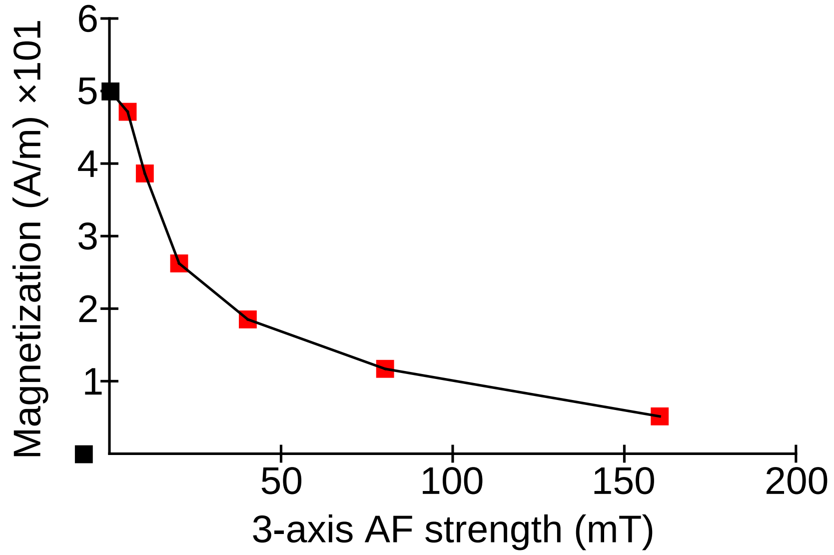

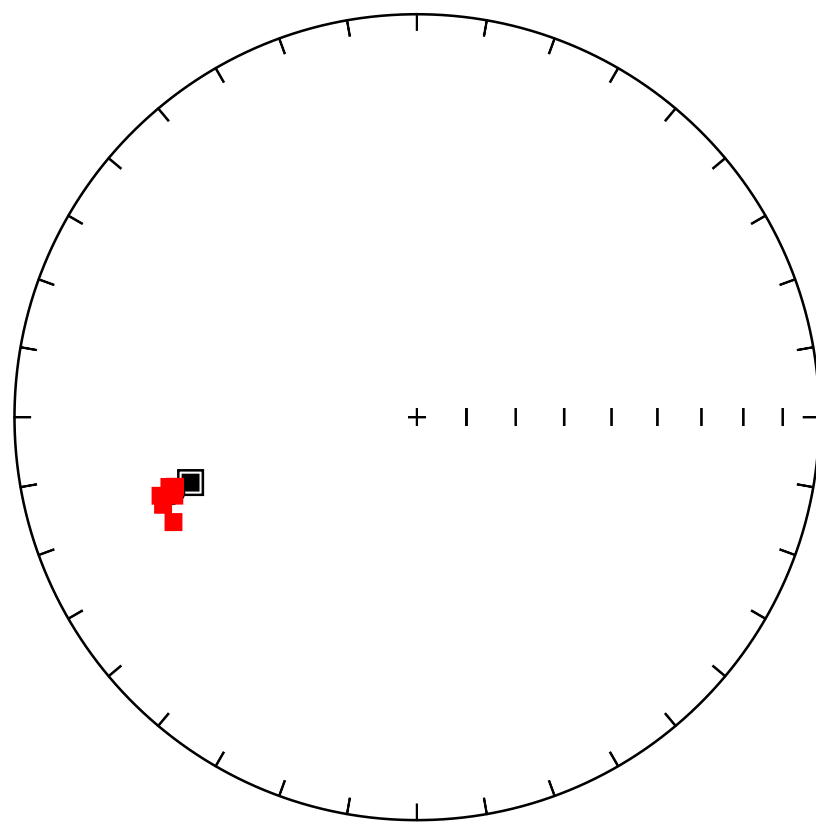

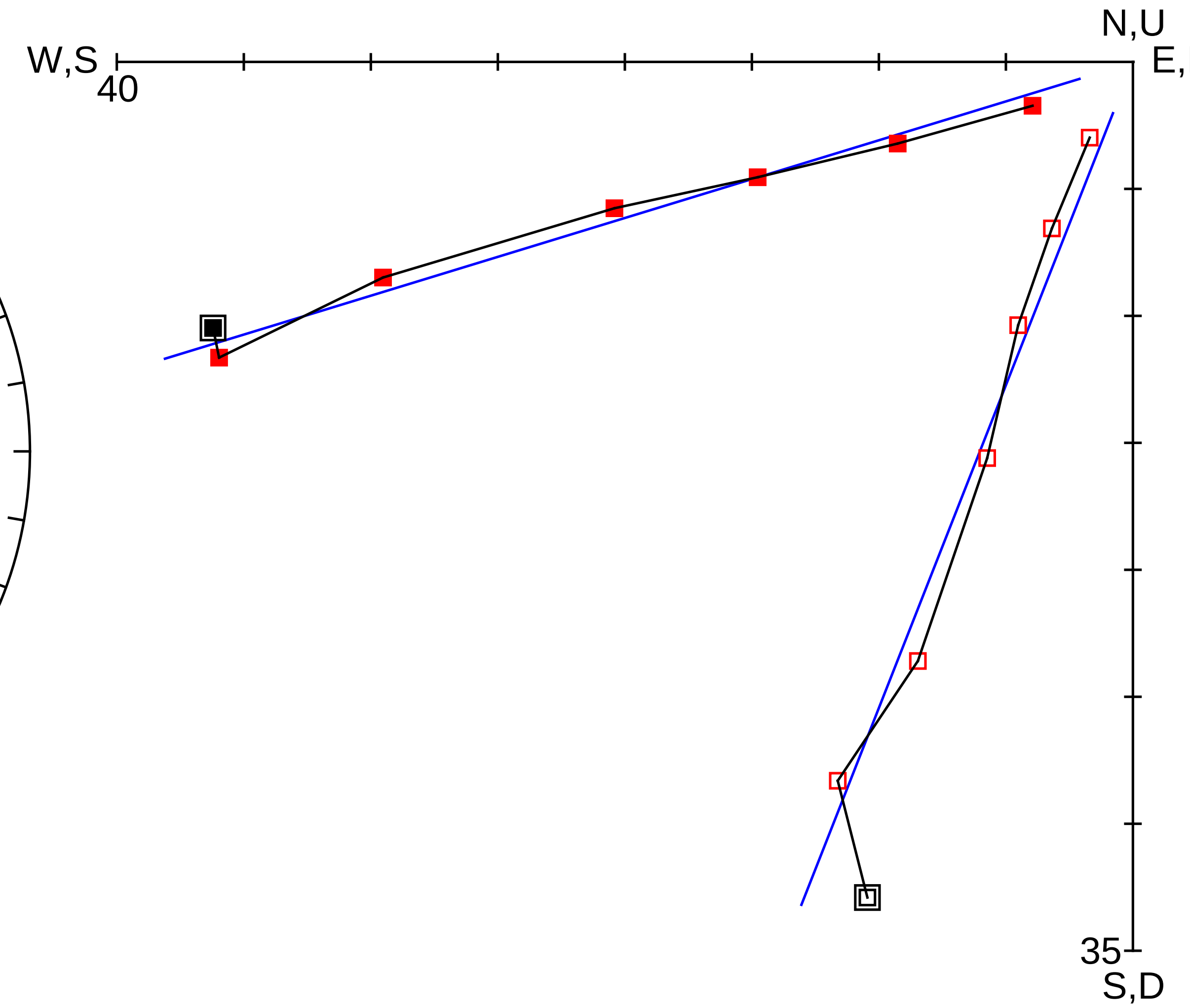

Sample: E1-1
Site: Estella

PCA dec 342.62 / inc 78.36 Fisher dec 335.6 / inc 72.7 / a95 10.7 / k 24.3
PCA MAD1 11.70 / MAD3 4.37
(0.19 -0.06 0.98)t

□ vertical
■ horizontal
Units: A/m ×102

Updated July 2017

	demag.	dec.	inc.	int.	m.s.
	0	346.2	85.7	8.28e-02	NaN
*	5	339.3	77.3	4.54e-02	NaN
*	10	347.2	78.5	3.01e-02	NaN
*	15	320.6	74.4	2.26e-02	NaN
*	20	29.5	80.4	1.79e-02	NaN
*	30	61.4	82.3	1.28e-02	NaN
*	40	10.9	82.3	7.47e-03	NaN

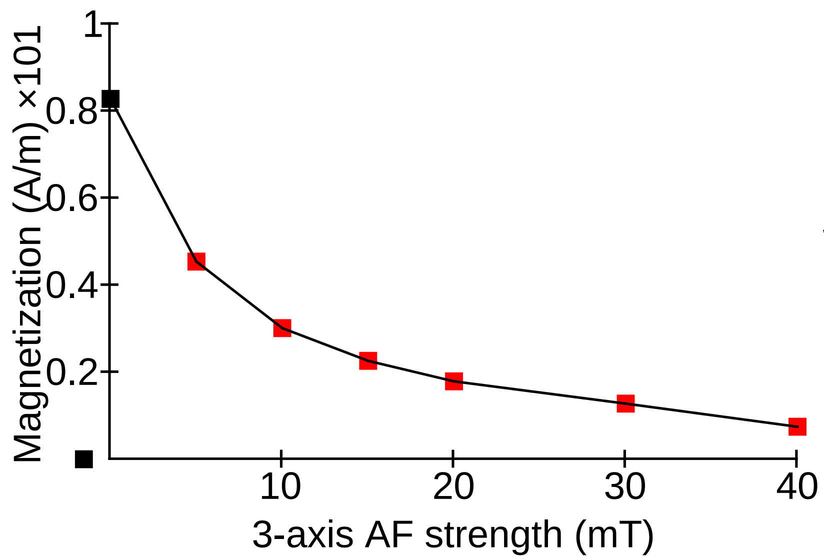

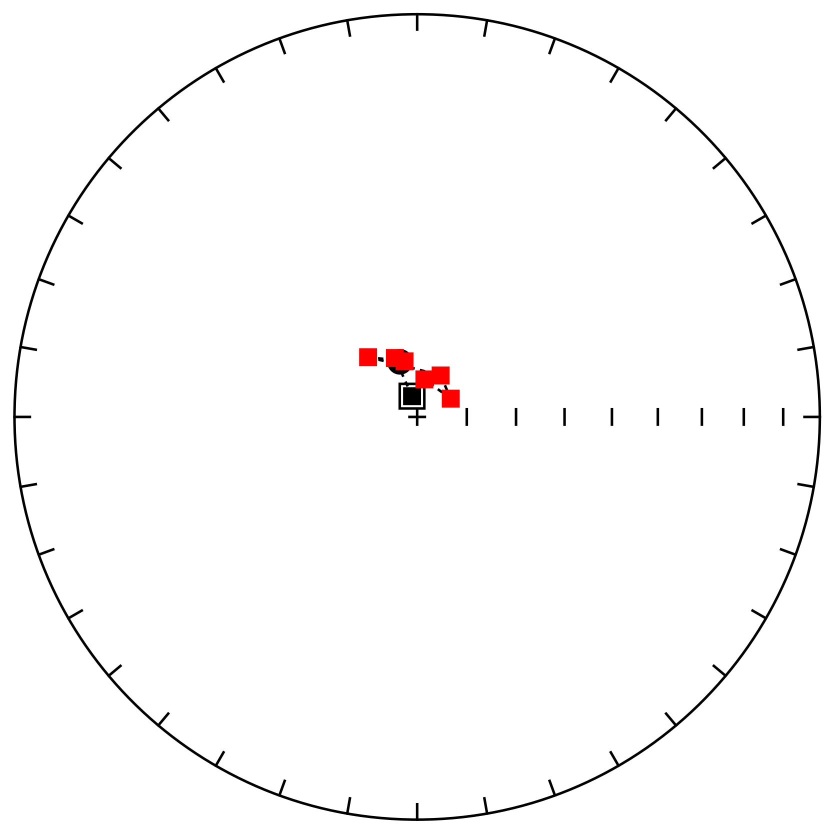

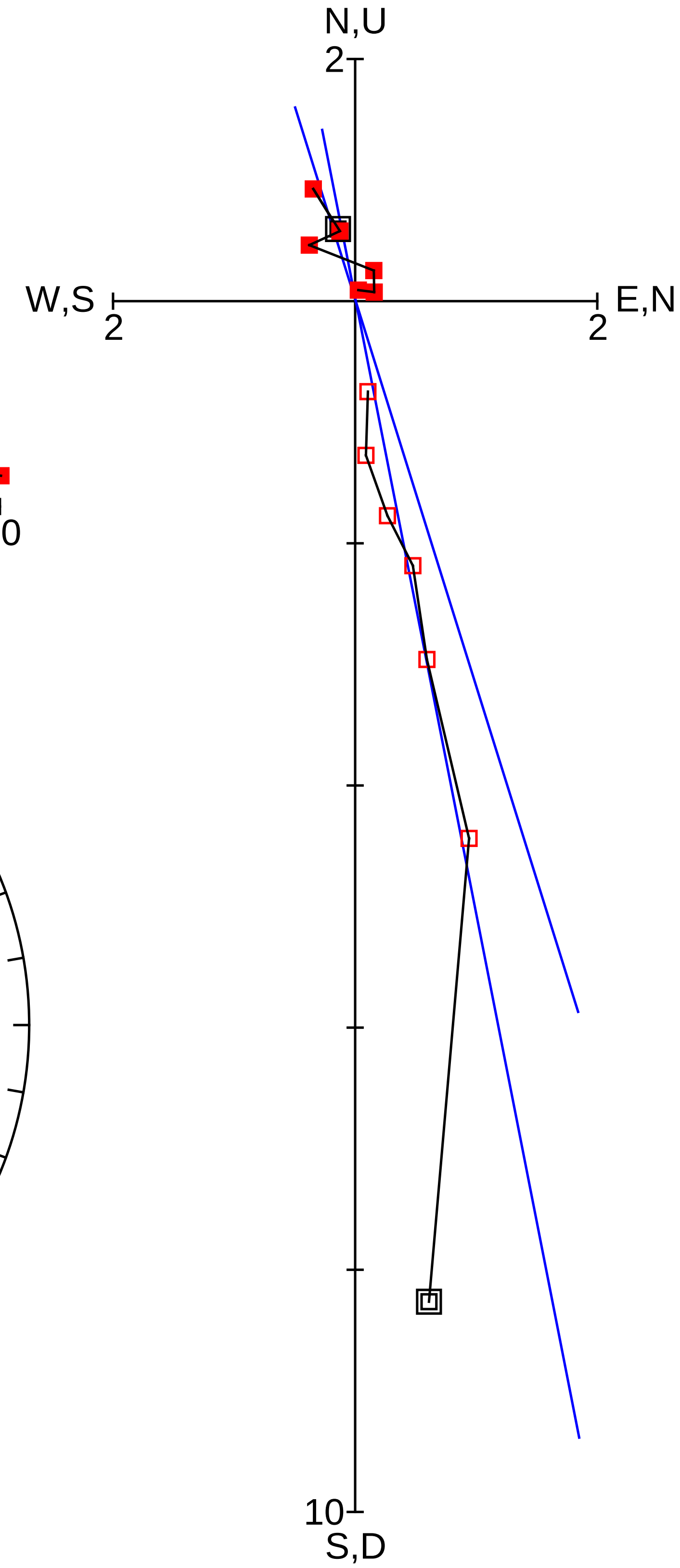

Sample: E2-2

Site: Estella

PCA dec 346.11 / inc 63.63 Fisher dec 335.6 / inc 72.7 / a95 10.7 / k 24.3
PCA MAD1 30.73 / MAD3 4.89
(0.43 -0.11 0.90)t

Updated July 2017

	demag.	dec.	inc.	int.	m.s.
	0	296.7	70.9	2.91e-02	NaN
*	5	344.7	61.3	1.94e-02	NaN
*	10	358.7	65.9	1.45e-02	NaN
*	20	327.1	65.3	1.02e-02	NaN
	40	200.6	81.2	6.42e-03	NaN

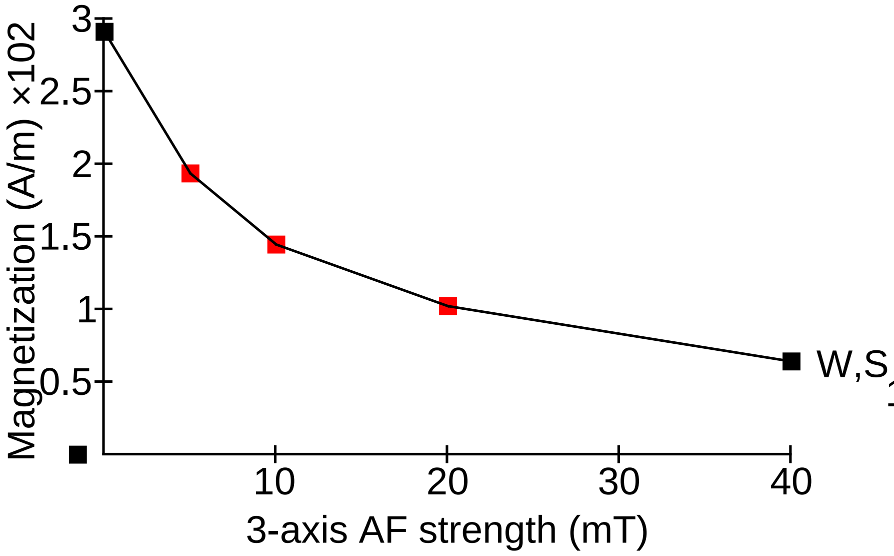

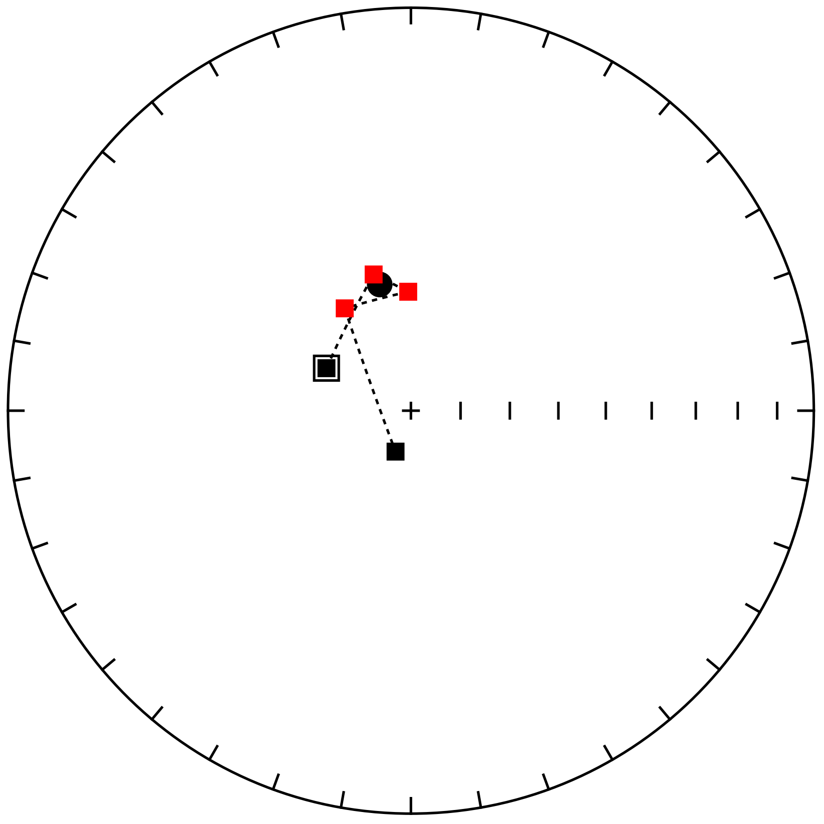

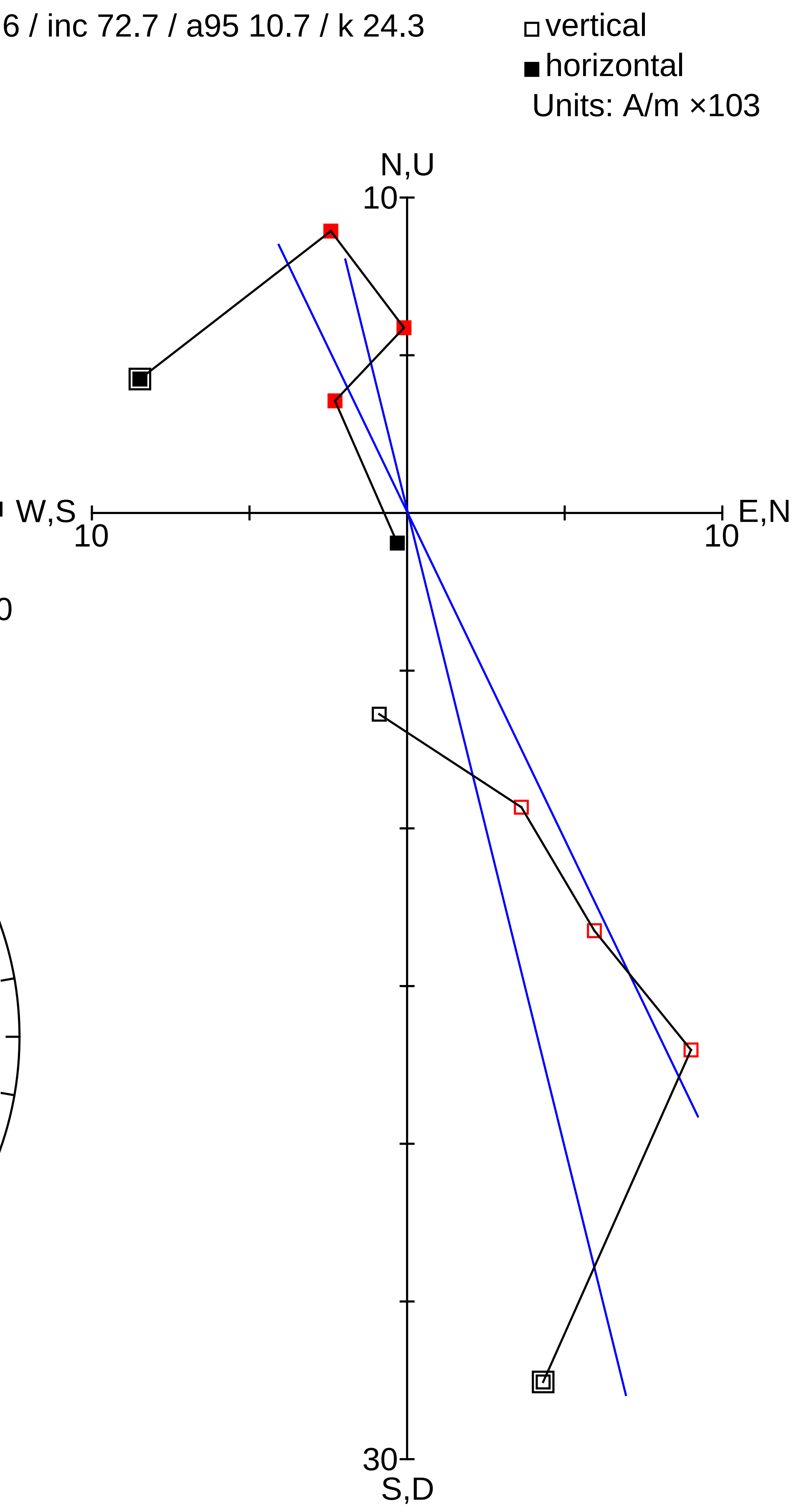

Sample: E3-2
Site: Estella

PCA dec 313.73 / inc 58.19 Fisher dec 335.6 / inc 72.7 / a95 10.7 / k 24.3
PCA MAD1 34.42 / MAD3 4.18
(0.36 -0.38 0.85)t

□ vertical
■ horizontal
Units: A/m ×103

Updated July 2017

	demag.	dec.	inc.	int.	m.s.
	0	324.5	47.2	4.44e-02	NaN
	5	320.4	48.8	2.50e-02	NaN
*	10	314.0	55.3	1.68e-02	NaN
*	20	319.4	62.6	1.15e-02	NaN
*	40	302.5	59.3	7.57e-03	NaN
*	50	308.9	62.8	5.21e-03	NaN

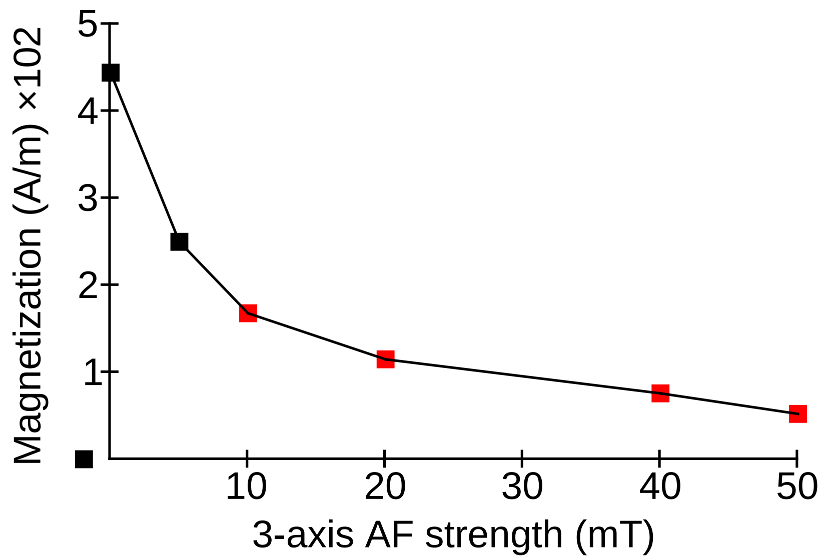

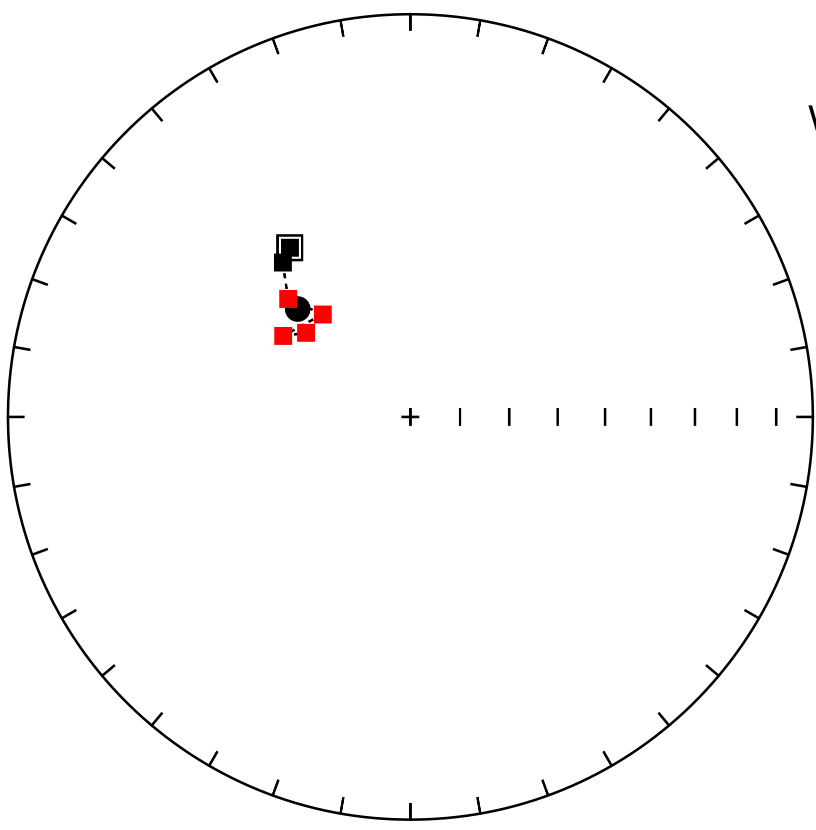

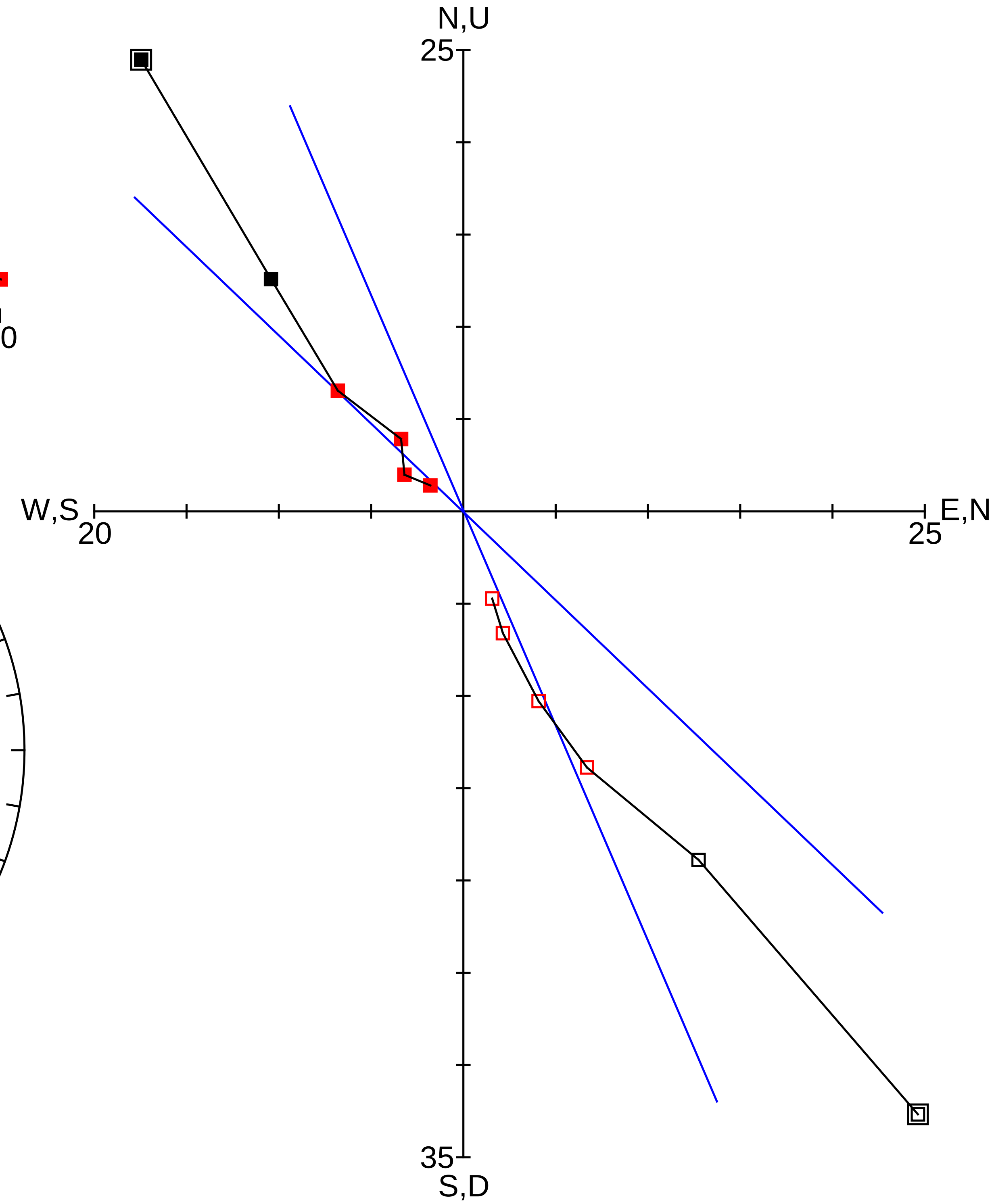

Sample: E4-2
Site: Estella

PCA dec 314.03 / inc 62.70 Fisher dec 335.6 / inc 72.7 / a95 10.7 / k 24.3
PCA MAD1 0.83 / MAD3 1.79
(0.32 -0.33 0.89)t

□ vertical
■ horizontal
Units: A/m ×102

Updated July 2017

	demag.	dec.	inc.	int.	m.s.
	0	321.8	68.0	5.84e-02	NaN
	5	326.6	65.9	3.14e-02	NaN
*	10	313.8	62.2	2.32e-02	NaN
*	15	315.4	64.9	1.96e-02	NaN
*	20	312.6	60.2	1.52e-02	NaN
	30	293.8	53.7	1.16e-02	NaN
	40	288.6	51.2	9.88e-03	NaN
	50	279.7	53.2	7.23e-03	NaN

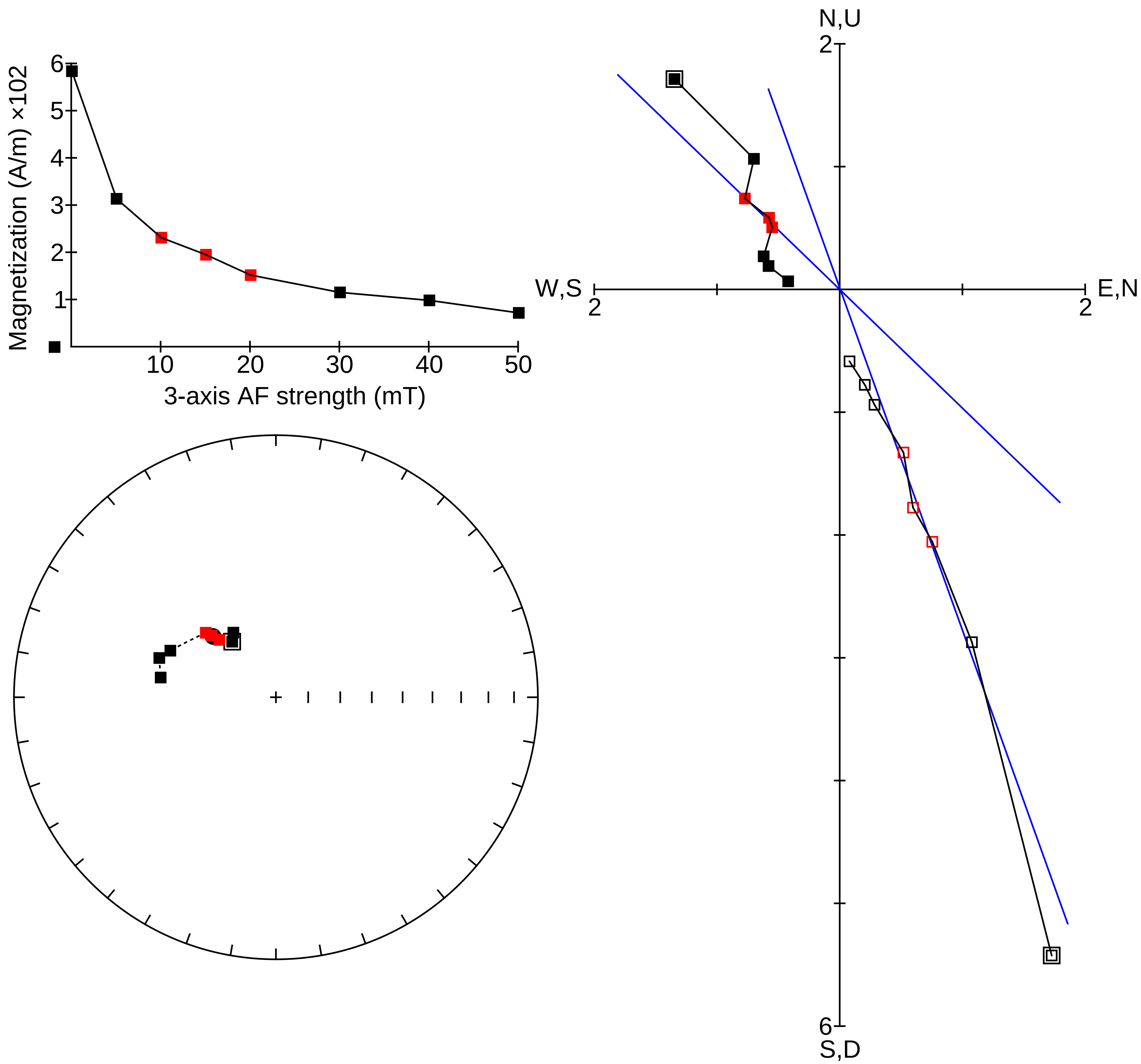

Sample: E5-2
Site: Estella

PCA dec 106.33 / inc 67.70 Fisher dec 335.6 / inc 72.7 / a95 10.7 / k 24.3
PCA MAD1 17.37 / MAD3 6.24
(-0.11 0.36 0.93)t

□ vertical
■ horizontal
Units: A/m ×102

Updated July 2017

	demag.	dec.	inc.	int.	m.s.
	0	78.5	66.7	5.40e-02	NaN
*	5	106.5	71.8	3.31e-02	NaN
*	10	111.6	70.0	2.25e-02	NaN
*	15	102.1	66.7	1.86e-02	NaN
*	20	108.9	53.9	1.73e-02	NaN
*	30	102.1	60.7	1.20e-02	NaN
*	40	0.0	0.0	0.00e+00	NaN
*	50	89.1	60.1	7.97e-03	NaN

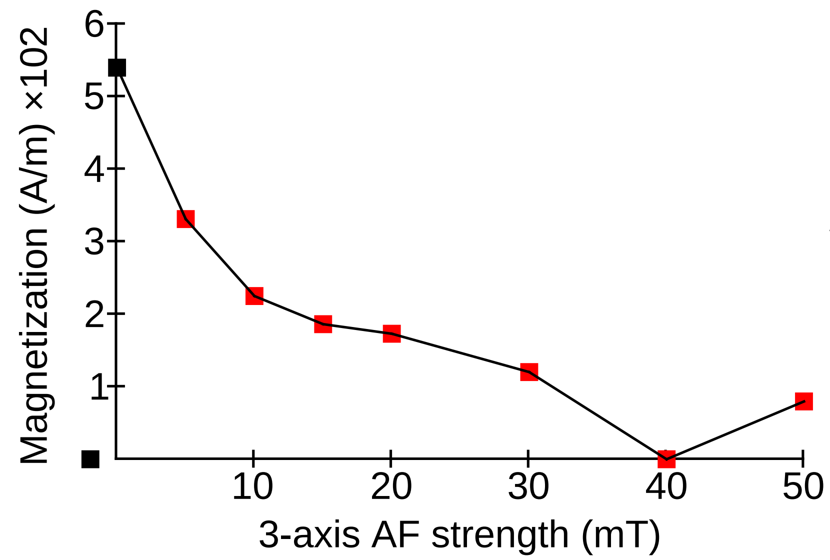

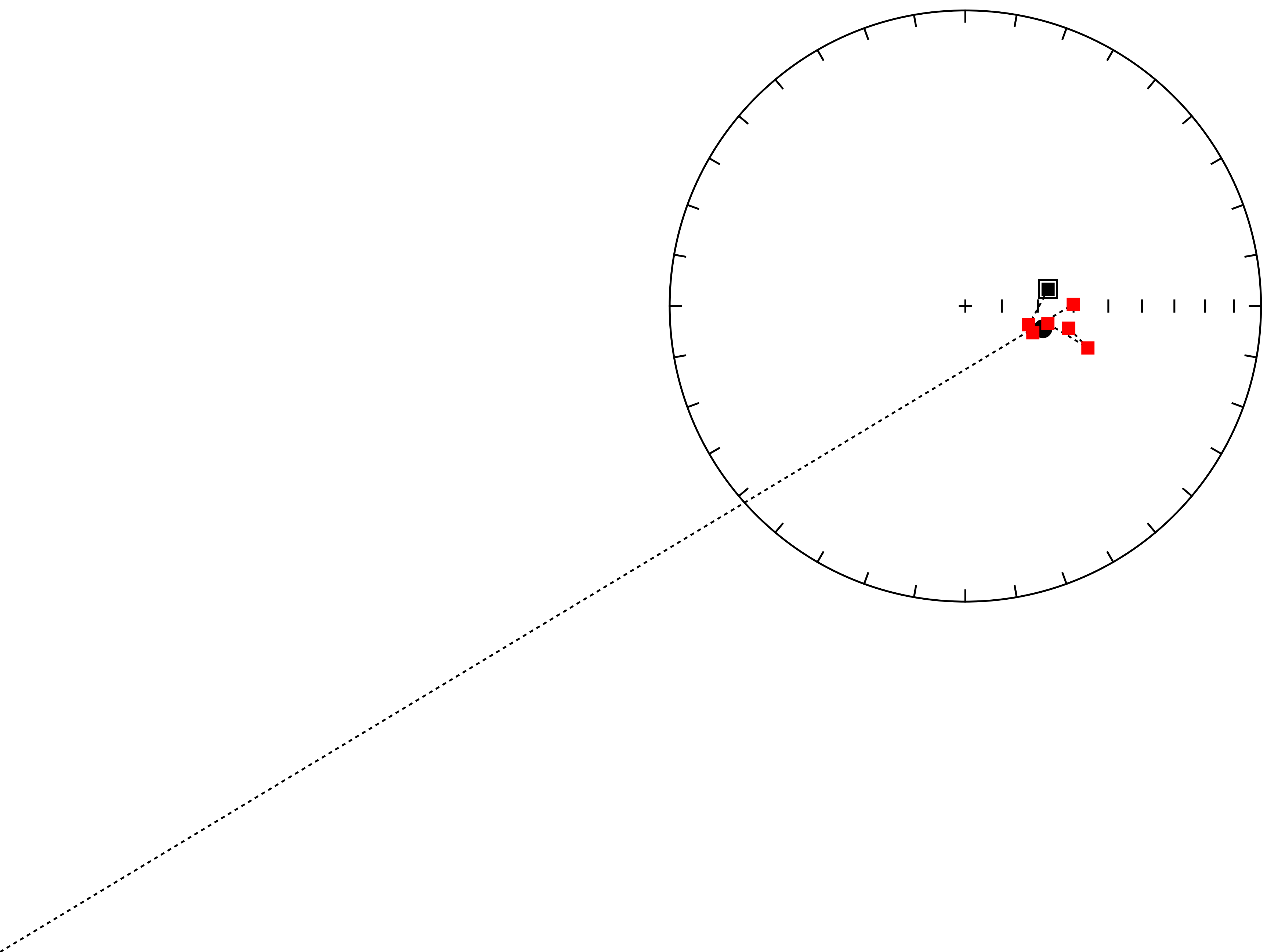

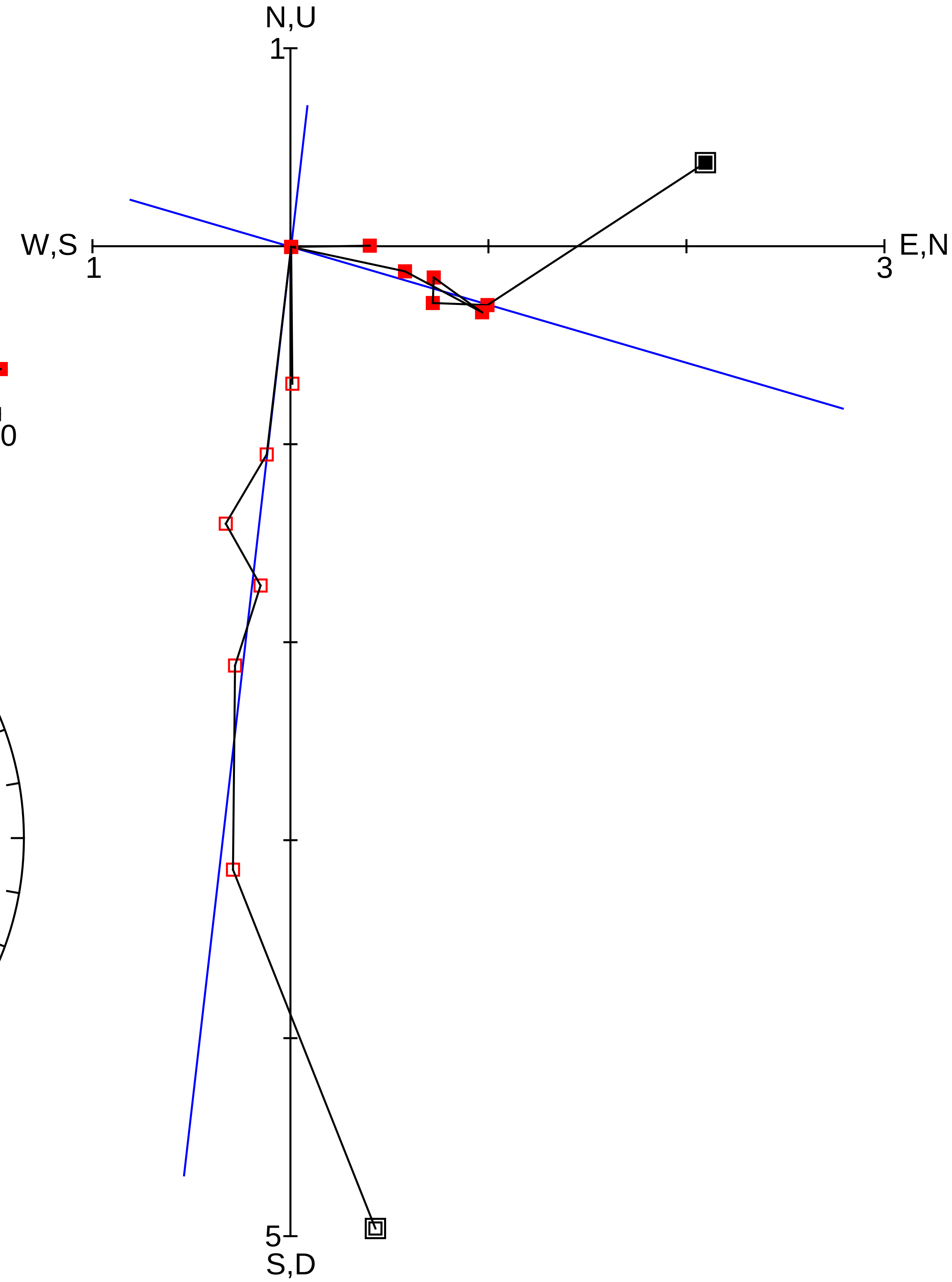

Sample: E6-3

Site: Estella

PCA dec 337.92 / inc 74.52 Fisher dec 335.6 / inc 72.7 / a95 10.7 / k 24.3

PCA MAD1 16.91 / MAD3 5.14

(0.25 -0.10 0.96)t

vertical

horizontal

Units: A/m ×102

Updated July 2017

	demag.	dec.	inc.	int.	m.s.
	0	12.0	81.4	6.36e-02	NaN
	5	27.8	73.9	3.49e-02	NaN
*	10	350.7	75.2	1.89e-02	NaN
*	15	311.0	72.4	1.44e-02	NaN
*	20	333.0	73.1	1.14e-02	NaN
*	30	357.7	75.9	7.89e-03	NaN
*	40	352.8	70.1	8.30e-03	NaN

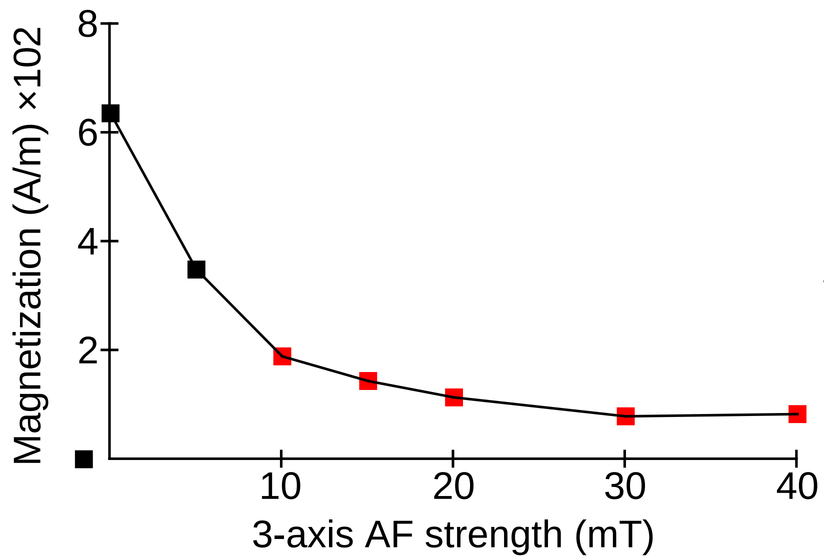

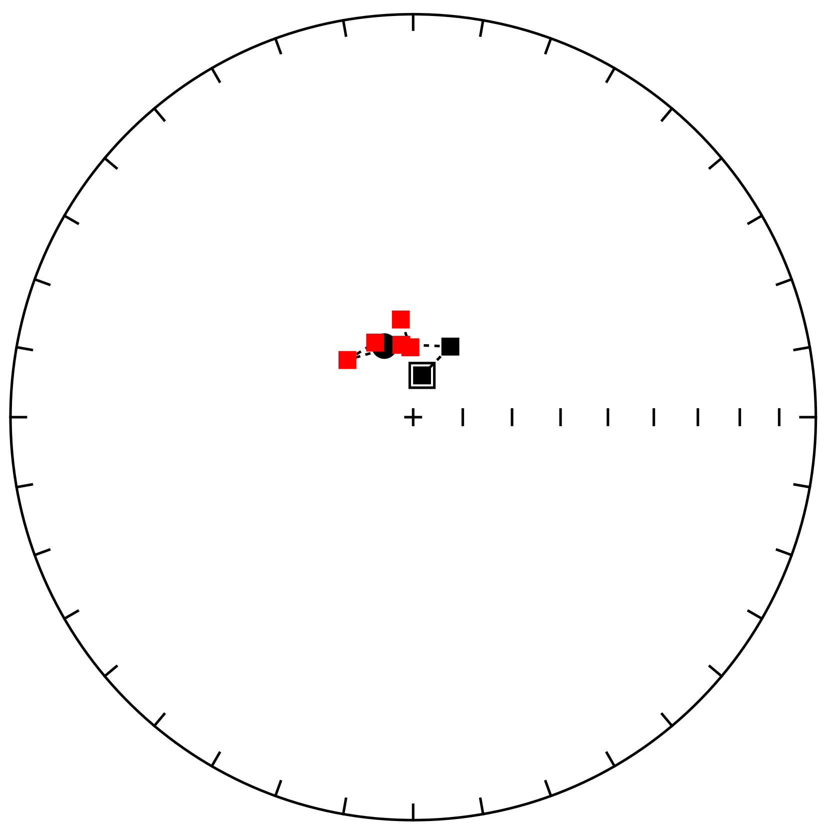

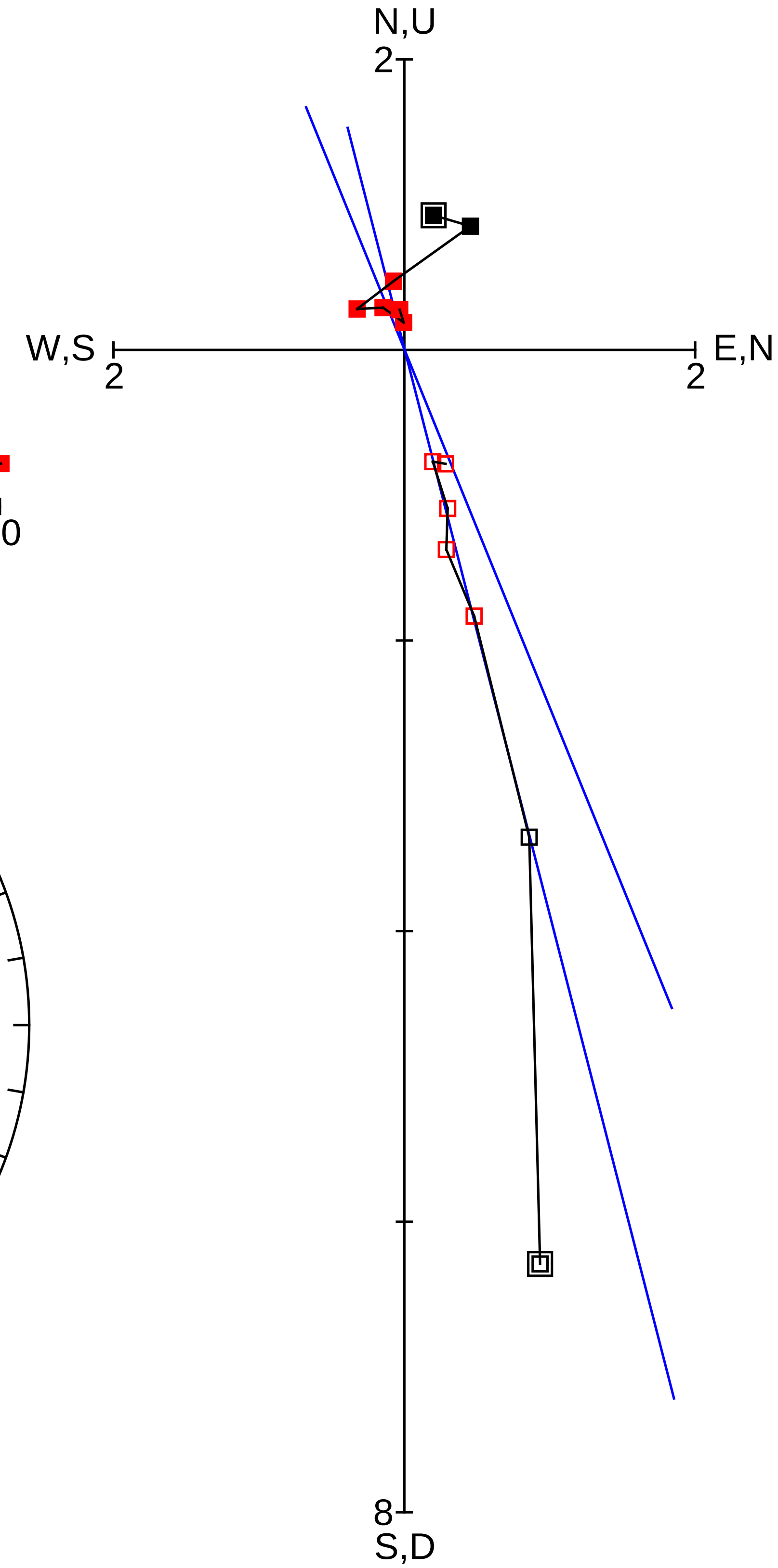

Sample: E7-2
Site: Estella

PCA dec 349.70 / inc 65.43 Fisher dec 335.6 / inc 72.7 / a95 10.7 / k 24.3
PCA MAD1 18.56 / MAD3 5.29
(0.41 -0.07 0.91)t

□ vertical
■ horizontal
Units: A/m ×102

Updated July 2017

	demag.	dec.	inc.	int.	m.s.
	0	355.4	66.3	5.08e-02	NaN
*	5	356.2	65.2	3.20e-02	NaN
*	10	352.1	63.1	1.91e-02	NaN
*	15	334.5	67.5	1.33e-02	NaN
*	20	331.3	69.7	9.90e-03	NaN
*	25	315.8	60.5	1.02e-02	NaN
	30	326.3	65.1	8.08e-03	NaN
	35	314.7	57.6	7.65e-03	NaN
	40	301.2	52.9	7.98e-03	NaN

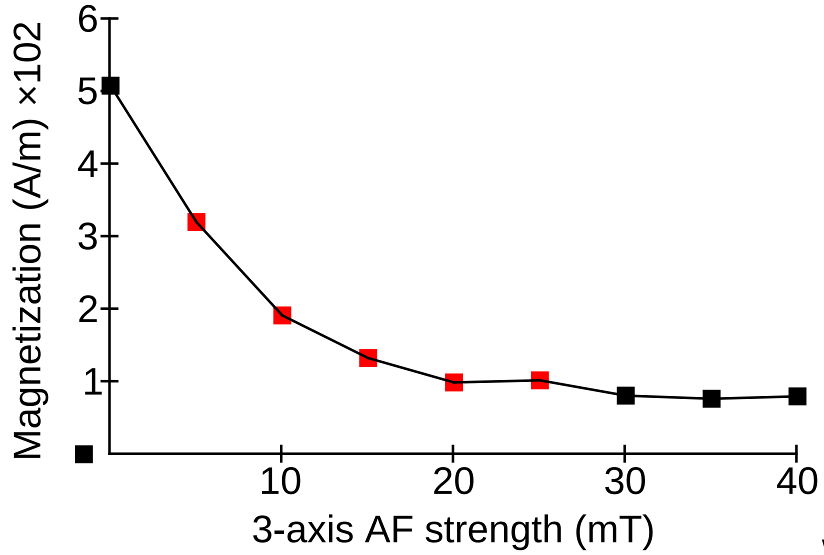

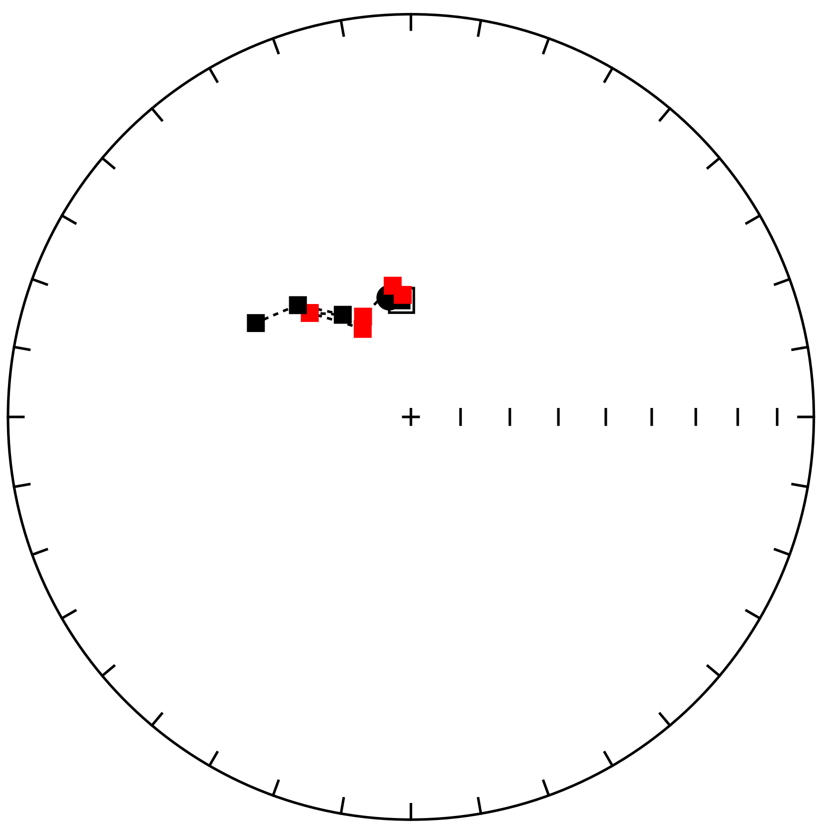

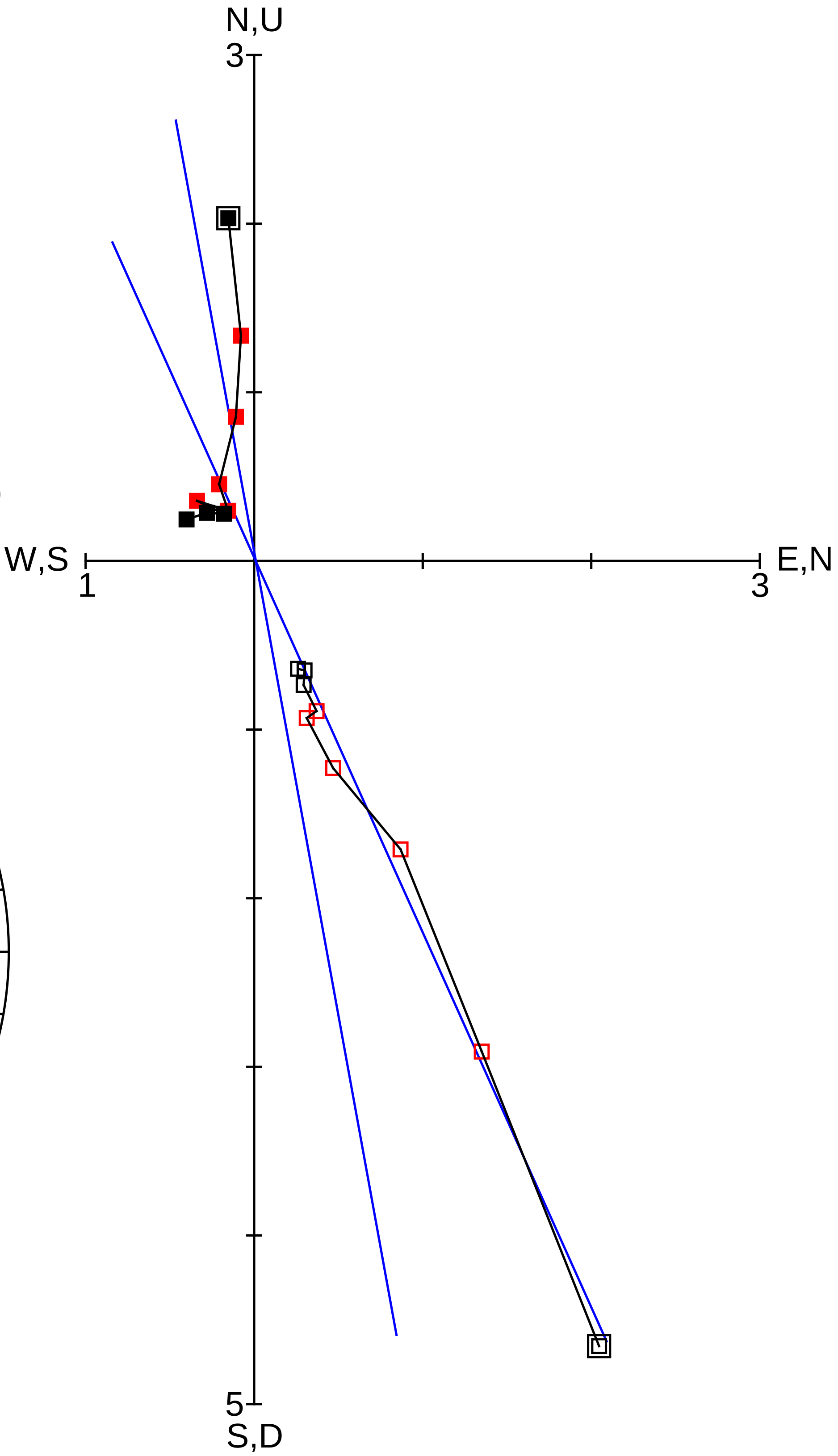

Sample: E8-3
Site: Estella

PCA dec 286.66 / inc 74.41 Fisher dec 335.6 / inc 72.7 / a95 10.7 / k 24.3
PCA MAD1 31.77 / MAD3 3.37
(0.08 -0.26 0.96)t

Updated July 2017

	demag.	dec.	inc.	int.	m.s.
	0	256.3	66.4	6.29e-02	NaN
*	5	292.9	75.0	3.13e-02	NaN
*	10	275.5	72.7	1.83e-02	NaN
*	15	280.7	71.0	1.13e-02	NaN
*	20	288.6	73.1	7.74e-03	NaN
*	30	265.4	84.9	6.87e-03	NaN
*	40	269.0	65.5	5.12e-03	NaN

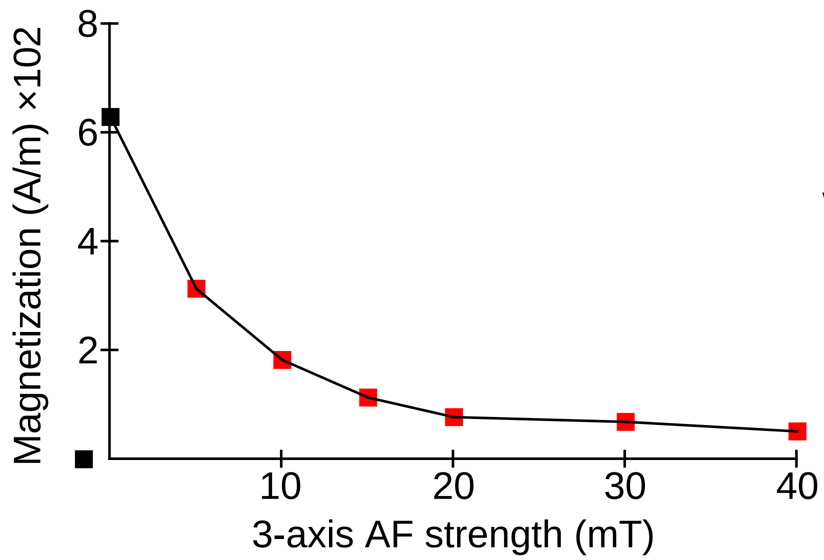

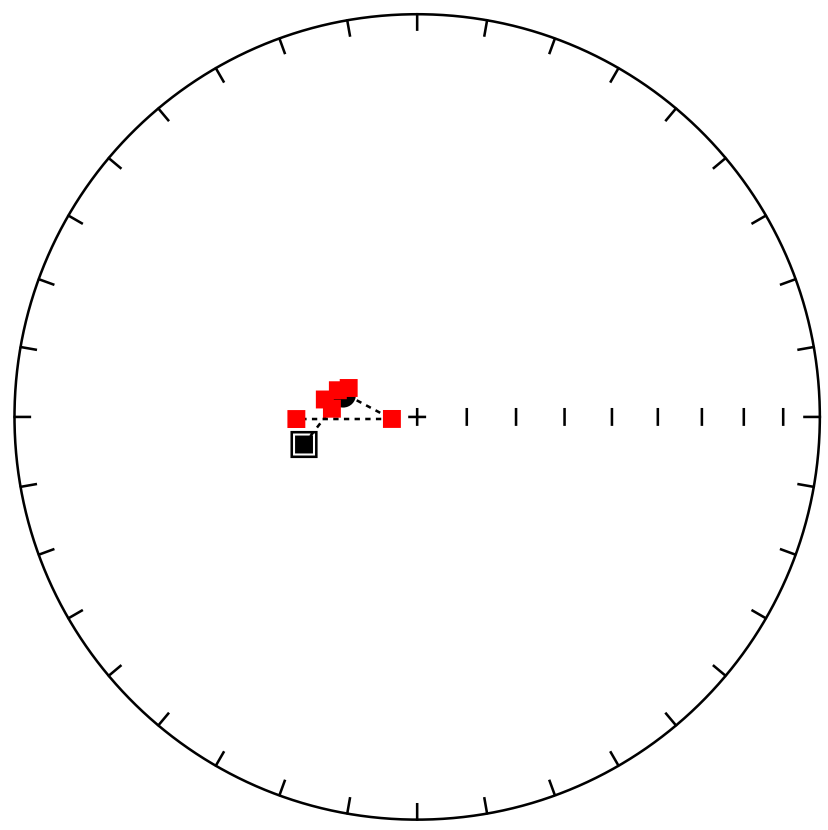

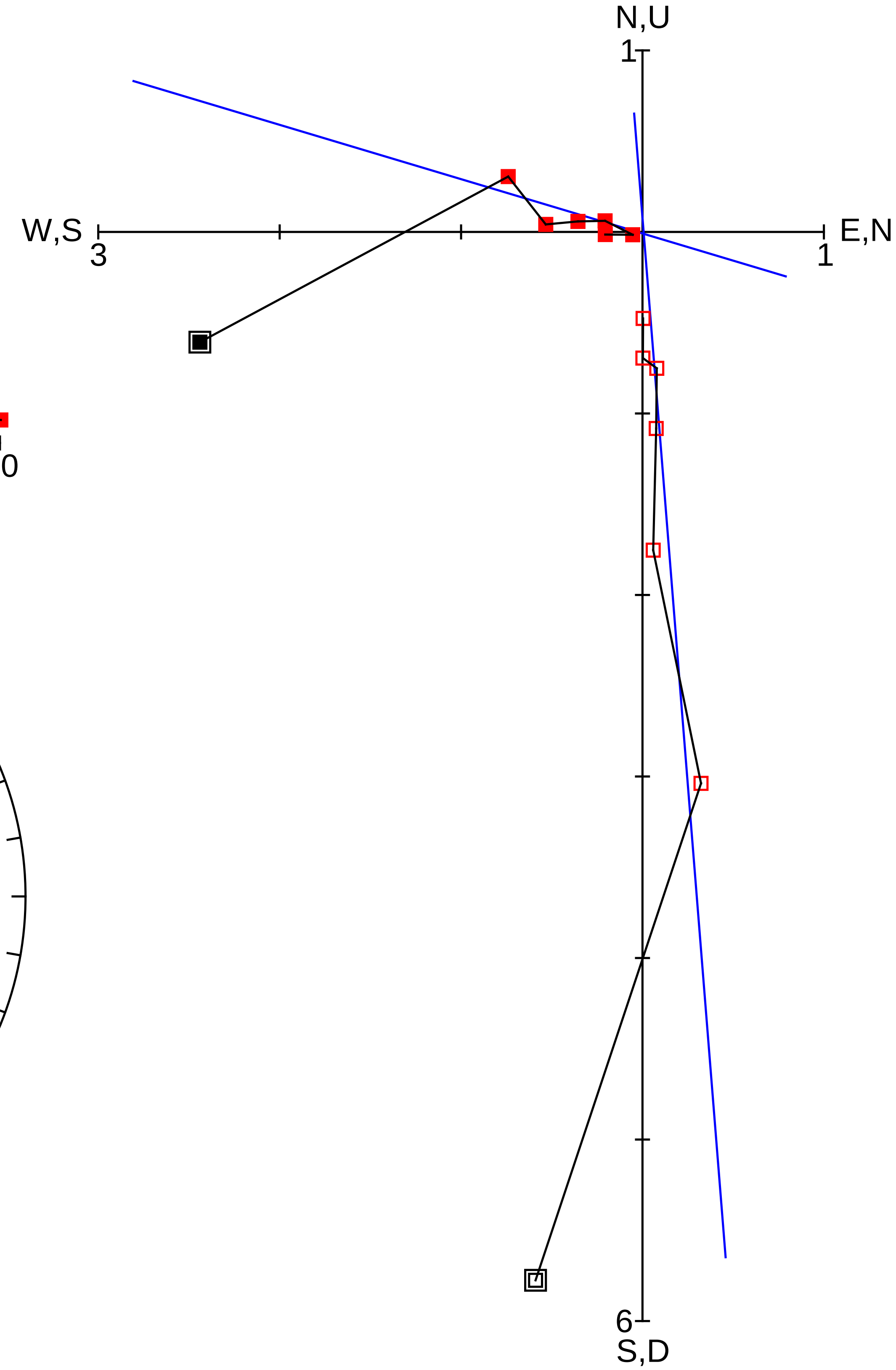

Sample: E9-1
Site: Estella

PCA dec 344.04 / inc 64.80 Fisher dec 335.6 / inc 72.7 / a95 10.7 / k 24.3
PCA MAD1 20.27 / MAD3 5.69
(0.41 -0.12 0.90)t

Updated July 2017

	demag.	dec.	inc.	int.	m.s.
	0	340.9	78.3	6.43e-02	NaN
*	5	343.5	68.0	3.66e-02	NaN
*	10	337.7	65.6	2.08e-02	NaN
*	15	354.4	57.0	1.40e-02	NaN
*	20	344.4	55.4	1.20e-02	NaN
*	30	352.7	51.2	1.10e-02	NaN
*	40	334.5	59.1	8.54e-03	NaN

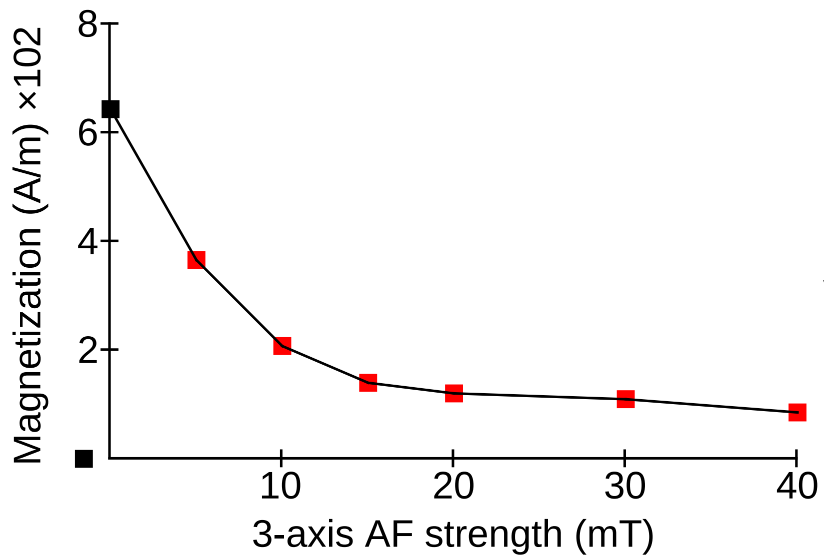

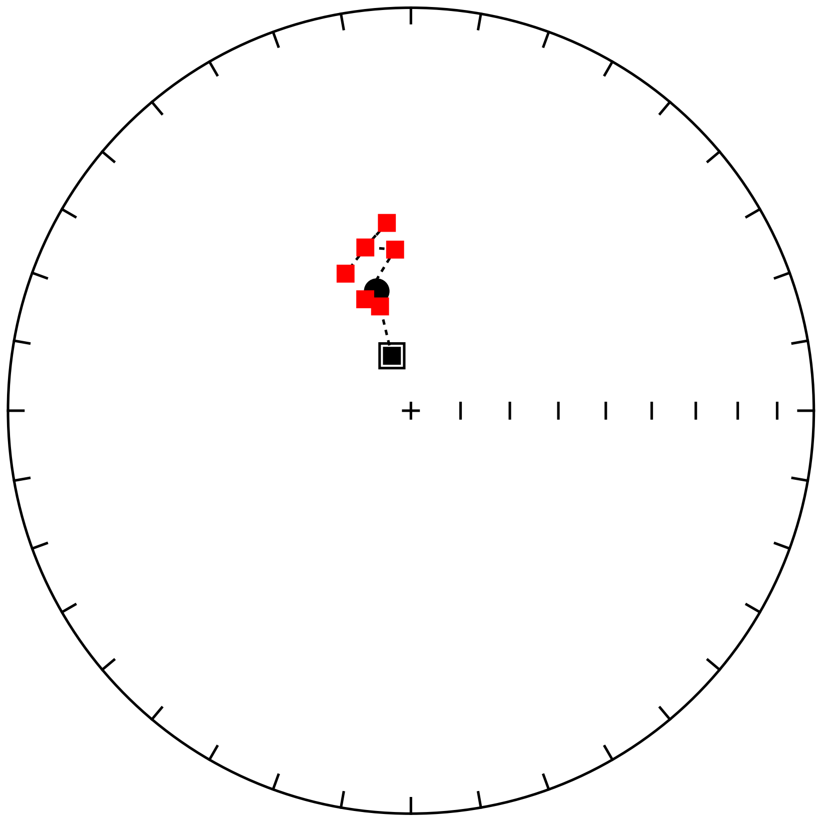

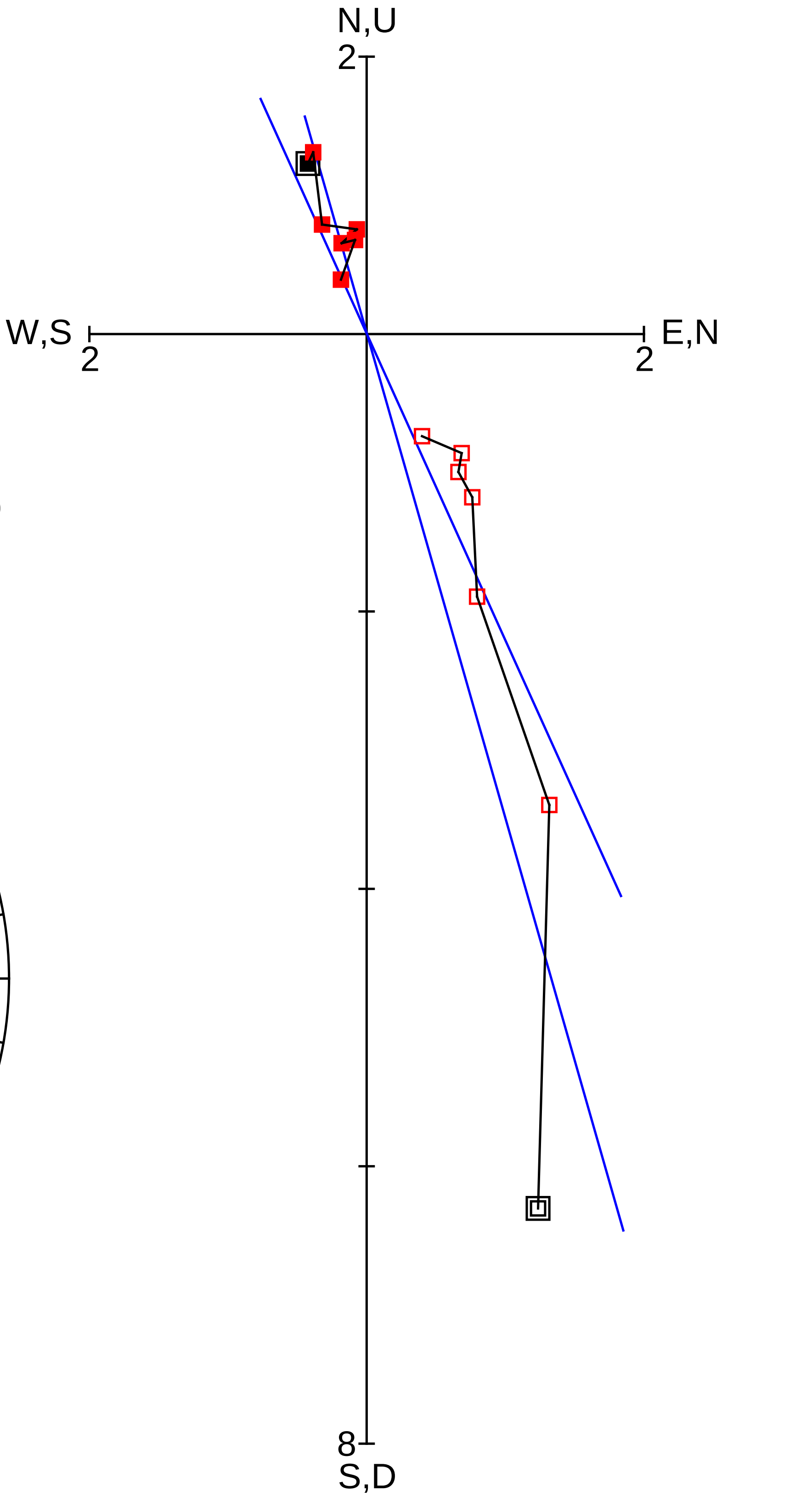

Sample: BR1-1

Site: Bull River

PCA dec 351.71 / inc 75.08 Fisher dec 10.2 / inc 66.9 / a95 6.2 / k 81.2
PCA MAD1 9.14 / MAD3 2.10
(0.25 -0.04 0.97)t

	demag.	dec.	inc.	int.	m.s.
	0	5.0	78.2	1.30e-01	NaN
	5	1.7	79.3	1.00e-01	NaN
*	10	353.9	75.0	6.99e-02	NaN
*	20	353.0	75.7	4.32e-02	NaN
*	40	341.6	74.5	2.17e-02	NaN
*	80	319.2	68.3	1.37e-02	NaN
	160	262.5	54.6	4.54e-03	NaN

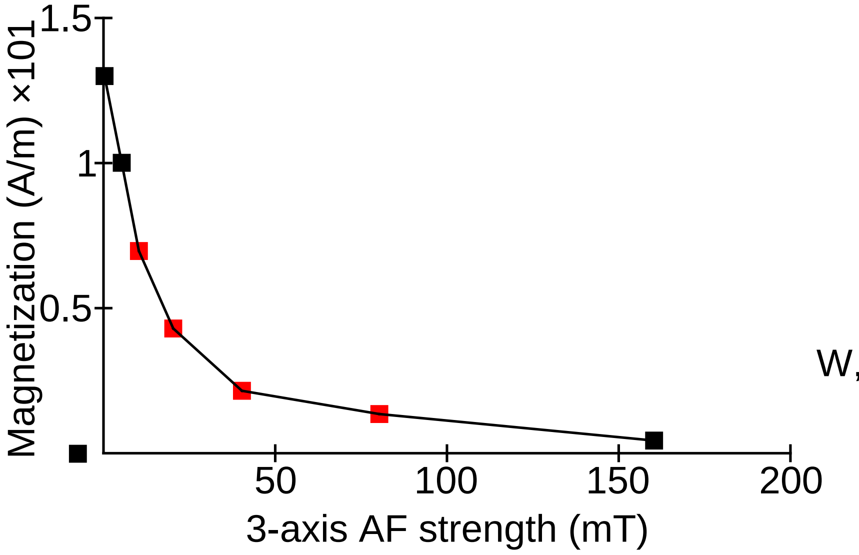

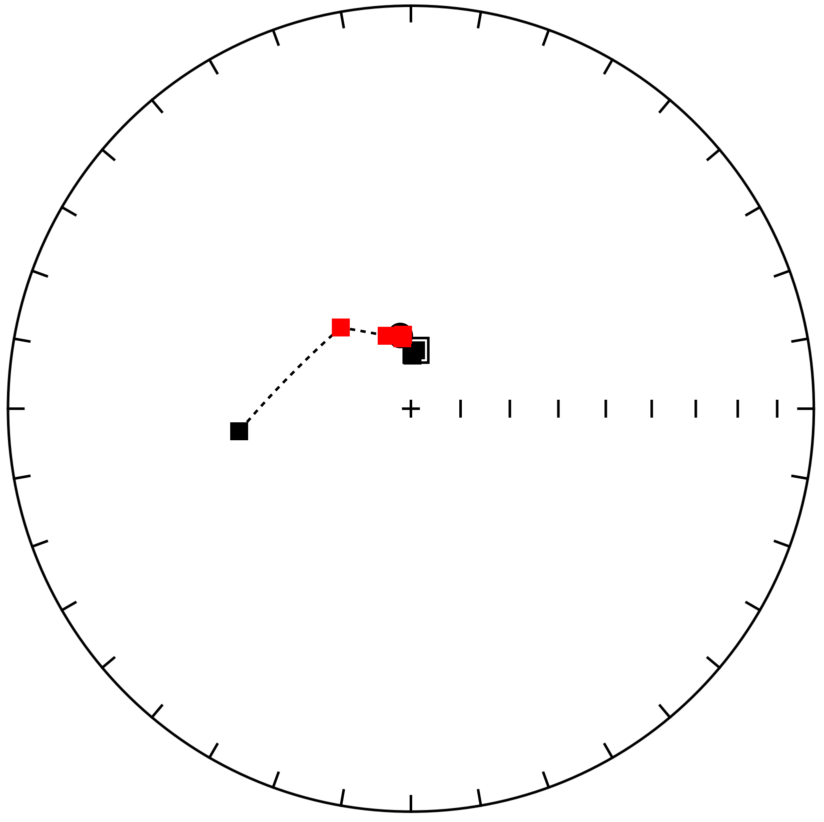

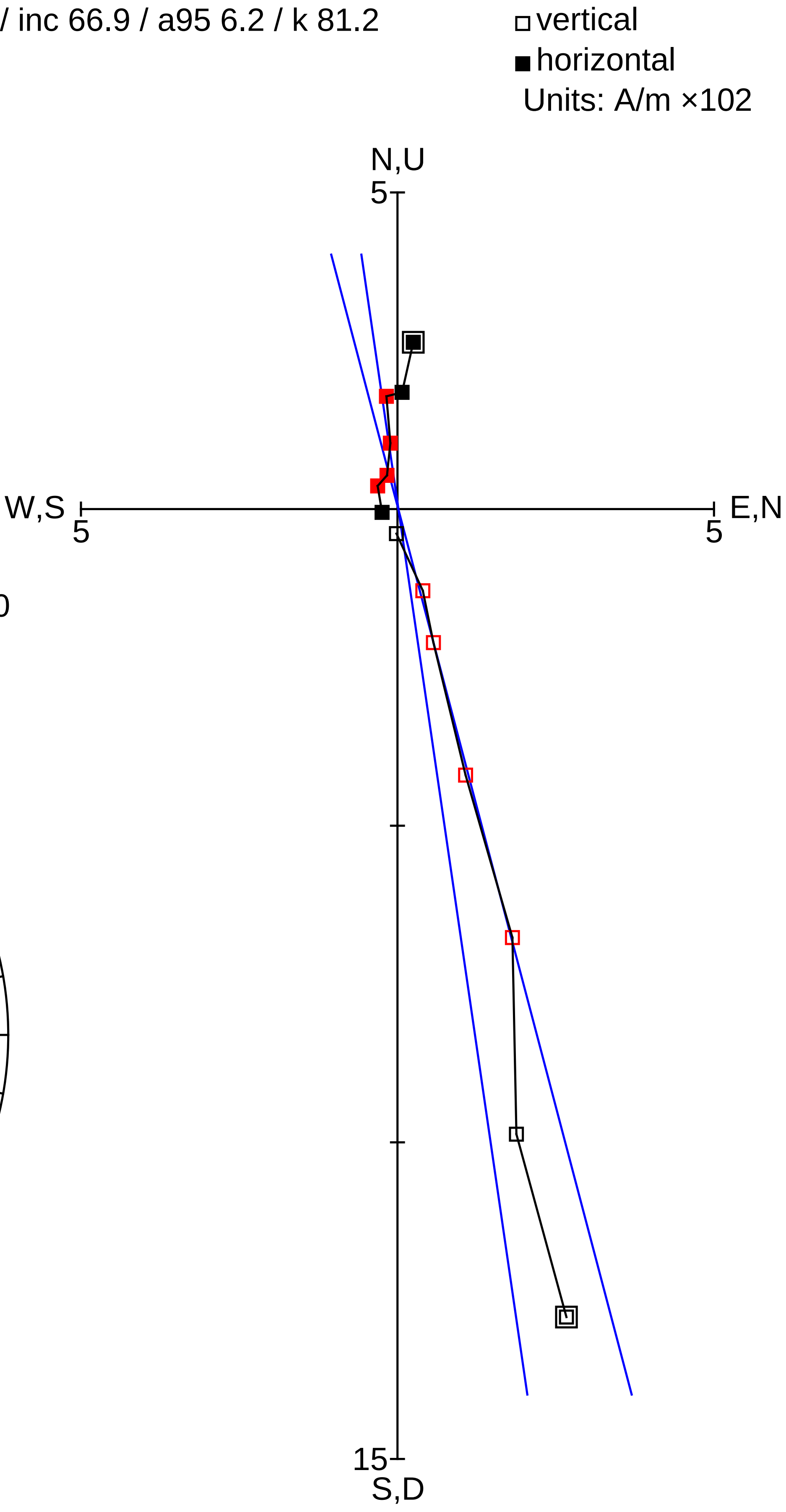

Updated July 2017

Sample: BR2-2

Site: Bull River

PCA dec 10.74 / inc 67.64 Fisher dec 10.2 / inc 66.9 / a95 6.2 / k 81.2

PCA MAD1 14.22 / MAD3 1.21

(0.37 0.07 0.92)t

□ vertical

■ horizontal

Units: A/m ×102

Updated July 2017

	demag.	dec.	inc.	int.	m.s.
	0	8.9	70.2	1.18e-01	NaN
*	5	11.2	68.1	9.83e-02	NaN
*	10	12.7	67.7	7.91e-02	NaN
*	20	5.2	65.7	4.93e-02	NaN
*	40	7.9	67.0	2.63e-02	NaN
	80	358.3	51.2	7.68e-03	NaN
	160	10.1	36.2	5.02e-03	NaN

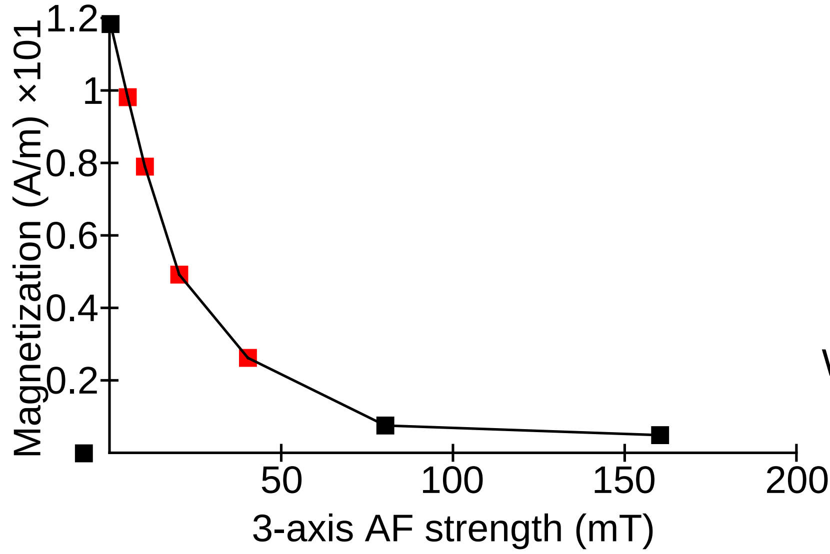

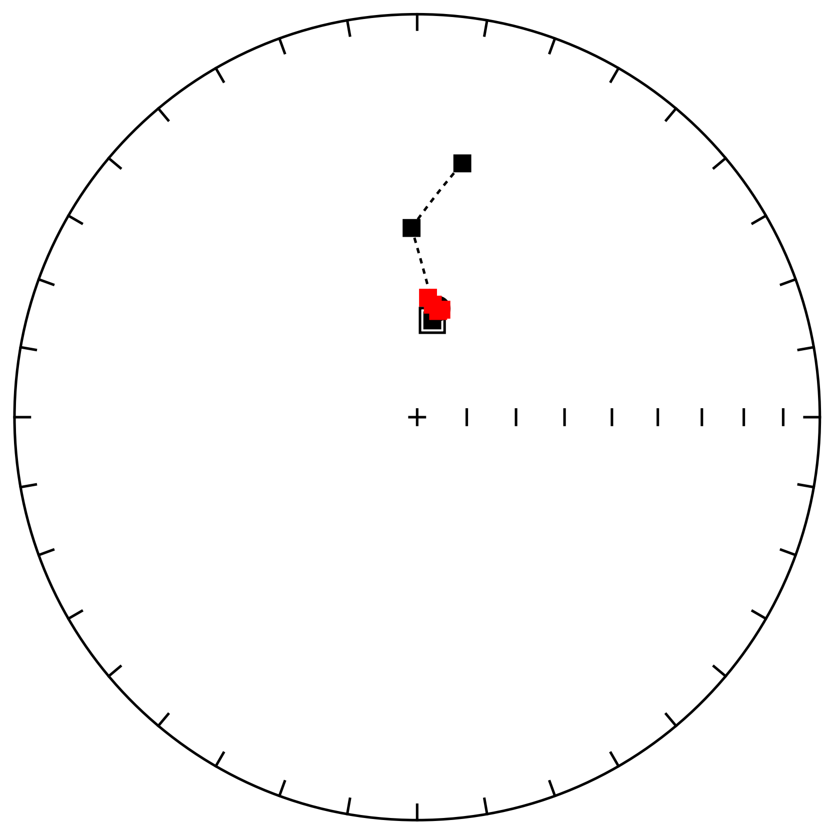

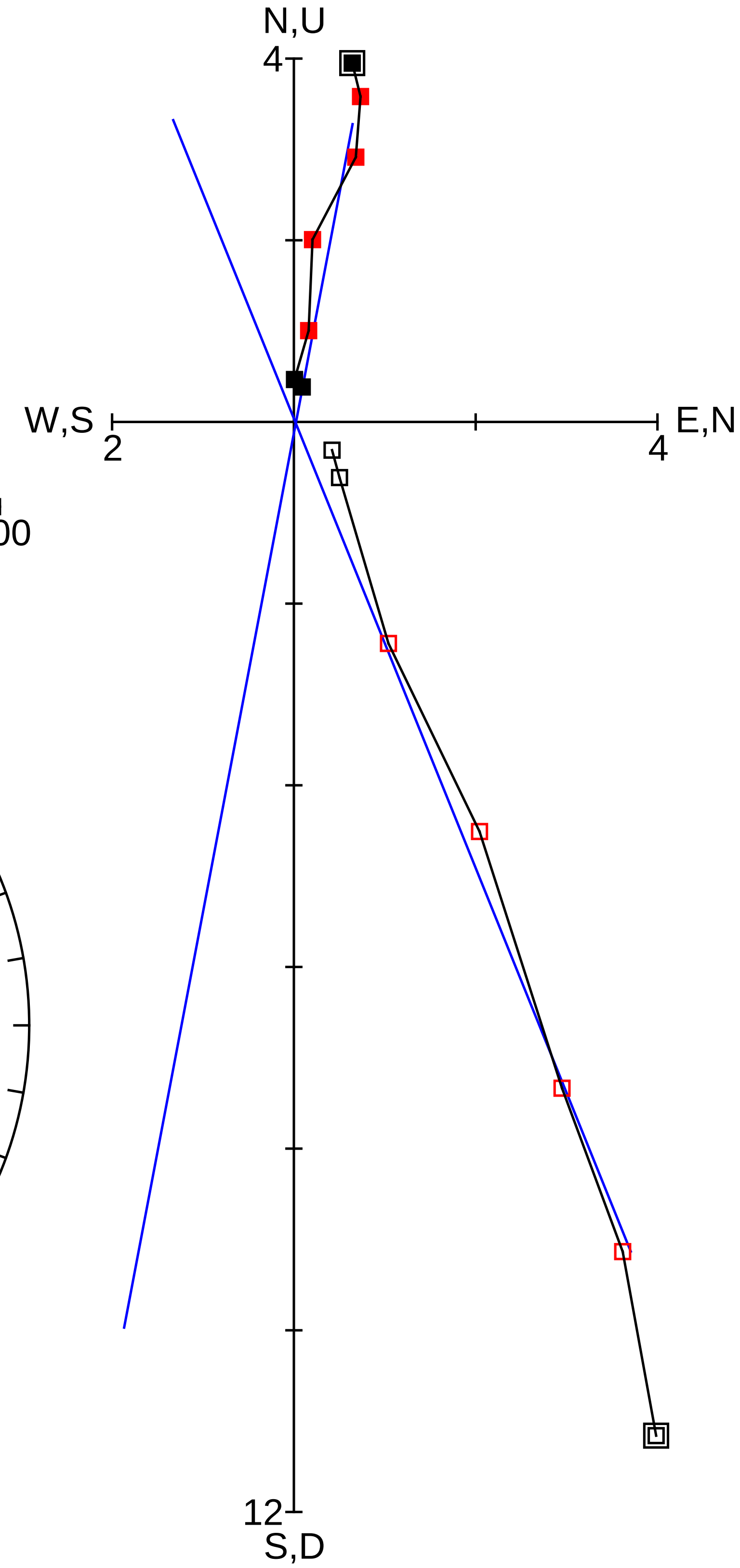

Sample: BR3-1
Site: Bull River

PCA dec 336.14 / inc 75.00 Fisher dec 10.2 / inc 66.9 / a95 6.2 / k 81.2
PCA MAD1 33.32 / MAD3 1.75
(0.24 -0.10 0.97)t

Updated July 2017

	demag.	dec.	inc.	int.	m.s.
	0	33.8	86.1	9.26e-02	NaN
	5	339.5	79.9	7.93e-02	NaN
*	10	339.0	75.8	6.40e-02	NaN
*	20	336.4	73.5	4.57e-02	NaN
*	40	321.7	74.3	2.80e-02	NaN
	80	319.6	57.7	1.56e-02	NaN
	160	298.4	55.7	6.84e-03	NaN

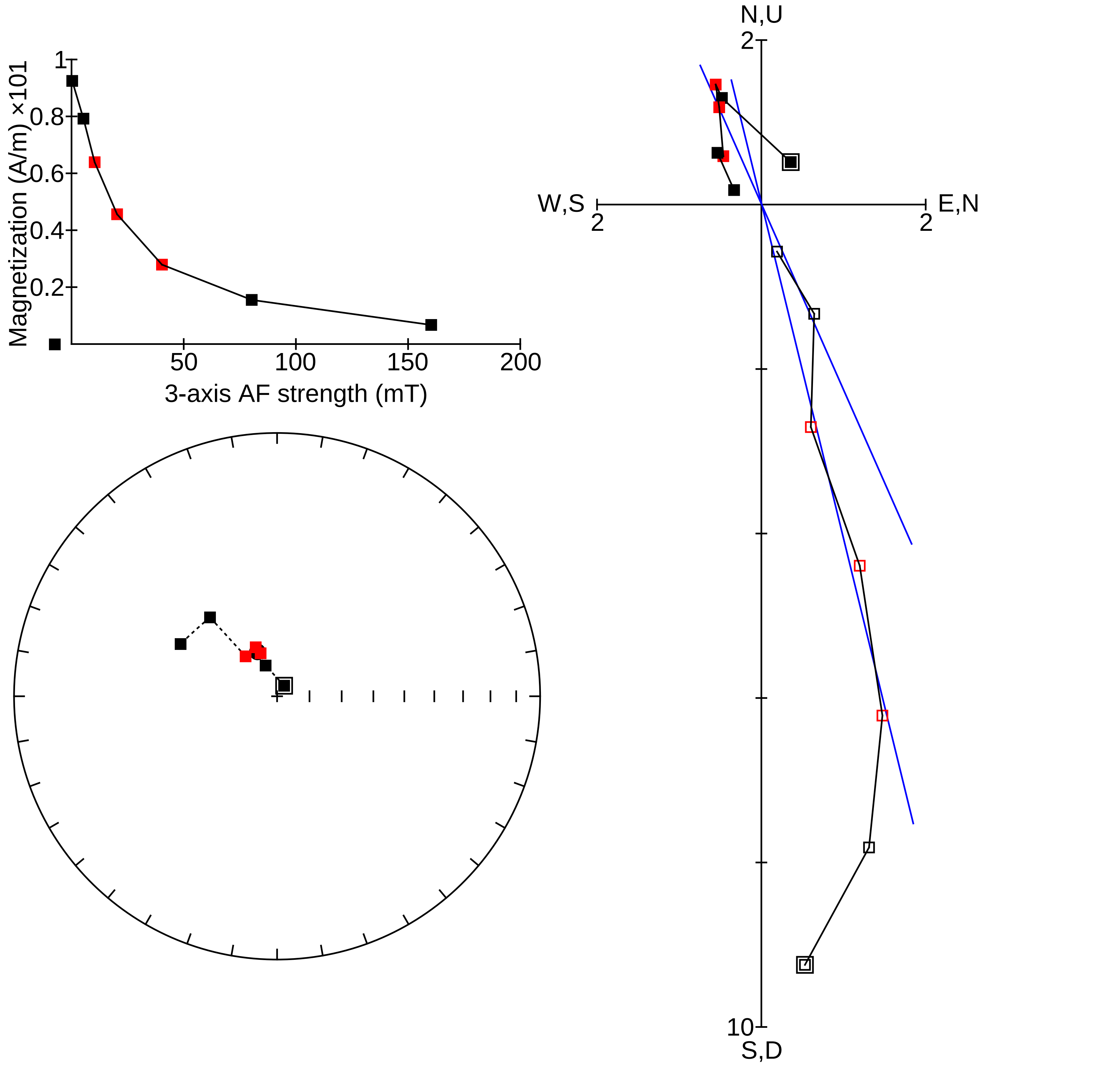

Sample: BR5-2
Site: Bull River

PCA dec 32.38 / inc 68.20 Fisher dec 10.2 / inc 66.9 / a95 6.2 / k 81.2
PCA MAD1 14.59 / MAD3 1.78
(0.31 0.20 0.93)t

□ vertical
■ horizontal
Units: A/m ×102

Updated July 2017

	demag.	dec.	inc.	int.	m.s.
	0	43.4	68.0	1.85e-01	NaN
*	5	35.1	68.5	1.39e-01	NaN
*	10	30.6	68.6	9.62e-02	NaN
*	20	23.5	65.2	5.61e-02	NaN
*	40	25.5	65.2	2.32e-02	NaN
	80	338.2	49.8	8.67e-03	NaN
	160	29.3	26.5	3.39e-03	NaN

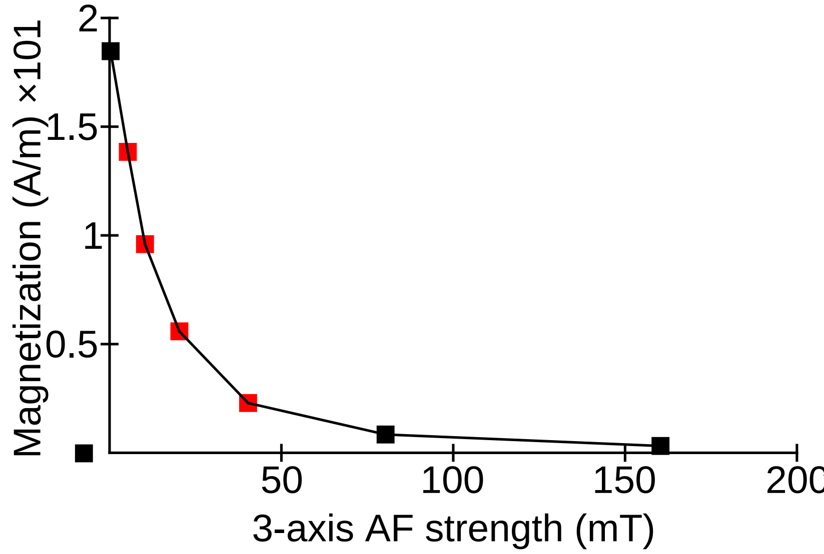

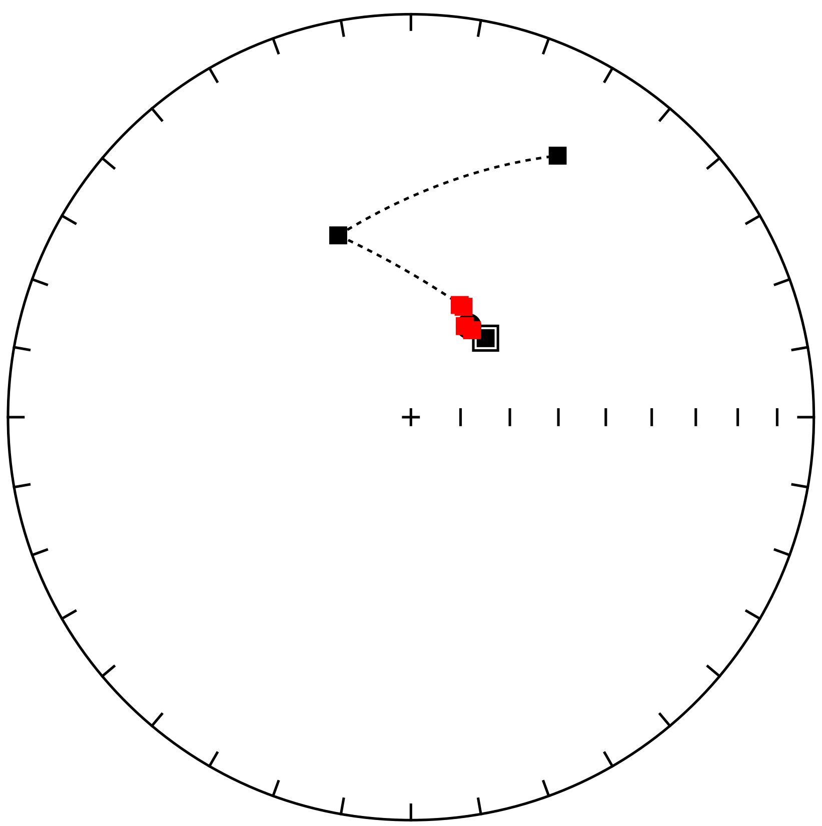

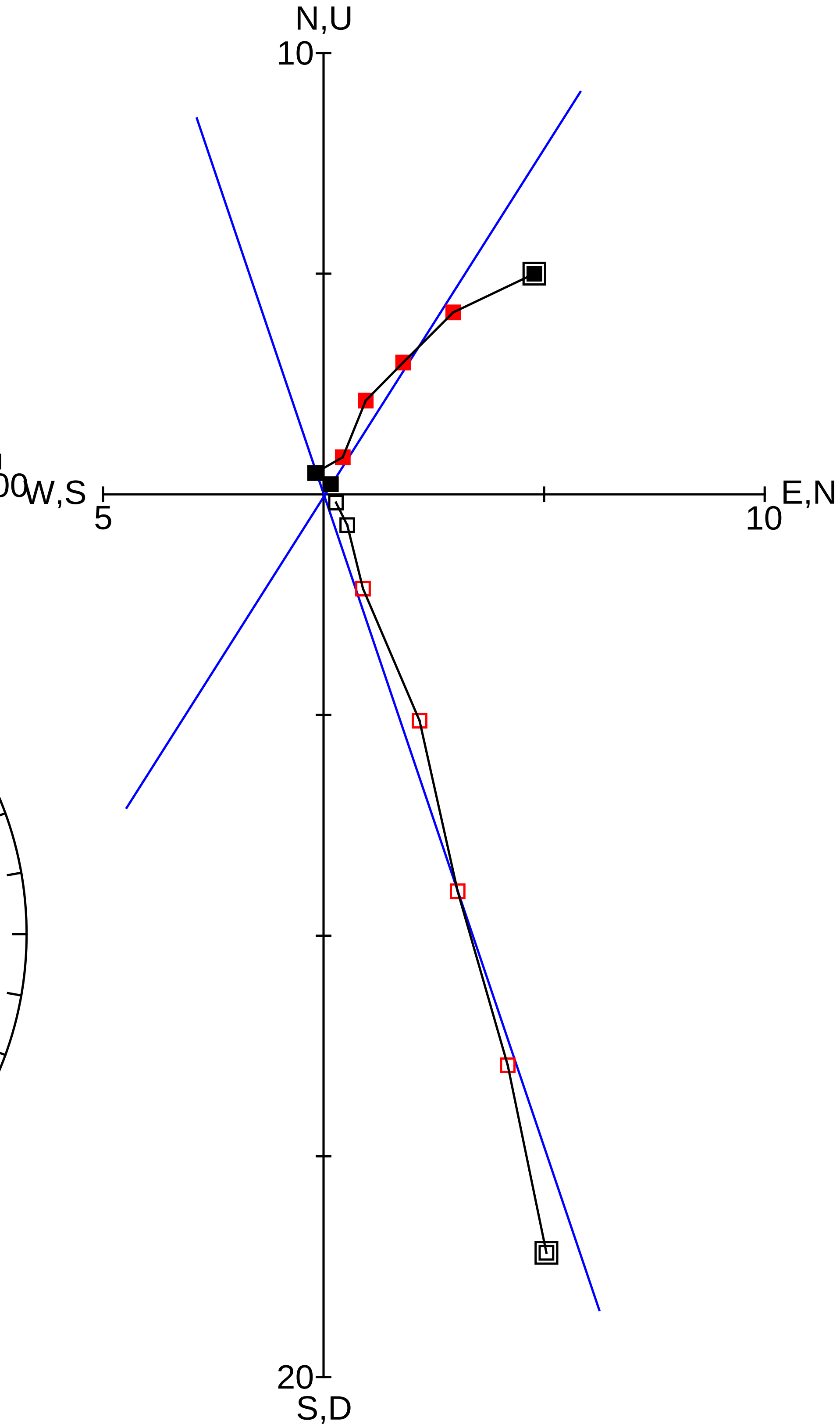

Sample: BR7-1

Site: Bull River

PCA dec 26.11 / inc 59.44 Fisher dec 10.2 / inc 66.9 / a95 6.2 / k 81.2

PCA MAD1 19.79 / MAD3 2.78

(0.46 0.22 0.86)t

□ vertical

■ horizontal

Units: A/m ×102

Updated July 2017

	demag.	dec.	inc.	int.	m.s.
	0	69.9	53.7	8.20e-02	NaN
	5	51.6	64.1	6.30e-02	NaN
	10	44.3	65.3	5.04e-02	NaN
*	20	26.0	60.9	3.37e-02	NaN
*	40	27.8	54.8	1.75e-02	NaN
*	80	18.6	54.4	7.38e-03	NaN
	160	353.2	-1.0	2.81e-03	NaN

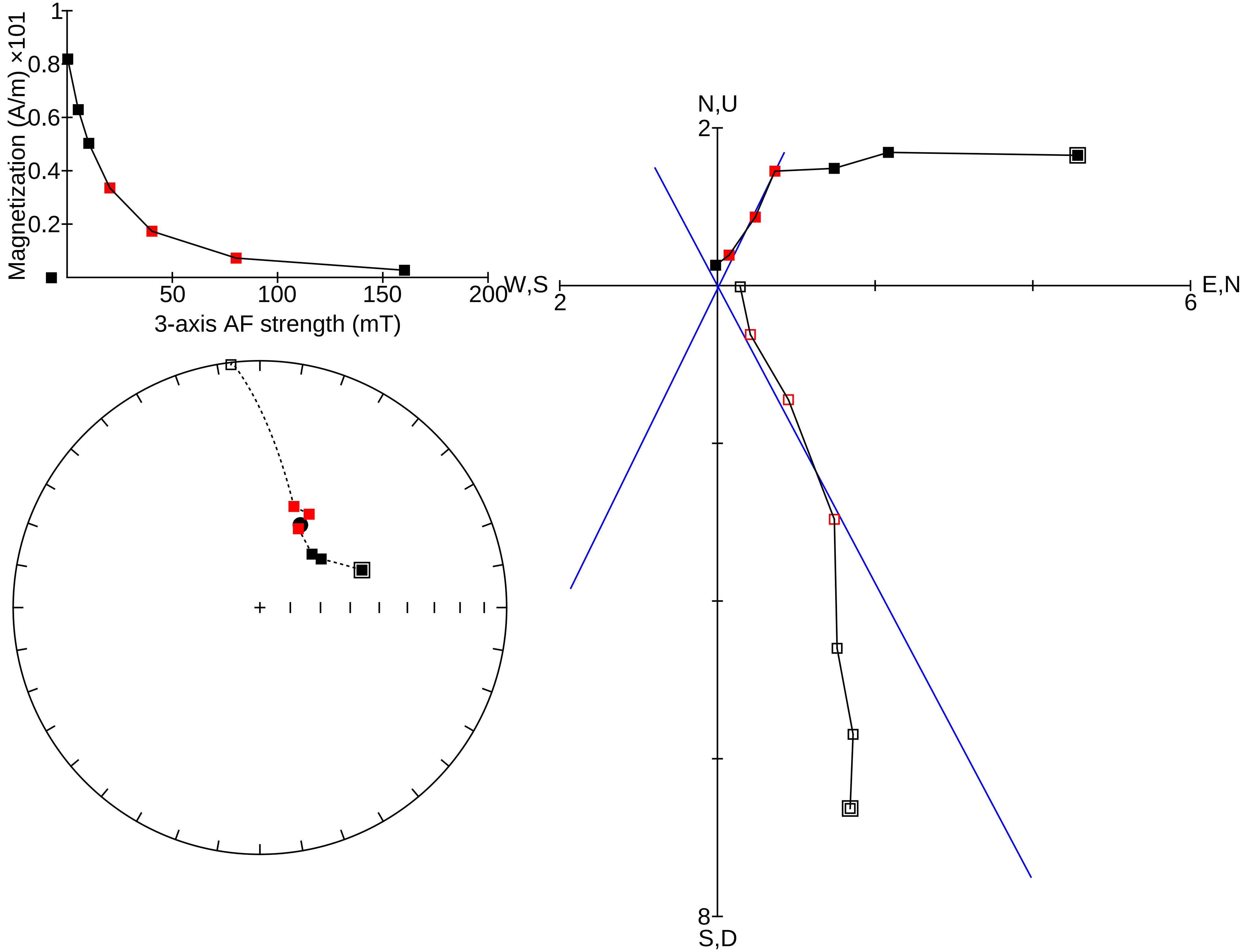

Sample: BR8-1

Site: Bull River

PCA dec 11.43 / inc 59.14 Fisher dec 10.2 / inc 66.9 / a95 6.2 / k 81.2
PCA MAD1 21.67 / MAD3 3.08
(0.50 0.10 0.86)t

□ vertical
■ horizontal
Units: A/m ×102

Updated July 2017

	demag.	dec.	inc.	int.	m.s.
	0	33.1	51.0	1.75e-01	NaN
*	5	14.9	59.3	1.23e-01	NaN
*	10	8.4	58.8	8.22e-02	NaN
*	20	4.8	60.7	4.87e-02	NaN
*	40	355.4	53.9	2.54e-02	NaN
*	80	351.2	45.3	1.21e-02	NaN
*	160	353.3	41.9	8.15e-03	NaN

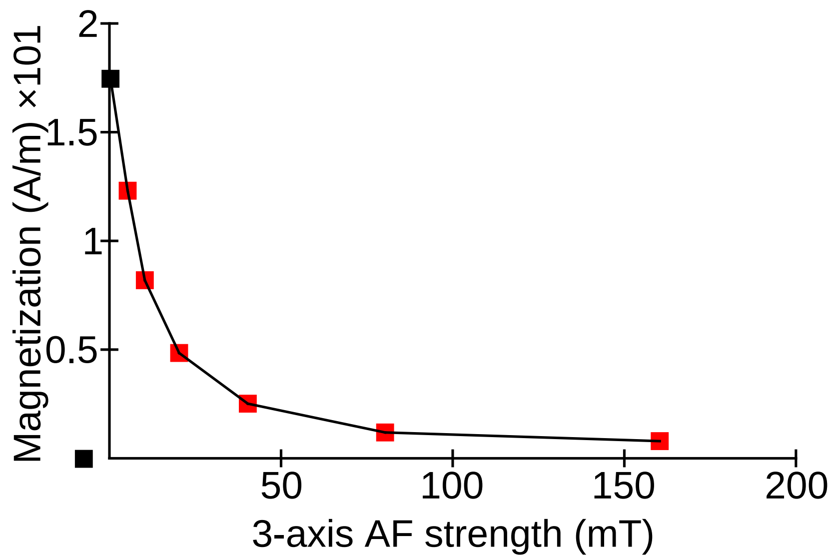

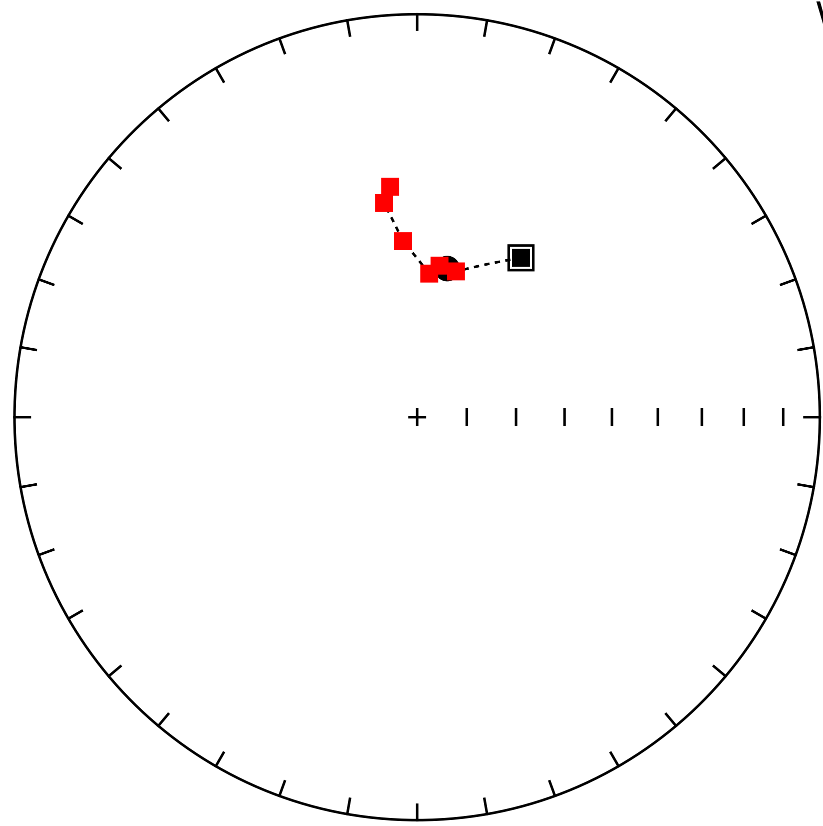

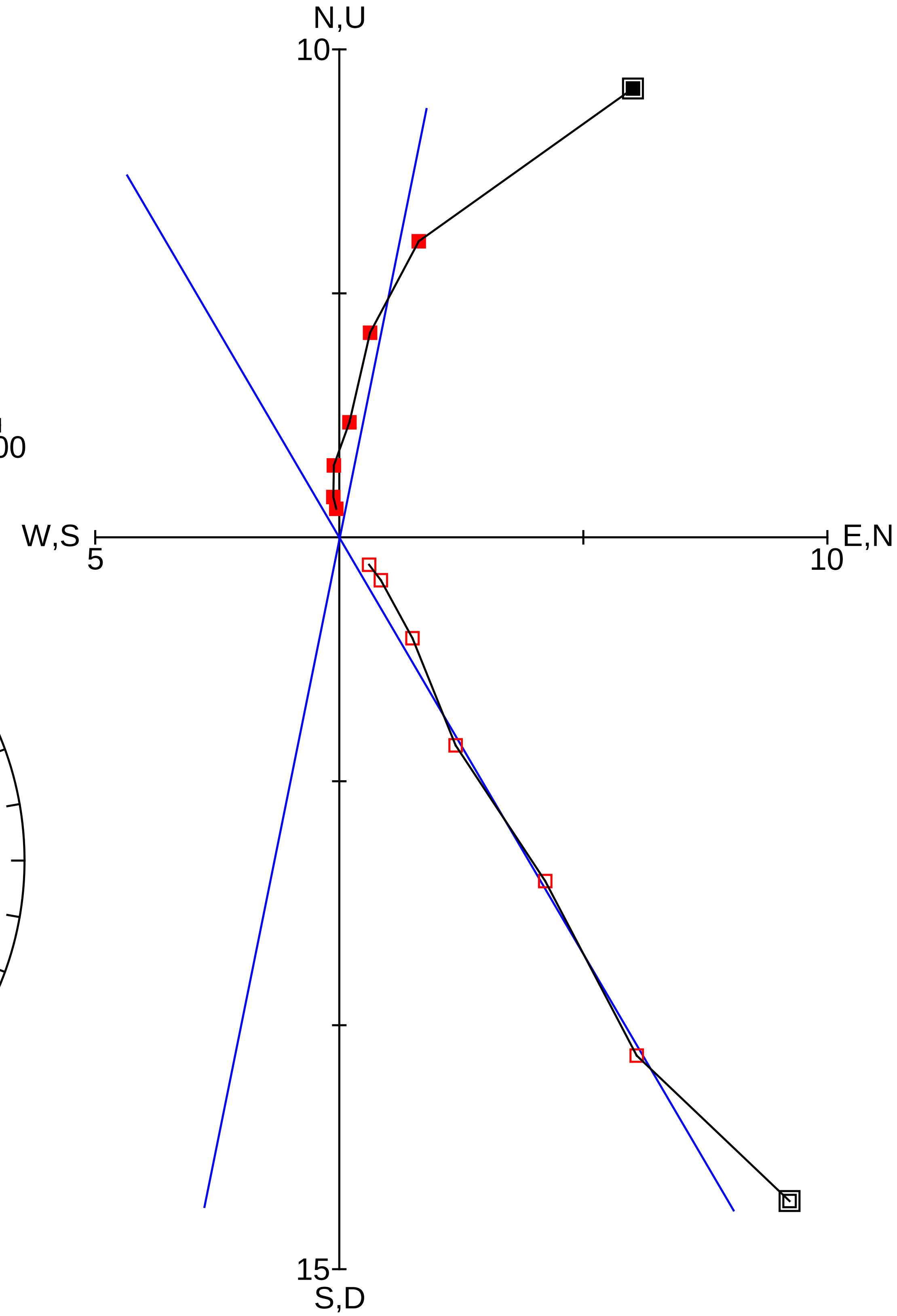

Sample: BR9-1

Site: Bull River

PCA dec 4.74 / inc 62.67 Fisher dec 10.2 / inc 66.9 / a95 6.2 / k 81.2

PCA MAD1 14.20 / MAD3 1.87

(0.46 0.04 0.89)t

Updated July 2017

	demag.	dec.	inc.	int.	m.s.
	0	9.1	58.9	2.14e-01	NaN
*	5	6.8	62.0	1.72e-01	NaN
*	10	359.2	63.7	1.20e-01	NaN
*	20	7.9	63.2	6.32e-02	NaN
*	40	12.9	63.6	2.22e-02	NaN
*	80	343.5	61.4	8.51e-03	NaN
	160	39.2	44.0	2.93e-03	NaN

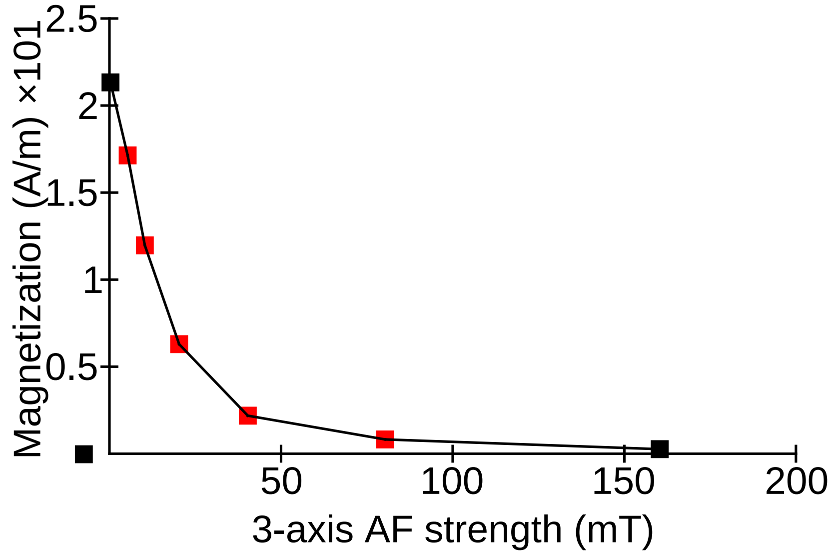

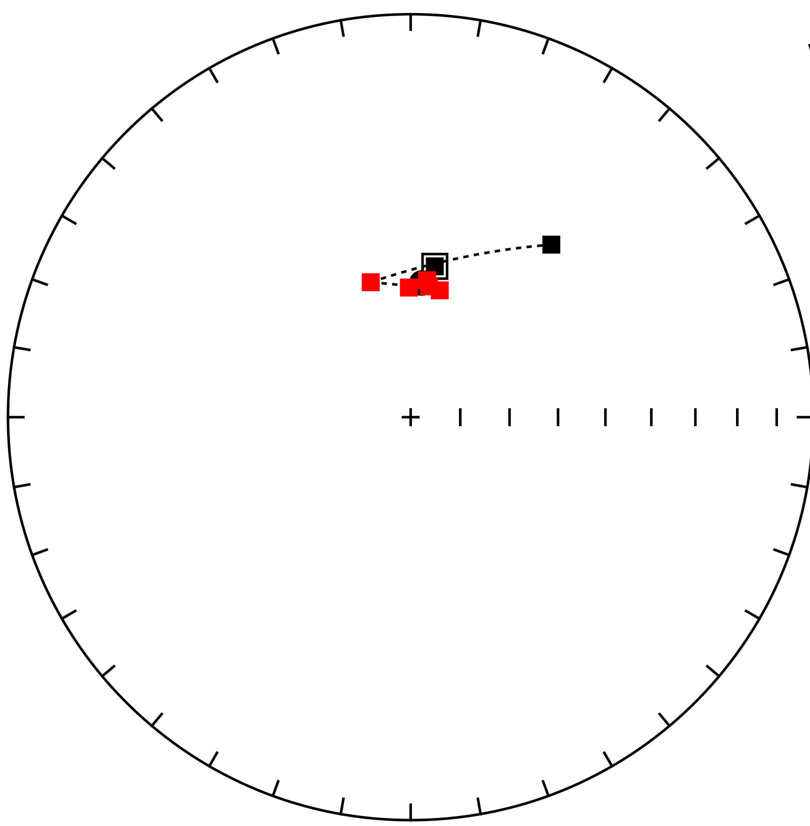

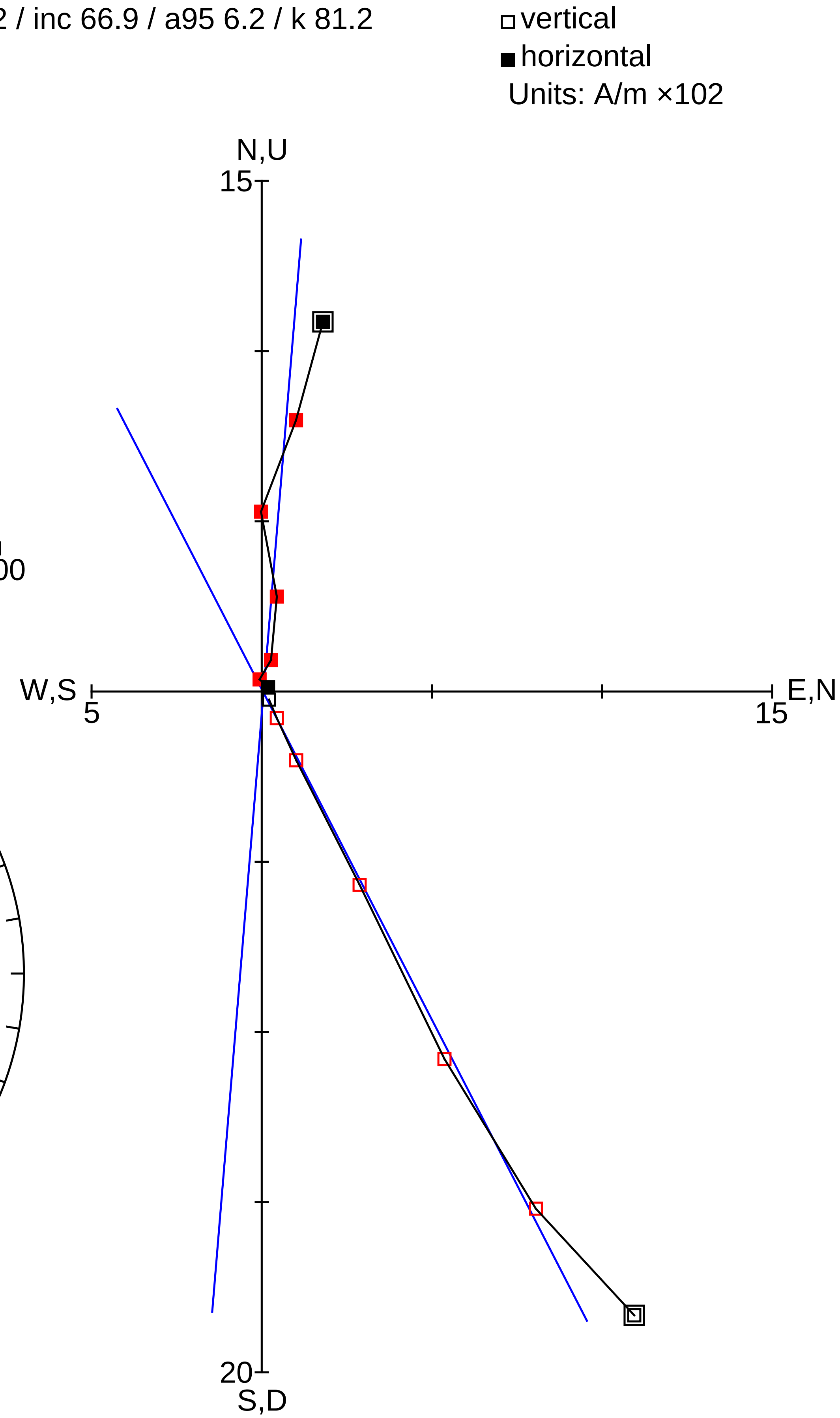

Sample: BR10-1

Site: Bull River

PCA dec 7.26 / inc 62.32 Fisher dec 10.2 / inc 66.9 / a95 6.2 / k 81.2

PCA MAD1 19.47 / MAD3 2.21

(0.46 0.06 0.89)t

□ vertical

■ horizontal

Units: A/m ×102

Updated July 2017

	demag.	dec.	inc.	int.	m.s.
	0	11.9	61.0	1.15e-01	NaN
*	5	7.5	63.1	8.48e-02	NaN
*	10	6.2	63.1	6.62e-02	NaN
*	20	8.4	59.6	4.23e-02	NaN
*	40	11.0	55.3	2.06e-02	NaN
*	80	357.6	47.0	9.60e-03	NaN
	160	340.8	9.2	4.34e-03	NaN